AD-A078 575 NATIONAL BUREAU OF STANDARDS WASHINGTON, D.C. 18/3, 18/8
OPERATION JANGLE. NEVADA PROVING GROUNDS, OCTOBER-NOVEMBER 1951, GAMMA RADIATION MEASUREMENTS, COSTRELL, LOUIS

UNCLASSIFIED WT-370 01 APR 52 AEC

1 OF 4
AD A
078575

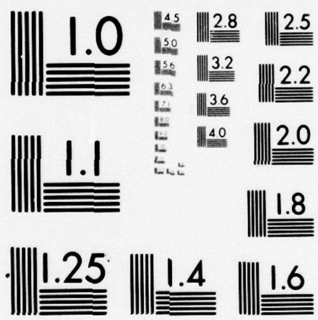

MICROCOPY RESOLUTION TEST CHART

AD-A078575

DI2018,856

UNCLASSIFIED

JANGLE

NEVADA PROVING GROUNDS
OCTOBER-NOVEMBER 195[illegible]

GAMMA RADIATION MEASUREMENTS

[redacted]

Classification (Cancelled) (Changed to UNCLASSIFIED)
By Authority of [illegible] 8/6/64
By [illegible] Date 8/11/64

CANCELED

ARMED FORCES SPECIAL WEAPONS PROJECT
WASHINGTON, D.C.

UNCLASSIFIED

WT-370

This document consists of 335 plus 4 pages (counting all preliminary pages in all reports and all unnumbered blanks)

Copy 199 of 243 copies, Series B

OPERATION JANGLE

GAMMA RADIATION MEASUREMENTS

Project 2.1a	Gamma Radiation as a Function of Time and Distance (WT-329)
Project 2.1b	Gamma Radiation as a Function of Time with Droppable Telemeters (WT-392)
X Project 2.1c-1	Aerial Survey of Distant Contaminated Terrain (WT-330)
X Project 2.1c-2	Aerial Survey of Local Contaminated Terrain (WT-351)
Project 2.1d	Monitor Survey of Ground Contamination (WT-381)
X Project 2.3-1	Total Gamma Radiation Dosage (WT-331)
Project 2.3-2	Foxhole Shielding of Gamma Radiation (WT-393)

Reproduced Direct from Manuscript Copy by
AEC Technical Information Service
Oak Ridge, Tennessee

SECRET
Security Information
CANCELED

UNCLASSIFIED

OPERATION JANGLE

PROJECT 2.1a

GAMMA RADIATION AS A FUNCTION OF TIME AND DISTANCE

by

L. Costrell

Radiation Physics Laboratory

April 1, 1952

National Bureau of Standards

Washington 25, D. C.

UNCLASSIFIED

CANCELED
SECRET
Security Information

RESTRICTED DATA
ATOMIC ENERGY ACT 1946
CANCELED

[redacted]

PROJECT 2.1a

UNCLASSIFIED

PREFACE

The measurement of residual gamma radiation intensity as a function of time and distance was undertaken by the National Bureau of Standards for the Signal Corps Engineering Laboratories, Fort Monmouth, New Jersey. Personnel participating in the project are listed below.

*Robert C. Bass	Participated in development work and field installations
Howard O. Cline	" " " " "
Louis Costrell	" " " " "
John A. Dickinson	" " " " "
*Thomas J. Hahn	" " " " "
Russell Little	" " " " "
*Hal O. Smith	" " " " "
Edward T. Sullivan	" " " " "
H. W. Koch	Participated in development work
Simon R. Mayerhofer	" " " "
Harold A. Thomas	" " " "
Bartlett Wong	" " " "
*Larry Creech	Participated in field installations
Owen H. Gailar	" " " "
*Keith Hartwig	" " " "
Robert J. Kennedy	" " " "
*James Meador	" " " "
*William Scott	" " " "

* Denotes Signal Corps personnel

UNCLASSIFIED

[redacted] [redacted]

ACKNOWLEDGEMENTS

The successful completion of this project was made possible only through the combined efforts of all the participants. In addition to the contributions of those listed in the preface, generous assistance and cooperation were received from Lt. Col. Merwin B. Forbes, Signal Corps Project Officer, Dr. Howard L. Andrews, Director of Program 2, Lt. Col. Edward A. Martell, AFSWP, and the members of their respective staffs.

Appreciation is also expressed to Ed Meyers, of the Squier Signal Laboratory, and his assistants for their excellent handling of the storage battery requirements in the field.

Allen E. Shoup and Charles A. Minor of the Shoup Engineering Company were responsible for the design and operation of the magnetic recorders and deserve considerable credit for their fine work and selfless cooperation. Herman Jensen of the Seeburg Corporation rendered valuable aid in the procurement of many components for the instruments.

Mention should also be made of the cooperation of Don Daybell, General Manager of the Haddock Engineering Company, who expeditiously handled our heavy construction requirements.

Dr. Harold A. Thomas, John A. Dickinson, Robert C. Bass, and Thomas J. Hahn contributed to the writing of the report. Howard O. Cline, Edward T. Sullivan, and Hal O. Smith are principally responsible for the assembly of the data in graph form. Appreciation is also expressed to William E. McClellan who fought the battle of procurement with much vigor and considerable success.

Particular acknowledgement is made of the invaluable contributions of Dr. Harold A. Thomas, of the Corona California Laboratories of the National Bureau of Standards, who headed the project prior to the field installation.

UNCLASSIFIED

[redacted]

PROJECT 2.1a

CONTENTS

[redacted] [redacted]

UNCLASSIFIED

PROJECT 2.1a

[redacted]

[redacted]

PROJECT 2.1a

ILLUSTRATIONS

[redacted] [redacted]

[redacted]

PROJECT 2.1a

[redacted]

[redacted]

[redacted]

PROJECT 2.1a

TABLES

[redacted] [redacted]

[redacted]

PROJECT 2.1a

ABSTRACT

Gamma ray dosage rates were determined as a function of time and distance. The method of measurement and the equipment used is described. Dose rates as a function of time were obtained for 27 stations on the surface burst and for 29 stations on the underground burst. Total dose data was obtained by integration of the dose rates. Dose rate and integrated dose as a function of time are presented for all of the stations. One hour dose rate contours are presented as well as 10 minute, 1 hour, and 10 hour integrated dose contours. All of the above mentioned data is presented in the form of curves. In addition 10 second dose versus distance curves for the surface and underground bursts are presented on a single graph for ready comparison.

CHAPTER 1

INTRODUCTION

1.1 PURPOSE

It has been demonstrated that in the case of an atomic bomb burst several hundred feet or higher above the ground the principal damage inflicted is due to blast and incendiary action. While the initial gamma radiation can constitute a personnel hazard over a limited area, residual contamination is relatively unimportant.[1,2] The Bikini Baker test demonstrated that underwater bursts can produce serious contamination over a considerable area, and it was anticipated that underground atomic explosions could produce similar effects. Since the blast damage of an underground explosion is considerably less than for an air burst, it was felt that radioactive contamination and the production of interdictory areas by an underground burst might represent a considerable portion of the military effectiveness of such a burst. The purpose of the measurements described in this report was to determine the radiation effects for underground and surface bursts.

1.2 STATION PATTERN

After consideration of variations in ground winds, wind variations with altitude and the limitations of the terrain, the station patterns of Fig 1.1 and 1.2 were used. The underground zero was located 2½ miles north of the surface zero on a line running approximately 5 degrees west of true north. For each burst an area of approximately 12 square miles was covered with stations extending to about 3 miles from the point of detonation.

1.3 RADIATION MEASUREMENT

Radiation intensities as a function of time and distance were measured. By integration of the rate data, total dose information was obtained. Dose and dose rate contours were then plotted.

---

1 The Effects of Atomic Weapons (Washington: Government Printing Office 1950) p 248.

2 Experience of Operation GREENHOUSE.

[redacted]

PROJECT 2.1a

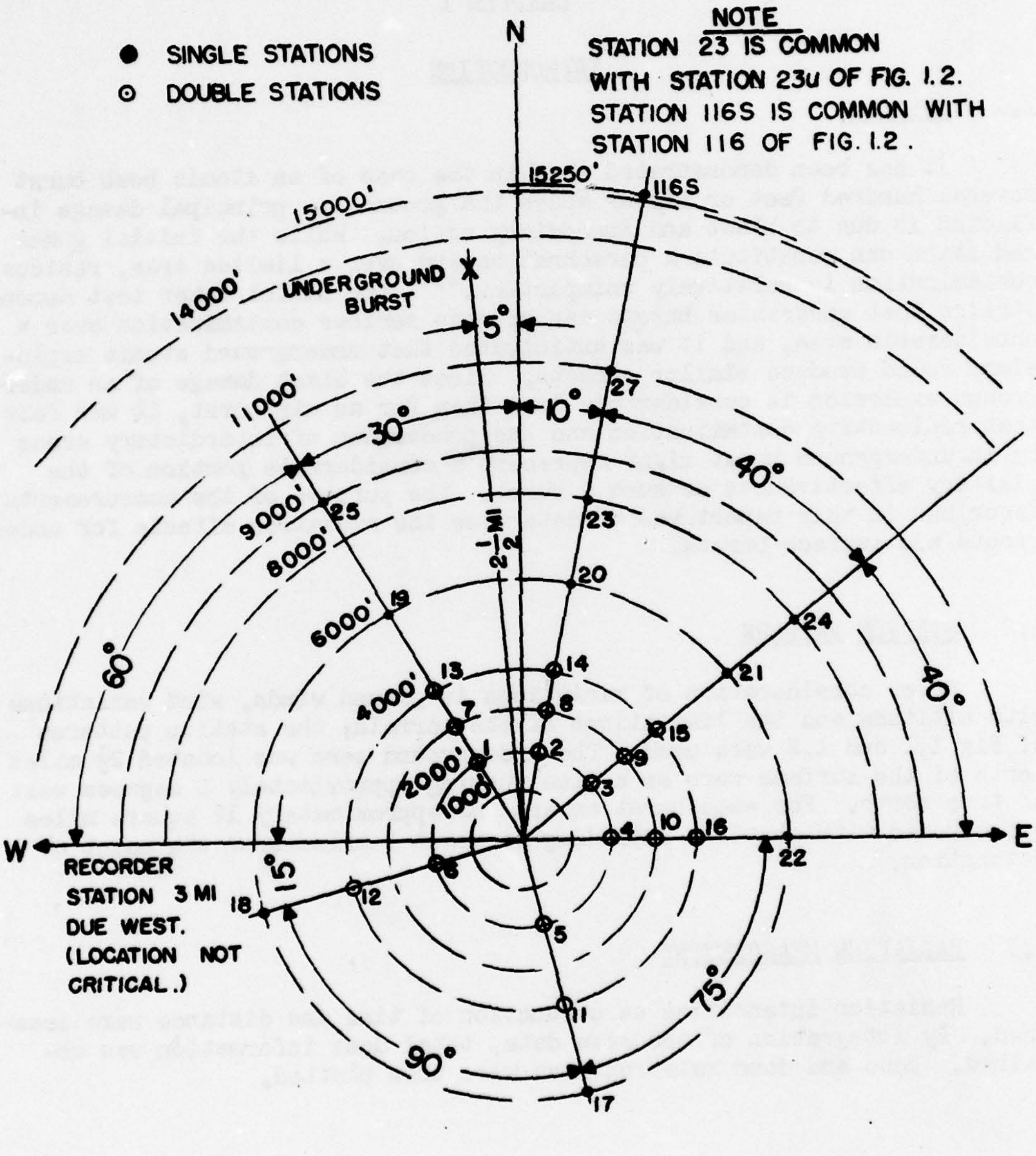

Fig 1.1 Station Pattern of Surface Burst

[redacted] [redacted]

PROJECT 2.1a

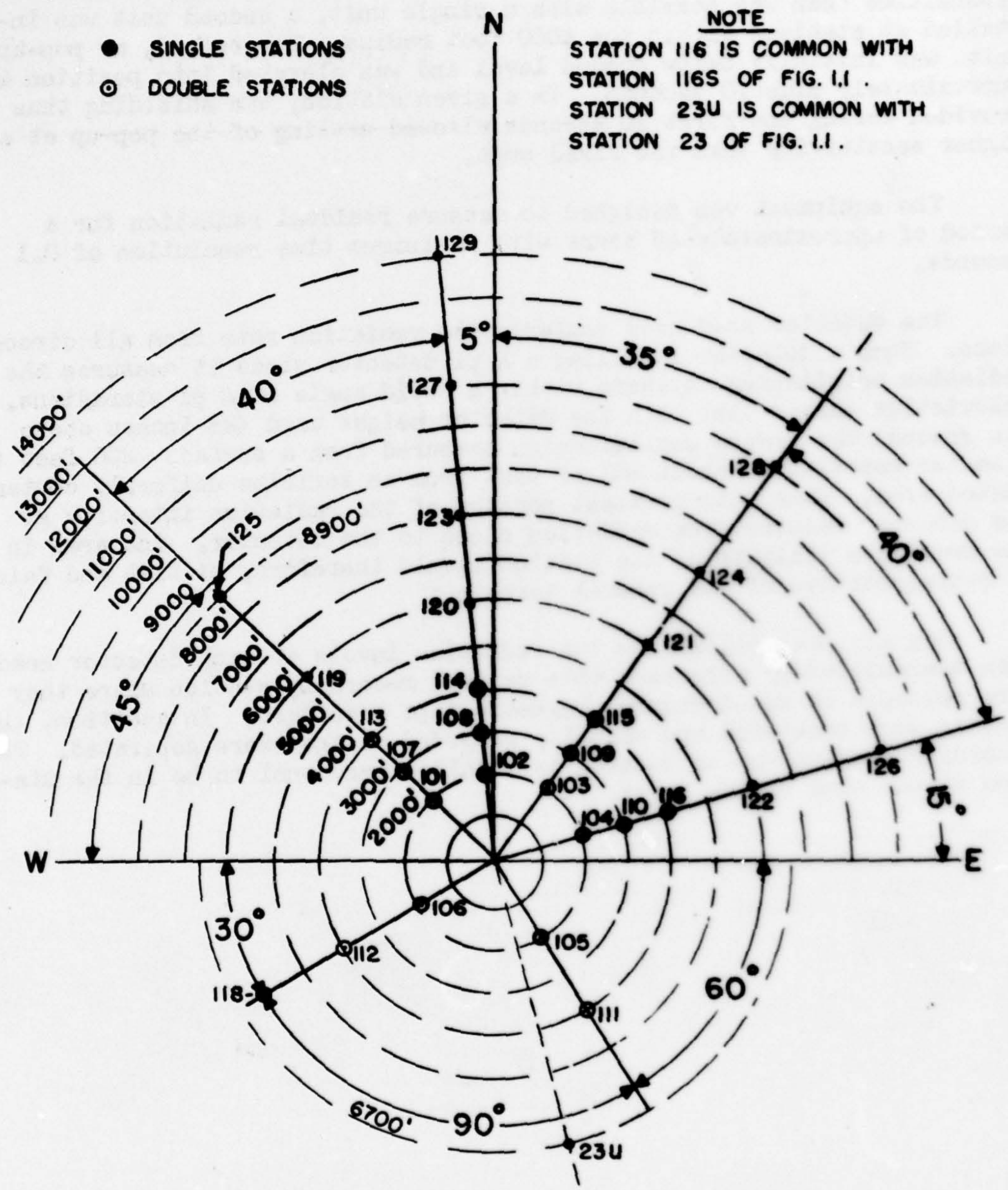

Fig 1.2 Station Pattern of Underground Burst

[redacted]

Since blast might have damaged some of the units within 4000 feet of zero and since it was desired to measure a greater range of radiation intensities than was possible with a single unit, a second unit was installed at stations within the 4000 foot radius. The second, or pop-up unit, was initially below ground level and was elevated into position at approximately plus 10 seconds. In a given station, the shielding thus provided during the first 10 seconds allowed setting of the pop-up at a higher sensitivity than the fixed unit.

The equipment was designed to measure residual radiation for a period of approximately 48 hours with a minimum time resolution of 0.1 seconds.

The detector head used measured the radiation rate from all directions. Such a detector is called a 4 pi detector since it measures the radiation originating anywhere within a solid angle of 4 pi steradians. Calculation shows[3] that with the detector height used (28 inches above the ground) the ground contamination measured from a surface 200 feet in diameter constitutes about 80% of that from an infinite uniformly contaminated area. Thus, the greatest portion of the radiation intensity at the detector results from radiation close to the detector. The area in the immediate vicinity of the station should therefore, be flat and fairly representative of the general terrain.

Signals proportional to the radiation levels at each detector head were transmitted by wire back to a central recording station where they were recorded on multi-channel magnetic tape recorders. In addition, the signals were monitored and manually recorded as they were generated. The recording station was so located as to allow personnel to be in the station at the time of the burst.

---

[3] The Effects of Atomic Weapons (Washington: Government Printing Office, 1950) p 431.

[redacted]

CHAPTER 2

RADIATION DETECTORS

2.1 STANDARD DETECTOR HEAD

Conversion of radiation intensity in roentgens per unit time to a usable electrical signal is the basic requirement of the detector head. Further conversion of this electrical signal for the purpose of transmission and recording may be necessary depending upon the type of recording system used. There are various methods of converting radiation levels to electrical signals, each offering various advantages and disadvantages for this particular application. The method chosen is essentially the same as that used in the GREENHOUSE tests and while later events have indicated that it is probably not the best, the limited time available for the construction of the required number of instruments made this choice mandatory. Theoretically, this method has the desirable characteristics of covering an unlimited range of radiation intensities, of giving a current signal proportional to the radiation intensity and of showing little energy dependence. When reduced to practice however, certain exceptions to these characteristics appear as will be discussed later.

The standard 4 pi detector consists fundamentally of a scintillating crystal, which produces light proportional to the radiation intensity, a light pipe for conducting the light from the crystal to a photoelectric device and the photomultiplier tube (PMT) located in a pit below ground for converting this light to an electrical current proportional to the light intensity. The crystal used is stilbene, 1.2 cm in diameter and 0.4 cm thick, mounted in a graphite block (Fig 2.1) to obtain electronic equilibrium and thus approach the characteristic of a free-wall ion chamber. The light pipe is an electropolished stainless steel tube 3/4 inch in diameter and 4 feet long. This tube conducts the light from the crystal, which is mounted about 28 inches above ground, to the PMT mounted below ground in the instrument pit, with a transmission efficiency of about 7%. The PMT is a 1P21 type tube mounted in a suitable light-proof housing which terminates the lower end of the light pipe. For mechanical protection the assembled unit is mounted in a 2 3/8 inch diameter dural tube the upper end of which is covered with a thin-wall hemispherical aluminum cap as shown in Fig. 2.2. The upper end of the dural tube has a reduced wall thickness to minimize absorption.

Since the PMT is also sensitive to gamma radiation, it must be either shielded or its sensitivity and energy dependence must be taken into

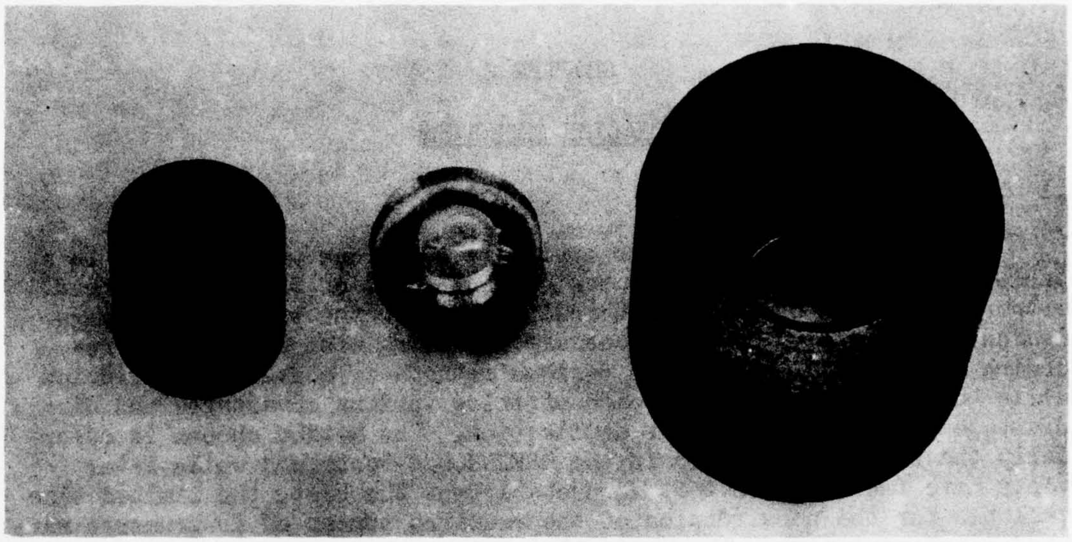

Fig 2.1 Graphite Block and Stilbene Crystal

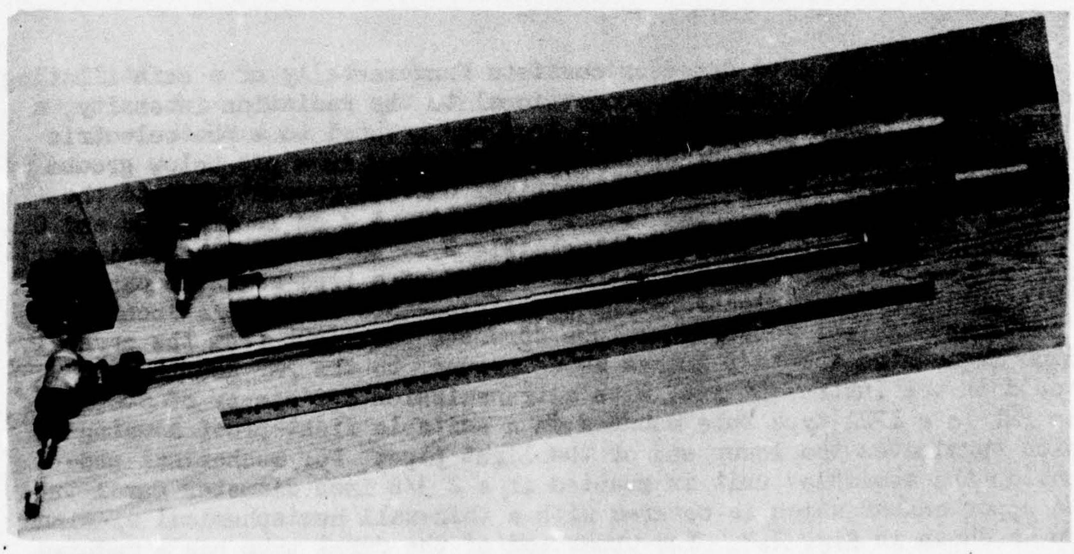

Fig 2.2 Standard Detector Head

account in the overall calibration. The preferable system of shielding was used. The amount of shielding required depends upon the relative sensitivity of the stilbene crystal and the PMT and upon the wave-length of the radiation involved. The crystal is somewhat more sensitive than the PMT but the light transmission loss in the light pipe is sufficient to off-set this and make shielding necessary. In fact, with the light pipe used, the PMT current output is approximately six times greater for radiation incident on the PMT than for the same radiation incident on the crystal alone. In the case of the surface detonation a major portion of the radiaton at the close-in stations during the first few milliseconds was probably due to neutron-gamma reactions with the nitrogen in the air and with various elements, such as chlorine, in the soil. This nitrogen reaction will produce gamma radiation with energies ranging up to 11 Mev necessitating considerable shielding. For the underground detonation the neutron flux should have been fairly well absorbed by the earth and as a consequence the amount of shielding required was considerably less.

The inherent shielding of the instrument shelter top is one foot of concrete. Additional shielding, consisting of 3 1/2 inches of lead surrounding the PMT, was used on the surface detonation for the fixed units at 2000 and 3000 feet and on one fixed unit at 4000 feet. However, comparison of the results for the stations with and without the additional shielding showed no great difference. A 2 1/2 inch lead shadow shield was used on all fixed units except where the 3 1/2 inch shielding was used.

The sensitivity of the detector head shown in Fig 2.2 is a function of PMT voltage. Therefore, the voltage was adjusted for each unit to obtain the desired sensitivity. The maximum sensitivity without excessive dark current is obtained with approximately 1000 volts on the PMT and is of the order of 10 r/hr. The lower limit of sensitivity is well beyond the required value and the unit may easily be adjusted to measure 10^8 r/hr which was beyond the maximum radiation rate measured. Throughout this seven decade range the current is a linear function of the radiation intensity (neglecting fatigue effects in the PMT).

Fatigue in the PMT has been investigated not only for this project but also by others and can constitute a serious problem in this type of application.[1] The magnitude of the fatigue effect depends in a complicated manner on the maximum plate current and the period of time in operation. It also varies considerably from one tube to another depending upon the exact time of tube seal-off relative to its stage of

---

1 Fitz-Hugh Marshell, J. W. Coltman, and L. P. Hunter, "The Photomultiplier X-ray Detector", Rev. Sci. Inst. 18, 504 (1947).

activation.[2] The fatigue problem was minimized in this application by limiting the maximum plate current to 600 microamperes and by using tubes that showed a minimum fatigue effect. Light calibrations were made just previous to zero time, at plus 10 minutes and at such other times as seemed necessary during the detectors operation. Thus sensitivity changes due to fatigue were measured. Also the light calibration served to detect changes in sensitivity as a result of blast.

2.2 HIGH SENSITIVITY DETECTOR HEAD

It was desired to measure radiation levels as low as a few mr/hr which is beyond the ultimate sensitivity of the standard detector. Certain modifications of the standard head could be made for distant stations that would enhance the sensitivity. These included elimination of the light pipe, larger photo-cathode surface and a larger crystal. These modifications led to the high sensitivity detector head assembly shown in Figs 2.3 and 2.4.

In this detector an anthracene crystal 3.2 mm thick and 4 cm in diameter was cemented to the end of a type 5819 PMT, covered with a carbon block, and this assembly shock-mounted on a bakelite disc. The assembly was covered with a thin-wall aluminum cover having a spherical top to shed fall out material. This complete unit screwed to the top of the standard dural tubes and so could be adapted to any station desired. The ultimate sensitivity of the unit is about one mr/hr.

Radiation shielding of the PMT was neither possible nor necessary for the high sensitivity detectors. Because of the large crystal and efficient light transmission, the effect of radiation on the PMT is negligible.

The stilbene crystals used in the standard detector show no temperature effects but the anthracene crystals used in the high sensitivity detectors are somewhat temperature dependent. A correction for this effect was anticipated, but study of temperature data taken in the field proved the correction to be negligible.

High sensitivity detectors were used in stations 17 through 25, 27, 116S, 117, 118, 122, 123, and 125 through 129. Standard detectors were used in all other stations.

---

[2] Ibid., p 508.

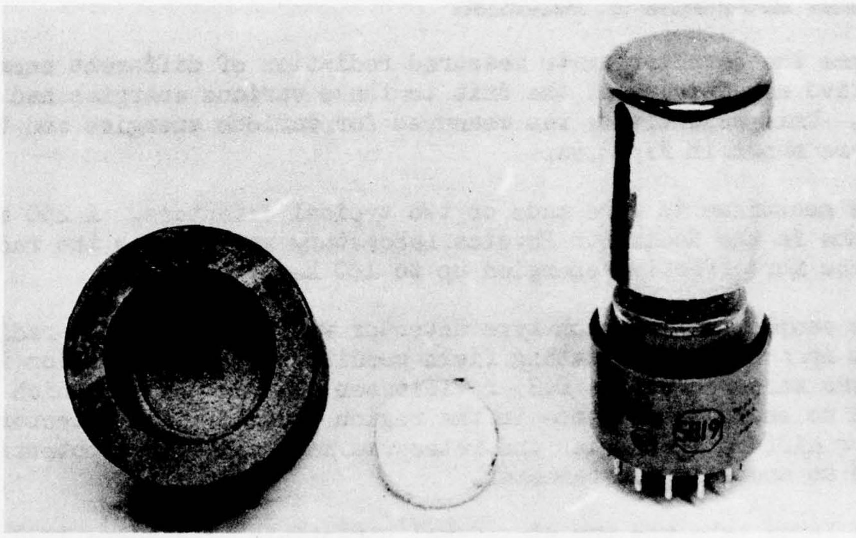

Fig 2.3 High Sensitivity Head, Tube and Crystal

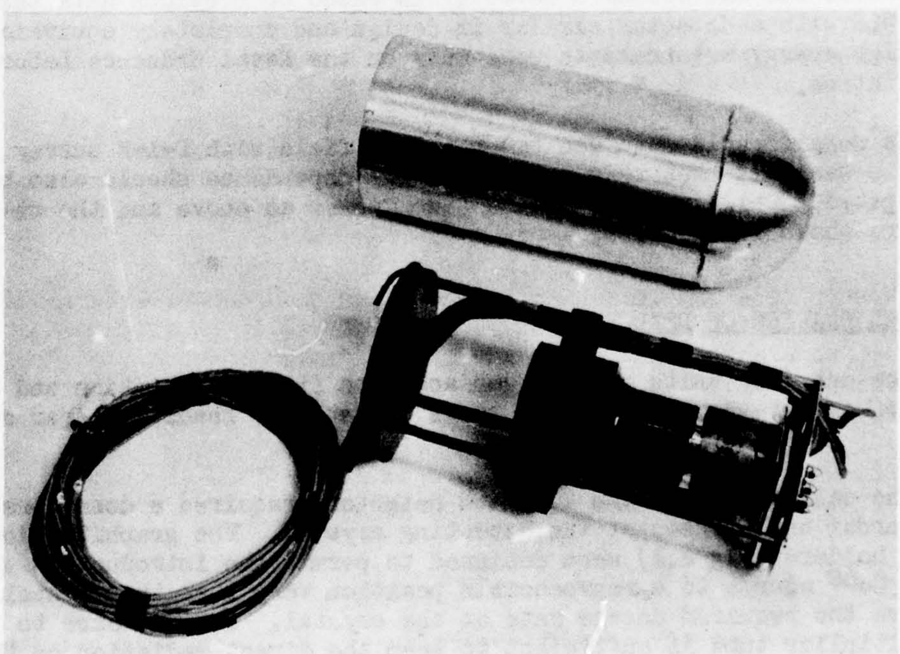

Fig 2.4 High Sensitivity Head

2.3 ENERGY DEPENDENCE OF DETECTORS

Since the detector units measured radiation of different energies, the relative sensitivity of the unit to these various energies had to be known. This sensitivity was measured for various energies and the results are shown in Fig 2.5a.

The measurements were made on two typical detectors. A 250 KV X--ray tube in the Radiation Physics Laboratory was used as the radiation source for effective energies up to 180 kev.

The sample unit of each type detector was mounted in the radiation beam in a manner simulating field conditions. The radiation intensity was measured with a 0.25 r Victoreen thimble chamber which exhibited no energy dependence in the region studied. The detector output for different energies and rates was measured with a potentiometer and an accurate microammeter.

The X-ray tube was run at several potentials with added lead and copper filtration to give desired effective energies. In order to extend the energy range a Co^{60} source (1.2 Mev) was also used. The curves shown were normalized to the Co^{60} energy point. The 3.5 Mev point shown on the curve for the standard detector is based on previous data taken at the NBS with a detector similar in design and completely equivalent. These high energy measurements were made on the Naval Ordnance Laboratory Betatron.

As considerable data was taken in the field with T-1-B survey meters it was felt that this meter's energy dependence should also be investigated. This was done in the same manner as above and the results are shown in Fig 2.5b.

2.4 CALIBRATION OF DETECTORS

The detector units required an accurate field calibration and the method of calibration for the two types of detector heads differed somewhat.

The calibration of the standard detectors required a dosage rate of the order of 10 r/sec at the detecting crystal. The graphite block crystal holders (Fig 2.1) were designed to permit the introduction of a 4 curie Co^{60} source to a reproducible position very near the crystal. This gave the required dosage rate at the crystal. The distance to the photomultiplier tube is sufficient to keep the direct radiation on the tube low enough to be unimportant.

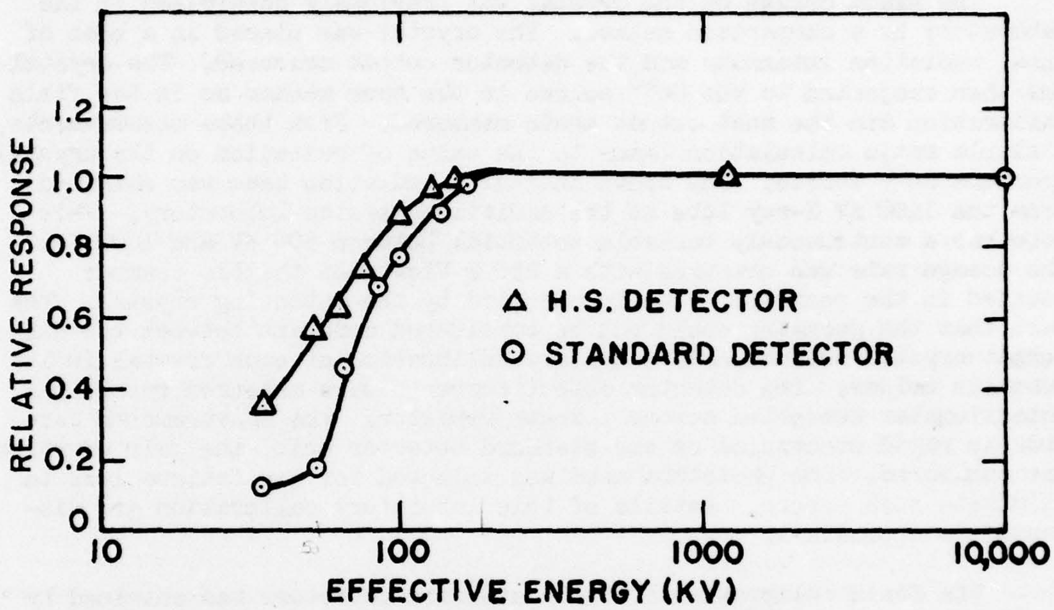

Fig 2.5a Detector Energy Dependence

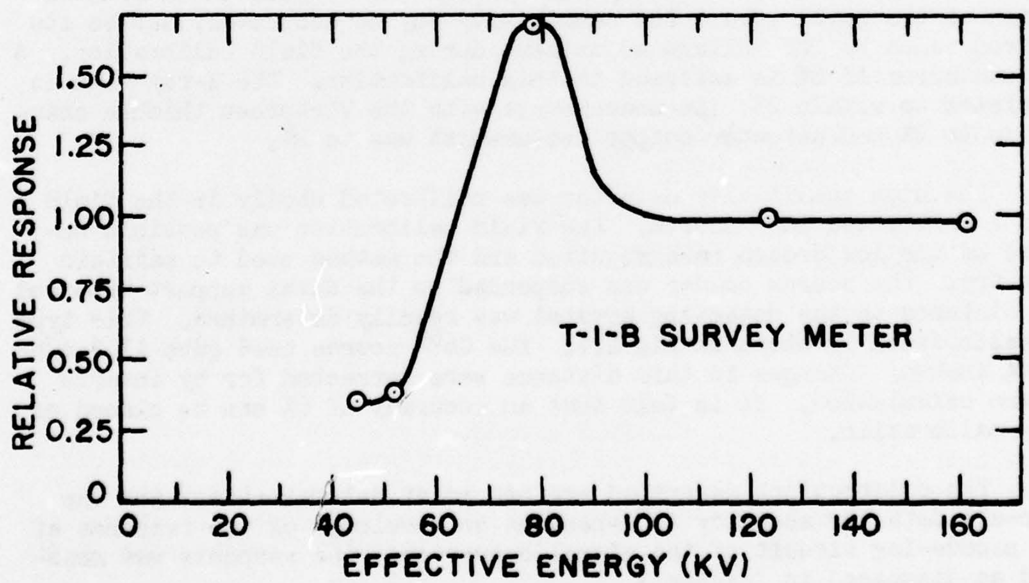

Fig 2.5b T-1-B Survey Meter Energy Dependence

The exact dosage on the crystal was previously determined in the laboratory by a comparison method. The crystal was placed in a beam of known radiation intensity and the detector output measured. The crystal was then subjected to the Co^{60} source in the same manner as in the field calibration and the unit output again measured. From these measurements, a simple ratio calculation leads to the value of radiation on the crystal from the Co^{60} source. The known intensity radiation beam was obtained from the 1400 KV X-ray tube at the Radiation Physics Laboratory. This tube has a continuously variable potential between 500 KV and 1400 KV. The dosage rate was measured with a 250 r Victoreen thimble chamber mounted in the position normally occupied by the detecting crystal. The fact that the geometry could not be considered constant between the different crystal holders made necessary calibration of each crystal in its graphite holder. The detector output currents were measured by using a potentiometer connected across a known resistor. The measurements were made in rapid succession on one standard detector unit, the gain of which was monitored. The phototube used was selected for low fatigue loss to eliminate such errors. Details of this laboratory calibration are discussed in Appendix A.

The field calibration of these standard detectors was obtained by again placing the Co^{60} in the crystal holder and use of the radiation rate for the particular crystal and holder as discussed above. Fig 2.6 shows the Co^{60} source mounted in position for calibration. The source holder is centered above the crystal by means of a steel plate mounted on top of the dural tube. The sensitivity may be accurately set to its desired value by PMT voltage adjustment during the field calibration. A maximum error of 6% is assigned to this calibration. The X-ray beam is regulated to within 2%, its measurement with the Victoreen thimble chamber is to 2% and detector output measurement was to 2%.

The high sensitivity detector was calibrated wholly in the field with a calibrated Co^{60} source. The field calibration was possible because of the low dosage rate required and the method used to maintain geometry. The source holder was suspended on the dural support tube and the distance to the detecting crystal was readily determined. This type of calibration is shown in Fig 2.7. The Co^{60} source used gave 11.3 r/hr at 24 inches. Changes in this distance were corrected for by inverse square calculation. It is felt that an accuracy of 6% can be placed on this calibration.

The calibrations described are one point determinations and the over-all detector accuracy is dependent on knowledge of the response of the pseudo-log circuit of the signal converter. The response was measured as discussed in Chapter 3.

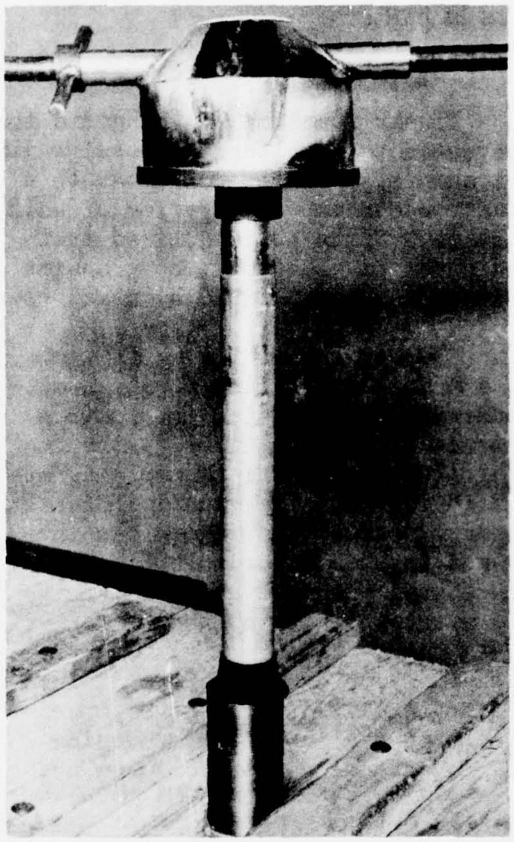

Fig 2.6 Calibration of Standard Detector Head

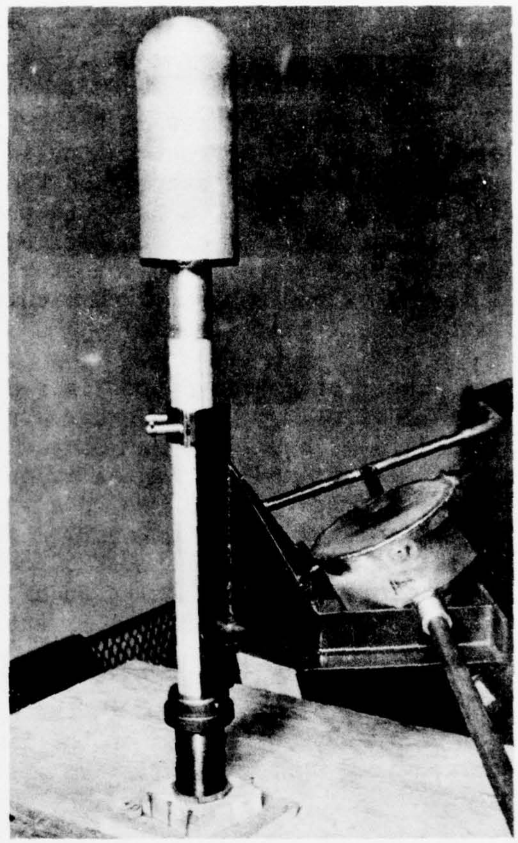

Fig 2.7 Calibration of High Sensitivity Detector Head

[redacted]

CHAPTER 3

TRANSMISSION AND RECORDING

3.1 GENERAL DESCRIPTION

The current output of the PMT is a linear function of the gamma intensity. The PMT current output is converted to a voltage by passing it through suitable resistors, and the voltage is, in turn, converted to a frequency by means of a balanced phantastron circuit, the period of which is a linear function of the applied voltage. Since it is desired that the current range of each detector head cover five decades, compression of the range is necessary. The compression is accomplished by means of a pseudo-logarithmic circuit.

The phantastron output is fed to a transmission line for transmitting the signal to the recorder station. The transmission line output is amplified, equalized and shaped by means of the amplifier at the recorder station and the signal is then applied to a multi-channel magnetic tape recorder as well as to a visual indicator. The visual indicator is a commercial "EPUT" meter.[1] A frequency versus time record can thus be obtained visually on the EPUT meter and is also recorded on the magnetic tape. Proper translation of this signal yields a gamma intensity versus time record. Fig 3.1 is a block diagram of the system.

The pseudo--log circuit and the phantastron circuit are modifications of the circuits used in the NBS Gamma Radiation Project of Operation GREENHOUSE. Because of the limited time available for producing the required units, alternative methods for signal conversion were not explored.

The fact that reasonable variation in line attenuation and other factors effecting the amplitude of the output signal can be tolerated in a frequency modulated system is the main advantage of converting the current signal to a frequency signal.

3.2 PSEUDO-LOG CIRCUIT

The pseudo-log circuit shown in Fig 3.2 converts the five decade current range (0.006 microamperes to 600 microamperes) into a voltage

---

1 Manufactured by Berkeley Scientific Corp., Richmond, California

[redacted]

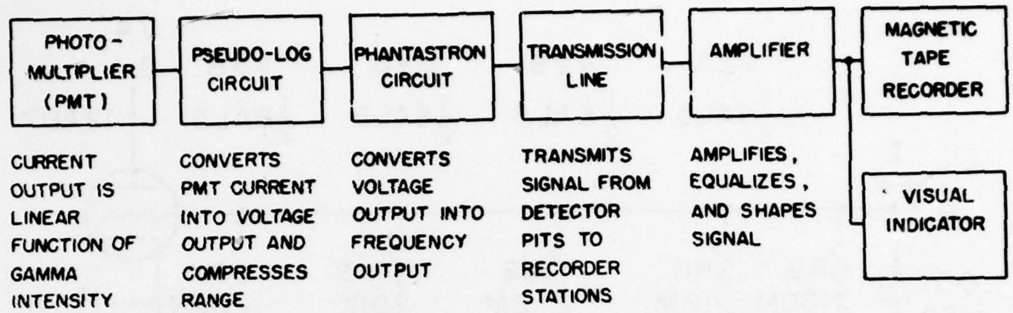

Fig 3.1 Block Diagram of System

of 0 to 26 volts. For an "ideal" diode, the diode resistance is infinite when the voltage applied between plate and cathode is negative, and is zero when the applied voltage is positive. In such a circuit, the current vs voltage characteristic is as shown in Fig 3.3.

At currents between zero and 0.06 microamperes, the current flows entirely through R9.[2] The voltage drop across R9 varies linearly with current, being 6 volts at 0.06 microamperes. As the current exceeds 0.06 microamperes, the drop across R9 exceeds 6 volts and diode V2A begins to conduct. When the voltage across R9 reaches 12 volts, the current through R9 is 0.12 microamperes and the current through R11 is $(12-6)/12 = 0.5$ microamperes. The total current is thus 0.62 microamperes at 12 volts. Similarly, the current is 6.18 microamperes at 18 volts, 59.7 microamperes at 22 1/2 volts and 595 microamperes at 26 volts. The values of the resistors, R11 through R14, have been chosen so as to give this current-voltage relation.

Since practical diodes do not have the infinite and zero resistance characteristics of "ideal" diodes, there is some departure from the ideal curves of Fig 3.3. In addition to the non-linearity introduced by the variation in voltage drop across the diode, there is a shift of the curves along the abcissa since the break (from non-conducting to conducting) in the characteristic of a hot cathode diode occurs when the plate is slightly negative with respect to the cathode. Since the instruments are individually calibrated, a small shift of the curves is of no consequence. A non-linearity could also be tolerated provided sufficient calibration points were taken. However, in the

---

2 The designation of all components has been chosen to agree with the detailed plans listed in Appendix C.

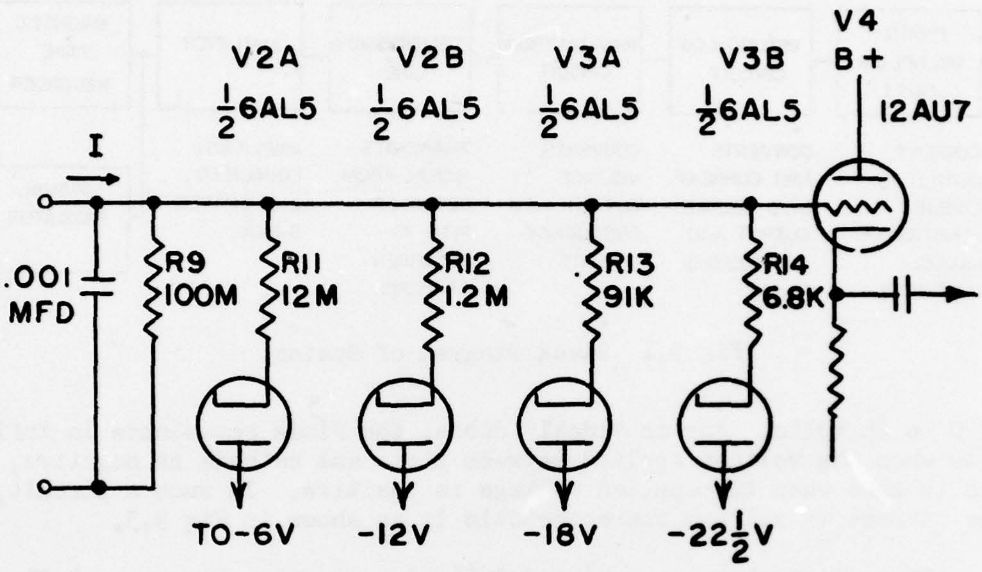

Fig 3.2 Pseudo-Log Circuit

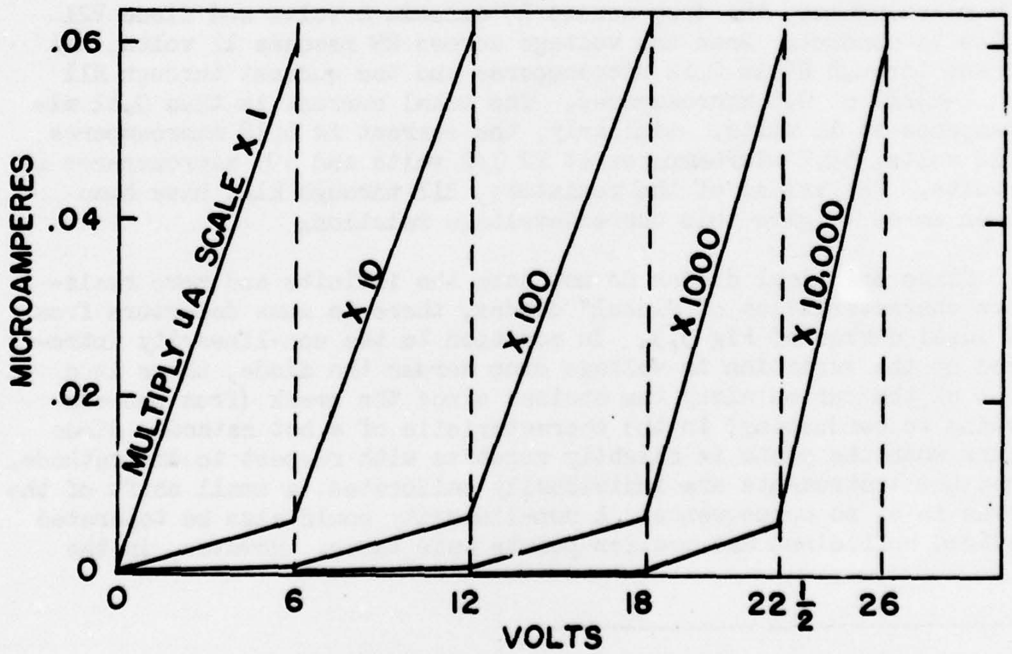

Fig 3.3 Current vs Voltage of Pseudo-Log Circuit of Fig 3.2

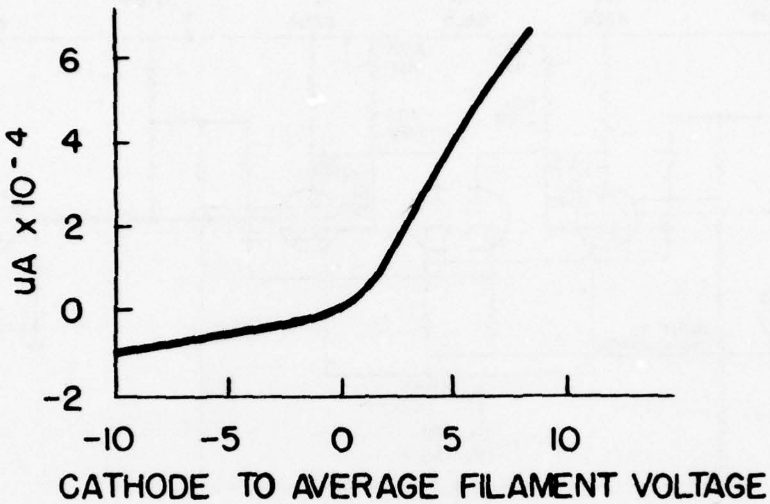

Fig 3.4 Heater to Cathode Leakage Current of a Typical 6AL5 Diode.

interest of reducing the work involved in calibration, linear curves are desirable. Fortunately, the tube drop changes only about 0.2 volts per decade[3] in the region of interest. The maximum departure from linearity is, therefore, about 0.025 volts. Since the first diode is biased, at 6 volts, the maximum departure from linearity is only about 0.4%, which is small enough to be ignored.

The upper current limit of the PMT is dictated by PMT fatigue and was chosen as 600 microamperes. Further reduction in the upper current limit was not considered advisable since it would necessitate a corresponding increase in the value of R9 (Fig 3.2) in order to work the phantastron circuit over a reasonable input voltage range. The maximum value of R9 is limited by leakage currents, principally heater to cathode leakage in the 6AL5 diodes and grid current in the 12AU7 cathode follower (V4). To limit the leakage, the 6AL5s were tested for heater to cathode current and the 12AU7s for grid current and only those tubes with low current were used. Since only aged tubes were used, the measurements were made after the tubes were aged. To still further limit the heater to cathode leakage current, the cathodes were biased 6 volts negative with respect to the negative sides of the filaments by returning the negative filament leads to plus 6 volts. Inspection of Fig 3.4 will show how such biasing is effective. The 6AL5 diodes were operated at reduced heater voltage to give additional reduction in the heater to cathode leakage.

[3] Chance, et al, Waveforms, New York; McGraw Hill (1949), p 61 (Fig 3.28).

UNCLASSIFIED

[redacted]

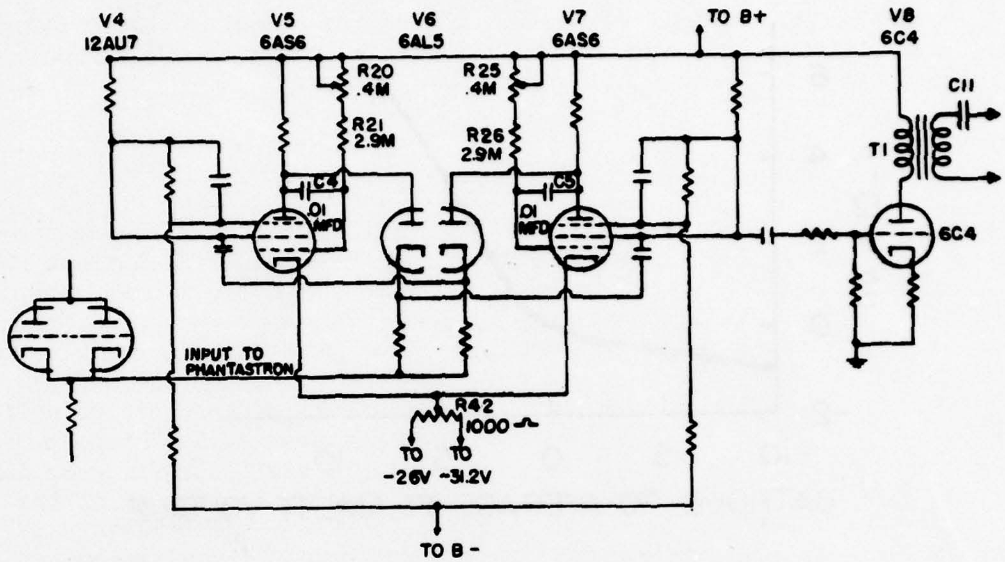

Fig 3.5 Phantastron Circuit

3.3 PHANTASTRON

The output of the pseudo-log circuit is applied to the grid of the cathode follower (V4 or Fig 3.2) and the cathode follower output is applied to the phantastron circuit, Fig 3.5. The cathode voltage of V4 is about 5 volts negative with respect to the grid and maintains this difference as the grid voltage changes. The phantastron circuit used is the balanced double screen coupled type described by Chance.[4] The output is approximately a square wave, the period of which varies linearly with the input voltage.

Adjustment of the phantastron is made by setting R20 and R25 at such values as to give a symmetrical phantastron output of approximately 100 cps with zero voltage on the grid of V4 (Figs 3.2 and 3.5). Then, with -22 1/2 volts on the grid of V4, R42 is adjusted to give 325 cps output frequency. The grid voltage of V4 is then returned to zero and R20 and R25 readjusted to approximately 100 cps. The output frequency for -22 1/2 volts on the grid of V4 is then readjusted to 325 cps, if necessary, by means of R42. By alternately adjusting the zero voltage and the -22 1/2 volt frequencies in this manner, proper adjustment is readily obtained. Since the converters are individually calibrated, precise adjustment is not necessary.

---

4 Ibid., p 199.

[redacted]

UNCLASSIFIED

The phantastron output is coupled to the transmission line by means of V8 and T1. The capacitor C11 serves simply to prevent DC timing signals from going through the transformer winding.

3.4 CALIBRATION OF SIGNAL CONVERTER

A one-point calibration of radiation intensity versus output frequency was made as described in Section 2.4. Since the PMT current output is linear with radiation intensity, complete calibration is obtained by supplementing this calibration point with current versus frequency data for all the decades. Microammeters capable of high accuracy in the low current range required were not available. Therefore the current calibration was taken for each instrument by means of the current calibrator of Fig 3.6 which eliminates the need for a precision microammeter. With S5 on "check", the helipot is set to give a desired reading on the precision voltmeter. Since the circuit resistance, consisting of the precision resistor selected by S6 in series with the microammeter resistance is known to high precision, the current through the microammeter is known accurately. The reading of the microammeter is noted and S5 switched to "read" so that the current flows through the signal converter. The helipot setting is then changed so as to reproduce the microammeter reading that was noted when S5 was on "check", and the corresponding output frequency noted. Thus, the absolute accuracy of the microammeter is of no importance since it is used only for comparison. The short time reproducibility of the microammeter is of importance and was found to be adequate.

The current versus frequency data was converted to current versus period (period = 1/f) and plotted. The current corresponding to the output frequency obtained for the radiation intensity calibration was noted and this figure used in determining the calibration constant, K, relating the radiation intensity to PMT current. All frequency data was converted to radiation intensity data by means of the curves and the calibration constants. Changes in the calibration constant were determined by periodic light calibrations as described below and in Section 2.1.

Decade voltage calibrations were also made for one point in each decade. Known voltages (4.5V, 10.5V, 16.5V, 21V and 24V) were applied to the grid of V4 (Figs 3.2 and 3.5). The output frequencies corresponding to these voltages were determined in the pre-shot calibrations. These calibrations were also applied automatically for approximately 3 seconds each, beginning 37 seconds before zero time and were also applied manually after the burst.

Light calibration that involved turning on a light so as to illuminate the PMT was also applied. Laboratory tests showed light output of the calibration light to be consistant within about 3%. Accordingly,

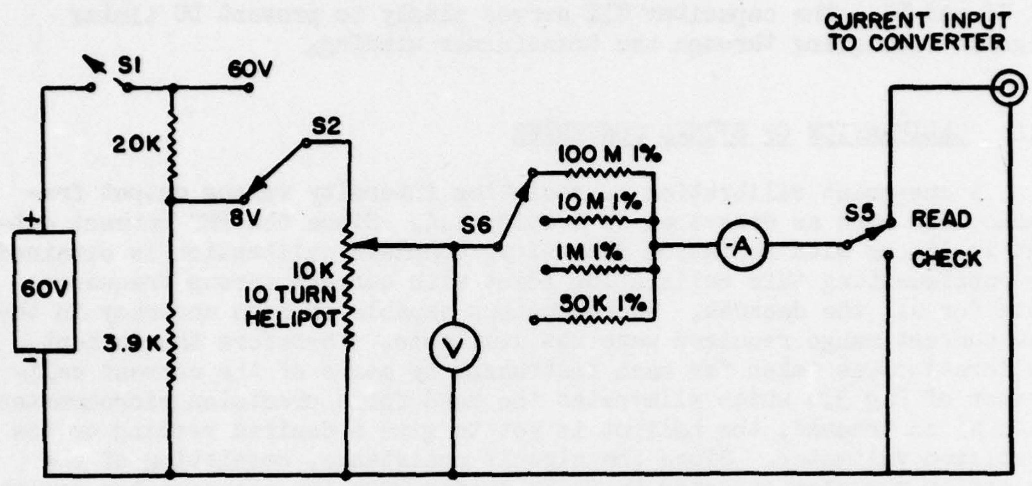

V IS A PRECISION VOLTMETER ($\frac{1}{4}$% FS)
WITH FULL SCALE RANGES OF 7.5V, 30V, & 75V

A IS RCA ULTRA SENSITIVE MICROAMMETER
TYPE WV-84A

Fig 3.6 Current Calibrator

small changes in calibration light output were attributed to changes in PMT sensitivity and proper correction factors applied to the data. In those instances where large changes in calibration light signal output were obtained, the data was considered suspect and was critically analyzed to determine whether the calibration light could be relied upon. This was determined by noting the consistency of the readings, by comparison of the dose rate readings with those of other instruments in the same location, and by observation of the general pattern of dose rate versus time and distance. Questionable data that could not be resolved was discarded. The light calibration was applied automatically for approximately 6 seconds beginning approximately 22 seconds before zero time. An 11 to 12 second light calibration was also applied automatically at about plus 10 minutes and 2 to 3 minute light calibrations were automatically applied at plus 12 hours, 24 hours, and 36 hours. Additional light calibrations were remotely introduced by the recorder station operator periodically after zero time. These calibrations were introduced as often as desired and for any desired time interval.

A 26 position stepping relay (hereafter referred to as the "stepper") was used to apply the calibrating signals. The stepper operated automatically from steps 1 to 9 at the rate of one step every 3 seconds by means

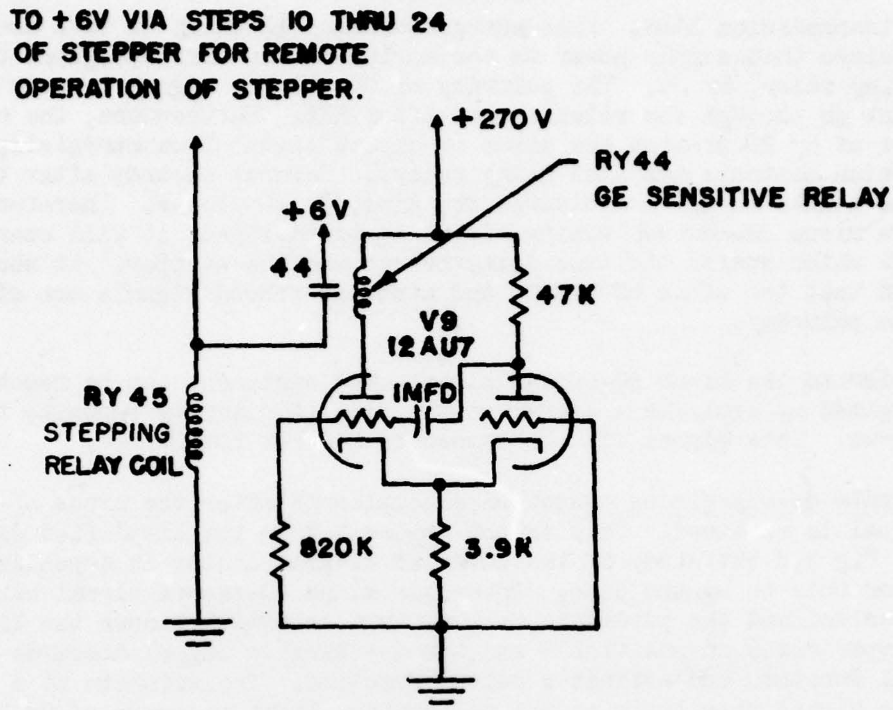

Fig 3.7 Circuit for Operating Stepping Relay

of the multivibrator circuit of Fig 3.7. At the end of 48 hours a timing motor caused the stepper to move from step 9 to step 10. Operation over the remaining steps was remotely controlled from the recorder station.

3.5 TIMING

Two timing signals, each of 2 to 3 seconds duration, were transmitted from the recorder station to each signal converter by means of the transmission line that was used to transmit the radiation intensity data to the recorder station. The first signal was received at minus one hour and served to energize the equipment. The one hour period was adequate for the equipment to attain thermal equilibrium and provide a background reading of sufficient duration. The second signal arrived at minus 40 seconds and served to start timers in the converter unit and to initiate calibration signals.

The transmission line used for transmission of data was also used for all timing signals and all calibration signals. The manner in which this was done will be explained with reference to the simplified relay diagram, Fig 3.8. The minus 60-minute signal is applied with the polarity indicated

on the transmission line. This energizes Relay 11 which in turn energizes relays that supply power to the equipment and also energizes the time delay relay, Ry 20. The polarity of the timing signal is such that it cannot go through the selenium rectifier RX2. Furthermore, the open contacts of Ry 20 prevent the minus 60-minute signal from energizing Ry 22 which controls the time delay relays. Several seconds after the minus 60-minute signal has cleared the line, Ry 20 closes. Therefore, when the minus 40-second timing signal is transmitted, it will energize Relay 22 which starts the time delay relays and the stepper. It should be noted that the minus 60-minute and minus 40-second signals are of the same polarity.

Prior to the minus 40-second signal, the equipment can be remotely de-energized by applying a signal to the line of polarity opposite to that shown. This signal will be passed by RX2 but not by RX1.

Remote de-energizing cannot be accomplished after the minus 40-second signal is received. This is not apparent from the simplified diagram of Fig 3.8 but study of the detailed diagram listed in Appendix C will show this to be the case. After the minus 40-second signal has been received and the automatic calibrations transmitted down the line, the stepper rests on position 9 and the de-energize signal discards its original function and assumes a second function. Transmission of a de-energize signal then turns on the calibration light by means of Ry 33 (Fig 3.8). Transmission of an energize signal turns off the calibration light. The energize and de--energize signals assume these new functions only when the stepper is on step 9, which is its normal resting position during the run. This means that during the run the light calibration is completely under the control of the recorder station operator.

At the end of 48 hours, the 48 hour timer causes the stepper to move to step 10 where the de-energize signal discards its second function and assumes a third function, which it retains for the remaining positions of the stepper. After the stepper has reached step 10, a de--energize signal moves the steppper one position; a second de-energize signal moves it another position; and so on. Thus, the operator at the recorder station is able to advance the steppers and introduce for any desired duration various decade voltage calibration signals as well as light calibration signals. As the recorder station operator remotely advances the stepper to step 26, the stepper returns to the homing position, step 1, and the batteries are disconnected from the equipment.

3.6 CONSTRUCTION OF SIGNAL CONVERTERS

The completed Signal Converters are shown in Figs 3.9, 3.10 and 3.11. Because of the difficulty in procuring components and because of

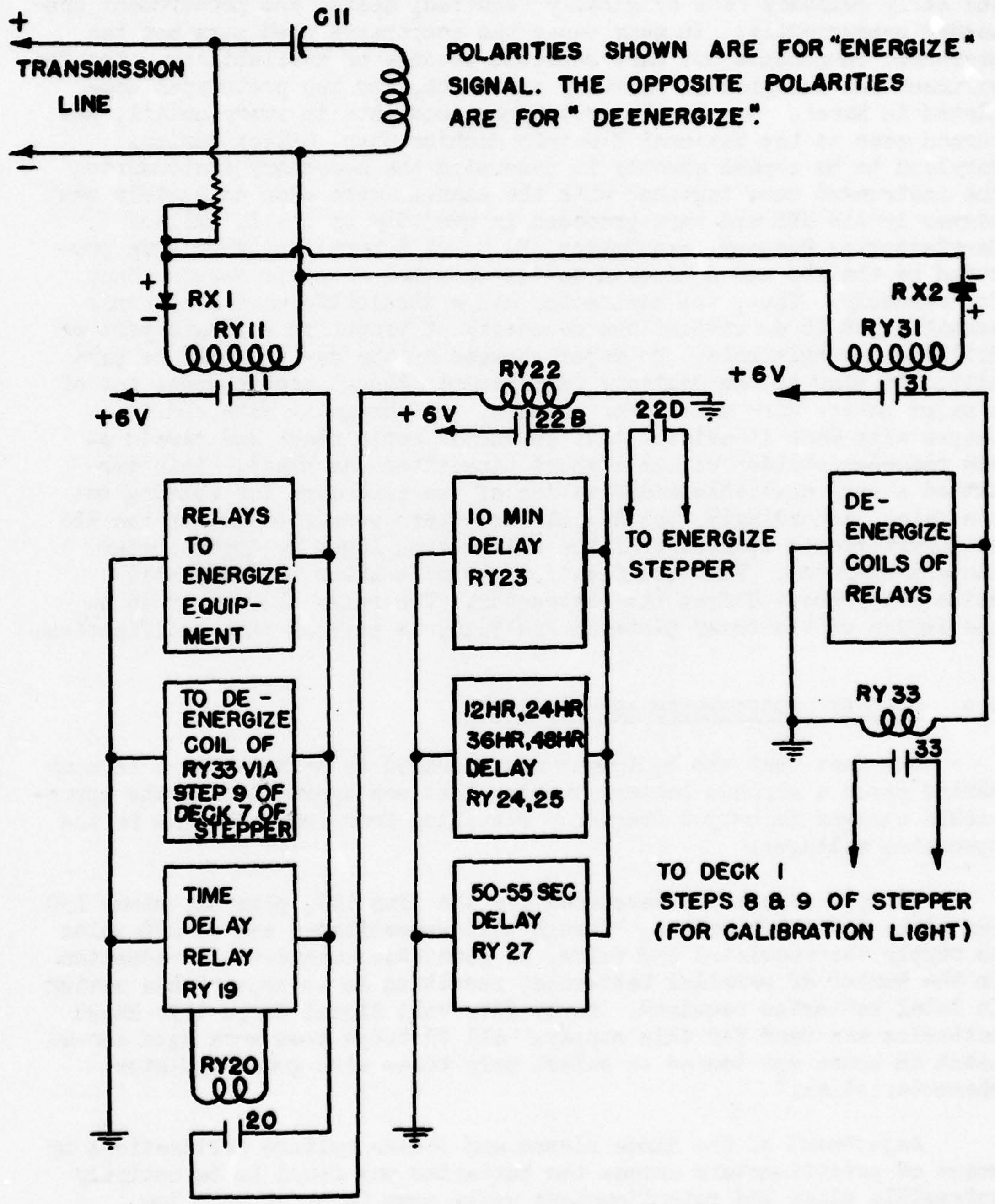

Fig 3.8 Simplified Relay Diagram

the early delivery date originally required, design and procurement proceeded concurrently. In many cases the components used were not the preferred components but were selected because of availability. The instrument was designed in February and March, and two prototypes completed in March. One of the prototypes, complete in every detail, was turned over to the National Electric Machine Shop, Silver Spring, Maryland to be copied exactly in producing the necessary instruments. The instrument case together with the chassis were also completely designed by the NBS and were produced in quantity by the D. Ballauf Manufacturing Company, Washington, D. C. All parts required were procured by the NBS and delivered to the National Electric Machine Shop for assembly. Thus, the contractor had a straightforward electronic assembly job to do without the necessity of procuring a single part or drilling a single hole. No major changes in the design could be permitted in view of the delivery requirements though some changes not of a major nature were made. For example, the change in site and in weapon size made it evident that personnel could reach and remain at the recorder station within a short time after the blast. This permitted a very desirable modification of the procedure for reading out the data. Accordingly, the Signal Converters were modified by the NBS to permit remote operation of the calibration light by the recorder station operator. This modification was made after the completed units were received from the contractor. The relay shown mounted on the inside of the cover plate in Fig 3.10, is part of this modification.

3.7 BATTERY REQUIREMENTS AND STABILITY

The fact that the equipment was required to operate for a 48 hour period posed a serious battery problem that was aggravated by the appreciable changes in output frequency resulting from small changes in the operating voltages.

VR type regulators were used for the plus 150, plus 90, minus 150 and minus 90 volt supplies. Though this necessitated use of 270 volts to supply the regulated 150 volts, it permitted considerable reduction in the number of parallel batteries, resulting in an appreciable saving in total batteries required. Forty-five volt Signal Corps type BA-26 batteries are used for this supply. All VR tubes used were aged for at least 48 hours and tested to select only tubes with good regulator characteristics.[5]

Adjustment of the diode biases and decade voltage calibrations by means of potentiometers across the batteries was found to be entirely unfeasible since the potentiometers would have to be of such low

[5] O. B. Rudolph, RSI, 21, 497 (1950)

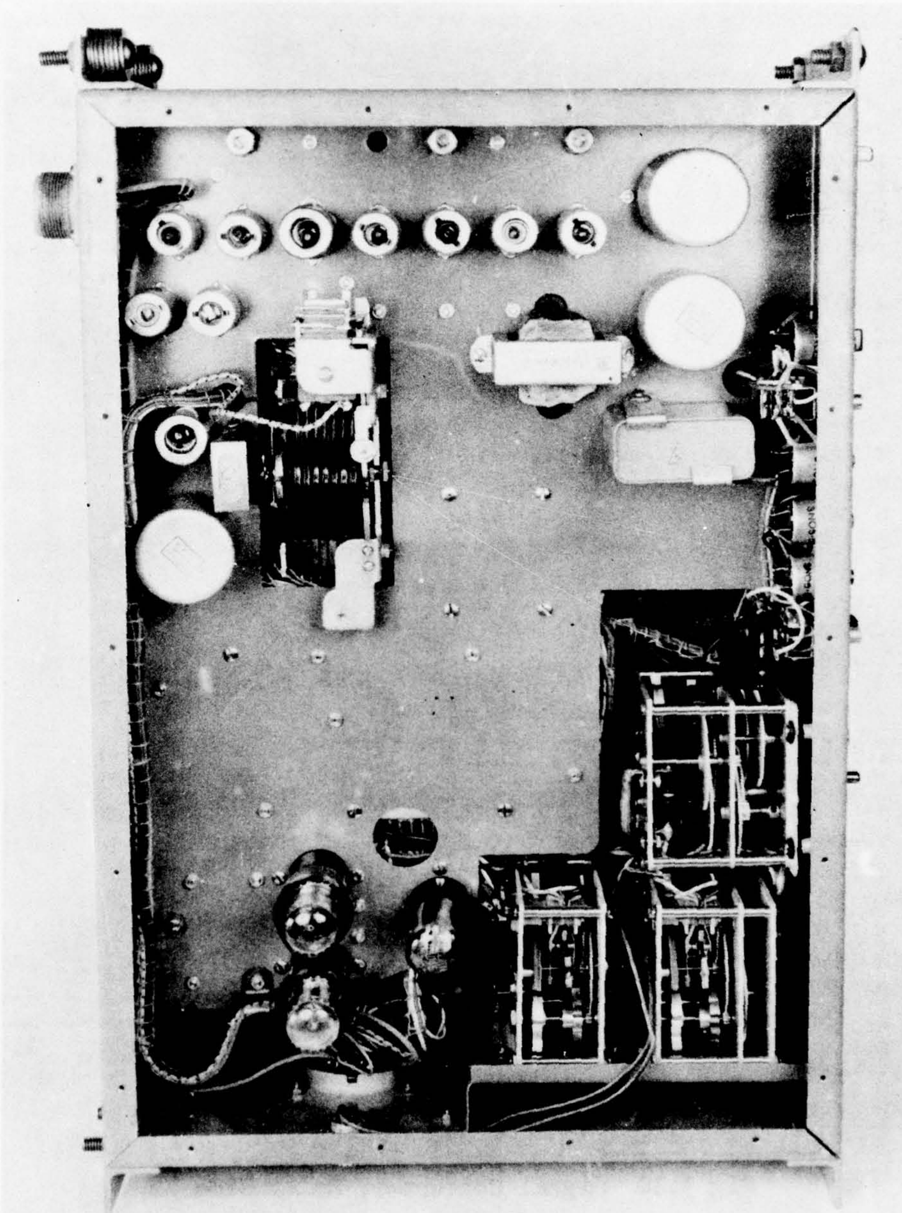

Fig 3.9 Signal Converter, Tube Side

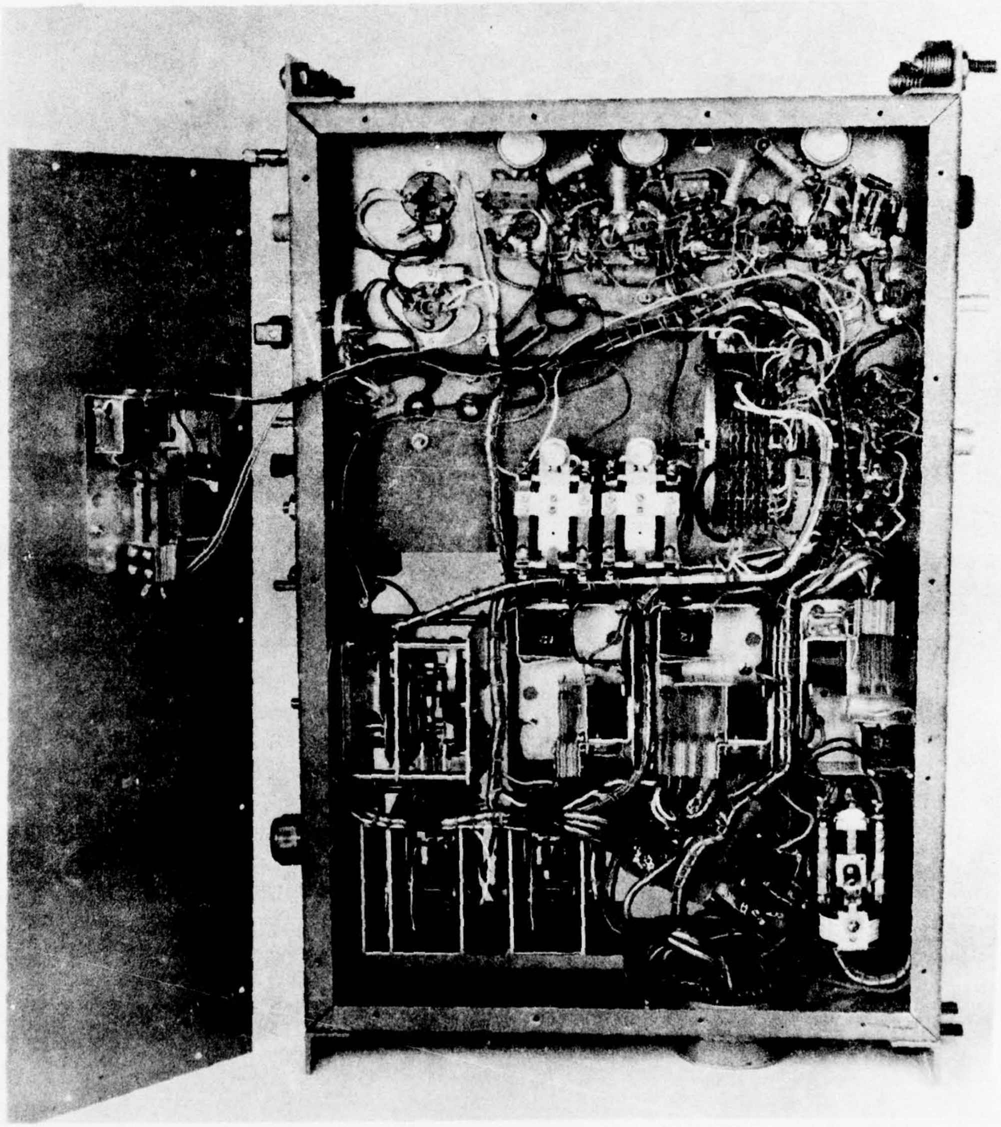

Fig 3.10 Signal Converter, Relay Side

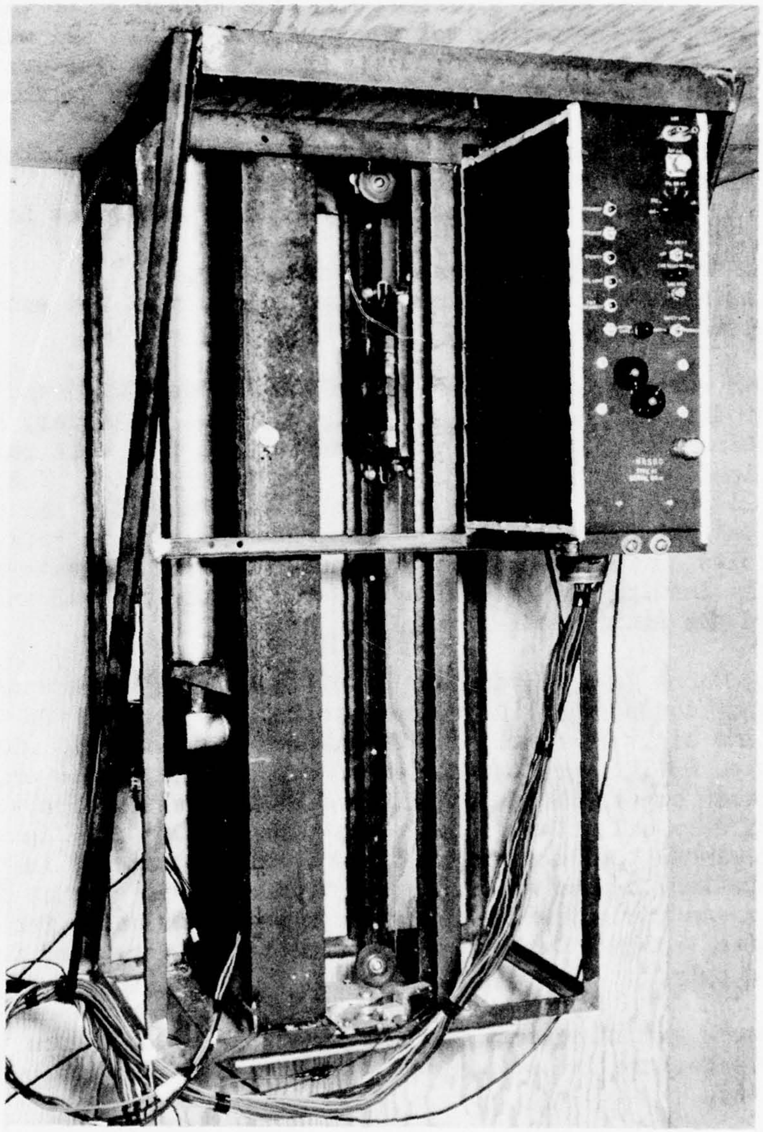

Fig 3.11 Signal Converter Mounted in Mock Up Pit

resistance that the battery requirements would be prohibitive. Accordingly, the voltages utilized were those obtainable directly from 1 1/2 volt batteries, Signal Corps type BA-15A. This accounts for the fact that the diode biases and the decade voltage calibrations are all multiples of 1.5 volts. Small deviations from the specified voltages are of no consequence since the signal converters are individually calibrated.

Selection of the battery supply for the phantastron cathodes presented particular difficulty because of the following:

(a) The output frequency is very sensitive to changes in this voltage.
(b) An adjusting potentiometer is necessary.
(c) The adjusting potentiometer resistance must not exceed about 1000 ohms.

Special mercury cell batteries, Mallory types 302204 and 302205 were used for this purpose. Two of the type 302204 batteries, each consisting of 16 mercury cells (1.3 volts each) in series, were paralleled and the combination placed in series with one type 302205. The latter consists of 16 cells arranged in two parallel strings of 8 cells in series with taps at every 2.6 volts. The potentiometer is bridged across 5.2 volts on the tapped battery thus providing adequate adjustment without unduly loading the batteries as would be the case if the potentiometer bridged the entire battery string.

Signal Corps BA-44 batteries (6 volt hot-shots) were used for supplying power to energize the relays, to run the timers, and to supply the calibration light current. Two 220-ampere hour six volt storage batteries (type BB-57) were paralleled to supply filament power. Resistors were placed across the diode bias and decade calibration voltage string across the mercury cell string, and across the calibration light batteries to eliminate the "sleeping voltage" peak that occurs in the early part of the battery discharge. To prevent undesirable circuit interactions, separate ground returns were found to be advisable for several of the circuits. Signal Corps type BA-26 batteries were used for the PMT voltage supply.

To assure good frequency stability as well as to reduce the probability of tube failure in service, all tubes used in the equipment were aged and tested.

3.8 MASTER CONTROL BOARD

Timing signals (see Section 3.5) were transmitted to the Signal Converters by means of the Master Control Board shown in Fig 3.12.

At minus one hour a pair of floating contacts supplied by the Edgerton, Germeshausen and Grier Company were closed and remained

closed until approximately plus one second. Closure of the minus one hour contacts energized relays in the master control board, thus starting the recorder motor, energizing the amplifier filaments (Section 3.9), and closing the relays in the amplifier chassis thus placing 90 volts DC across the transmission line. The 90 volts constitutes the timing signal that energizes the signal converters and the PMTs.

The minus 60-second signal was similar to the minus one hour signal. By means of a 20 second time delay relay, the minus 40-second timing signal was derived from this signal and was sent down the transmission lines to start the converter timers and initiate calibration signals as described in Section 3.5.

Since many detectors were dependent on each Master Control Board, it was essential that the Master Control Boards be so designed as to reduce to a minimum the probability of malfunctioning. For this reason, two independent relays were paralleled in all places in the Master Control Board where closure is essential. Similarly, where the circuit must not fail to open after a few seconds, the contacts of two independent relays were connected in series.

3.9 TRANSMISSION, AMPLIFICATION AND RECORDING

The data from the Signal Converters was transmitted to the recording station by means of twisted pair wire, Signal Corps type WD-1/TT. Though this is nominal 600 ohm line for audio frequencies, the impedance varies considerably with frequency and is quite different for the wet and dry conditions. Since the line lengths did not exceed 8 or 9 miles and since the maximum frequency transmitted was less than 500 cps, the termination impedance was not critical, any reasonable termination being satisfactory. As stated in Section 3.5, the transmission lines carried the timing signals and the calibration signals as well as the radiation intensity data.

Because of the attenuation characteristics of the line, equalization and amplification of the signal was necessary at the recording station. The equalization and amplification was accomplished by means of the amplifier circuit of Fig 3.13.

Unit controls for energizing and de-energizing the signal converters individually were included in the amplifier chassis.

Four amplifiers and unit controls for four converters were mounted on a single chassis as shown in Fig 3.14. To permit rapid construction of the units, all parts were mounted on a panel and the panel mounted on a chassis. Six assemblies were then mounted in a standard relay rack.

UNCLASSIFIED

[redacted]

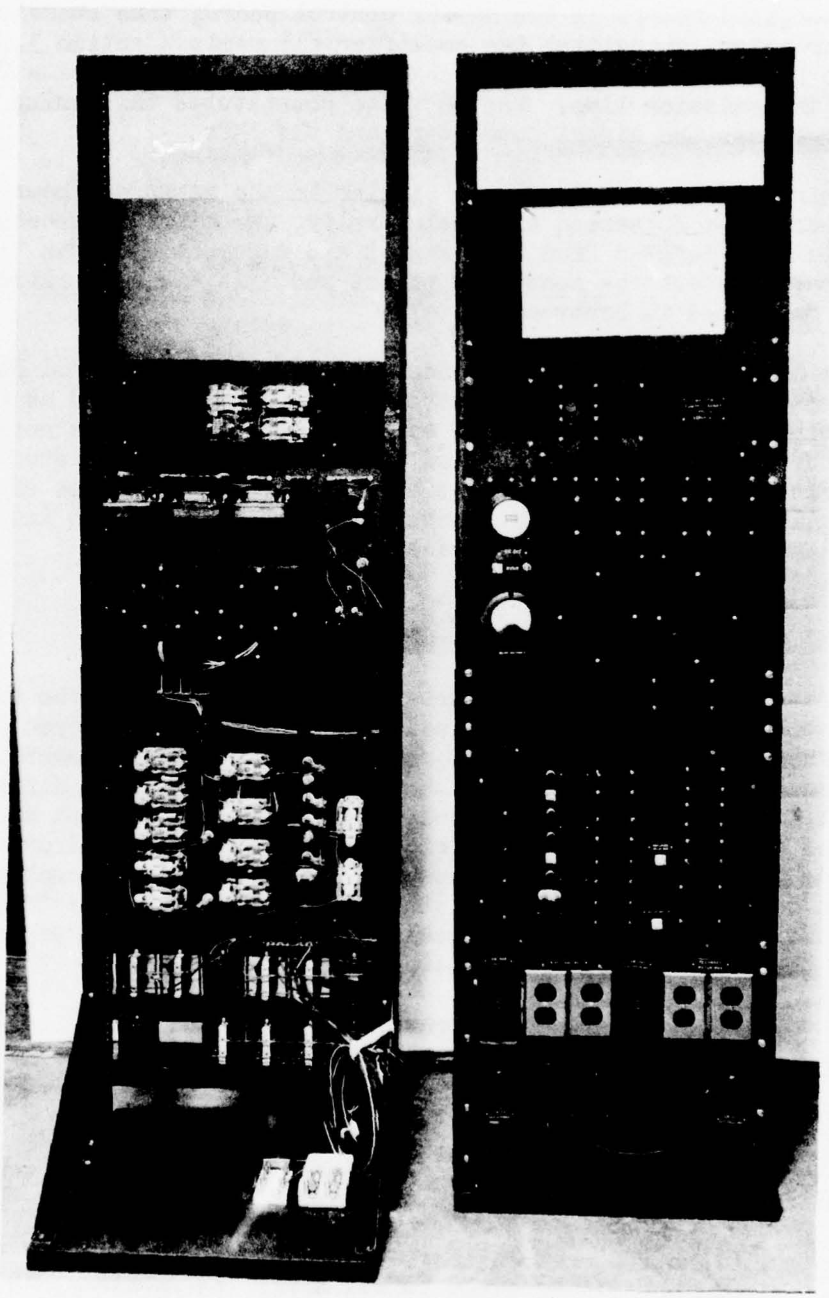

Fig 3.12 Master Control Board

[redacted] [redacted]

UNCLASSIFIED

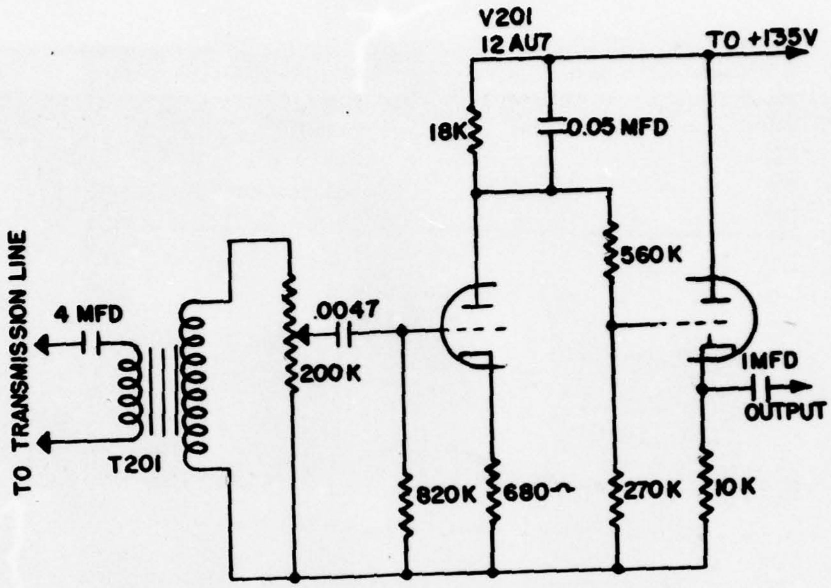

Fig 3.13 Amplifier Circuit

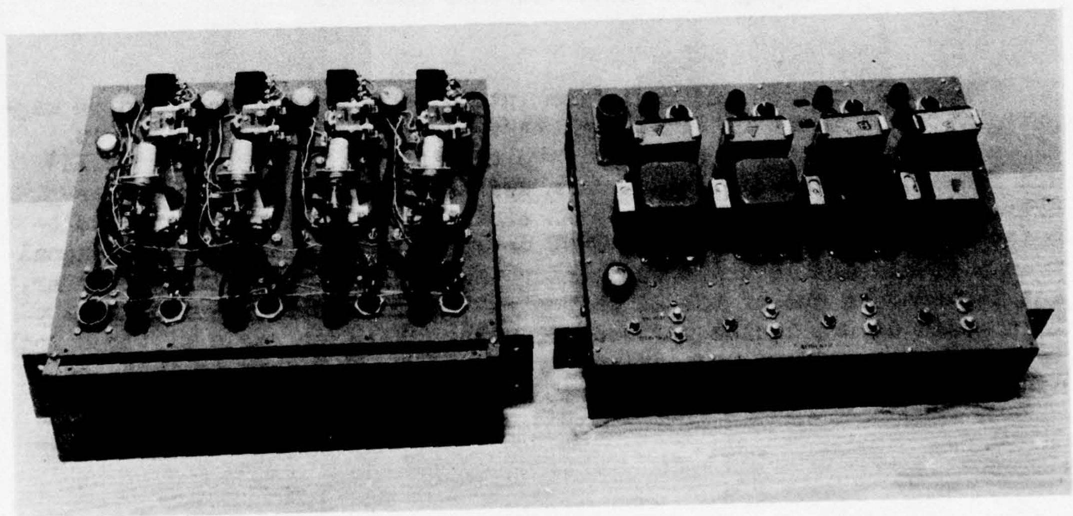

Fig 3.14 Amplifiers

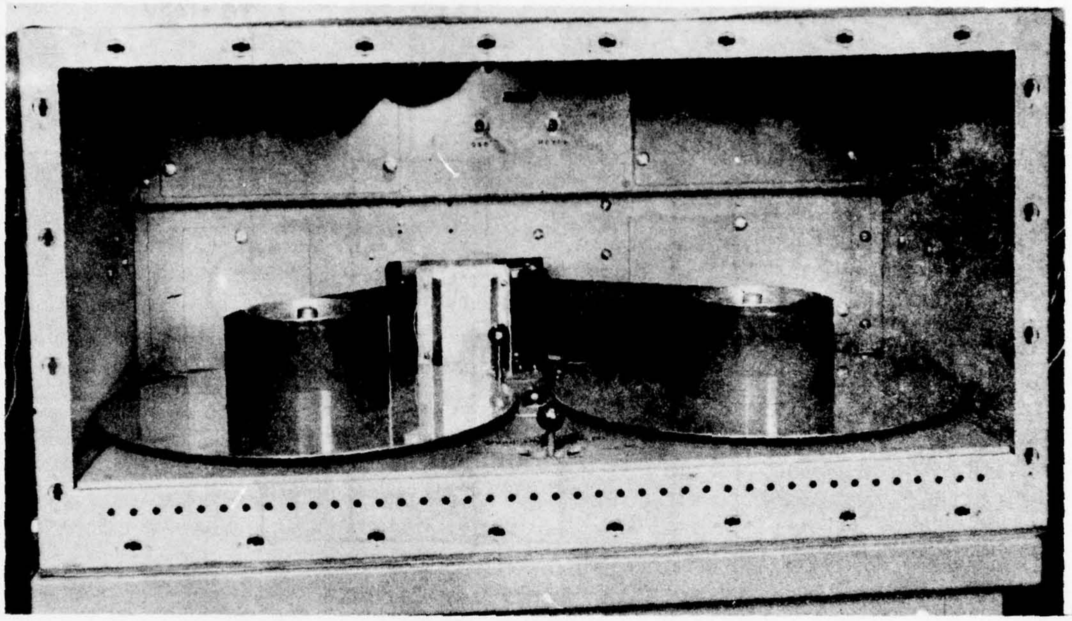

Fig 3.15 Magnetic Tape Recorder

The calibration and radiation intensity data were recorded on magnetic tapes by means of 24 channel tape recorders,[6] one of which is shown in Fig 3.15. The output of the amplifiers (Figs 3.13 and 3.14) was fed to the recorder heads via a switch box. The switch box permitted connecting any channel to an oscilloscope and vacuum tube voltmeter as well as to a Berkeley EPUT meter.[1] A 500 cps reference signal from a stable and accurate oscillator that was built into the recorder, was recorded on one of the 24 channels. The recording was made at a tape speed of 0.4 inches per second, using 6000 foot reels of three inch tape.[7] The recorders were driven by governed a-c motors so that the tape speed was essentially independent of power frequency.

---

6 Manufactured by Shoup Engineering Co., Chicago, Ill.

7 Manufactured by Minnesota Mining Co., Minneapolis, Minn.

3.10 READOUT OF DATA

The data was read out by two methods; visual readout at the time of occurrence and tape readout.

Visual readout at time of occurrence was used as the data came over the line. It can be used only when a resolution of not less than five minutes is adequate. If the operator concentrates on reading out only a few stations, resolutions of the order of a few seconds can be obtained. In general, visual readout data was used after the first ten minutes.

Visual readout was accomplished by means of Berkeley EPUT meters which count the cycles in a given time interval (one second or 10 seconds, as desired), display the result for a desired time intervals (up to 5 seconds), and automatically continue this cycle of operation. The accuracy of the EPUT meter, as used in this application, is plus or minus one cycle. By using three instruments, the operators could scan all the stations on each burst within five minutes. Each operator concentrated on a single station for the first five minutes thus obtaining good visual data on three stations after plus 10 seconds. The frequency data was converted to period (1/f). Then, by use of the calibration curves, the calibration constants and the calibration data received during the run (see Section 3.4), the radiation intensity data was plotted. Thus the desired radiation intensity data was available in the desired form shortly after it occurred. This is an important advantage of the visual readout. Other important advantages are that the data is obtained even if a recorder should fail after the first ten minutes, and also there is a considerable saving in total time and manpower over that required for readout from the tape recordings. It should be noted that the operator had complete control of the light calibrations in that he could put them in remotely from the recorder station at any time, for any desired time interval and as often as desired. This fact has already been pointed out in Section 3.4 but is of sufficient importance to be mentioned again.

Tape readout can be done at any time after the recording, since all of the radiation intensity data and the calibrations are permanently recorded on the magnetic tape. In case of obvious errors in the visual readout, the visual data can be checked against the tape data. In general, tape readout was used only where visual readout could not be used. Tape readout was used to obtain the pre-burst calibration data (minus 37 to minus 16 seconds) and the radiation intensity data for the first ten minutes. The playback console[6] used for tape readout is shown in Fig 3.16.

The signal data between plus 5 seconds and 10 minutes and the preburst calibrations were obtained by direct tape readout. This was accomplished by playing back the original or re-recorded tape in the

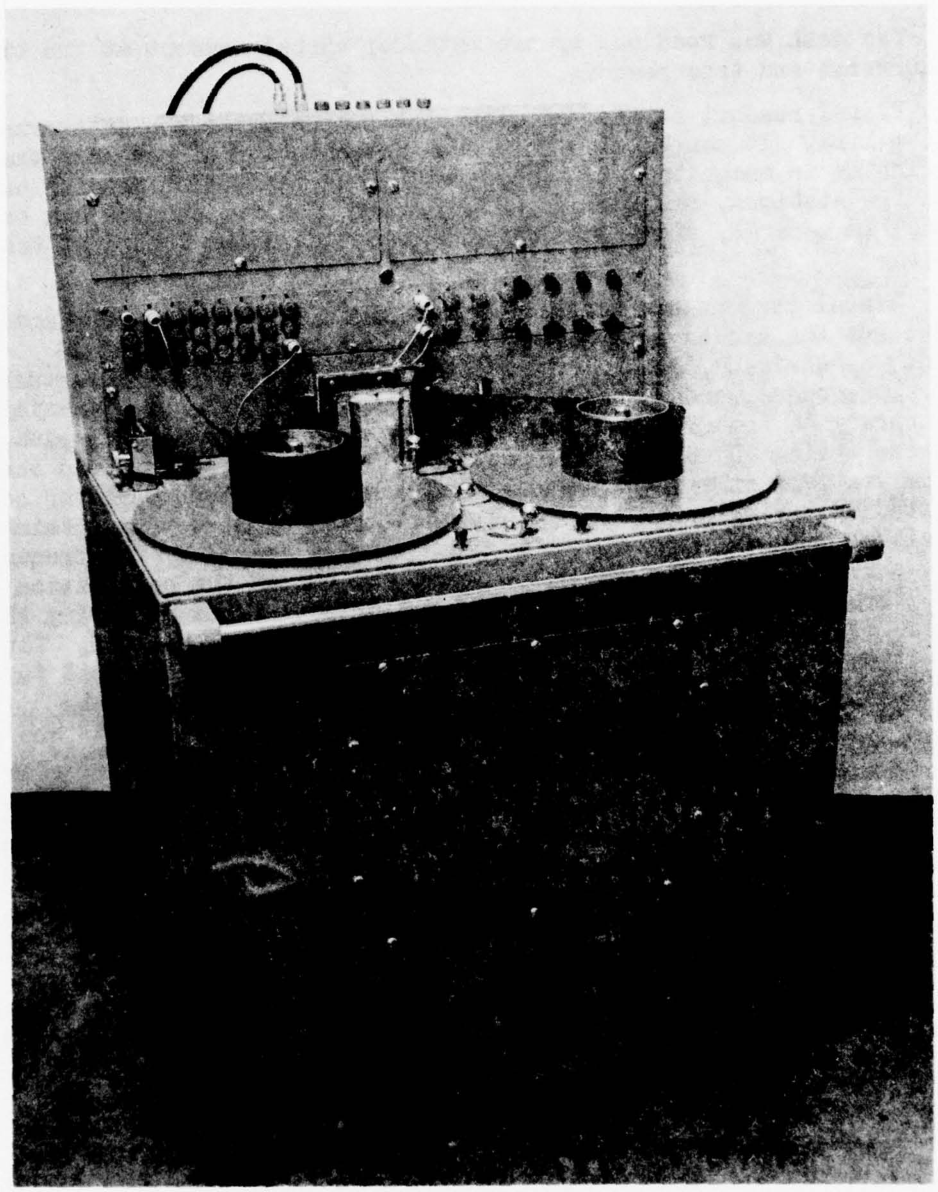

Fig 3.16 Magnetic Tape Playback Console

playback console and feeding the playback signal to an EPUT meter, the visual display of which was noted and recorded by the operator. Since there was variation in the speed of the playback unit, the EPUT meter was slightly modified to use the recorded 500 cps reference signal as a time base in place of the crystal oscillator in the EPUT meter. Because of the use of the reference oscillator in this manner, variations in the recording speed and readback speed and stretching or shrinking of the tape could not affect the accuracy of the data. Fig 3.17 is a block diagram of the readout system used without re-recording and Fig 3.19 is a diagram of the system used with re-recording. The scaler was a conventional Higinbotham type diode coupled scaler.[8] Fig 3.18 is a circuit diagram of the univibrator type pulse shaper used. The 500 cps reference signal was fed to a scaler, the output of which triggered the gate circuit of the EPUT meter. Thus, when a scale of 512 was selected, the gate duration was 512/500 seconds in terms of recording time. The signal frequency was calculated as the EPUT reading times 500 cps divided by the scaling factor. Since the counting interval and the display interval of the EPUT were of equal duration, the tabulated readings provided their own time base.

In most instances re-recording was used since this slowed down the tape by a factor of two thus permitting readout of the data with considerably less difficulty on the part of the operator. This slowdown was accomplished by re-recording at a speed of 8 inches per second and playing back the re-recording at 4 inches per second. As mentioned earlier the original recording was made at a speed of 0.4 inches per second. The re-recorder unit[6] is a console similar in appearance to the playback console of Fig 3.16. The playback speed of 4 inches per second was chosen in order to expedite readout of the data and also because the output data signal at that speed was much more satisfactory than at 0.4 inches per second for feeding the electronic equipment.

From zero time to about plus 5 seconds, resolution of the order of a tenth of a second was desired. The playback was indirectly slowed down by a factor of 20 by playing back at a speed of 0.4 inches per second the re-recordings mentioned earlier. The data originally recorded in 0.1 second was thus played back in two seconds. As shown in Fig 3.20, the re-recorded data signal was applied directly from the playback unit to one channel of a double channel Brush Oscillograph[9] via a current limiting resistor. The reference signal was applied to a scaler, the output of which was applied to the second channel of the oscillograph. For the first 0.5 seconds of signal data the reference was applied directly to the oscillograph without going through the

---

[8] W. A. Higinbotham, RSI 18, 706 (1947).

[9] Manufactured by Brush Development Co., Cleveland, Ohio.

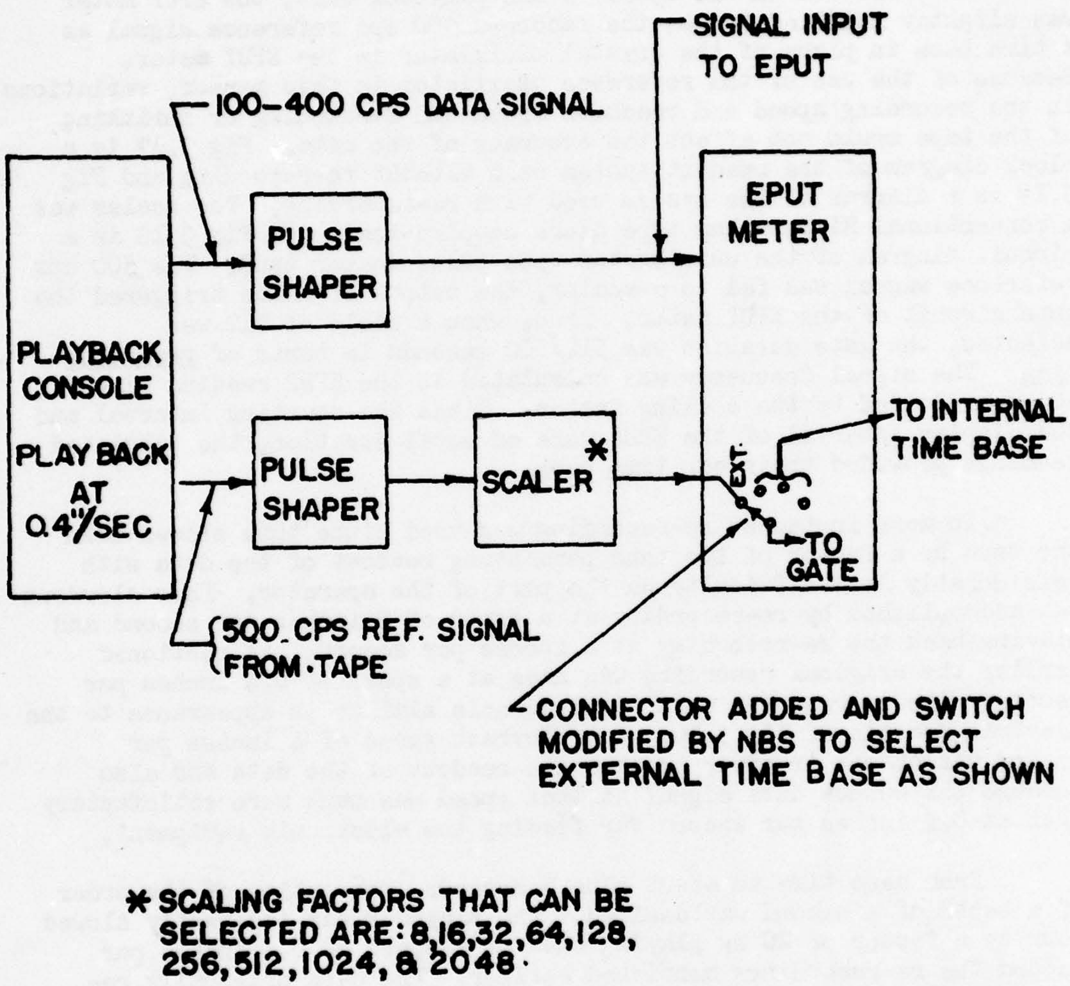

Fig 3.17 Block Diagram of Direct Tape Readout without Re-recording

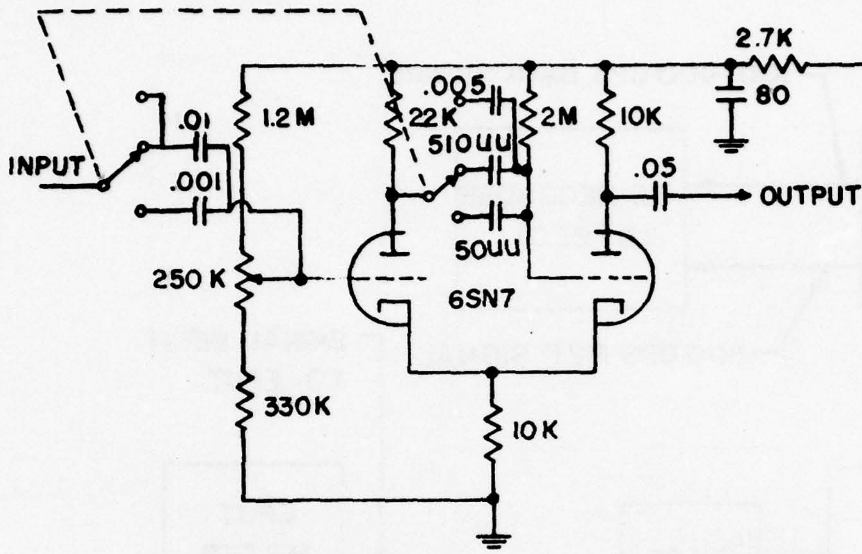

Fig 3.18 Pulse Shaper of Figs 3.17, 3.19 and 3.20

scaler. Thus, direct comparison of the data and reference cycles was possible to high accuracy. The high readout accuracy possible cannot be utilized at 0.1 second resolution because of an accuracy limitation that was encountered. It was found that results obtained for a constant frequency signal varied by several percent in one-tenth second intervals but averaged out over a second. The reason for this was found to be that the horizontal stretch of the tape was not uniform along a vertical line. At the tape speed of 0.4 inch per second, a tape stretch in one channel of one mil with respect to the reference channel results in an error of 2 1/2 percent in a one-tenth second interval. The variation was reduced considerably by shifting the reference signal from the bottom of the tape (channel 24) to a channel near the center (channel 13). However, variations up to 3 percent (average about 1.8 percent) were still obtained for one-tenth second intervals. The variations were, of course, much less, for 0.2 and 0.3 second intervals. Since the bottom channel was particularly bad, its use was abandoned. The tape stretch consideration effects only the data in the first few seconds. Since the error factor (Fig 3.21) is smallest at the high frequencies obtained in the first few seconds, the radiation intensity error is not as seriously affected as might otherwise be the case and the accuracy obtained is entirely acceptable.

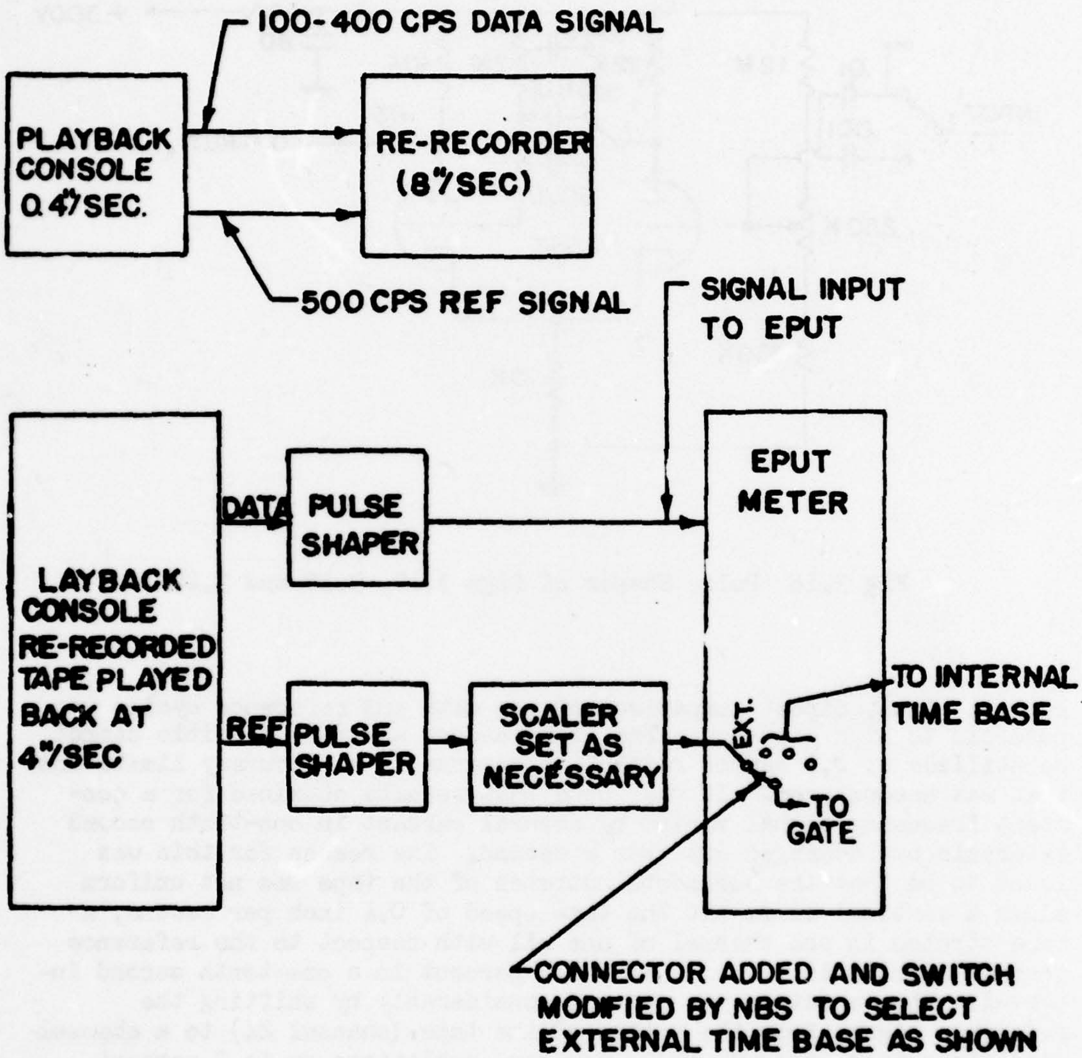

Fig 3.19 Block Diagram of Direct Tape Readout Using Re-recording

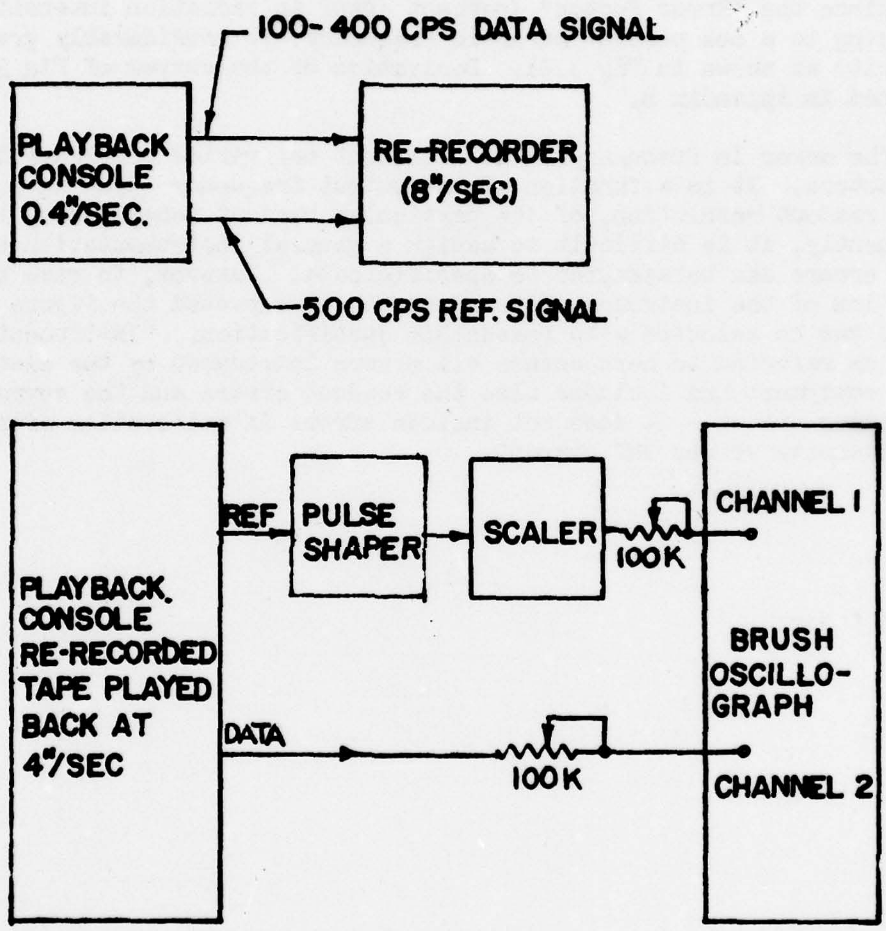

Fig 3.20 Block Diagram of Tape Readout for One-Tenth Second Resolution

3.11 INSTRUMENTATION ERRORS

The pseudo-logarithmic frequency modulated system used makes it imperative that the errors in the frequency be reduced to a minimum. This is so since the "Error Factor" (percent error in radiation intensity corresponding to a one percent error in frequency) is considerably greater than unity as shown in Fig 3.21. Derivation of the curves of Fig 3.21 is explained in Appendix B.

The error in frequency is not constant but varies considerably with many factors. It is a function of the output frequency (see Fig 3.21), of the readout resolution, of the particular readout scheme used, etc. Consequently, it is difficult to assign a general instrumentation error, though errors can be assigned to specific data. However, to give some indication of the instrumentation errors to be expected the figure 10 percent can be selected with reasonable justification. "Instrumentation error" as referred to here covers all errors introduced by the electronic equipment and includes also the readout errors and the current calibration errors. It does not include errors in calibration of radiation intensity versus PMT current.

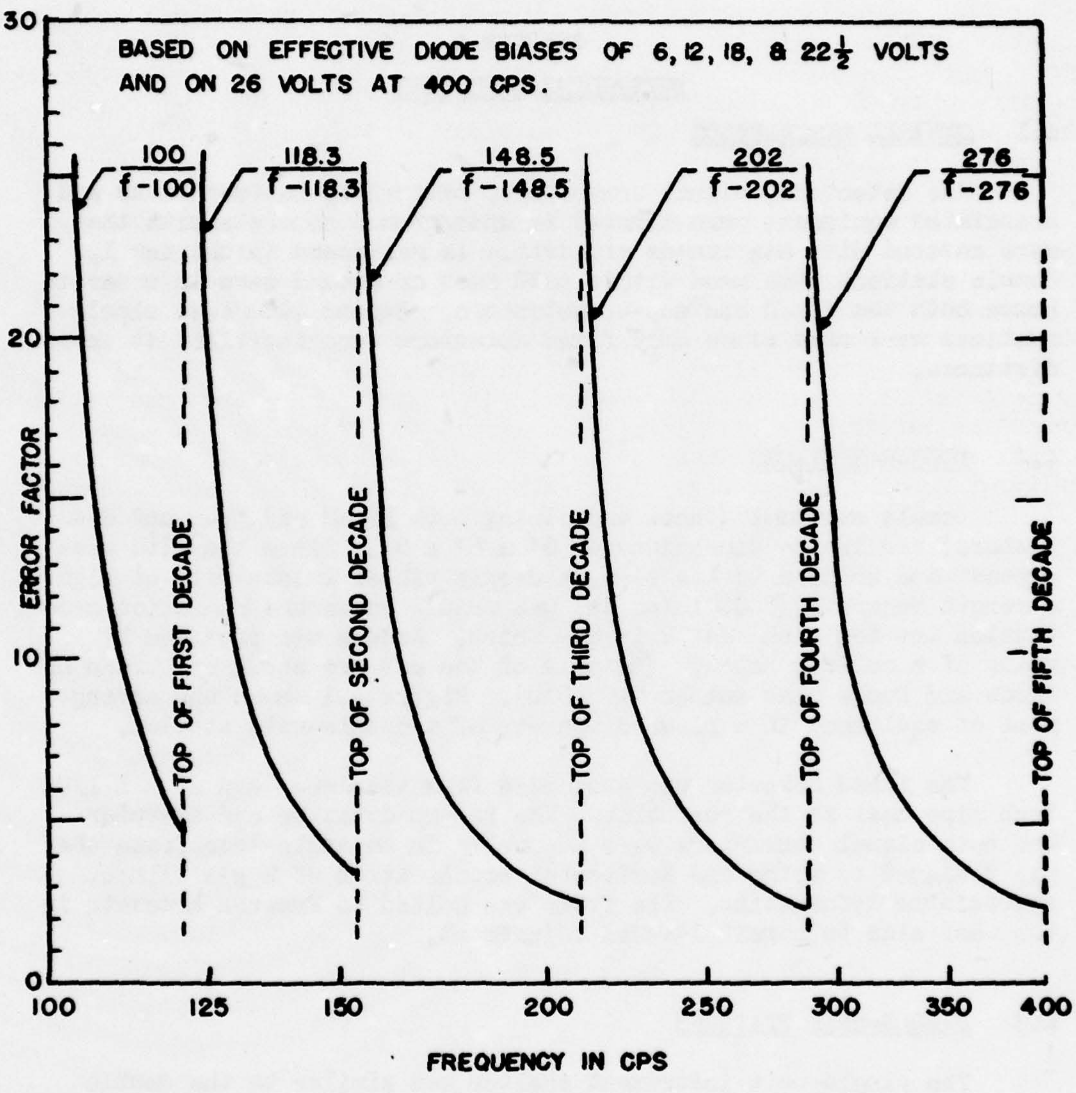

Fig 3.21 Error Factor (Percent Error in Radiation Intensity Corresponding to One Percent Error in Frequency)

[redacted]

CHAPTER 4

MECHANICAL EQUIPMENT

4.1 GENERAL DESCRIPTION

The detectors, signal converters, batteries, battery racks and associated equipment were mounted in underground concrete pits that were covered with six inches of earth. As mentioned in Chapter 1, double stations were used within 4000 feet of ground zero in order to house both the fixed and pop-up detectors. Beyond 4000 feet single stations were used since only fixed detectors were installed at these distances.

4.2 DOUBLE STATIONS

Double stations (those containing both fixed and "pop-up" detectors) had inside dimensions of 6' x 6' x 6'. Since the pits were precast and shipped to the site, a deeply ribbed 2 inch wall of high strength concrete (5000 lb/sq in) was used. To secure radiation protection the top slab was 12 inches thick. Access was provided by means of a rolling hatch. (Details of the pit are shown on Bureau of Yards and Docks plan number 510, 910). Figure 4.1 shows the arrangement of equipment in a plywood mock-up of a double-unit station.

The fixed detector was suspended from the lower end of a 2 1/2 inch pipe cast in the roof slab. The pop-up detector and elevator and both signal converters were supported in an angle-iron frame that was designed to withstand horizontal acceleration of 2 g's without appreciable deformation. The frame was bolted to Truscon brackets in the roof slab to permit lateral adjustment.

4.3 SINGLE-UNIT STATIONS

The single-unit instrument shelter was similar to the double unit station shelter in mechanical details. However, the size of the single-unit station was 4' x 6' x 4' and the sliding hatch cover was the full width of the shelter.

A small frame suspended from the roof slab by four bolts was used to support the signal converter in the small pit. One inch pipe sleeves around each of the four suspension bolts allowed appreciable tolerance.

[redacted]

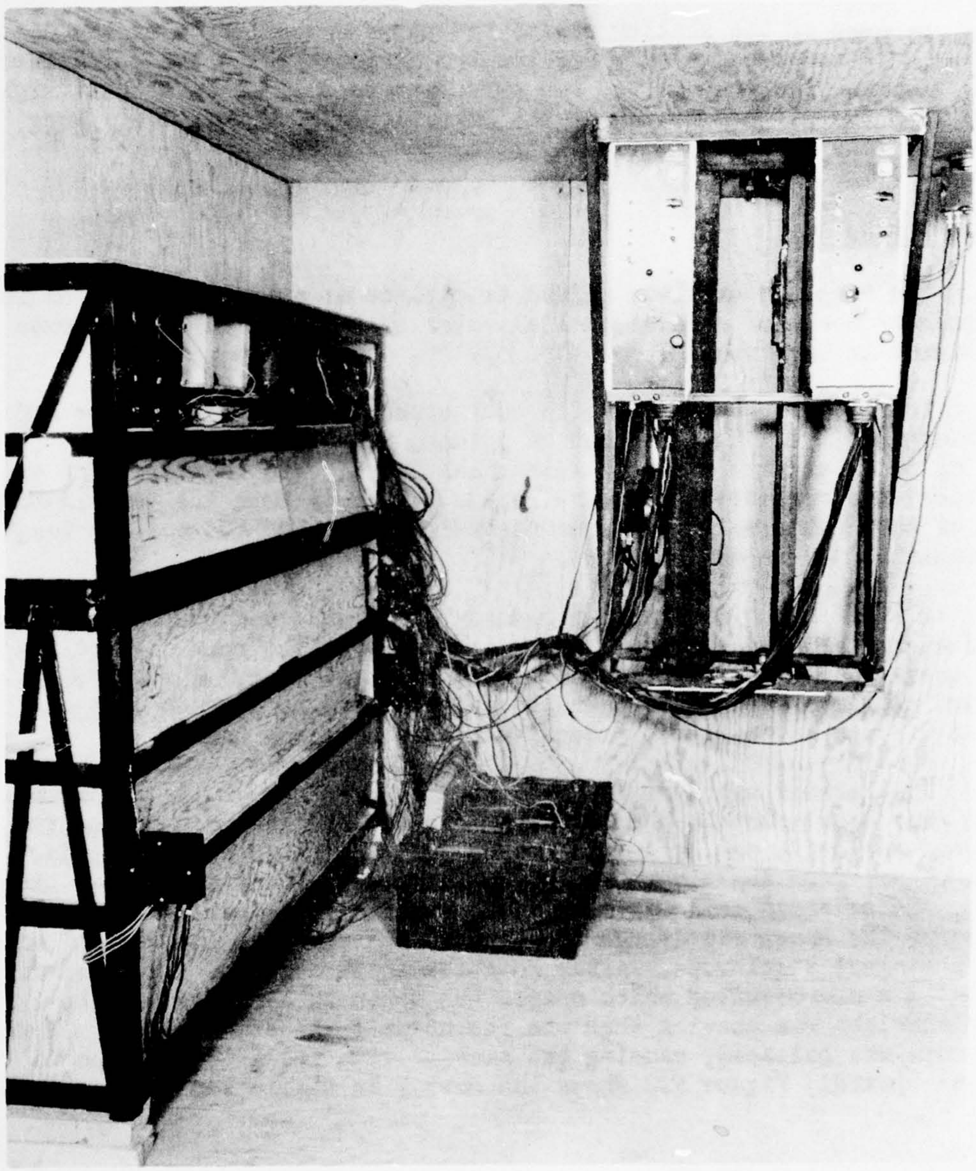

Fig 4.1 Interior View of Mock-Up of Large Pit

A Truscon bracket was cast in one wall three feet above the floor to secure the battery rack.

Because of the shallowness of the pit and the length of the detector head and tube, a sump was located directly below the 2 1/2 inch pipe sleeve. The sump served two purposes; to collect water that might seep into the pit and to permit the insertion of the relatively long detector tube through the sleeve in the cover slab.

4.4 POP-UP UNIT

The "pop-up" unit was raised into place at approximately plus 10 seconds by means of a mechanical elevator system mounted in the frame mentioned in Section 4.2.

The elevator consisted of a counterweight running in guides and a carrier running in a second set of guides. The carrier was locked in the up position with a simple mechanical latch. The counterweight and carrier were connected with wire rope attached to both the top and bottom of each frame so that the counterweight, carrier and the two lengths of cable formed an endless belt.

A 2 1/2 inch internally threaded pipe positioned the detector unit in the carrier, and a 3 inch pipe sleeve cast in the roof slab of the pit provided a guide for the detector unit as it rose. A mushroom-shaped aluminum cap placed over the guide sleeve to exclude dust and water was displaced by the ascension of the detector unit.

The carrier was normally held at the lower end of its run by means of a rope lock mounted on an aluminum plate. The lock consisted of a grooved bar and a cam linked to an eccentric operated by a solenoid. Upon signal from the timing motor, approximately 10 seconds after time zero, the solenoid coil was energized, pulling the armature inward and rotating the eccentric enough to withdraw the cam from its contact with the stainless steel rope. After rotation of 30 degrees, the eccentric actuated a micro-switch which opened the solenoid circuit. As the counterweight was heavier than the pop-up unit, it started downward when the rope was released, causing the carrier with its detector tube to travel upward. Figure 4.2 shows the device in the locked position.

4.5 ACCESSORY EQUIPMENT

Portable davits, capable of handling in excess of one-half ton were provided for lowering equipment into the pits. A special lifting platform utilizing a small truck jack was used for lifting the heavy frames into position in the double stations.

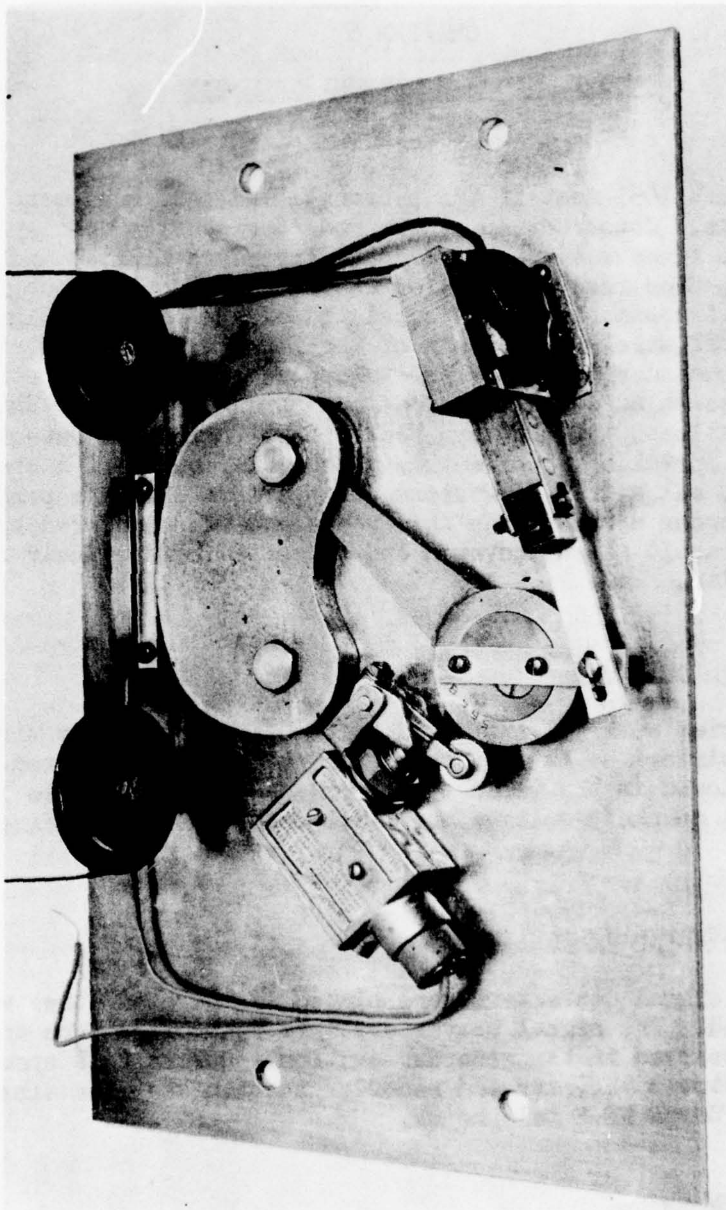

Fig 4.2 Rope Lock Assembly; Locked

[redacted]

CHAPTER 5

FIELD INSTALLATION AND EQUIPMENT

5.1 GENERAL

By 21 August 1951 most of the personnel and test equipment had arrived at the site. Construction of the recorder station and laying of the transmission lines was done by Haddock Engineers Limited and their sub-contractors. The recorder station was a 20 foot by 40 foot frame structure. The transmission lines consisted of 112 pairs of Signal Corps type WD-1/TT wire. Eighty-six of the lines were used as signal lines and the remainder for spare and telephone lines. The instrument shelters were assembled at the base camp and transported as a unit to their field locations. The battery racks, unit frames and detector units were then installed. While this mechanical equipment installation was in progress, all signal converters were given a complete performance test at the recorder station. In this way any damage incurred by the converters in transit was discovered and corrected before their installation in the pits.

5.2 BATTERY INSTALLATION

The batteries were all installed in the pits before any wiring was begun. In wiring the battery bank, all joints were soldered and enough slack allowed in the wires to prevent damage by possible shock displacement. A complete voltage check was made after the wiring was completed.

5.3 SIGNAL CONVERTER INSTALLATION

After the signal converters were placed in the pits, they were thoroughly tested. The signal converters were controlled from and signal output observed in the recorder station. During this operation communication between the pits and recorder station was maintained by means of Signal Corps EE-8 telephones.

5.4 CALIBRATION

As mentioned in Section 3.4, current calibrations were made to obtain plots of current versus period for each signal converter. These plots related the radiation intensity to the frequency output of the

[redacted] [redacted]

instruments. The current calibration plot was used during the cobalt calibration in setting the sensitivity of the detector. As explained in Section 2.4, the radiation intensity due to the Co^{60} calibrating source was known for each detector. The desired PMT current output resulting from the cobalt radiation was thus readily determined as the ratio of the desired sensitivity in microamperes per roentgen per hour to the radiation intensity in roentgens per hour due to the calibrating source. The frequency output corresponding to the desired output current was determined by reference to the current calibration graphs that related PMT output current to converter unit frequency. In setting the sensitivity the PMT high voltage was adjusted to give the proper frequency with the Co^{60} calibrating source in position. The calibration light was then adjusted so that it produced PMT currents far larger than expected background values.

5.5 FINAL ADJUSTMENTS

A few days prior to shot day, final adjustment of the pop-up mechanism was made. The pits were then closed and covered with six inches of earth. Some difficulty with ditch digging machinery was experienced in that they frequently cut the cables leading from the various pits to the recorder station. For this reason a checkout of all cables was made after pit covering by activating the signal converters and observing the output.

5.6 VISUAL READOUT

The visual readout system used during the test made radiation intensity data available a short time after the burst. Visual readout gave all the required data, except the short time resolution information, and considerably speeded data interpretation. Figure 5.1 shows the operators manning the station during visual readout, while Fig 5.2 shows the readout equipment. The control and magnetic recording equipment is shown in Fig 5.3.

5.7 TRANSPORTATION

Two jeeps, two weapons carriers and two 6 x 6 2 1/2 ton trucks were used to transport personnel and equipment in the field. Other vehicles were also supplied when necessary.

UNCLASSIFIED

[redacted]

PROJECT 2.1a

Fig 5.1 Operators Manning Station During Visual Readout

[redacted] [redacted]

UNCLASSIFIED

UNCLASSIFIED

[redacted]

PROJECT 2.1a

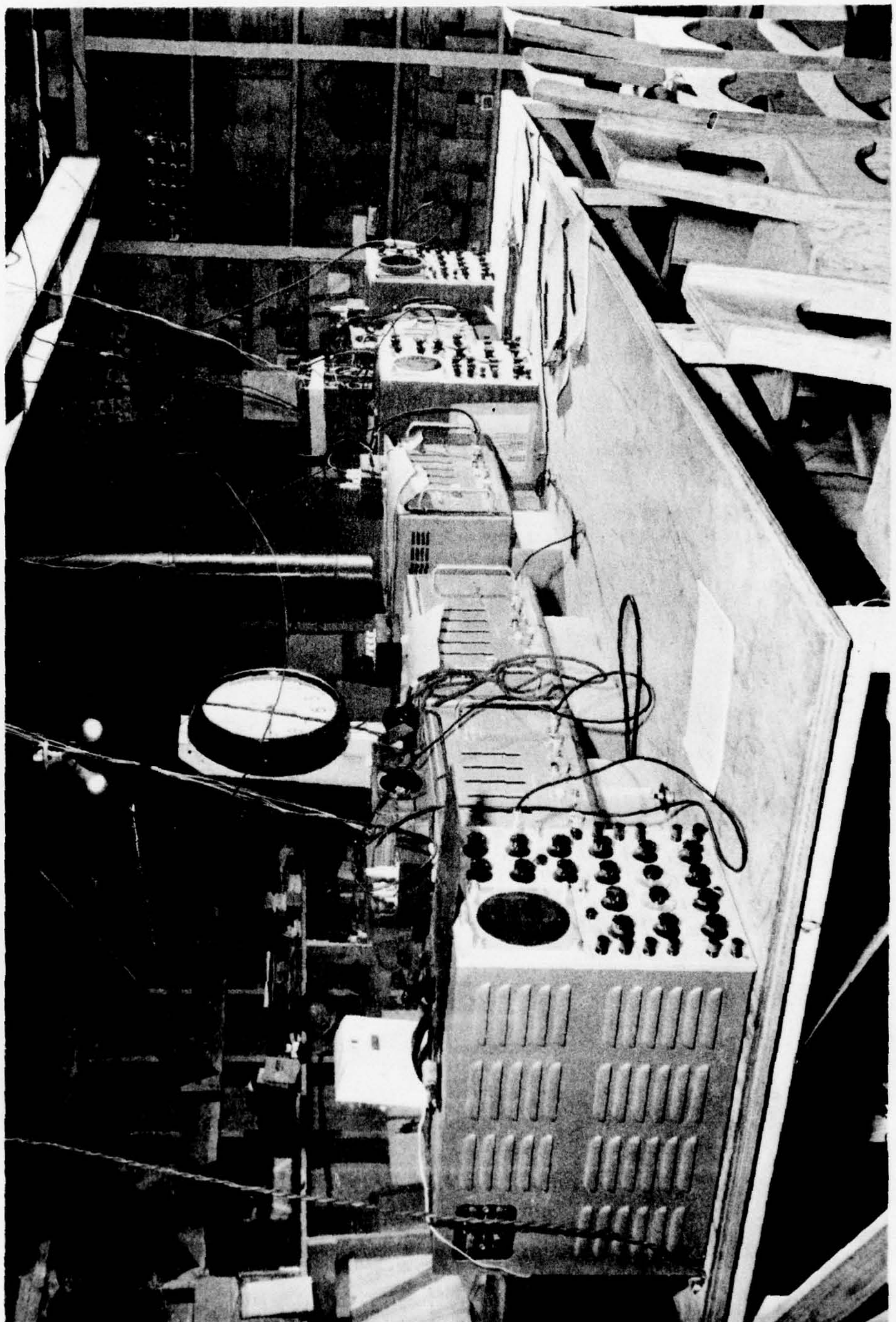

Fig 5.2 Readout Equipment

[redacted] [redacted]

UNCLASSIFIED

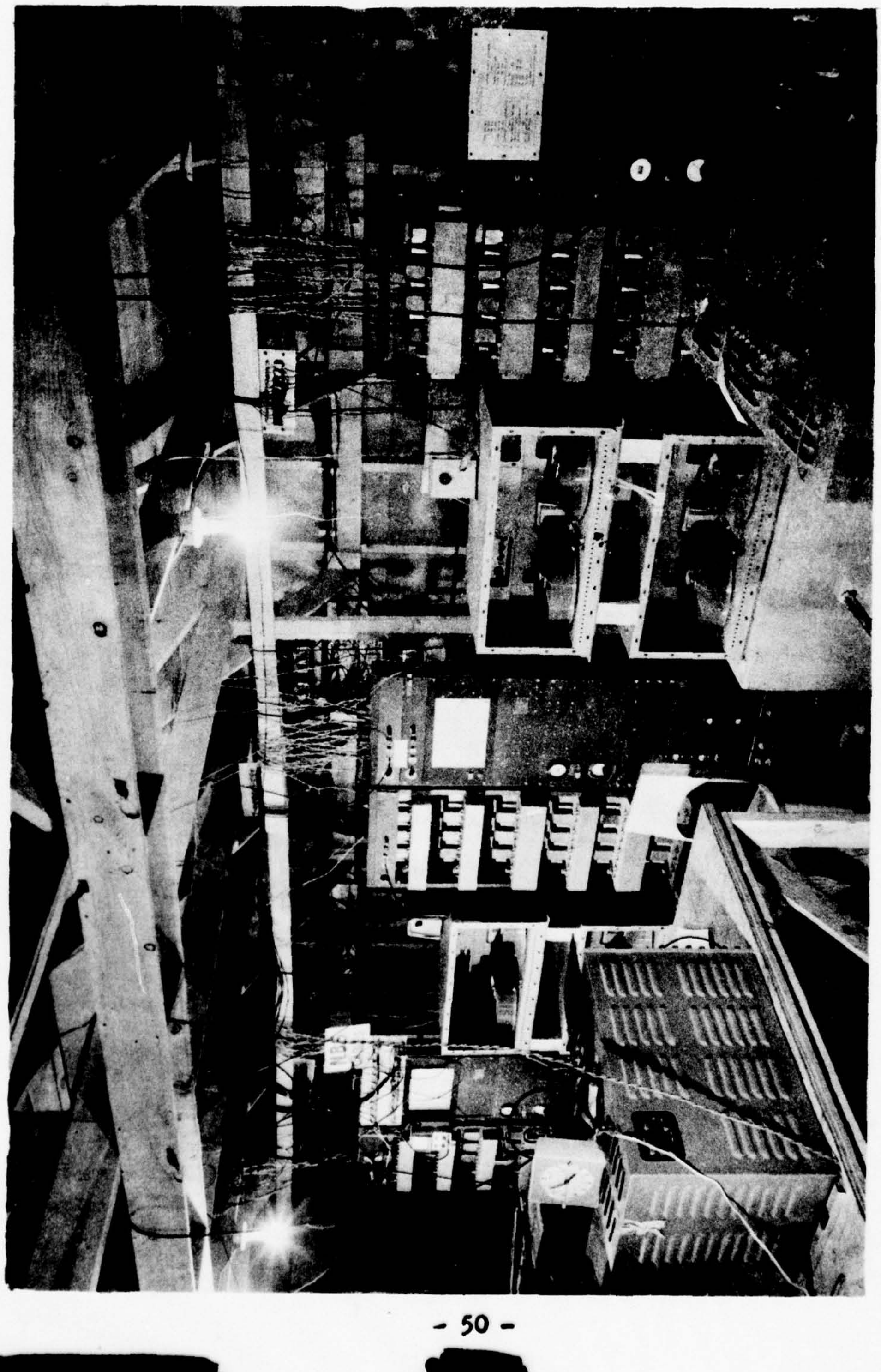

Fig 5.3 Control and Recording Equipment

CHAPTER 6

RESULTS

6.1 GENERAL

Good data was obtained from all of the 56 stations used. The only instrument failures encountered occured in stations with two instruments one of which operated successfully. Eighty-three of the 86 instruments installed performed properly. This operational performance of 94% is considered satisfactory. The calibration was found to be in error on four of the instruments (1P, 2P, 14P, 101). However, the data was corrected by comparison with data from the companion units at the same stations.

6.2 GAMMA DOSE RATE

The gamma dose rate data obtained is plotted on Fig 6.1 through 6.12 as a function of time. Fig 6.1 through 6.6 are for the surface burst and Fig 6.7 through 6.12 for the underground burst. All stations on a given radial are plotted on a single graph. Station locations are shown on Figs 1.1 and 1.2.

Zero time was clearly indicated on the Brush oscillograph tape (see Section 3.10) by the sudden change in signal frequency and is considered to be accurate to within two milliseconds. The one-tenth second intensity reading was taken as the average reading between 0.05 second and 0.15 second. Analysis of preliminary data obtained by John Malik[1] shows that for the underground burst the dose rate is essentially constant over this interval. Therefore, the two millisecond accuracy applies also to the one-tenth second interval for the surface burst. For an air burst Malik's data shows a considerable change in dose rate over the period of 0.05 second to 0.15 second. Averaging the intensity data over this period gives a reading that corresponds to about 0.093 seconds instead of 0.10 seconds for an air burst. For the surface burst it is therefore reasonable to assume that the 0.10 second readings given actually occur at between 0.094 and 0.098 second.

6.3 GAMMA TOTAL DOSE

Total dose information was obtained by integration of the dose rate curves of Figs 6.1 through 6.12. The total dose curves are plotted on the same graphs as the dose rate curves from which they are

[1] John Malik, Preliminary Report, LASL, BUSTER/JANGLE Project 10.6

[redacted]

PROJECT 2.1a

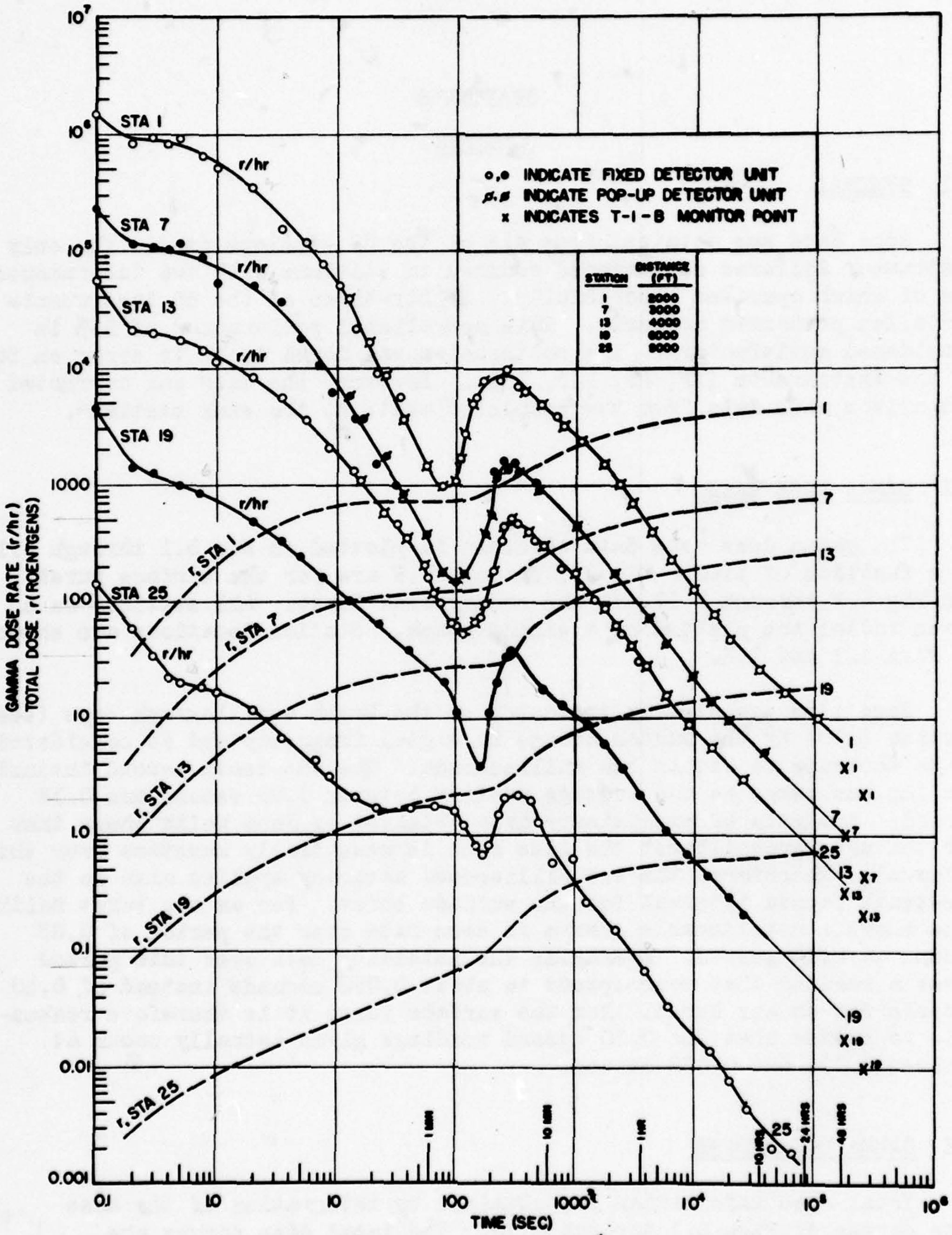

Fig 6.1 Surface Burst, Dose Rate and Total Dose vs Time (Dose received in first 0.1 second not included. See para 6.3. Station locations on Fig 1.1.)

[redacted] [redacted]

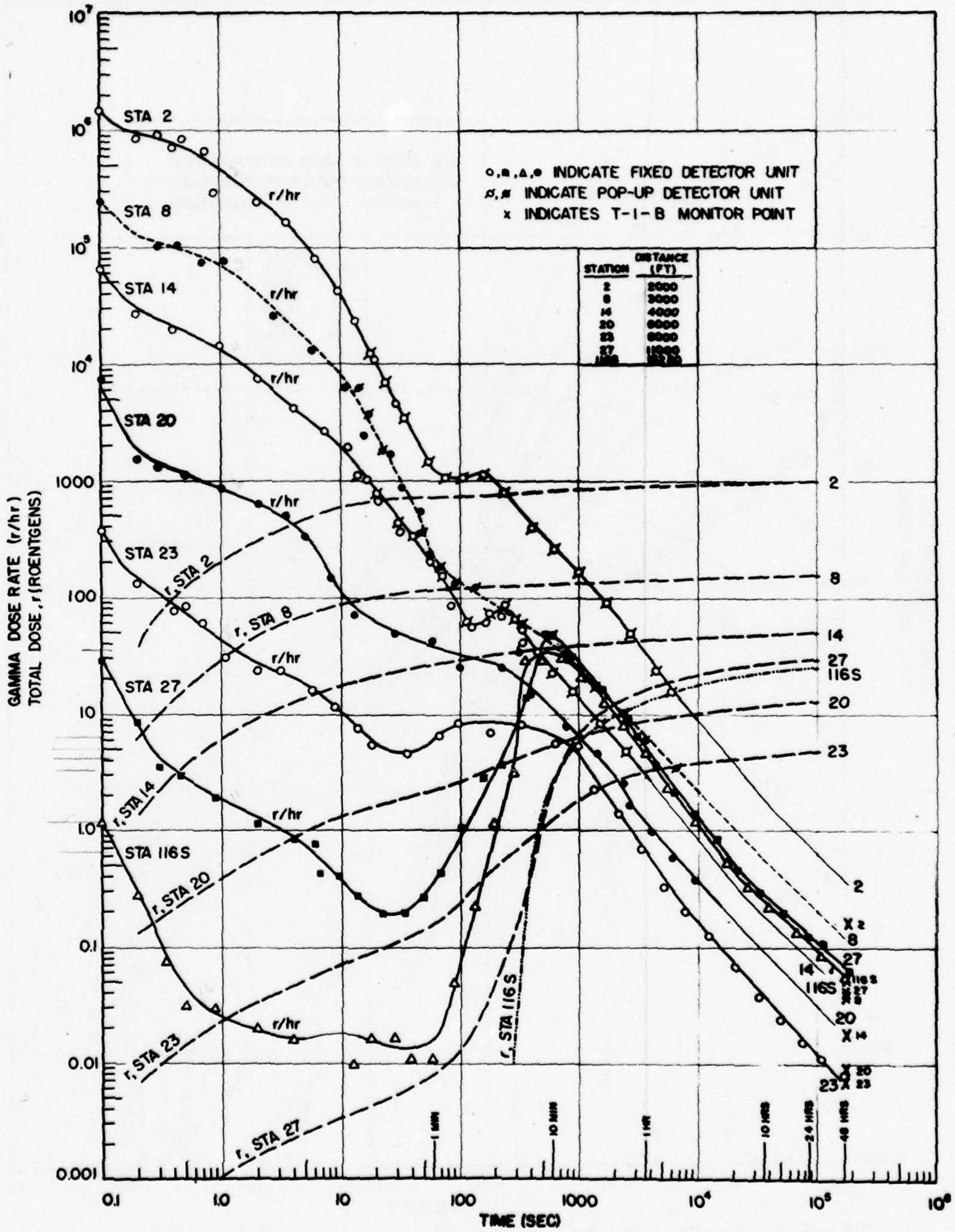

Fig 6.2 Surface Burst, Dose Rate and Total Dose vs Time (Dose received in first 0.1 second not included. See para 6.3. Station locations on Fig 1.1.)

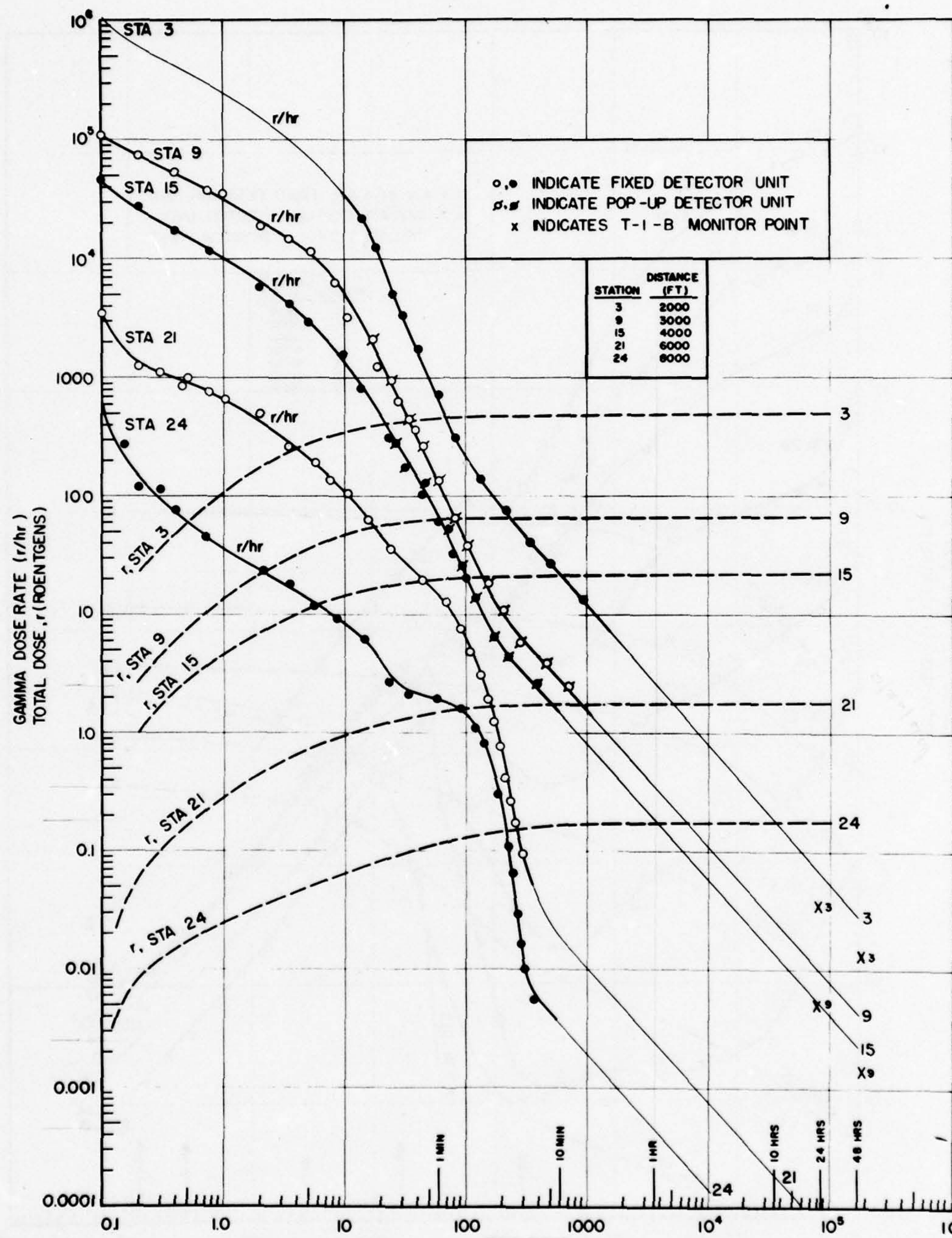

Fig 6.3 **Surface Burst, Dose Rate and Total Dose vs Time (Dose received in first 0.1 second not included. See para 6.3. Station locations on Fig 1.1.)**

[redacted]

PROJECT 2.1a

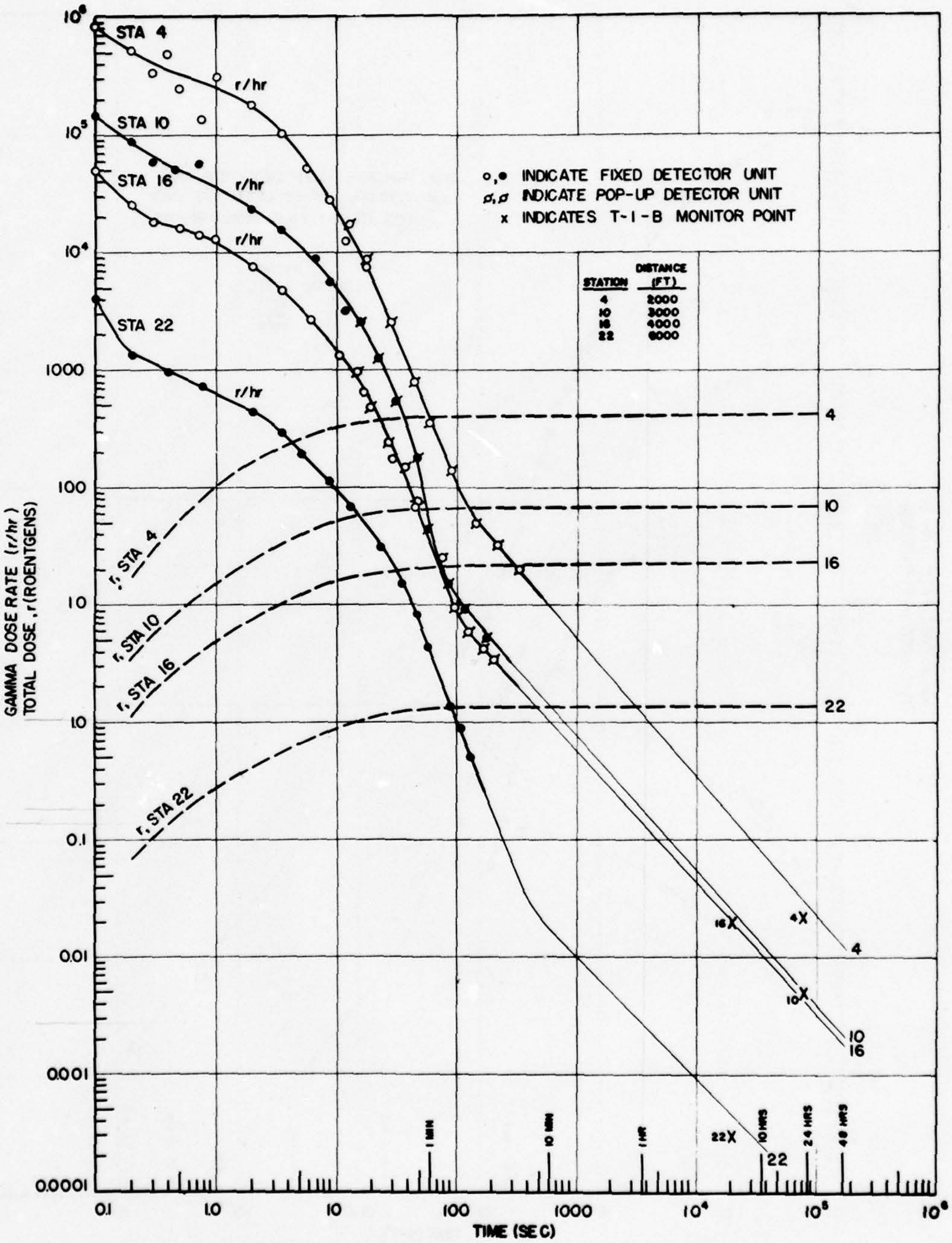

Fig 6.4 Surface Burst, Dose Rate and Total Dose vs Time (Dose received in first 0.1 second not included. See para 6.3. Station locations on Fig 1.1.)

[redacted] [redacted]

[redacted]

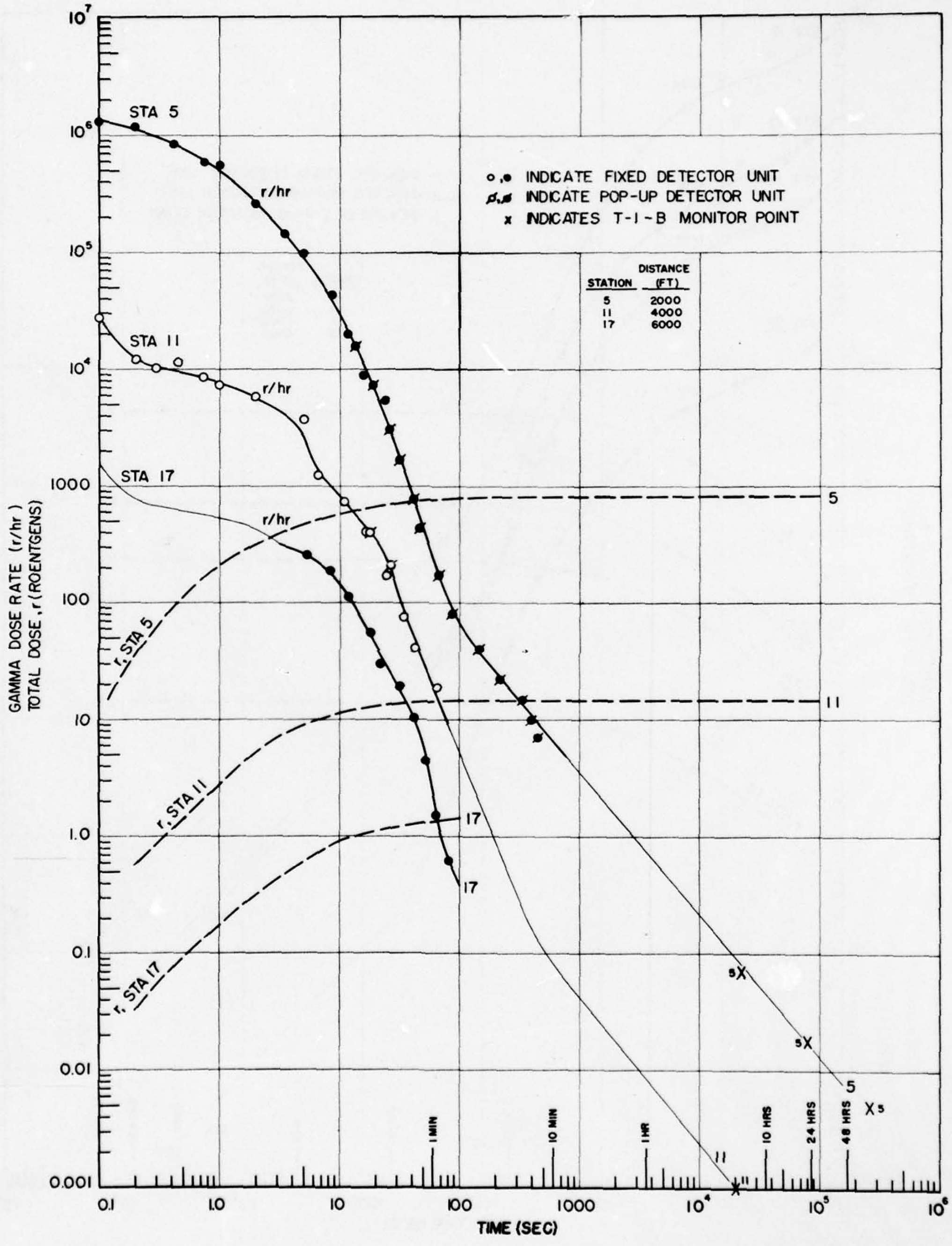

Fig 6.5 Surface Burst, Dose Rate and Total Dose vs Time (Dose received in first 0.1 second not included. See para 6.3. Station locations on Fig 1.1.)

[redacted]

[redacted]

PROJECT 2.1a

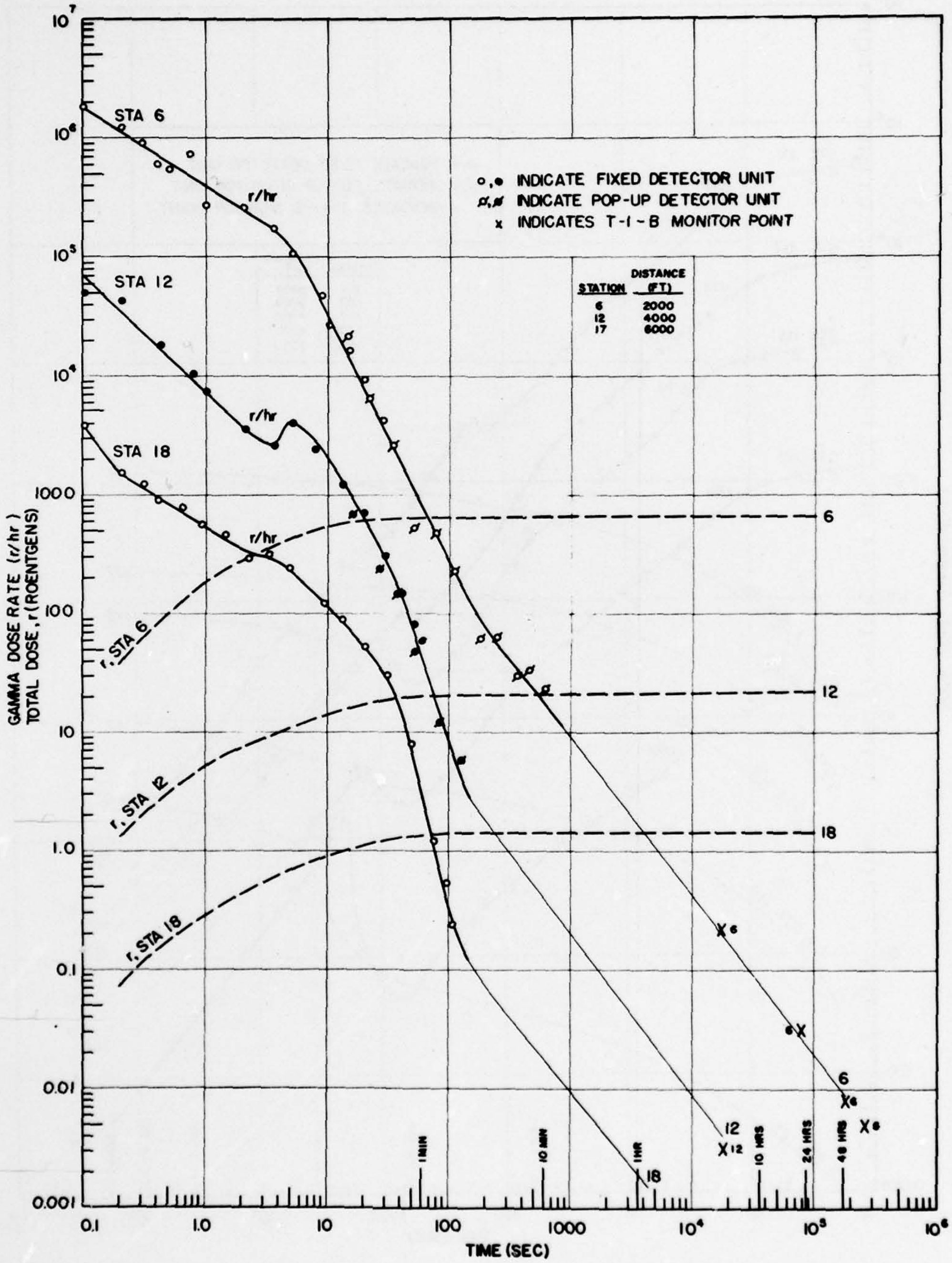

Fig 6.6 Surface Burst, Dose Rate and Total Dose vs Time (Dose received in first 0.1 second not included. See para 6.3. Station locations on Fig 1.1.)

[redacted] [redacted]

UNCLASSIFIED

[redacted]

PROJECT 2.1a

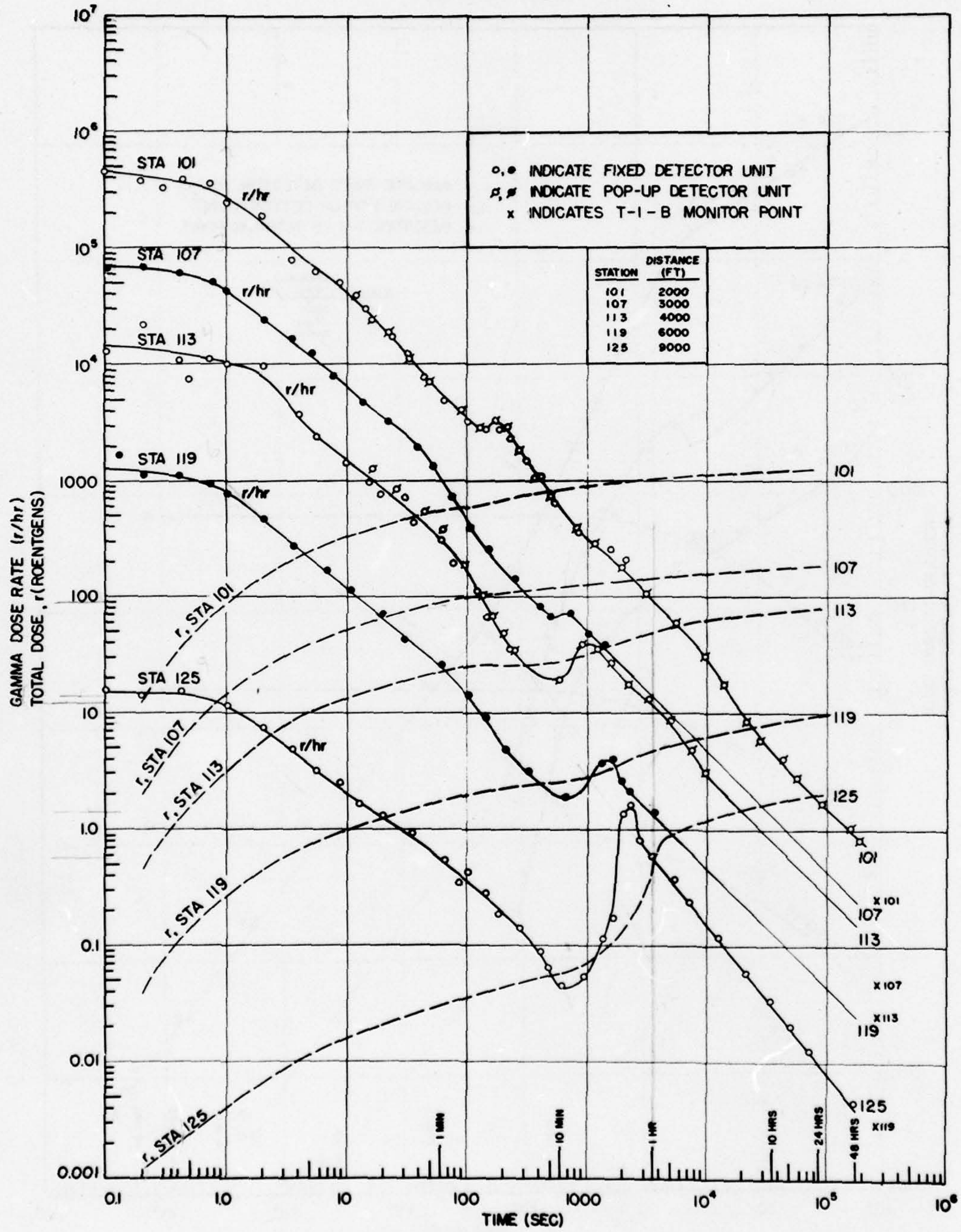

Fig 6.7 Underground Burst, Dose Rate and Total Dose vs Time (Dose received in first 0.1 second not included. See para 6.3. Station locations on Fig 1.2.)

[redacted]

UNCLASSIFIED

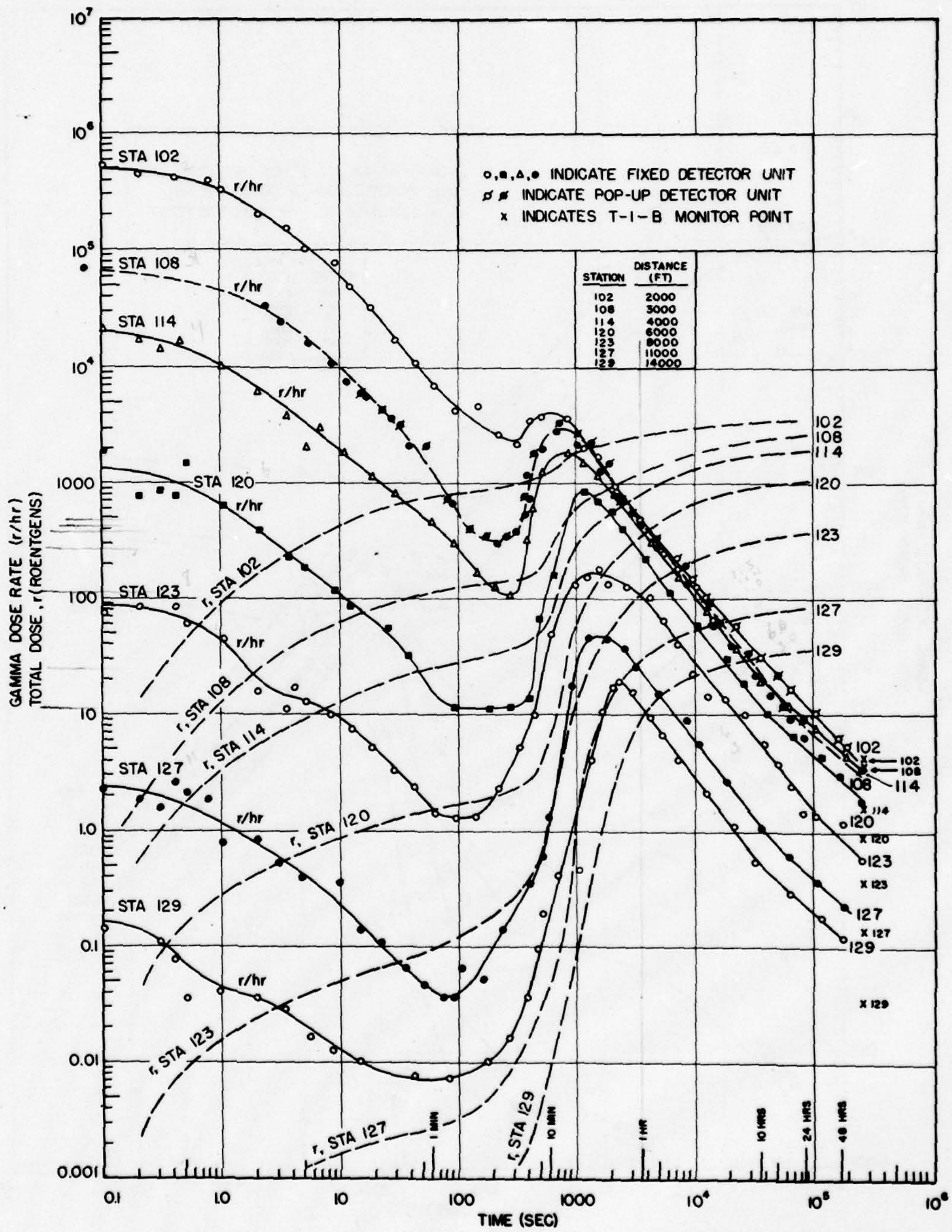

Fig 6.8 Underground Burst, Dose Rate and Total Dose vs Time (Dose received in first 0.1 second not included. See para 6.3. Station locations on Fig 1.2.)

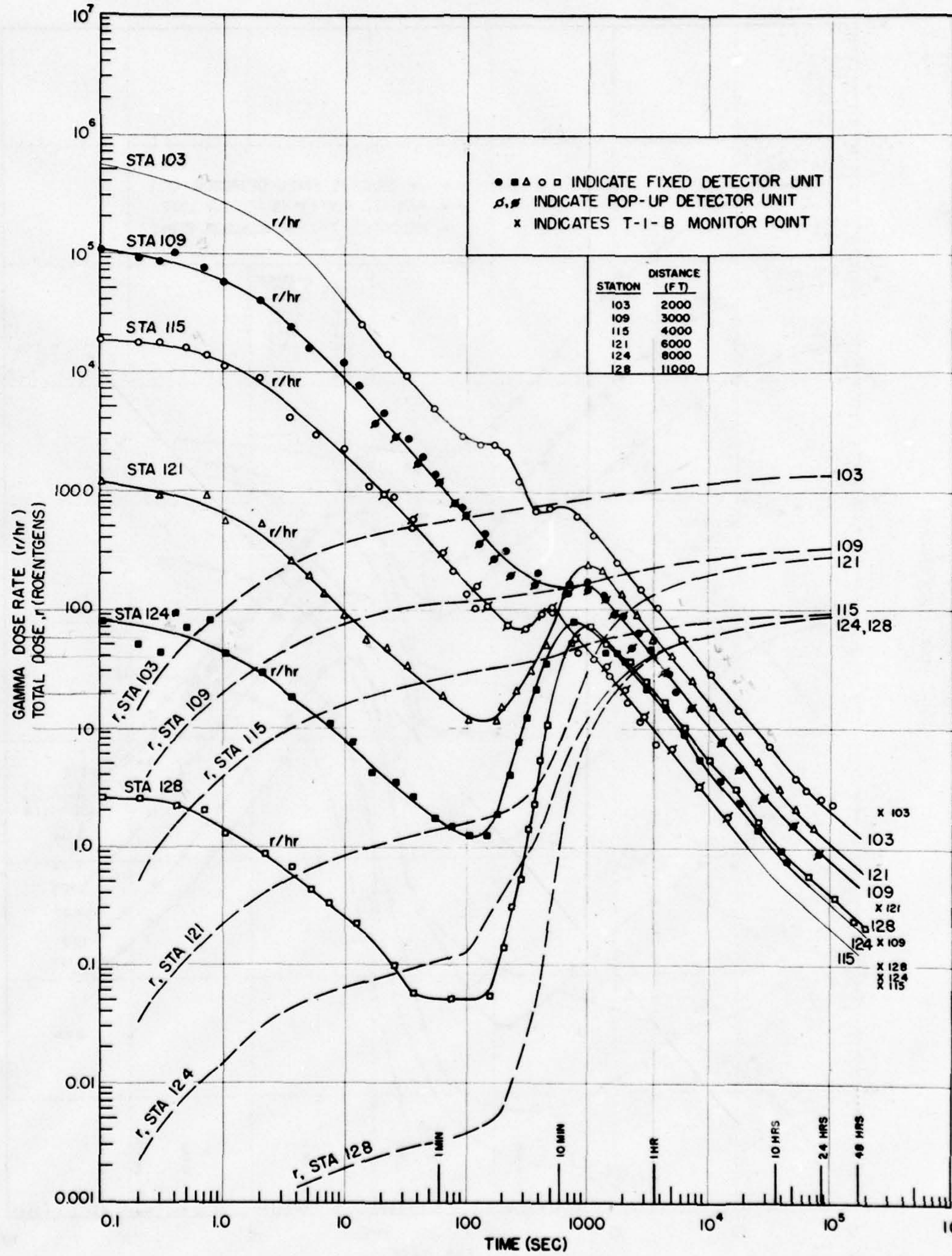

Fig 6.9 Underground Burst, Dose Rate and Total Dose vs Time (Dose received in first 0.1 second not included. See para 6.3. Station locations on Fig 1.2.)

[redacted]

PROJECT 2.1a

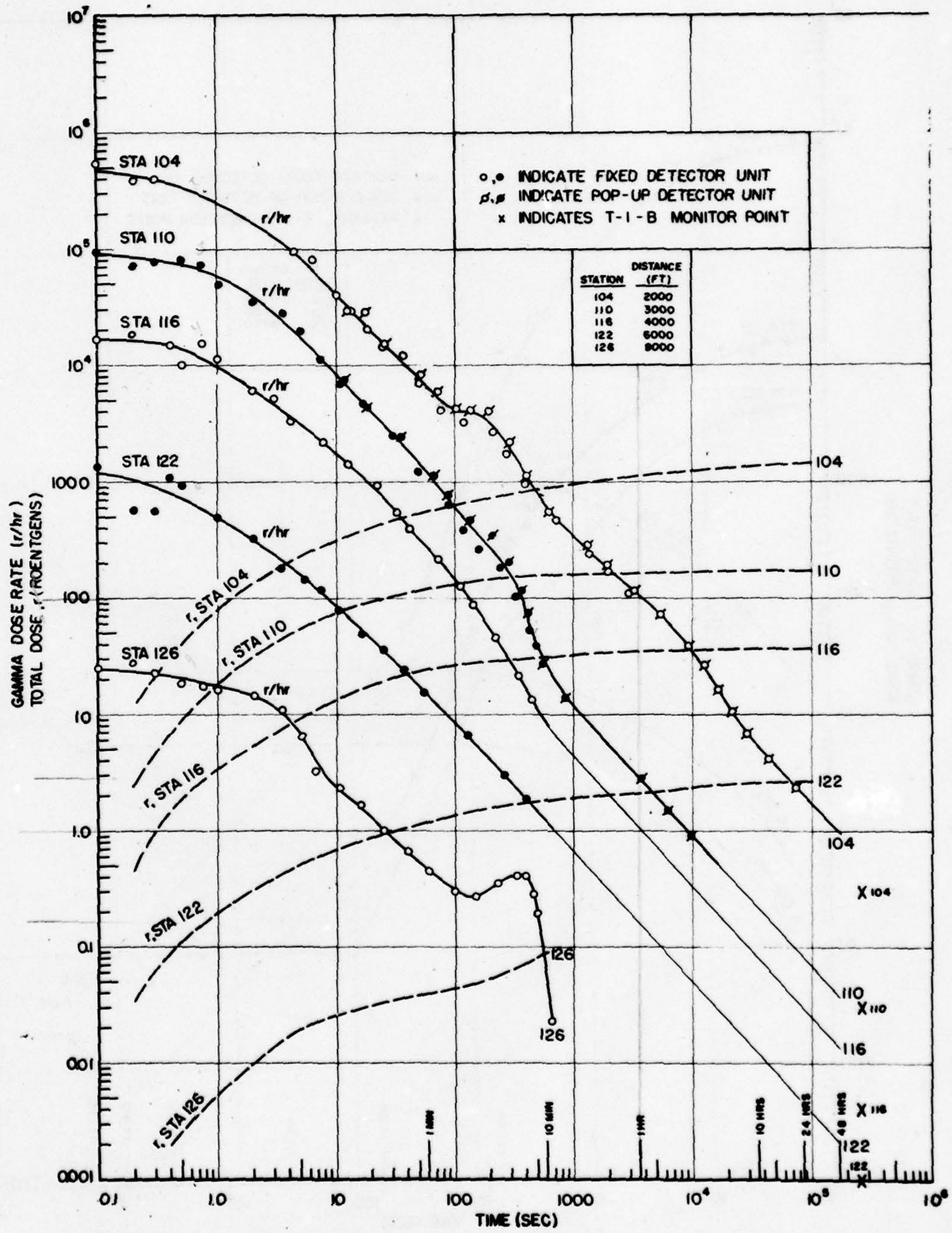

Fig 6.10 Underground Burst, Dose Rate and Total Dose vs Time (Dose received in first 0.1 second not included. See para 6.3. Station locations on Fig 1.2.)

[redacted] [redacted]

[redacted]

PROJECT 2.1a

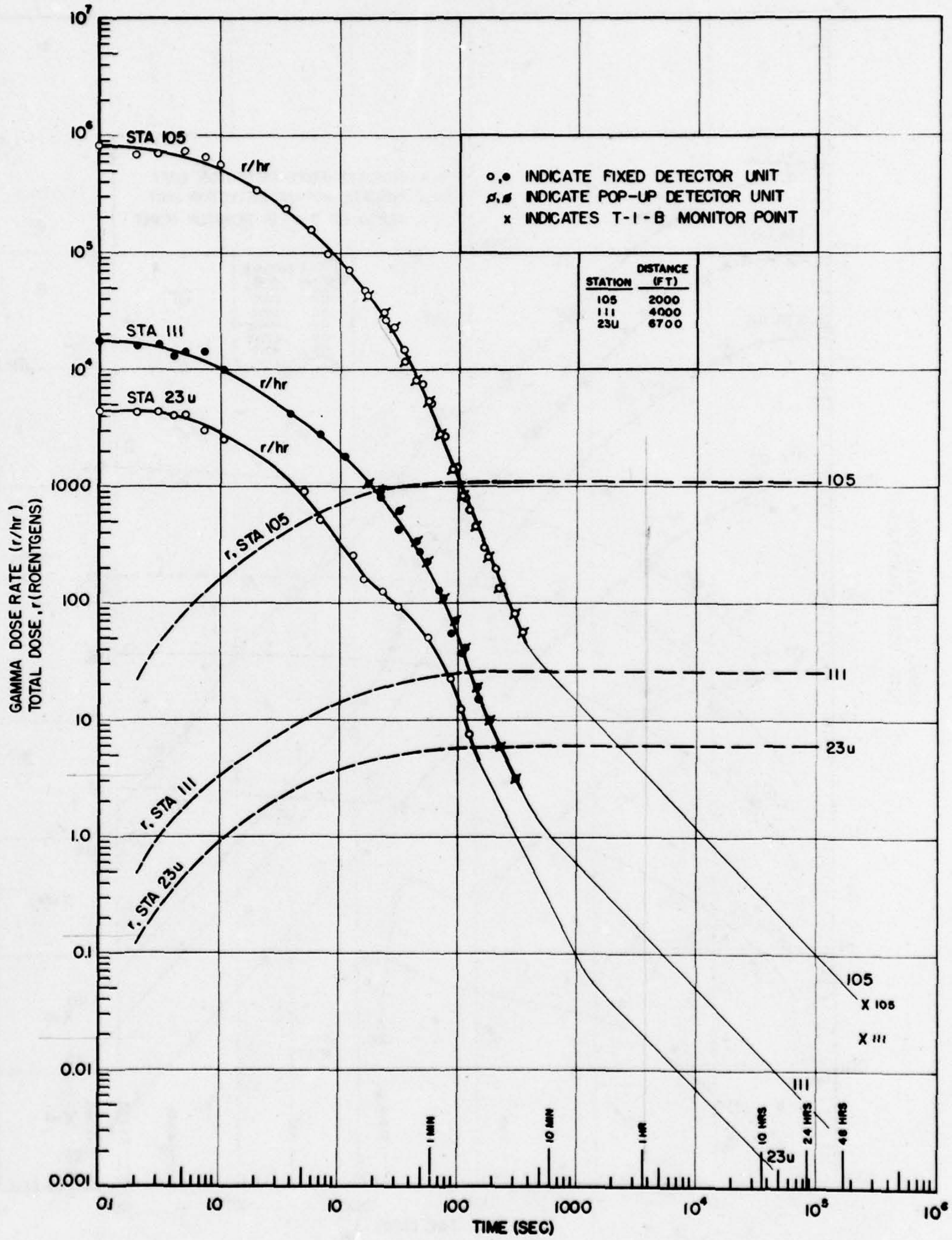

Fig 6.11 Underground Burst, Dose Rate and Total Dose vs Time (Dose received in first 0.1 second not included. See para 6.3. Station locations on Fig 1.2.)

[redacted]

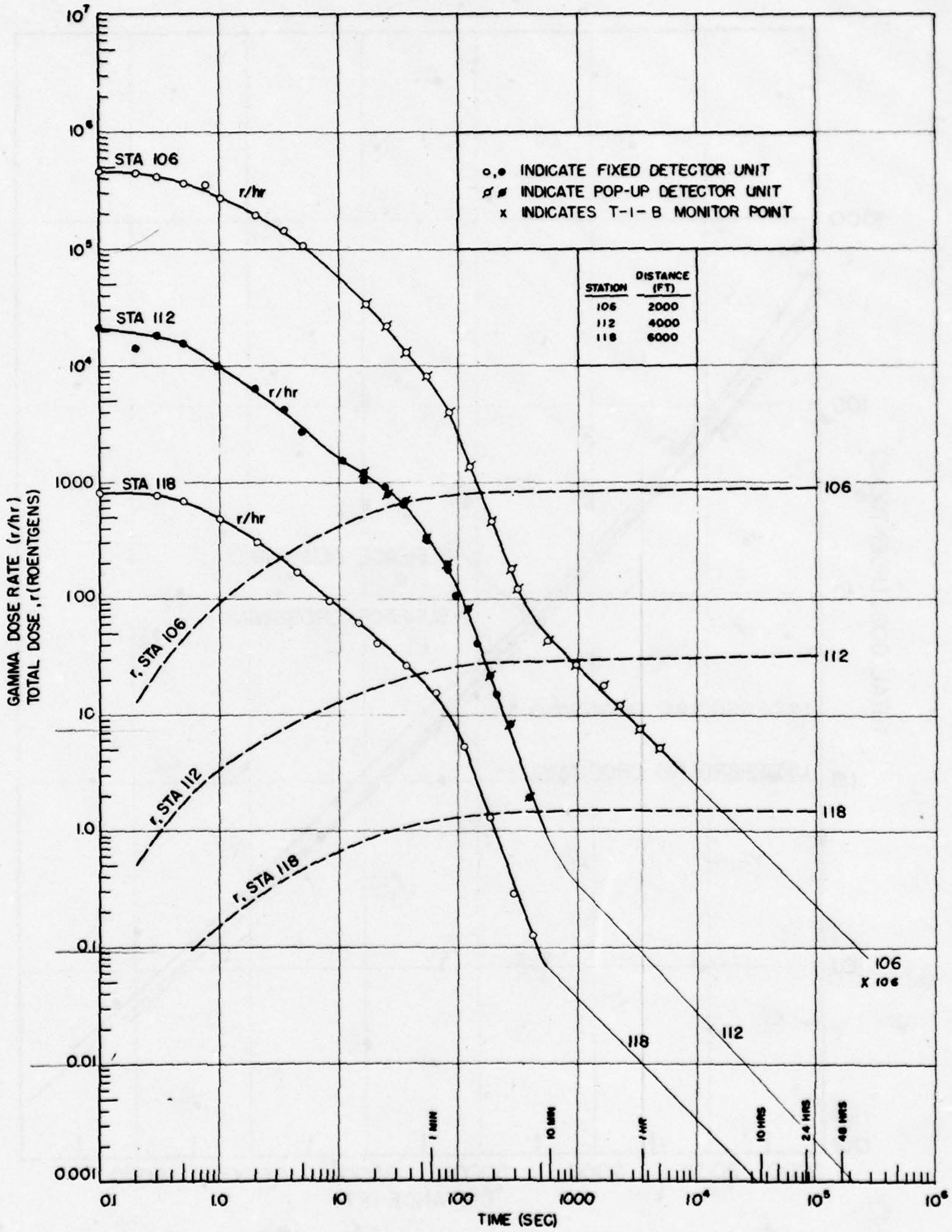

Fig 6.12 Underground Burst, Dose Rate and Total Dose vs Time (Dose received in first 0.1 second not included. See para 6.3. Station locations on Fig 1.2.)

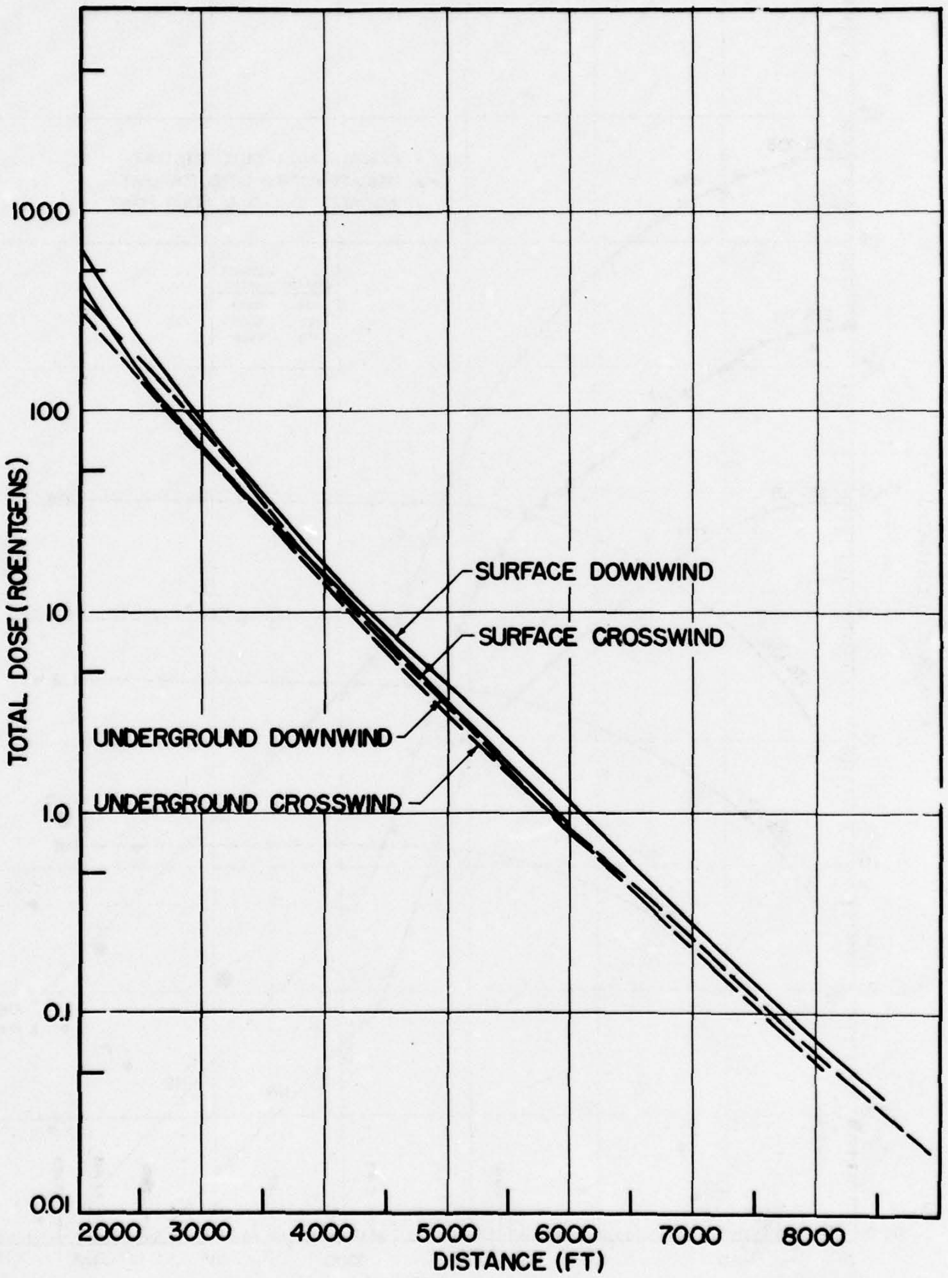

Fig 6.13 Surface and Underground Burst Total Dose at 10 Seconds (Dose received in first 0.1 second not included.)

PROJECT 2.1a

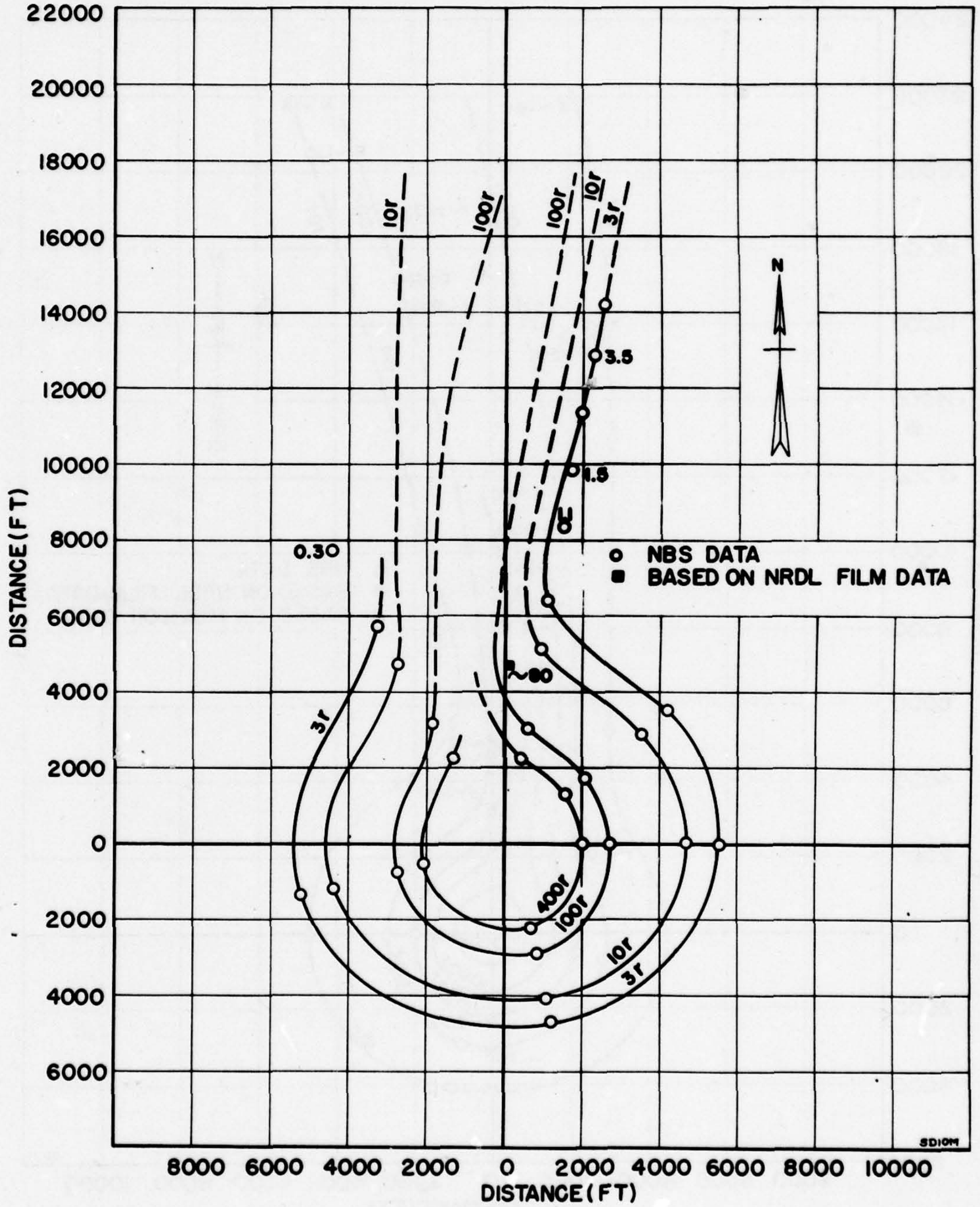

Fig 6.14 Surface Burst, Iso-Dose Contours at 10 Minutes (Dose received in first 0.1 second not included.)

[redacted]

PROJECT 2.1a

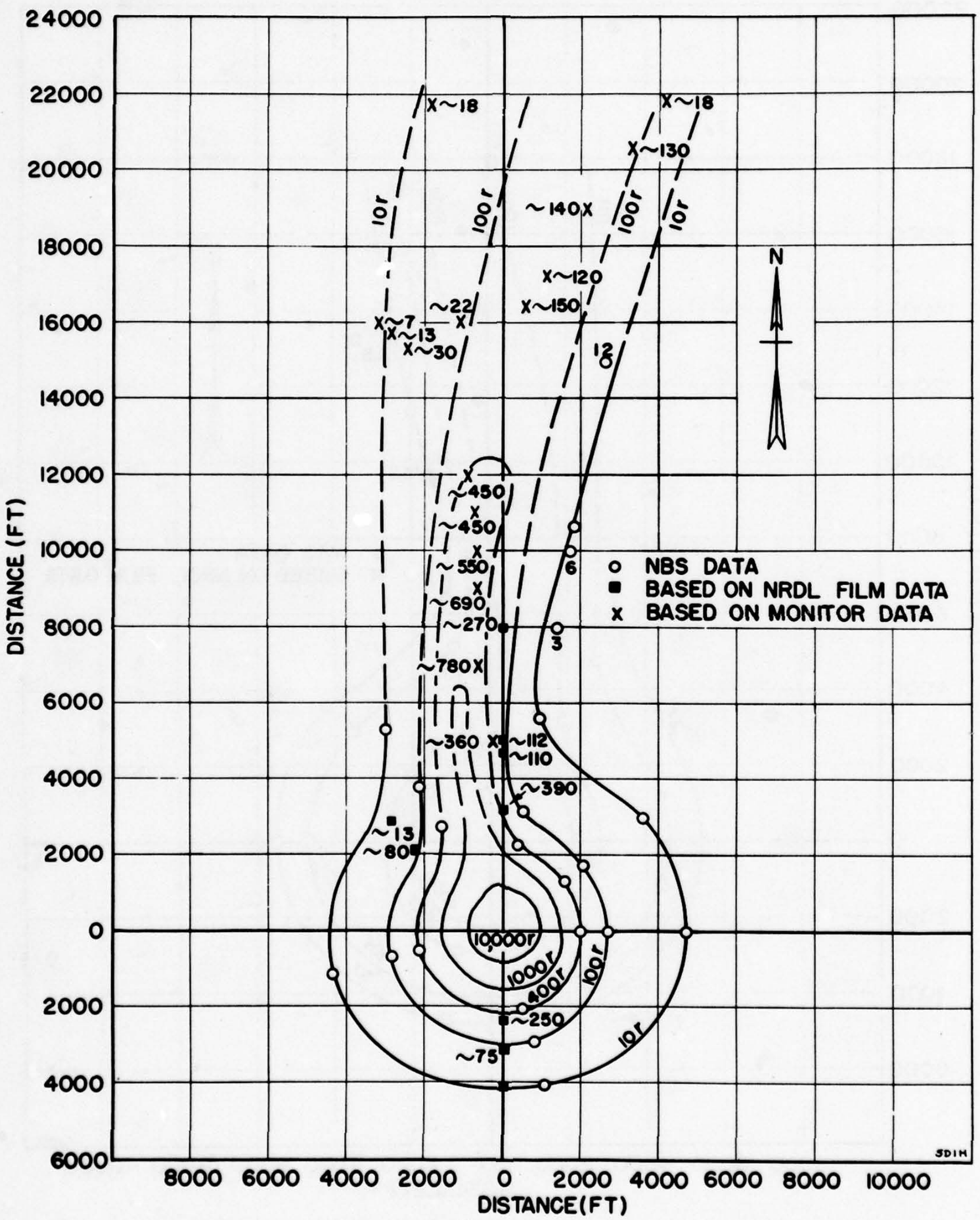

Fig 6.15 Surface Burst, Iso-Dose Contours at 1 Hour
(Dose received in first 0.1 second not included.)

[redacted]

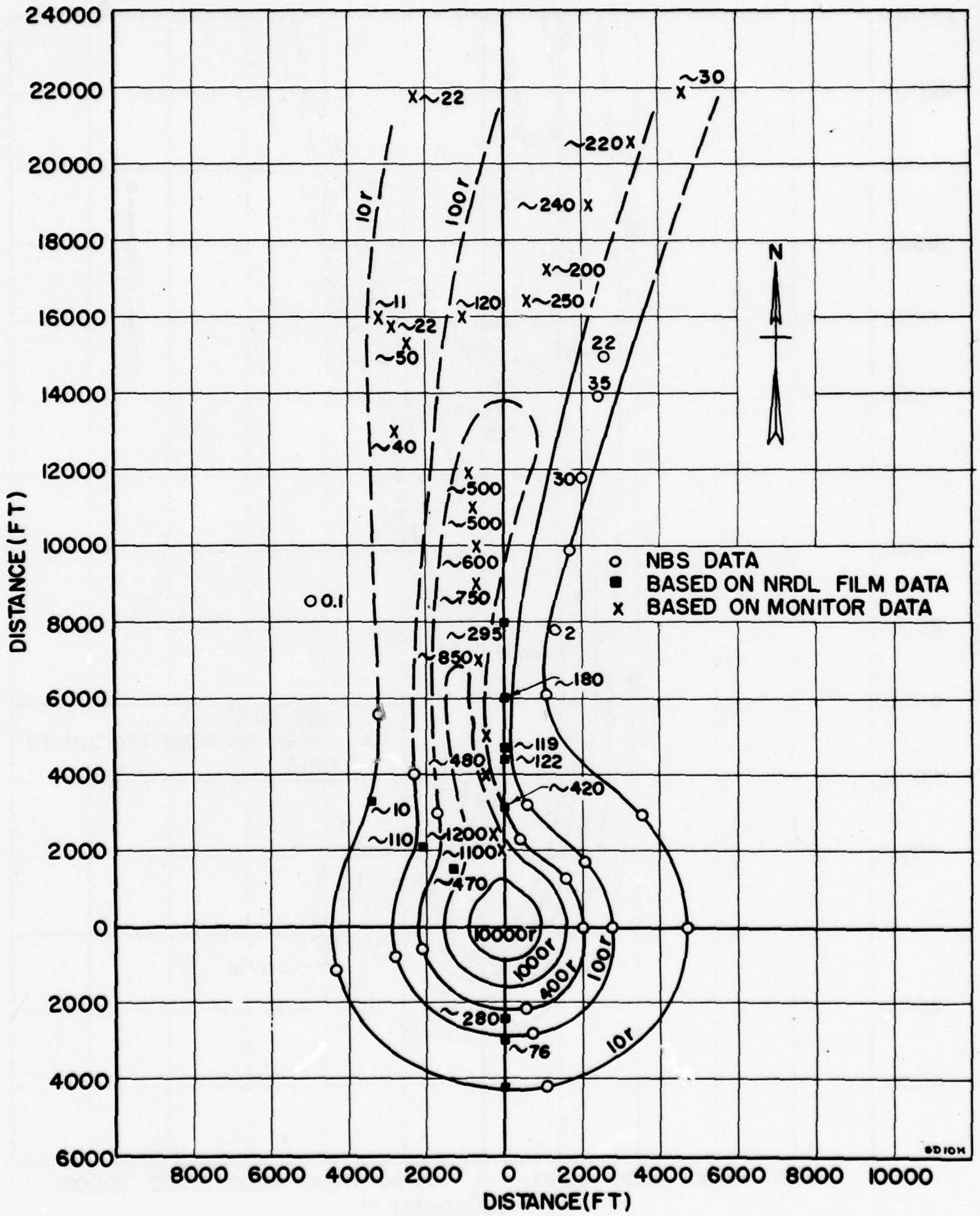

Fig 6.16 Surface Burst, Iso-Dose Contours at 10 Hours
(Dose received in first 0.1 second not included.)

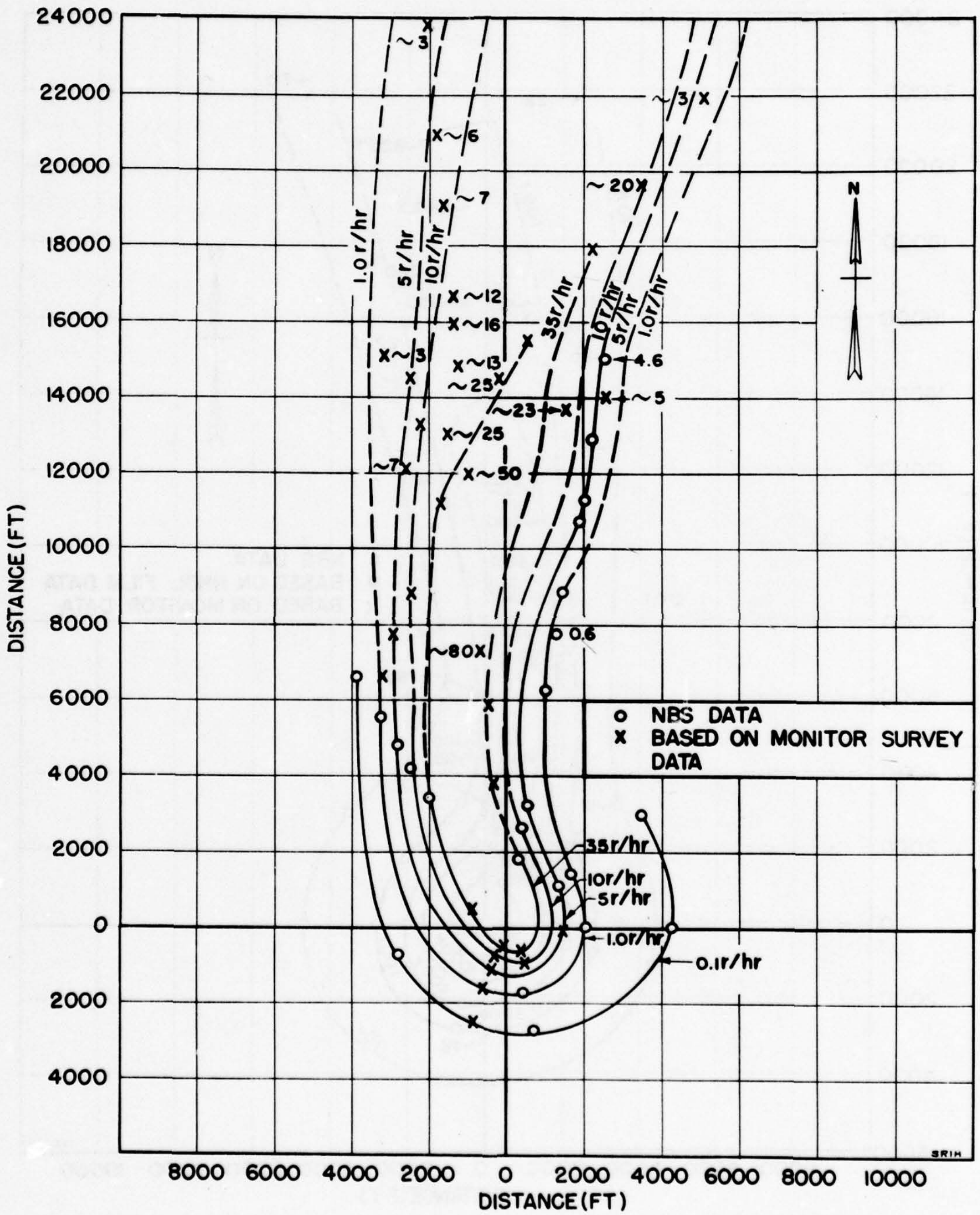

Fig 6.17 Surface Burst, Iso-Rate Contours at 1 Hour

[redacted]

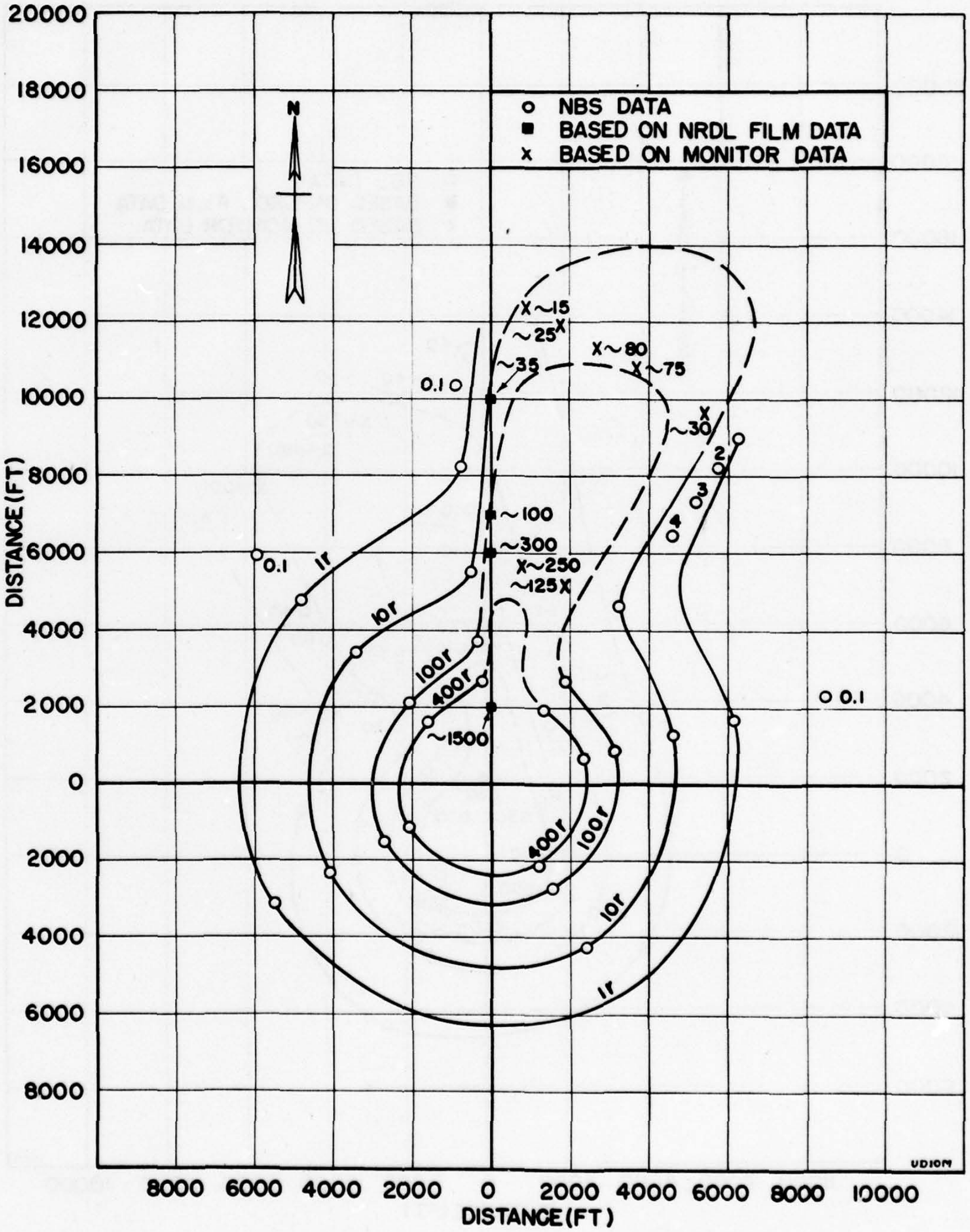

Fig 6.18 Underground Burst, Iso-Dose Contours at 10 Minutes (Dose received in first 0.1 second not included.)

[redacted] [redacted]

UNCLASSIFIED

[redacted]

PROJECT 2.1a

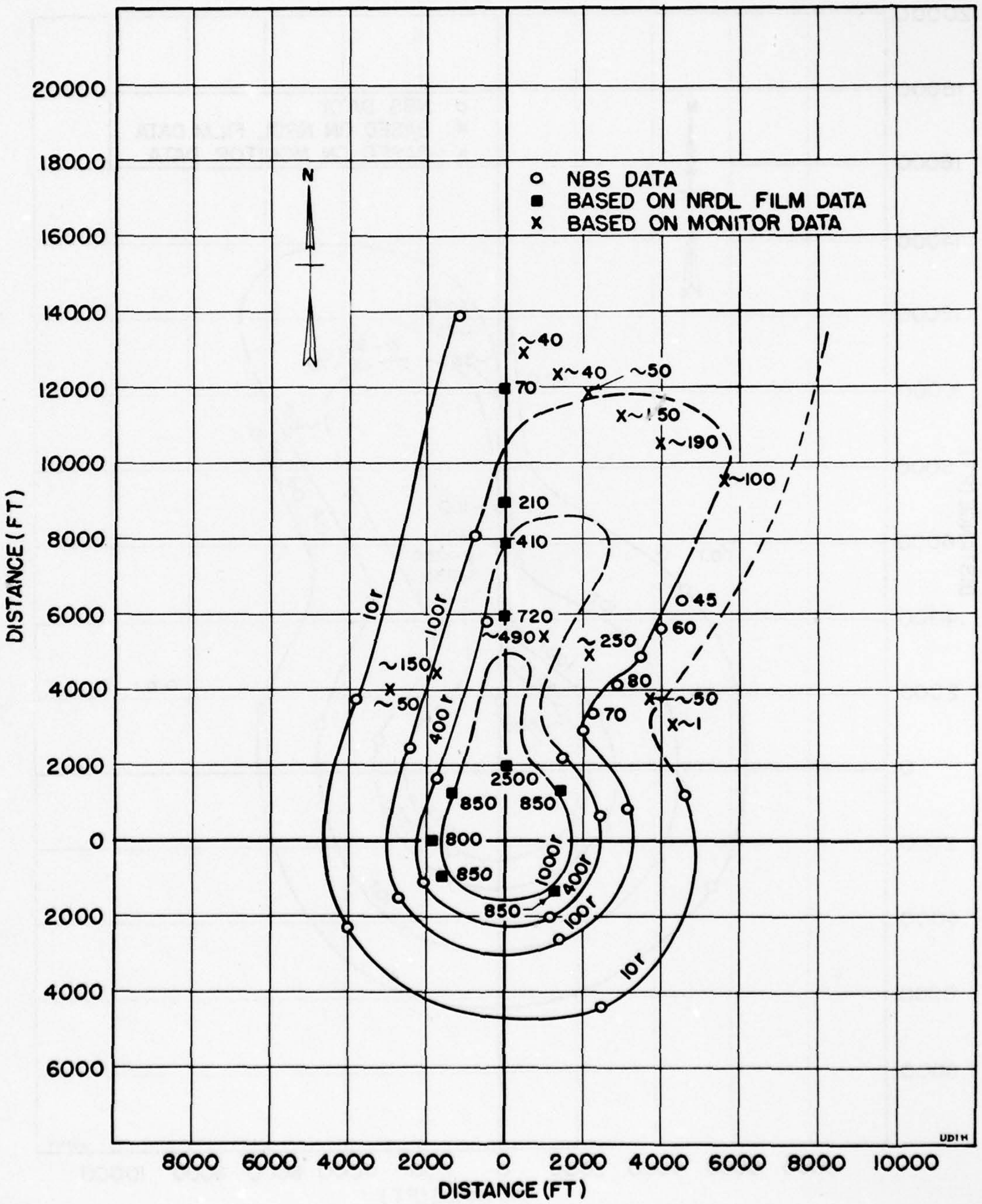

Fig 6.19 Underground Burst, Iso-Dose Contours at 1 Hour
(Dose received in first 0.1 second not included.)

[redacted]

UNCLASSIFIED

[redacted]

PROJECT 2.1a

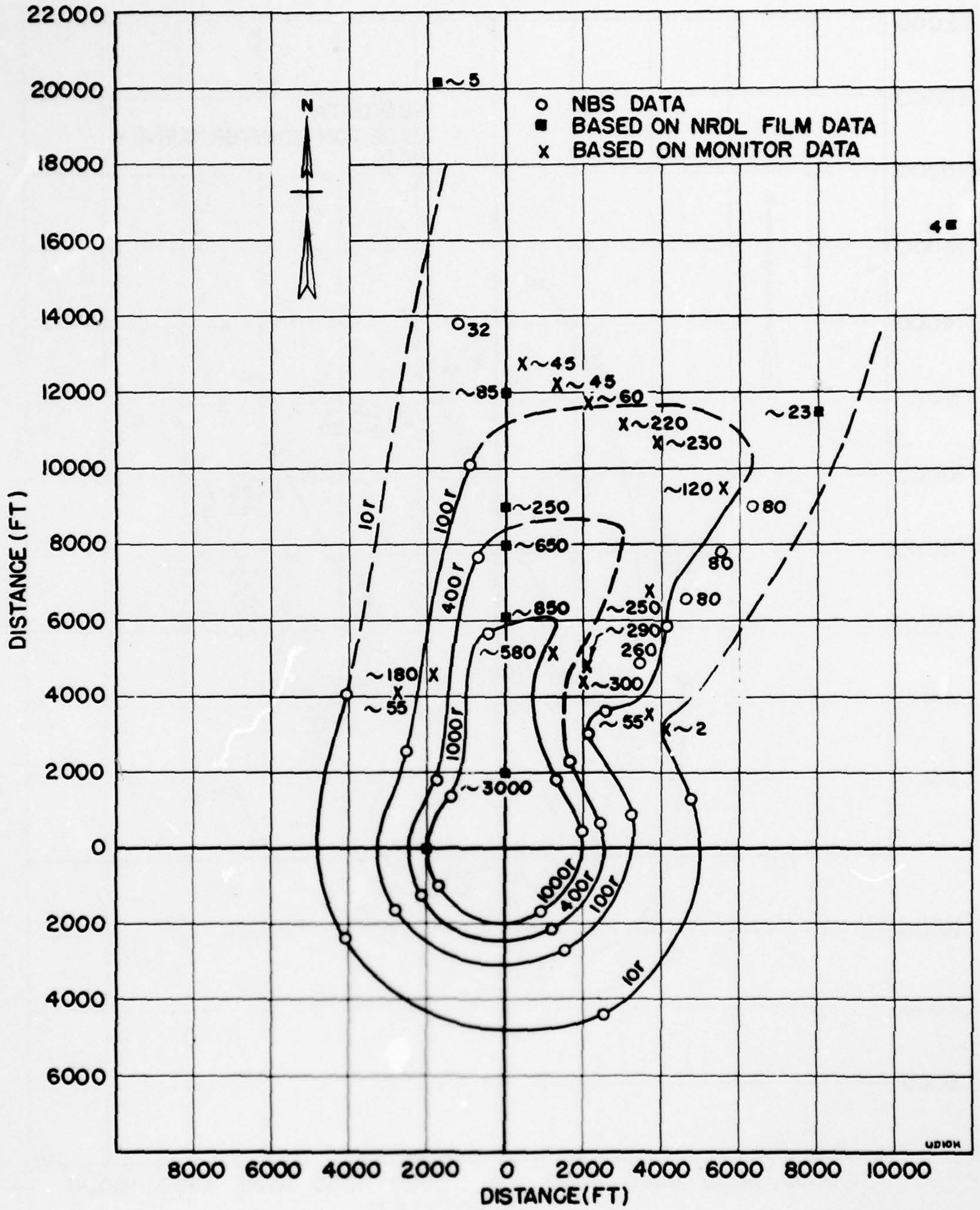

Fig 6.20 Underground Burst, Iso-Dose Contours at 10 Hours
(Dose received in first 0.1 second not included.)

[redacted] [redacted]

UNCLASSIFIED [redacted]

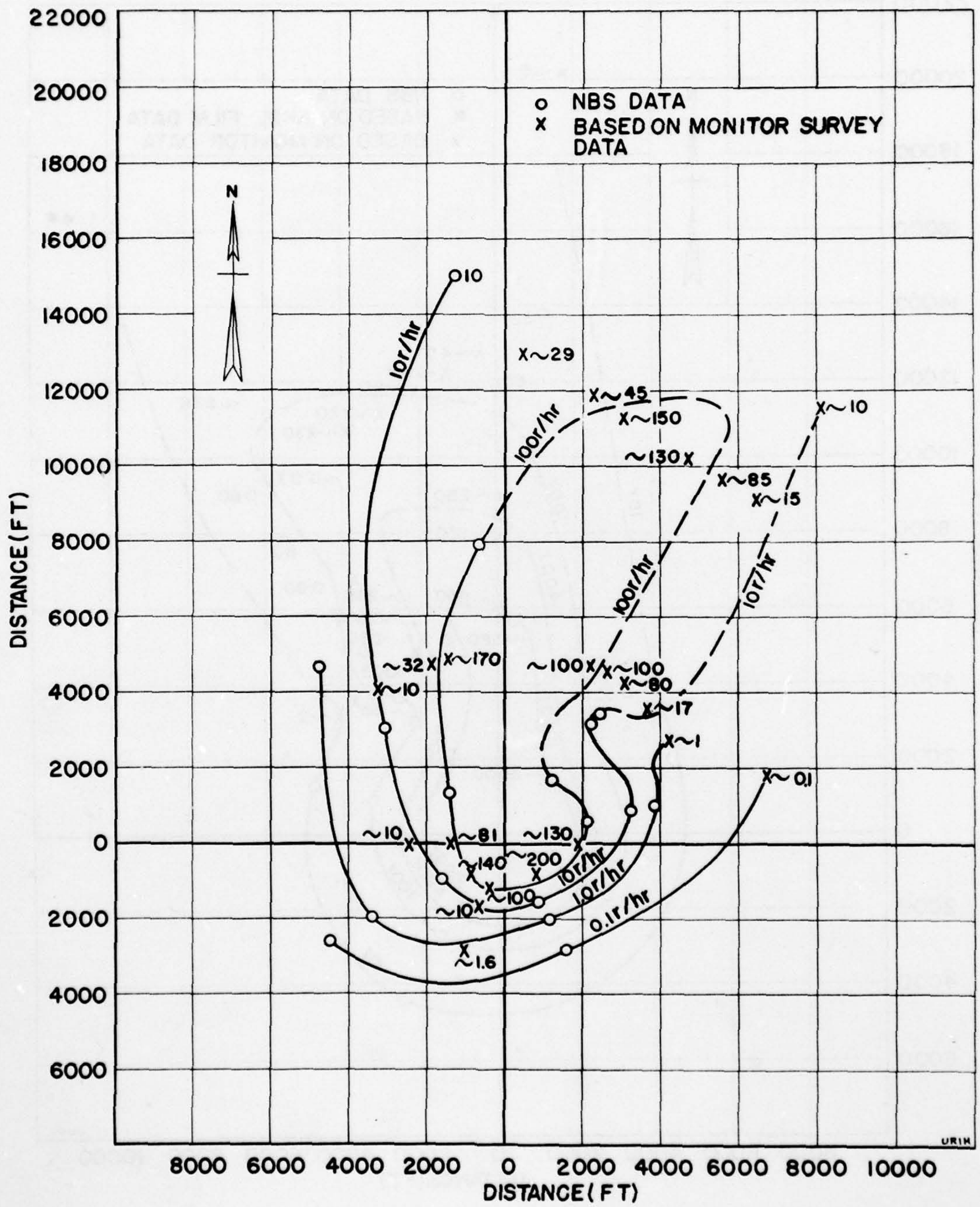

Fig 6.21 Underground Burst, Iso-Rate Contours at 1 Hour

[redacted] UNCLASSIFIED

derived. The total dose curves do not include the dose occuring within the first 0.1 second. However, analysis of Malik's preliminary data shows that for the underground burst the total dose received within the first one-tenth second is about 10% of that received between 0.1 second and 1.0 second. Also, based on Malik's preliminary airburst data, it is concluded that for the surface burst the total dose received within the first 0.1 second is slightly less than that received between 0.1 second and 1.0 second. Total doses at 10 seconds for the surface and underground bursts are shown for comparison in Fig 6.13.

6.4 CONTOURS

Iso-dose and iso-rate contours are shown on Figs 6.14 through 6.21. These curves are derived from the curves of Fig 6.1 through 6.12 supplemented by monitor, dosimeter and film data. The iso-dose contours are for 10 minutes, one hour and ten hours. The iso-rate contours are for one hour only. Areas included within the iso-dose and iso-rate contours are listed in Appendix E.

The contour areas shown in Figs 6.14 through 6.16 and 6.18 through 6.20 and tabulated in Appendix E are somewhat low since they do not include the dose received within the first one-tenth second. The resulting displacement of the total dose contours varies from a fraction of one percent in the downwind direction on the surface and underground bursts to a maximum of 3% in the crosswind and upwind directions on the surface burst. For the underground burst, the total dose contour maximum displacement from this cause is about 2.4% in the crosswind and upwind directions. The corresponding increases in total dose contour areas resulting from consideration of the dose received in the first one-tenth second amounts to about 8% for the surface burst and 6% for the underground burst.

6.5 MONITOR DATA

Monitor data obtained by various parties showed considerable disagreement. However, it did provide an order of magnitude check and was useful in extending some of the curves. Monitor data points are shown on Figs 6.1 through 6.12.

Most of the monitor data was taken with Tracerlab type T-1-B, ionization chamber type, survey meters which show some energy dependence and some directional dependence. However, the errors due to energy and directional dependence do not exceed 15% which is less than the overall accuracy of the monitor readings.

6.6 ACCURACY

The maximum error in dose rate and total dose, assuming no energy dependence, is considered to be about 25% with the mean error appreciably less. The error consists of an estimated 10% instrument error (Section 3.11), a six percent calibration error (Section 2.4), and additional errors, not readily evaluable, resulting from the exigencies of field operations.

The energy dependence curves of Figs 2.5a and 2.5b show an appreciable drop in detector response below 90 kev for the standard detector, below 80 kev for the high sensitivity detector, and below 60 kev for the T-1-B survey meter. In determining the corrections due to the detector energy response, the curves of Fig 20 of the Project 2.4c report dated 20 April 1952 were converted to equivalent roentgens per unit time as a function of energy by multiplying the gamma ray flux density by the energy and by the true absorption coefficient for air. It was arbitrarily assumed that the dose rate contribution above 700 kev was equal to that betwen 250 and 700 kev. This data, considered in conjunction with the curves of Fig 2.5a, was used to calculate the energy dependence correction factors for the residual radiation. The correction factors thus obtained were 1.3 for the standard detector and 1.2 for the high sensitivity detector. (Section 2.2 lists the types of detectors used in the various stations.) Similarly, consideration of Fig 2.5b gives an energy dependence correction factor of 1.1 for the T-1-B survey meter for the residual radiation. The energy dependence corrections have not been applied to the data in this report because of the large uncertainties in the spectral distribution and because the correction factors are appreciably less at early times at close in stations where the high energy radiation contribution is significant. Where the high energy contribution is less than that upon which the above correction factors have been based, the correction factors will be increased. However, in the most pessimistic case, assuming a complete absence of any contribution above 250 kev, the energy dependence correction factors are increased by only 2%. On the other hand, where the high energy contribution exceeds that upon which the energy dependence correction factors have been based, these factors are decreased. The correction factors listed above can, therefore, be considered to be maximum values.

As mentioned in Section 6.4 the total dose contour areas do not include the dose received in the first one-tenth second. The effect of the first one-tenth second dose is to increase the contour areas by about 8% for the surface furst and 6% for the underground burst. The maximum error in contour areas due to energy dependence of the detectors is about 9%.

Because of the limited number of NBS stations, it was necessary to supplement the station data with monitor and film badge data in

order to plot the contours. The accuracy of the contour areas is limited by the questionable accuracy of this supplementary data. However, since total dose and dose rate decrease rapidly with distance, large errors in total dose and dose rate produce small errors in contour area. With due consideration to all of the above factors, the contour areas are considered to be accurate to within 25%.

6.7 CONCLUSIONS

No conclusions are drawn in this report since the bursts were not of operational size. Significant conclusions can be drawn only after the data presented herein has been scaled to operational size weapons. The scaling and subsequent analysis of the scaled results is to be accomplished by the Armed Forces Special Weapons Project.

CHAPTER 7

RECOMMENDATIONS

7.1 INSTRUMENTATION

As mentioned in Section 2.1, scintillation detectors similar to those developed for Operation GREENHOUSE were used since time did not permit investigation of other types of detectors. Scintillation detectors have several disadvantages including the high voltage requirements, the large variation in gain with small changes in high voltage, the fatigue effects, the shielding requirements, etc. The expenditure of considerable effort and material was therefore necessary to properly utilize the scintillation detectors for this project.

It is recommended that the ionization type detectors be investigated for possible future use. However, it should be pointed out that there are difficulties such as recombination losses and sensitivity problems associated with ionization chambers. It is suggested that the SANDSTONE report on gamma measurements with ionization chambers be studied.[1] Another possibility is presented by the halogen type Geiger-Mueller counters in which the current is a function of radiation intensity.

The conversion of radiation intensity data to frequency variations is a highly satisfactory procedure provided that suitable circuits are developed that do not have severe voltage stability requirements. Though other conversion schemes may be simpler, the ease with which FM data can be transmitted and recorded and the high accuracy with which it can be readout are compelling arguments for the use of an FM system.

The continued use of simultaneous visual readout and magnetic recording is recommended. However, the recording should be limited to that period during which time resolution requirements or inability of personnel to man the recording station preclude the use of visual readout. In this connection it should be stressed that the advantages of visual readout are sufficient to warrant transmission over considerable distances, if necessary, to permit personnel to man the recorder station. By use of visual readout the necessity for recording over a long period is eliminated. The recorder speed can therefore be increased considerably resulting in improvement in frequency response and short time resolution. It is suggested that a recorder speed of no less than two inches per second be used.

---

[1] F. R. Shonka and G. S. Pawlicki, Report of LAJ-5 on Gamma Measurement, (Secret), 1 September 1948.

7.2 FIELD OPERATION

Considering the size of this operation, a relatively small crew was used in both the development and field work. Since most of the field crew participated in the development work, the personnel were well trained and thoroughly familiar with the equipment. This was of considerable importance in the successful completion of the project since the crew was able to work at high efficiency without the confusion associated with a large group. The continued use of small, highly trained crews is strongly advised. Sufficient time should be allowed for the field installation so that the schedules are not upset by the inevitable delays resulting from equipment failures, weather, and the other unpredictables that invariably arise.

Because of the difficulties associated with field work, considerable advance planning is advisable. As much of the work as can feasibly be completed prior to the field operation should be accomplished in the laboratory. The number of components to be assembled in the field should be reduced to a minimum by advance assembly. This policy was adhered to in this operation even to the extent of shipping kits containing the exact hardware, cables, and hook-up wire (cut to size, stripped, and tinned) for each pit. Such planning contributed appreciably to the high efficiency obtained in the field.

Shipments should be made early and preferably by sealed vans that are met at their destination by members of the field crew. The project group must assume complete responsibility for receiving supplies.

The crew should work in small groups. In general, two man groups are the most efficient. Safety considerations preclude the use of one man working groups.

Adequate transportation is a necessity. A ten man crew operating at maximum efficiency requires six or seven vehicles. Vehicles should be permanently assigned to the crews and proper steps taken to avoid pirating of vehicles.

Base camps should be located close to the test area. Travel time between Camp Three and the test area was excessive. The use of small advance base camps would add materially to working efficiency.

[redacted]

APPENDIX A

CRYSTAL CALIBRATION DATA

The various crystals were calibrated in the laboratory to determine the amount of radiation received from the Co^{60} source. This dosage rate was then used as a constant in the actual field calibration of the instrument.

It was found that the crystals had to be individually calibrated from a consideration of the geometry involved. The Co^{60} could not be positioned with the same geometry from crystal to crystal, but for a given crystal the geometry was reproducible. The crystal was exposed to radiation from the 1400 KV X-ray tube and the detector output measured. The dose rate at the crystal was carefully measured with a 250 r Victoreen thimble chamber. The same crystal was then exposed to the Co^{60} source and the detector output again measured. From these two detector readings and the chamber reading the effective radiation on the crystal was easily found. The sensitivity of the detector used to measure these crystal outputs was kept low and the phototube was selected to minimize errors due to fatigue of the tube. The detector outputs were measured with a Rubicon Potentiometer. This method of calibration bases the sensitivity of the unit in the field on the X-ray beam from the 1400 KV tube.

The results of this laboratory calibration are shown in Table A.1 which lists crystal calibration constants in roentgens per second.

In order to make possible more flexible field calibration which involved use of a different source in calibration than was used in the laboratory, several crystals were calibrated with two sources and a correlating factor that repeated itself to within about 8% was determined. This measurement showed source B to be effectively 4.2 times as strong as source A.

[redacted]

[redacted]

PROJECT 2.1a

TABLE A.1

Crystal Calibration

Source A and Crystal Series A

Crystal No.	r/sec.	Crystal No.	r/sec.	Crystal No.	r/sec.
A1	4.115	A18	4.11	A34	4.11
A2	3.96	A19	3.96	A35	4.421
A3	4.296	A20	4.16	A36	3.98
A4	4.27	A21	4.083	A37	4.18
A5	4.37	A22	4.26	A38	4.084
A6	4.16	A23	4.32	A39	4.39
A7	4.04	A24	4.27	A40	4.18
A8	4.102	A25	4.19	A41	4.00
A9	4.065	A26	4.135	A42	4.31
A10	4.19	A27	4.47	A43	4.45
A11	4.06	A28	4.10	A44	4.10
A12	4.287	A29	4.214	A45	4.03
A13	4.345	A30	5.48	A46	4.225
A14	4.878	A31	4.02	A47	4.06
A15	4.02	A32	4.57	A48	4.02
A16	4.14	A33	4.051	A49	4.14
A17	4.126			A50	3.974

[redacted] [redacted]

[redacted]

PROJECT 2.1a

TABLE A.1 (Cont.)

Source B and Crystal Series B

Crystal No.	r/sec.	Crystal No.	r/sec.	Crystal No.	r/sec.
B1	17.30	B18	18.08	B34	17.96
B2	17.40	B19	19.90	B35	15.8
B3	19.48	B20	16.30	B36	17.12
B4	18.48	B21	18.68	B37	16.35
B5	17.50	B22	18.24	B38	17.05
B6	18.51	B23	16.79	B39	17.71
B7	18.42	B24	18.88	B40	18.98
B8	16.24	B25	17.45	B41	17.54
B9	16.8	B26	19.69	B42	17.71
B10	17.45	B27	18.50	B43	17.78
B11	16.54	B28	19.18	B44	17.76
B12	17.87	B29	18.45	B45	19.22
B13	18.62	B30	18.20	B46	17.25
B14	17.80	B31	18.79	B47	19.52
B15	16.77	B32	15.75	B48	17.58
B16	17.86	B33	19.10	B49	17.48
B17	18.22			B50	19.16

[redacted] [redacted]

[redacted]

APPENDIX B

CALCULATION OF DECADE FREQUENCIES, CURRENT VERSUS VOLTAGE CHARACTERISTICS, AND ERROR FACTOR

For the frequency range of 100 to 400 cycles per second, the corresponding period (1/f) is 10,000 to 2500 microseconds. The five decades cover a total of 26 volts. Assuming, that the effective diode biases are equal to the applied biases,[1] the voltages on the grid of V4 (Fig 3.2) corresponding to the various decades are as listed in the first two columns of Table B.1. The total change in period of 7500 microseconds (10,000-2500) covers 26 volts, giving 288.5 microseconds per volt. Since the first decade covers 6 volts, the frequency range is 10,000 to 8269 microseconds and the corresponding frequency range is 100 to 121 cps.

In the following discussion the symbols used are:

- I = current (microamperes)
- V = voltage (volts)
- f = frequency (cps)
- P = period = $10^6/f$ = (microseconds)

TABLE B.1

Calculation of Decade Frequencies

Decade No.	Voltage Range	Period (Microseconds)	Frequency (cps)
1	0-6V	10,000 to 8269	100 to 121
2	6-12V	8,269 to 6538	121 to 153
3	12-18V	6,538 to 4807	153 to 208
4	18-22½V	4,807 to 3510	208 to 285
5	22½-26V	3,510 to 2500	285 to 400

The total PMT current corresponding to the voltages at the tops of the various decades is given in Table B.2

The diode resistance has been taken as 300 ohms when the applied voltage exceeds the bias, and as infinite when the bias exceeds the applied voltage.

---

[1] Though this is not strictly true, the difference is small and does not affect the method of analysis used herein.

[redacted] [redacted]

TABLE B.2

PMT Current

(See Fig 3.2. All currents given in microamperes)

V	I through R9	I through R11	I through R12	I through R13	I through R14	I Total
6	.06	0	0	0	0	.06
12	.12	.50	0	0	0	.62
18	.18	1.00	5.0	0	0	6.18
$22\frac{1}{2}$	.225	1.38	8.75	49.5	0	59.9
26	.26	1.67	11.7	87.9	493	595.

The "Error Factors" (See Section 3.11 and Fig. 3.1) are as given in Table B.3.

TABLE B.3

Error Factors

Decade No.	Error Factor
1	$\frac{100}{f-100}$
2	$\frac{118.3}{f-118.3}$
3	$\frac{148.5}{f-148.5}$
4	$\frac{202}{f-202}$
5	$\frac{276}{f-276}$

The derivation of the Error Factor for decade number 4 is given below. Derivations for the other decades are similar.

From Tables B.1 and B.2, the two points listed below are obtained on the straight line relating the period to the PMT current:

I = 6.18 microamperes at P = 4807 microseconds

I = 59.9 microamperes at P = 3510 microseconds

The equation of the straight line that includes the above points is:

$$I = -41{,}500 \times 10^{-6}\, P + 206$$

since $P = 10^6/f$

$$I = \frac{-41{,}500}{f} + 206$$

$$\frac{dI}{df} = \frac{41{,}500}{f^2}$$

$$\text{Error Factor} = \frac{dI}{I} \div \frac{df}{f}$$

$$= \frac{dI}{df} \cdot \frac{f}{I}$$

$$= \frac{41{,}500}{f^2} \cdot \frac{f}{\dfrac{-41{,}500}{f} + 206}$$

$$= \frac{41{,}500}{f^2} \cdot \frac{f^2}{206f - 41{,}500}$$

$$= \frac{202}{f-202}$$

[redacted]

APPENDIX C

DETAILED PLANS LIST

The plans listed below are detailed drawings of the National Bureau of Standards signal converter and accessory equipment. The listing is for information only; but, if desired, the plans may be obtained from the NBS upon request.

Titles	Number
Relay Diagram	D-500-32-3
Circuit Diagram	D-500-34-3
Bill of Materials	A-500-39-1
Amplifier Type II	C-500-48-4
Master Control Board Type 13	D-500-57-3
Calibrator Type 12	C-500-56

Examples of the calibration and monitor forms used in field operations are also available upon request.

[redacted]

AD-A078 575 NATIONAL BUREAU OF STANDARDS WASHINGTON, D.C. 18/3, 18/8
OPERATION JANGLE. NEVADA PROVING GROUNDS,OCTOBER-
NOVEMBER 1951, GAMMA RADIATION MEASUREMENTS, COSTRELL, LOUIS
UNCLASSIFIED WT-370 01 APR 52 AEC

2 OF 4
AD A
078575

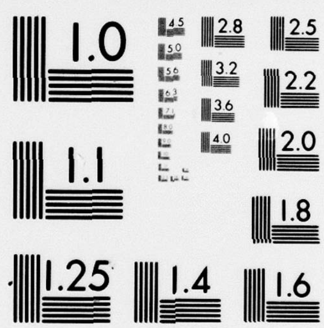

MICROCOPY RESOLUTION TEST CHART

APPENDIX D

<u>WIND</u> <u>DATA</u>

To aid in analysis of the contours presented in the text, the following wind velocity information is given.

TABLE D.1

Conditions at the Time of the Surface Burst

Height (ft)	Direction (Degrees)	Speed (mph)
0	190	2.3
6000	170	15.0
10000	200	36.8
14000	210	46.0

TABLE D.2

Conditions at the Time of the Underground Burst

Height (ft)	Direction (Degrees)	Speed (mph)
0	210	4.6
6000	190	5.8
10000	230	24.2
14000	250	28.8

APPENDIX E

AREAS WITHIN CONTOURS

The areas included within iso-dose and iso-rate lines on the various contours are shown in the tables below.

TABLE E.1

Surface Burst, Iso-Dose Contours at 10 Minutes

Value of iso-dose line (roentgens)	Included area (sq. miles)
400	greater than 0.6
100	" " 3.
10	" " 4.
3	" " 6.

TABLE E.2

Surface Burst, Iso-Dose Contours at 1 Hour

Value of iso-dose line (roentgens)	Included area (sq. miles)
10,000	0.10
1,000	0.38
400	1.0
100	greater than 3.
10	" " 6.

PROJECT 2.1a

TABLE E.3

Surface Burst, Iso-Dose Contours at 10 Hours

Value of iso-dose line (roentgens)	Included area (sq. miles)
10,000	0.10
1,000	0.43
400	1.2
100	greater than 3.
10	" " 6.

TABLE E.4

Surface Burst, Iso-Rate Contours at 1 Hour

Value of iso-rate line (roentgens/hr.)	Included area (sq. miles)
35	greater than 1
10	" " 3
5	" " 4
1	" " 6
0.1	" " 8

TABLE E.5

Underground Burst, Iso-Dose Contours at 10 Minutes

Value of iso-dose line (roentgens)	Included area (sq. miles)
400	0.70
100	1.9
10	4.2
1	greater than 6.

TABLE E.6

Underground Burst, Iso-Dose Contours at 1 Hour

Value of iso-dose line (roentgens)	Included area (sq. miles)
1,000	0.47
400	1.1
100	2.7
10	greater than 6.

TABLE E.7

Underground Burst, Iso-Dose Contours at 10 Hours

Value of iso-dose line (roentgens)	Included area (sq. miles)
1,000	0.70
400	1.4
100	3.0
10	greater than 8.

TABLE E.8

Underground Burst, Iso-Rate Contours at 1 Hour

Value of iso-dose line (roentgens/hr)	Included area (sq. miles)
100	1.7
10	greater than 5.
1	" " 7.
0.1	" " 8.

[redacted]

UNCLASSIFIED

OPERATION JANGLE

PROJECT 2.1b

GAMMA RADIATION AS A FUNCTION OF TIME WITH DROPPABLE TELEMETERS

by

EDWARD JAMES CARIS, JR.

and

JOHN H. TERRY
CDR., USN

April 30, 1952

DEPARTMENT OF THE NAVY
BUREAU OF AERONAUTICS
WASHINGTON 25, D. C.

NAVAL AIR DEVELOPMENT CENTER
JOHNSVILLE, PA.

UNCLASSIFIED [redacted] [redacted]

[redacted] UNCLASSIFIED

PROJECT 2.1b

UNCLASSIFIED

CONTENTS

UNCLASSIFIED [redacted] [redacted]

UNCLASSIFIED [redacted]

PROJECT 2.1b

CONTENTS (Cont)

UNCLASSIFIED

[redacted] [redacted]

[redacted]

PROJECT 2.1b

UNCLASSIFIED

ILLUSTRATIONS

UNCLASSIFIED

[redacted] [redacted]

UNCLASSIFIED

[redacted]

PROJECT 2.1b

UNCLASSIFIED

TABLES

UNCLASSIFIED

[redacted]

UNCLASSIFIED

PROJECT 2.1b

ABSTRACT

Five droppable telemetering units, AN/USQ-1, were emplaced at varying distances from the detonation points of each of the two shots of Operation JANGLE, the closest at 1,000 feet, the furtherest at 3,000 feet. They were monitored from 0 to + 15 minutes by ground- and air-based receivers, AN/ARR-29. The data obtained are exhibited as continuous curves of roentgens per hour versus time. Subsequent air drops of AN/USQ-1 units into the crater areas were unsuccessful. Recommendations are made for further development of the telemetering system.

CHAPTER 1

HISTORICAL BACKGROUND AND OBJECTIVES

1.1 HISTORICAL BACKGROUND

Operations CROSSROADS and SANDSTONE both indicated that radioactive contamination of the ambient surface would be a major hazard if an atomic detonation were to take place at low altitude over land or at shallow depths in the sea.

The possibility of defining such contaminated areas by measurements in a low flying aircraft was soon suggested and during 1949 and 1950 two complementary sets of radiac equipment were developed by the Bureau of Aeronautics as a tentative answer to the problem. The first of these was the AN/ADR-4 surface-radiation survey equipment; the second was a telemetering system consisting of a droppable gamma intensity transmitter, AN/USQ-1, and a receiver, AN/ARR-29, descrived in the present report. The two types of equipment are to be regarded as complementary for reasons detailed in Chapter 5, Discussion.

The telemetering system was designed and developed under considerable time pressure in order to obtain some preliminary information on its performance in Operation GREENHOUSE. No time was available to test it thoroughly either in the laboratory or in the field. The number of drops made prior to Operation GREENHOUSE by Navy testing facilities probably amounted to 10 or 20 at most.

In Operation GREENHOUSE approximately twenty-five AN/USQ-1 units were dropped of which about 40 per cent operated successfully. The failures were largely due to mechanical difficulties following the high "g" impact on landing which prevented proper erection of the whip antenna.

Prior to Operation GREENHOUSE, and before the antenna erection difficulties were evident, the telemetering system was proposed for use in Operation WINDSTORM. The proposed project was subsequently incorporated in the program of Operation JANGLE, the scaled-down, continental version of WINDSTORM. Unfortunately, the few months between the termination of GREENHOUSE and the initial phases of BUSTER and JANGLE were insufficient to introduce any significant improvements in the AN/USQ-1. Indeed, the deterioration of available AN/USQ-1 units under the tropical conditions of Eniwetok required that available time be devoted to rehabilitation, i.e., to eliminating corroded connections, fungus accumulations, and the selection of the few batteries which had not been completely exhausted by high tropical temperatures.

1.2 OBJECTIVES

The objectives of the present project were two-fold:

(1) To measure the initial gamma intensity and subsequent fall-out intensity due to the atomic detonations proposed, at least as far as the time constant or response characteristics of the AN/USQ-1 units would permit. This measurement was to be accomplished by mounting a minimum of five AN/USQ-1 units on concrete blocks located radially outward from the zero points at intervals of about 250 feet. These units were to be monitored for the most part by a ground-based set of receivers and in part by receivers in the P2V-2 project aircraft circling nearby.

(2) To determine gamma intensity in and around the craters by dropping AN/USQ-1 units from the P2V-2 and monitoring them from the airplane. These units were to be dropped as soon as the cloud had dissipated and it was evident that no hazard to personnel on the ground was involved.

The use of a ground-based set of receivers to monitor the fixed units on the ground was primarily a carry-over from the plans for Operation WINDSTORM. WINDSTORM was planned for an Alaskan area in which the weather was characterized by rapid change from unlimited to zero visibility. It was therefore anticipated that a weather change might take place on shot days which would render flight operations impossible without delaying the detonation schedule. As a supplementary measure, therefore, a ground-based set of portable receivers was constructed utilizing a gasoline engine-driven electrical power supply which could be placed on elevated ground and used to monitor the fixed units regardless of the weather.

CHAPTER 2

INSTRUMENTATION

2.1 GENERAL

The radiac telemetering system consists of a droppable frequency modulated VHF transmitting unit AN/USQ-1 and a VHF radio receiver AN/ARR-29. These units are shown, respectively, in Figures 2.1 and 2.2. Block diagrams of their components and interconnections are shown in Figures 2.3 and 2.4. Tables 2.1 and 2.2 contain pertinent data.

The purpose of this system is to provide a means of measuring, with remote indication, gamma radiation present in locations inaccessible because of geographic, military, or radiological safety reasons. Determination of the relation between gamma intensity and time in such areas is of particular importance in planning military operations, such as amphibious landings.

2.2 AN/USQ-1 TRANSMITTER

A complete AN/USQ-1 unit consists of a detecting ionization chamber connected to a high frequency transmitter by amplifying and modulating circuits, a mechanical timer, batteries, an air brake device used to slow the speed of descent and reduce forward motion after launching, a crushable shock nose, and an erecting mechanism to bring the whip antenna into the vertical shortly after impact. These components are illustrated diagrammatically in figure 2.5.

2.2.1 Detecting Circuit

The gamma-data channel consists merely of an ionisation chamber and its associated d-c amplifier. The ionization chamber is constructed of 20 mil brass, one inch in diameter and two and one-half inches long. The d-c voltage output of the gamma-data channel is proportional to the gamma radiation incident on the AN/USQ-1 unit.

A detailed study of the response of the chamber to radiation of varying energy has not been made. It is known that the chamber has a peak response in the 100-250 kev range and that the response decreases to 500 kev, leveling off thereafter for higher energies. The chamber is directionally shielded by battery and other components when installed in the AN/USQ-1 case. It has been found, however, that the response changes very little when the AN/USQ-1 is rotated in the path of incident radiation. In addition, the AN/USQ-1 units are always calibrated in a fully assembled condition.

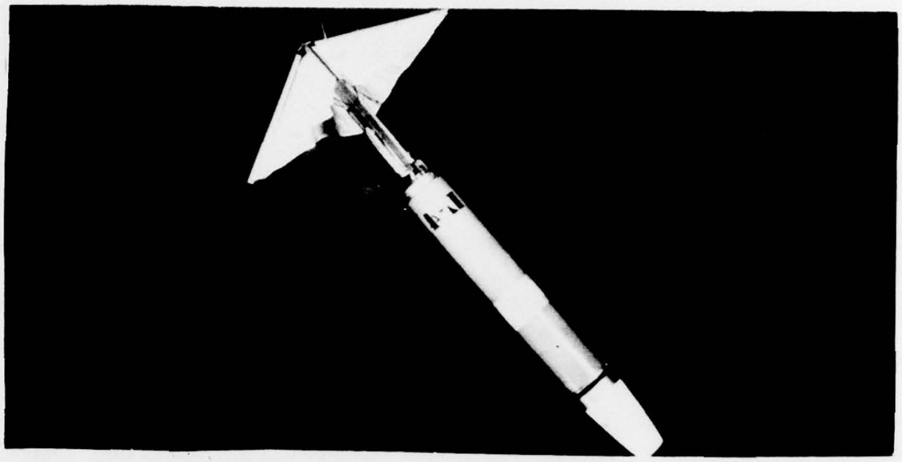

Figure 2.1 AN/USQ-1 Gamma Intensity Telemetering Transmitter

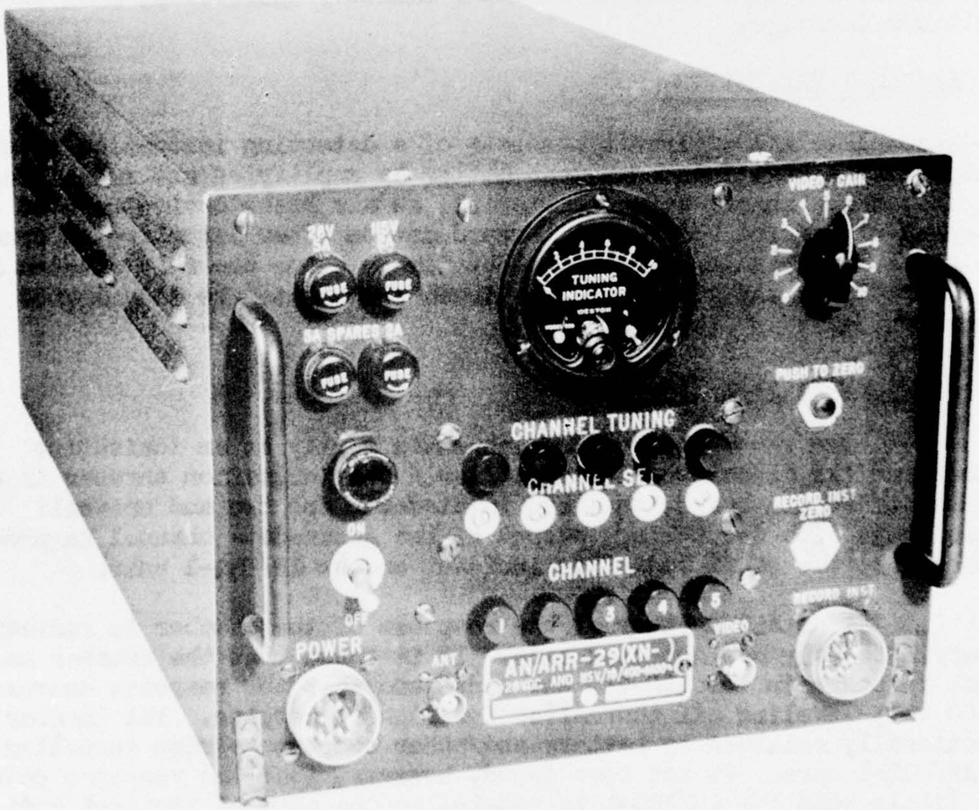

Figure 2.2 AN/ARR-29 Gamma Intensity Telemetering Receiver

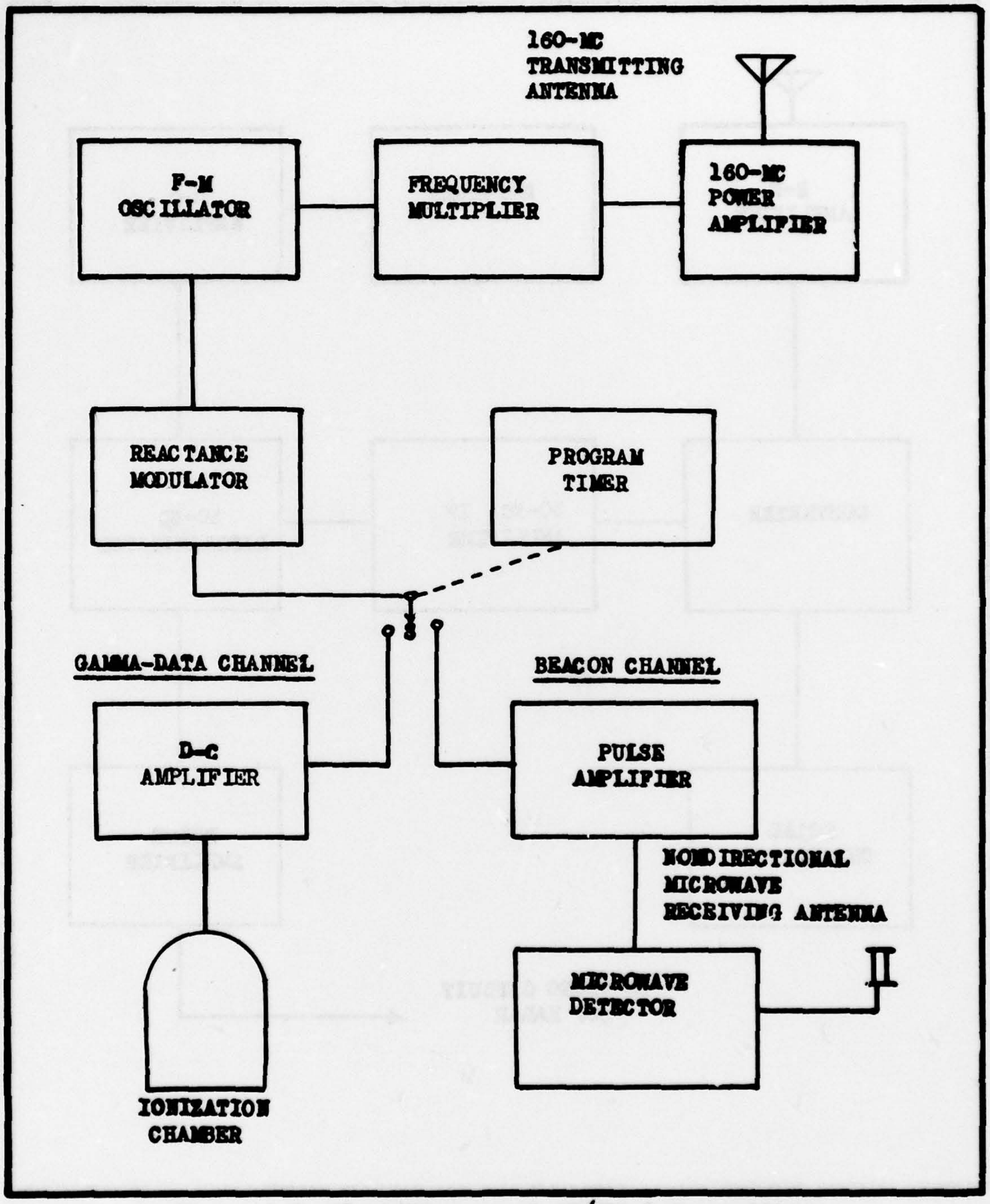

Figure 2.3 Block Diagram of AN/USQ-1 Transmitter

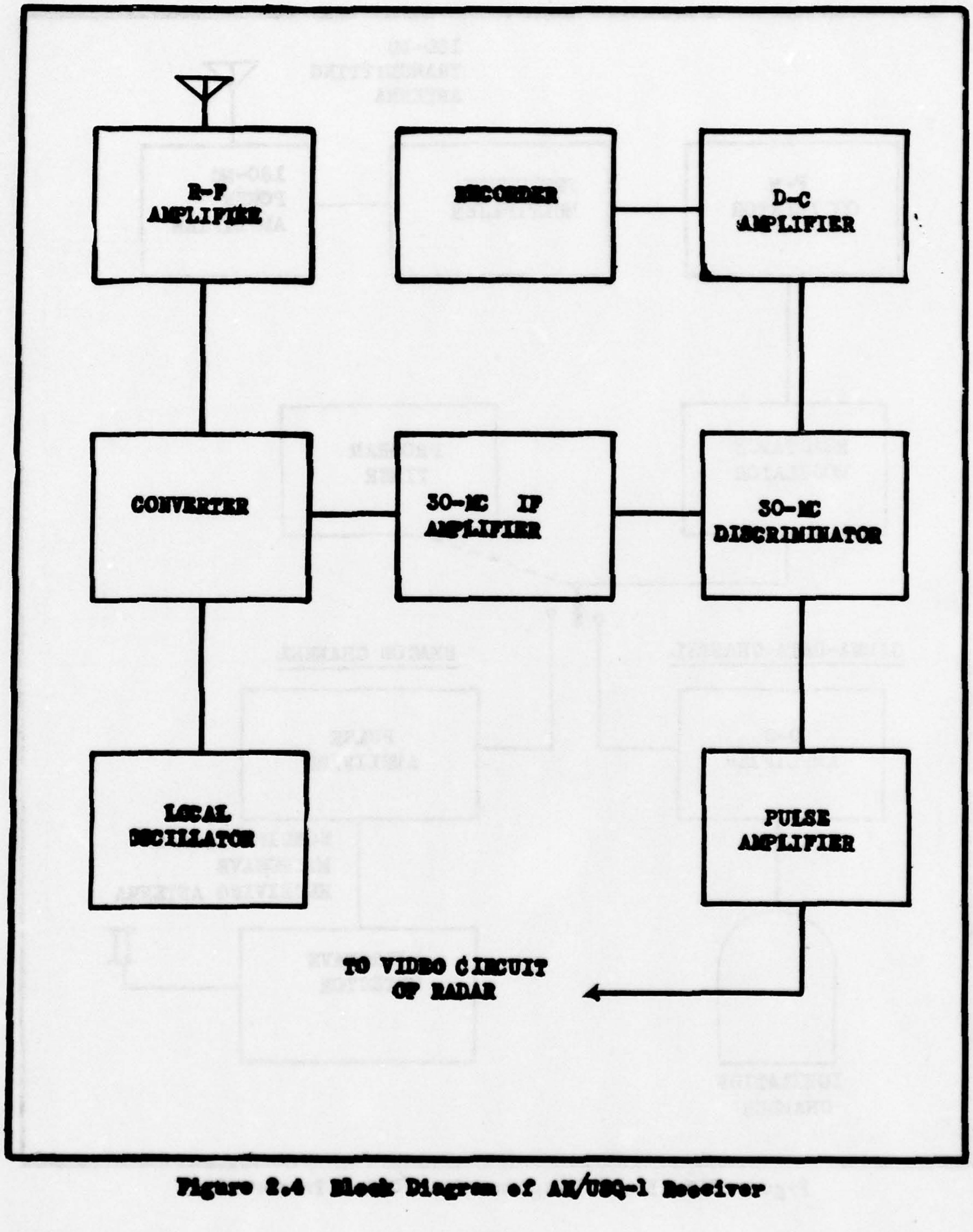

Figure 2.4 Block Diagram of AN/USQ-1 Receiver

PROJECT 2.1b

TABLE 2.1

Data for AN/USQ-1 Telemetering Transmitter

Physical Data	
Length (in.)	Approximately 40
Diameter (in.)	4 7/8
Weight (lb)	Approximately 14
Transmitting Frequency[a]	
Type A	162 mc/sec
Type B	164 mc/sec
Type C	166 mc/sec
Type D	168 mc/sec
Type E	170 mc/sec
Beacon receiving frequencies (cm)	8.5 and 3
Maximum recommended launching speed (knots)	150
Type radiation	Gamma
Range	0.5 to 500 r/hr (in two ranges)
Low range unit	0.5 to 17 r/hr
High range unit	13 to 500 r/hr

(a) Each AN/USQ-1 unit is preset at the factory

TABLE 2.2

Data for AN/ARR-29 Telemetering Receiver

Physical Data

Unit	Weight (lb)	Length (in.)	Width (in.)	Height (in.)
Receiver	25	21 1/4	10	7 5/8
Recorder	30	10	9 1/2	13

Power Requirements

DC	AC
None	115 v, 100 va 320-1,760 cps (Receiver only)

Miscellaneous Data

Radar video pulse output impedance . . . . 2000 ohms

Receiver frequency band . . . . 160-172 mc/sec

PROJECT 2.1b

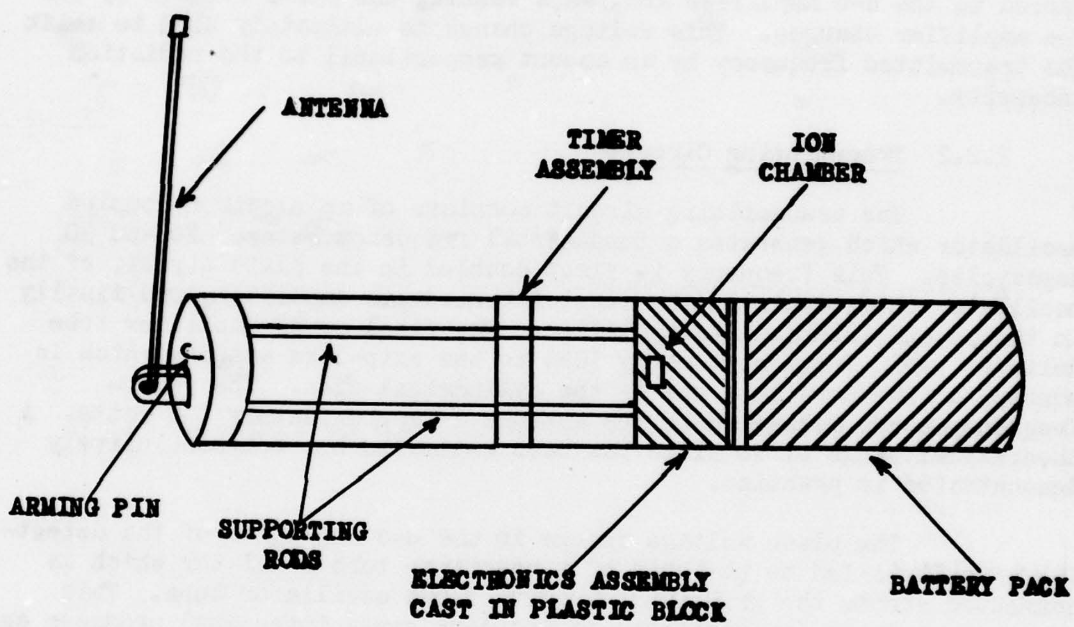

Figure 2.5 Cross-section of AN/USQ-1

[redacted]

The central grid of the ion chamber is connected directly to the grid of an electrometer tube and a high-valued resistor. The output of the electrometer tube is further amplified by a d-c amplifier. When the transmitter is exposed to gamma radiation, the air in the ionization chamber becomes ionized causing a minute current to flow in the grid circuit of the electrometer tube. The flow of grid current is transferred to the d-c amplifier and, as a result, the plate voltage of the d-c amplifier changes. This voltage change is ultimately used to shift the transmitted frequency by an amount proportional to the radiation intensity.

2.2.2 Transmitting Circuit

The transmitting circuit consists of an electron-coupled oscillator which generates a fundamental frequency between 20 and 30 megacycles. This frequency is first doubled in the plate circuit of the oscillator tube, again in the first intermediate amplifier, and finally in the second intermediate amplifier. The final power amplifier tube delivers radio-frequency energy (CW) to the whip-like antenna which is mounted on the parachute end of the cylindrical case. The radio-frequency-power delivered to the antenna is approximately 0.4 watts. A theoretical range of 20 miles has been estimated but not conclusively demonstrated in practice.

The plate voltage change in the d-c amplifier of the detecting circuit is fed to the grid of a reactance tube modulator which is connected across the grid tank circuit of the oscillator tube. This change in voltage (proportional to incident gamma intensity) produces an increase in the oscillator fundamental frequency. The transmitting unit then radiates a new frequency slightly higher than when not in a radiation field, the greater the gamma intensity, the greater being the frequency shift. The circuit is essentially linear and a gamma intensity of 500 r/hr will produce a maximum shift of 500 kilocycles in a normal unit.

It will be evident from the preceding discussion that the measurement of radiation intensity depends upon measuring the frequency shift of the oscillator relative to the frequency which would be transmitted in a radiation-free field. If, therefore, the radiation-free field frequency were to shift during the course of the measurements, the apparent relative shift of the radiation-modulated frequency would be in error. Clearly, some method must be introduced to check the radiation-free frequency at regular intervals to establish the "zero" position or reference level from which the radiation-modulated frequency is displaced. This check is accomplished by providing a timing mechanism which interrupts the modulating circuit at predetermined intervals and so permits the unit to send forth its radiation-free field frequency at corresponding intervals.

[redacted]

[redacted]

It is perhaps well to note here that a shift in the radiation-free frequency or "zero" position does not affect the actual displacement of the radiation-modulated frequency relative to that new "zero" frequency. For example, if the "zero" frequency shifts upward by one-half a megacycle, then correspondingly, the frequency in a 500 r/hr field will shift by one-half a megacycle. The point to the preceding discussion is that the shift of the "zero" frequency must be known if the radiation-modulated frequency shift is to be correctly measured.

The frequencies for which the AN/USQ-1 units are normally tuned are tabulated in Table 2.1. These represent radiation-free field frequencies. A unit tuned to 162 Mc will radiate on this frequency in a radiation-free field, shifting to a maximum of 162.5 Mc in a field of 500 r/hr for a normal unit.

2.2.3 Power Supply

Power for the AN/USQ-1 unit is supplied by a set of specially made batteries which provide 1.25 volts for filaments and 300 volts for plate circuits. In continuous operation, the battery voltage drops to about one-quarter of the initial value in about five hours with a corresponding decrease in transmission range of about one-half. For the intermittent operation for which they were originally designed, the AN/USQ-1 units would transmit five minutes out of every hour for forty-eight hours.

2.2.4 Timing Mechanism

The timing mechanism of the transmitting unit utilizes a self-winding electric clock which rotates various cams. These cams cause microswitches to operate and thus to turn on various sections of the transmitter at the proper time. The timing mechanism is located directly above the resin block in which the electronic circuits are potted.

2.2.5 Launching Method

The AN/USQ-1 unit is normally launched from the tail of the dispensing airplane in order to minimize aerodynamic difficulties. Immediately on leaving the airplane, an arming pin is pulled and the unit's electrical power and clock mechanism are thereby turned on. A small air brake rapidly slows the unit and permits greater accuracy in delivering it in a specified area than would be possible with a parachute. The air brake is automatically jettisoned on impact with the ground.

The electronics equipment is protected from damage due to landing shock by encasing the entire circuit assembly in plastic material. The acceleration experienced by the unit upon landing on

[redacted] [redacted]

concrete is approximately 2,500 g. The construction and encasing techniques used are similar to those employed in the proximity fuze.

In addition, a nose made of cellular cellulose acetate is affixed to the front of the unit to absorb the shock of landing. This nose is crushed and normally falls away from the unit.

After impact, two sets of coiled leaf springs snap out and cause the unit to come to rest. A gravity mechanism then comes into play which is intended to bring the whip antenna into a vertical position. The failure of this mechanism to operate properly has been a major source of trouble with the present AN/USQ-1 unit.

Figure 2.6 shows a properly functioning AN/USQ-1 unit immediately after being dropped from the project airplane.

2.3 AN/ARR-29 RECEIVER

The AN/ARR-29 receiving and recording equipment is basically a conventional f-m receiver equipped with an Esterline-Angus ink recorder. The receiver incorporates push-button tuning for five channels. Each channel is provided with a fine tuning control which is used in conjunction with a tuning meter to tune in accurately the incoming frequency during the radiation-free field transmissions of the AN/USQ-1 unit being monitored. As noted previously, this procedure affords a method of "zeroing" the amount of frequency displacement due to the radiation field.

The channel push buttons and associated circuits have been so designed and constructed that on depressing a button, not only does the channel change but indications are made on the right edge of the recorder paper to indicate which channel is being recorded. Timing markers appear on the left edge of the recorder paper to determine the relation between radiation intensity and time.

2.3.1 Receiving Circuit

The receiver contains two grounded-grid radio-frequency amplifiers stagger-tuned for stability and wide band pass (10 Mcs). The local oscillator is of the electron-coupled type and operates 30 Mcs below the received signal. Since the radio-frequency amplifiers are fixed tuned, tuning to the five different channels is accomplished by changing the frequency of the local oscillator with push buttons. Fine tuning is possible with a vernier capacitor.

Figure 2.6 AN/USQ-1 After Drop From Aircraft

Frequency conversion or heterodyning of the received signal and local oscillator frequency is accomplished by coupling the local oscillator signal and the radio-frequency fed to the grid of the mixer tube.

The plate circuit of the mixer stage and the intermediate amplifiers are tuned to the difference frequency of 30 Mcs. (local oscillator frequency subtracted from received signal frequency). The intermediate frequency stages have a band pass of about 2.4 Mcs at the half-power points. The wide band pass is obtained by leading both the primary and secondary winding of the intermediate frequency transformer with a resistance of 15,000 ohms.

Only one limiter stage is used. Limiting is accomplished in the last intermediate frequency stage by grid rectification. The discriminator which detects or demodulates the received signal is a conventional Foster-Seeley type of circuit.

The d-c output of the discriminator is fed to a balanced d-c amplifier which in turn drives the pen of the recorder. The receiver also has a timer which sends a voltage every five minutes to the recorder to operate an auxiliary pen for time marks.

The timer is accurate at least to the half-second. In practice, the paper speed of the recorder, normally four inches per minute, is checked at frequent intervals with a stop watch.

2.4 MODIFICATIONS FOR OPERATION JANGLE

The modifications entailed by the requirements of the present project were somewhat more extensive than had originally been anticipated:

(1) The permissible gamma intensity range of the AN/USQ-1 had to be increased from a maximum of 500 r/hr to a maximum of 50,000 r/hr and the units calibrated in that range.

(2) The timing cycle had to be changed from intermittent to delayed continuous operation.

(3) The negative frequency drift incident to continuous operation had to be corrected as far as practicable.

(4) Provisions had to be made to permit remote starting of the units.

(5) The radiation-free field frequencies had to be changed and new frequencies selected to minimize interference from other transmissions in the congested 160-170 Mc band.

(6) A mobile cart had to be constructed and equipped with two gasoline engine-driven generators and three AN/ARR-29 receivers to permit reception in the field a few miles from the point of detonation.

(7) For each shot, five telemetering units had to be mounted on specially designed concrete blocks spaced at intervals radially outward from the zero point.

2.4.1 Increase in Intensity Range

Thirty AN/USQ-1 transmitting units were set aside for ground based measurements and modified in accordance with the following program:

Intensity Range	Number of Units
0-500 r/hr (no change required)	10
0-5,000 r/hr	10
0-50,000 r/hr	10

The first approach to increasing intensity range was to evacuate the ionization chambers sufficiently to reduce resultant ionization at high intensity levels. Tentative objectives were one-tenth of an atmosphere for the 0-5,000 r/hr range and one-hundredth of an atmosphere for the 0-50,000 r/hr range.

To accomplish the desired evacuations, a vacuum pumping system was designed utilizing components on hand in the laboratory. It consisted of a mercury diffusion pump in series with Hi-Megavac oil pump, a large tank and needle valves, plus accurate vacuum-measuring instruments.

The technique used was to drill into the ionization chamber and solder a soft copper tube and flange assembly to the brass base of the ionization chamber. The short tube was then soldered to a long copper tube leading to the large vacuum tank. The system enabled the ionization chambers to be reduced to pressure levels as low as eight microns of mercury. Many chambers were evacuated to various degrees of vacuum.

The evacuated chambers were tested by exposing them to known gamma intensity fields and measuring the amount of frequency shift produced in the transmitter. Intensity versus frequency deviation curves were plotted for many degrees of vacuum. During these investigations it was learned that the range of an ionization chamber is not doubled by decreasing the pressure in the chamber by one half; i.e., the intensity range is not a linear function of gas pressure within the ionization chamber.

A pressure of 30 microns of mercury was necessary to increase the intensity range to 0-50,000 r/hr. Four units were evacuated to this pressure and sealed. After allowing the units to stand for 24 hours, they were again checked against known gamma intensity fields. The results indicated loss of vacuum. The loss was found to be due to the diffusion of air molecules from the resin casting, in which the detector circuits were potted, coming through the rim of the polystyrene cap which constituted the inaccessible end of the ionization chamber. Further efforts to investigate the evacuation technique were abandoned for the following reason: The AN/USQ-1 ionization chamber was designed to operate at atmospheric pressure and none of the seals throughout were made with a view to maintaining sustained pressure differentials. It was therefore evident that, if the evacuation technique were to be use, a minor redesign would be necessary to secure effective seals throught. Such a modification would involve removal of the circuits from the potting compound, work to secure better seals, followed by repotting to resist shock, and accomplish with great care to retain the high impedance properties of the final assembly. It was considered simpler to adopt the second approach outlined below.

The second approach to increasing intensity range was to cut into the plastic material in which the electrometer circuit was embedded and change the value of the high megohm resistor. (See Figure 2.7.) This approach looked feasible provided the high insulation properties of the electrometer circuit were not destroyed in the process.

The electrometer circuit consists of a 333 megohm resistor, 3 subminiature tubes, and several capacitors and resistors. These elements are housed in a silver-plated box which is filled with a mineral wax (ceresin) whose resistivity is about 10^{14} centimeter-ohms. The wax is nonhygroscopic and insures good insulation for the sensitive electrometer circuit which generates and amplifies a current of about one-thousandth of a microampere for a 500 r/hr unit and about one-tenth of a microampere for a 50,000 r/hr unit. Leakage paths and moisture cannot be tolerated in such a circuit.

In order to enter the electrometer circuit, it was necessary to mill the resin casting away from the top of the electrometer housing. The housing was then cut by a small vertical milling tool, thus exposing the ceresin wax covering the electrometer components. The transmitter casting was then mounted upside down and illuminated with an infrared lamp. The wax melted and drained from the housing.

The value of the 333 megohm resistor was changed to 30 megohms for the 0-5,000 r/hr units and the test unit was checked against a known field intensity to determine the multiplying factor. The unit worked satisfactorily and the desired multiple factor of ten was obtained. The unit was repotted with the special wax and completely resealed.

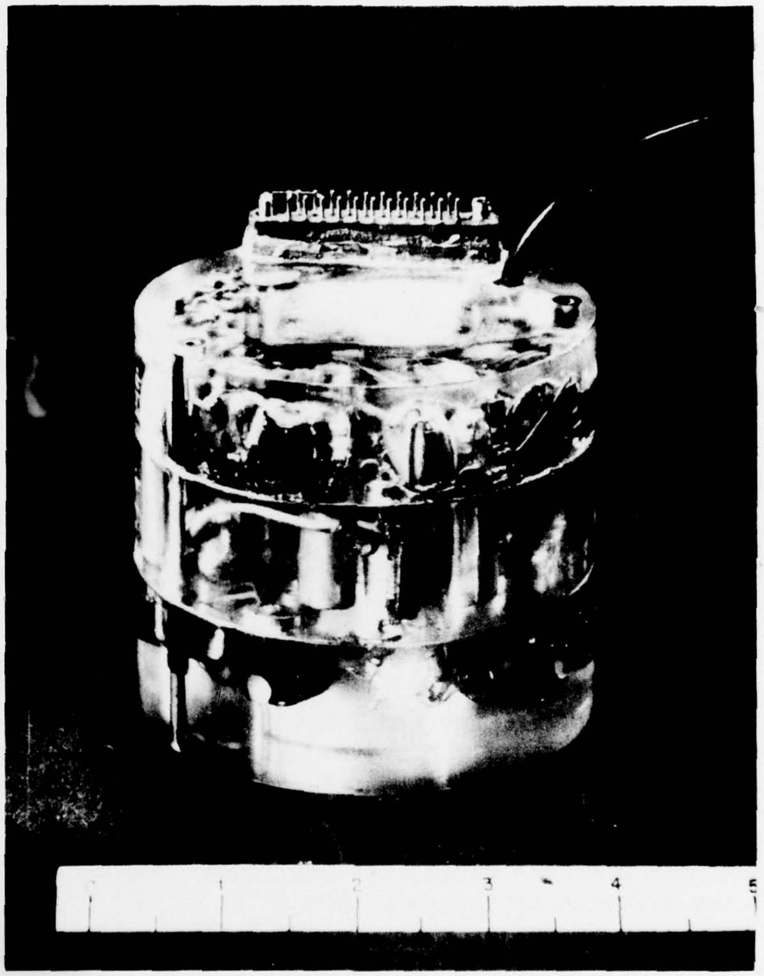

Figure 2.7 Electronic Circuits Embedded in Plastic

Further check indicated some leakage, giving a final multiplying factor of about nine.

The same long and tedious procedure was followed in obtaining units in the 0-50,000 r/hr range. The humidity of the laboratory was held as low as possible (about 20 per cent relative humidity). The handling of all electrometer components was effected with tweezers. After insertion of the new resistor (3 megohms), the repotting was done with extreme care. A blast of dry air passed over dry ice was used to solidify the liquid wax so that none would drain into the ionization chamber through the rim of the polystyrene seal. All units were repotted, sealed, and checked against known fields of high intensity.

2.4.2 Calibration

The low range 0-500 r/hr AN/USQ-1 units were calibrated at the Naval Air Development Center, Johnsville, Pa., using a thirty-curie Co^{60} source. An approximate calibration of the intermediate and high range units was made with the same source in order to determine the evacuation necessary for high ranges in the first approach and to determine the resistor size necessary for high ranges in the second approach. These two or three centimeters from the source with consequent poor geometry. The calibration of the intermediate and high range units was therefore checked by using a collimated beam from high power x-ray equipment at the National Bureau of Standards.

The National Bureau of Standards x-ray equipment includes filters to secure monoenergetic radiation. The response was determined at radiation energies of 100 kev and 1 mev for dosage rates extending over the appropriate range of the units. Figures 2.8, 2.9, and 2.10 show the calibration curves obtained for each of the three ranges, the last two being determined at 1 mev on the Bureau of Standards x-ray machine. As indicated on the calibration chart, while the 50,000 r/hr units do have that possible range, the particular resistor value selected gave a full scale frequency change of 500 Kc at 43,000 r/hr. This rate was considered to be adequate, however, and further alteration of the resistor was not made. The tests determined the linear response of each unit, the exact multiplying factor resulting from the change of the high megohm resistor, and the radiation level at which the ionization chamber became saturated.

As previously stated, in paragraph 2.2.1, the energy response curves for the AN/USQ-1 are only approximately known. The Bureau of Standards tests verified the existence of a peak response in the 100-250 kev range. Since it was expected that the gamma radiation to be measured at the test site would lie in the 1 mev region, however, more extensive calibrations were not conducted in view of the limited time available.

[redacted]

PROJECT 2.1b

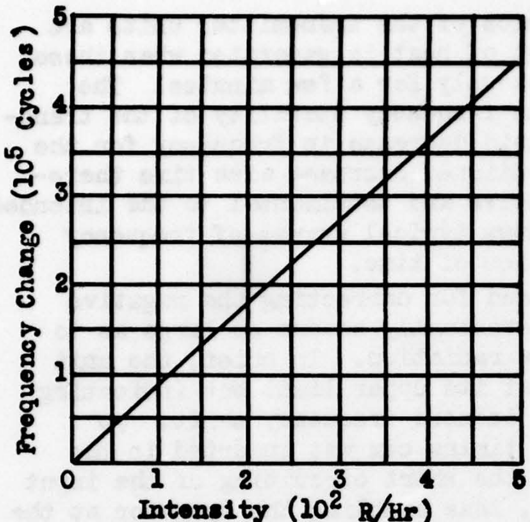

Figure 2.8 500 R/Hr Unit

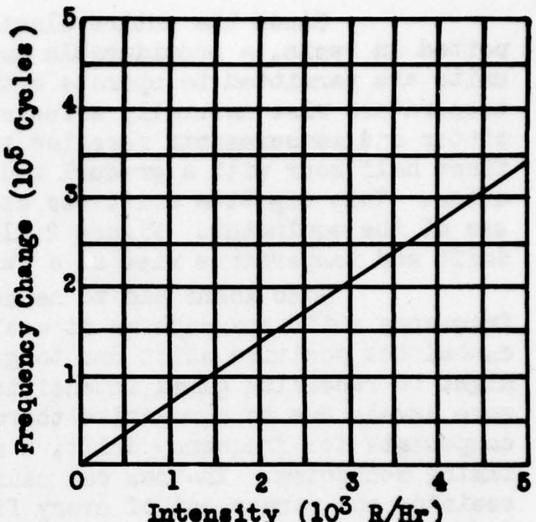

Figure 2.9 5,000 R/Hr Unit

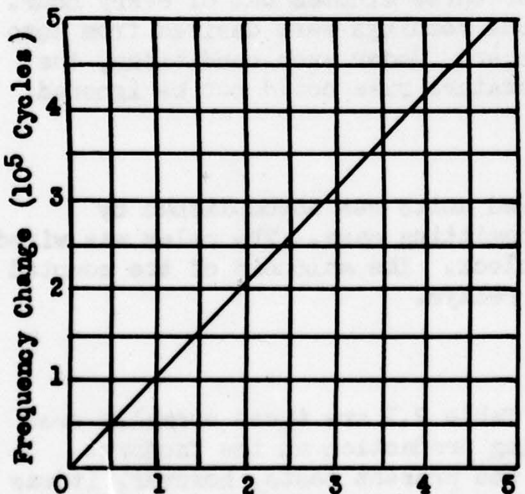

Figure 2.10 50,000 R/Hr Unit

NOTES

1. 500 R/Hr units calibrated against 33 curies of cobalt 60. 5,000 R/Hr units and 50,000 R/Hr units calibrated with Bureau of Standards x-ray equipment at one Mev.

2. Variation of all curves with radiation energy is negligible above 300 Kev.

Frequency Change Versus Roentgen/Hour for Three Ranges of AN/USQ-1

[redacted] [redacted]

2.4.3 Frequency Drift Correction

Since the entire electronics of the transmitter units are potted in resin, a considerable amount of heat is generated when these units are permitted to operate continuously for a few minutes. The temperature rise naturally affects the frequency stability of the transmitter and measurements revealed a rapid decrease in frequency for the first half hour with a gradual and continued decrease with time thereafter. This negative drift was excessive and detrimental to the intended use of the equipment. Figure 2.11 shows typical curves of frequency drift and temperature rise as a function of time.

Some means had to be devised for correcting the negative frequency shift inasmuch as it could eventually become so large as to cancel the positive shift due to gamma radiation. In brief, the unit might be receiving gamma intensities at its upper limit but indicating zero levels due to a negative thermal induced frequency shift. To compensate for frequency drift, a new timing cam was inserted in the timing mechanism. The new cam caused the short circuiting of the input resistor one minute out of every five, thus enabling the operator at the AN/ARR-29 receiver to "zero beat" his receiver units on the transmitter at regular intervals.

It is perhaps well to note that this problem of frequency drift was not quite as significant in Operation GREENHOUSE where the units were transmitting for only two or three minutes out of every hour. In Operation JANGLE, however, continuous readings were desired from zero time on to at least +15 minutes or longer. Under such conditions, the effects of heat accumulation and temperature rise could not be ignored.

2.4.4 Remote Starting

Remote starting of the fixed units was accomplished by mounting a 4 PDT relay inside the transmitting case. The relay was wired to two microswitches and an electric clock. The solenoid of the mounted relay was connected to the AEC timing relays.

2.4.5 Interference

The frequencies listed in Table 2.1 are those normally used by the AN/USQ-1. They are preset during production at the factory. During the course of preparations for the present tests, however, it was discovered that the 160-170 Mc band was being utilized by several other groups; e.g., radsafe field monitors and remote controlled "weasel" samplers. The 0.4 watts put out by the AN/USQ-1 were almost completely masked by radiation from there other systems and it was practically impossible to distinguish interference from legitimate signals. This difficulty was particularly marked due to the broad band receiving characteristics of the AN/ARR-29 receivers. Nevertheless, the units were

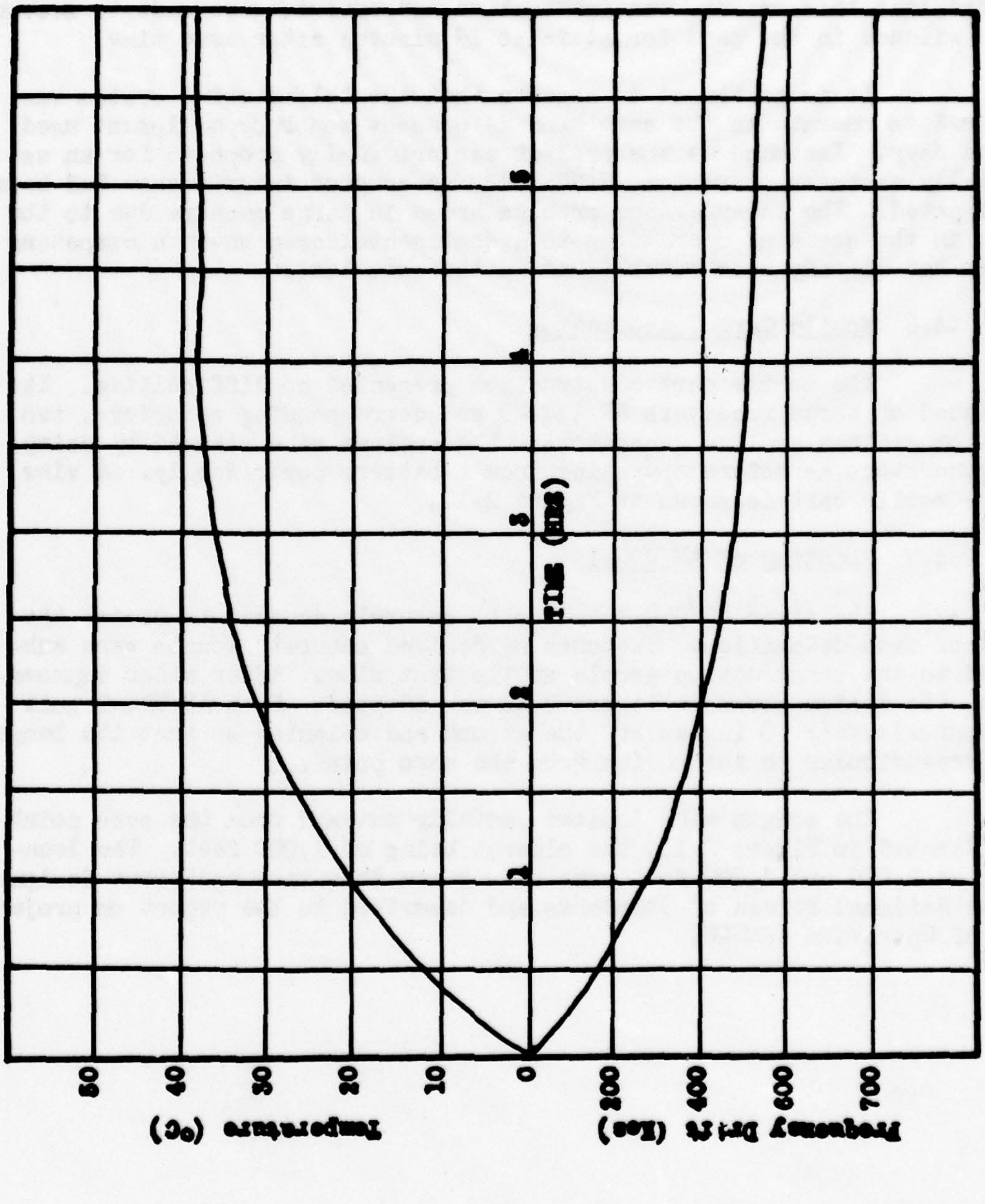

Figure 2.11 Frequency Drift and Temperature Versus Time for Continuous Operation of AN/URC-1 Units

modified, insofar as possible, to obtain new frequency emissions as far as possible from other interfering signals in the band. These new frequencies are listed in Tables 3.1 and 3.2. Subsequent experience demonstrated that this measure was ineffective and efforts were made to secure radio silence in the band for at least 15 minutes after zero time.

It is pertinent to observe that the telemetering system was designed to operate in the same band as present sonobuoy equipment used by the Navy. Inasmuch as the project was originally proposed for an essentially overseas operation, WINDSTORM, no serious interference had been anticipated. The interference problem arose in large measure due to the shift in the scene of operations to a continental area where a competing system had already been established in the same band.

2.4.6 Mobile Cart Construction

The mobile cart construction presented no difficulties. It consisted of three receivers AN/ARR-29 and corresponding recorders, two gasoline engines and two generators. The engines were started by using the generators as motors operating from a battery power supply. A view of the mobile cart is shown in Figure 2.12.

2.4.7 Mounting of AN/USQ-1

The fixed AN/USQ-1 had to be securely mounted to resist the shock of each detonation. Sketches of desired concrete mounts were submitted to the construction people at the test site. After minor improvements, the design shown in Figure 2.13 was adopted. Each AN/USQ-1 unit was approximately 30 inches off the ground and oriented so that its length was perpendicular to the radius from the zero point.

The mounts were located radially outward from the zero point as indicated in Figure 2.14, the closest being at 1,000 feet. The locations at 2,000 and 3,000 feet were near gamma dose rate equipment designed by the National Bureau of Standards and described in the report on project 2.1a of Operation JANGLE.

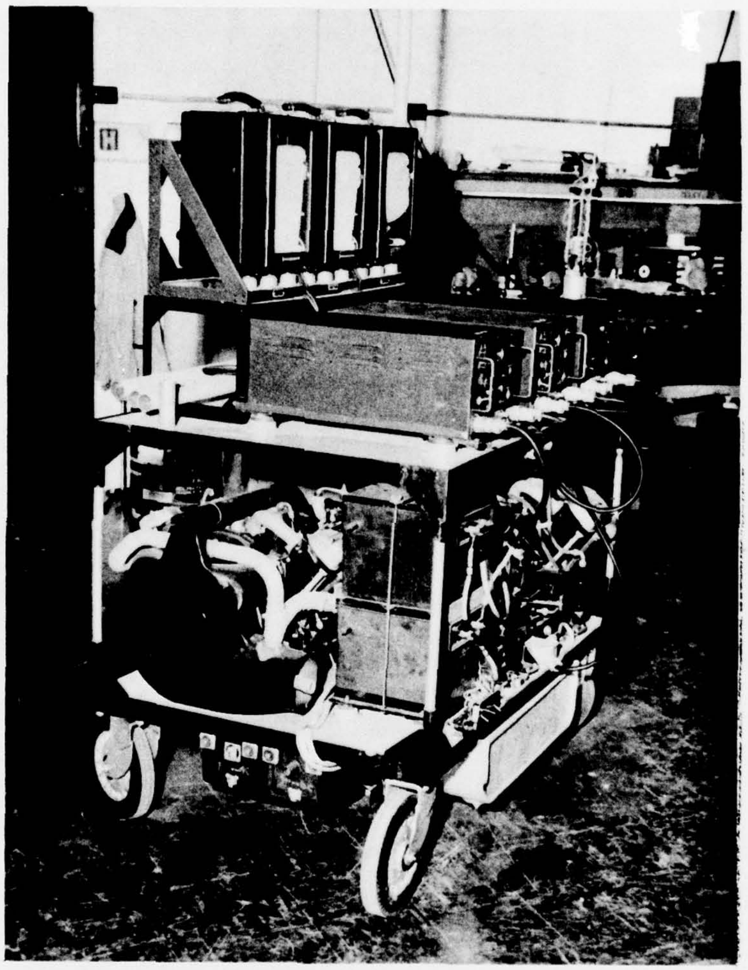

Figure 2.12 Mobile Cart for Ground-based AN/ARR-29 Receivers

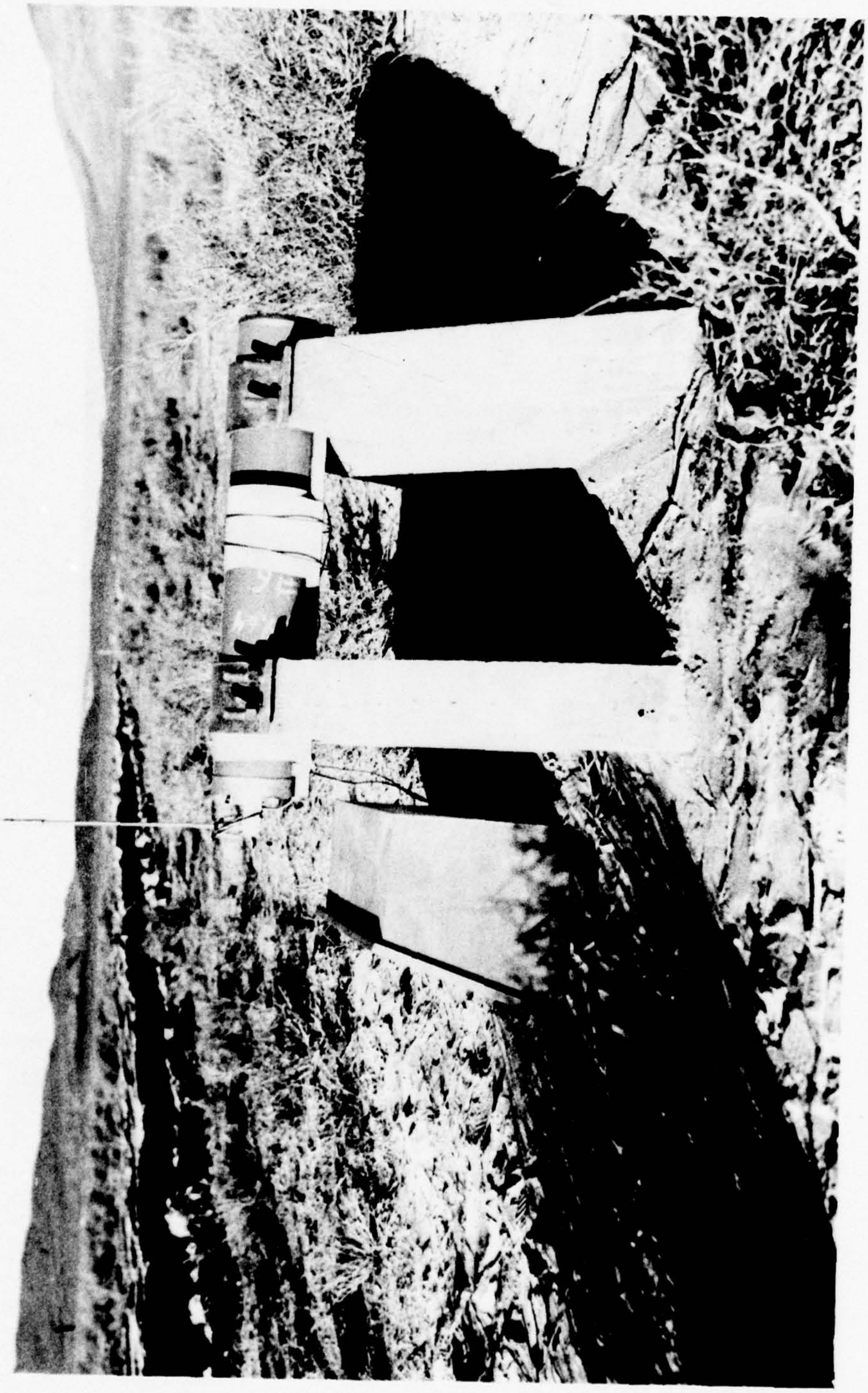

Figure 2.13 Ground-based AN/USQ-1 On Concrete Mount

UNCLASSIFIED

[redacted]

PROJECT 2.1b

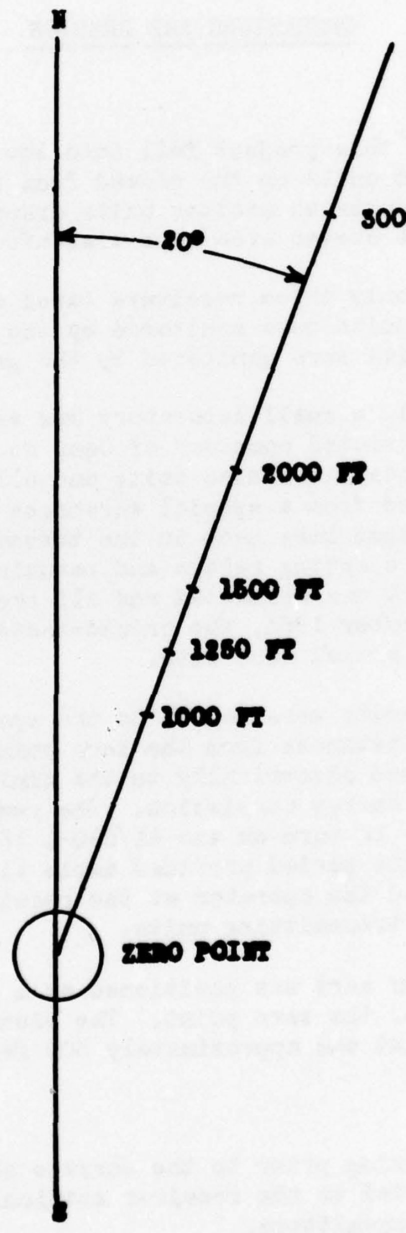

Figure 2.14 AN/USQ-1 Positions with Respect to Zero Point

[redacted]

UNCLASSIFIED

[redacted]

CHAPTER 3

OPERATIONS AND RESULTS

3.1 GENERAL

The operations of this project fell into two parts: (1) The monitoring of the fixed units on the ground from zero time on to plus fifteen minutes (2) Efforts to monitor units dropped from the project P2V-2 airplane into the crater area some time after the shot.

Since there were only three receivers based on the ground, two of the five fixed ground units were monitored by the P2V-2 circling nearby. The three innermost units were monitored by the ground-based receivers.

On 6 November 1951, a small laboratory was established in a Quonset hut located in the restricted compound of Camp No. Three at the test site in Nevada. The modified radiac units and all electronic testing instruments were removed from a special warehouse and transported to the laboratory. Final changes were made in the transmitting units, e.g., installation of remote starting relays and retuning to new frequencies. The mobile receiver cart was assembled and all receivers given a preliminary check. On 8 November 1951, the ground-based telemetering system was transported to the actual test site.

In the field the units were bolted to the special concrete mounts positioned at various distances from the zero point. The remote starting relays were connected electrically to the timing signal relays provided by the Atomic Energy Commission. The remote starting relay system made it possible to turn on the AN/USQ-1 15 minutes ahead of zero time. The 15 minute period provided ample time for the transmitters to warm up and permitted the operator at the receiver unit to zero beat the receivers with the transmitting units.

The mobile receiver cart was positioned on a sloping mountain side about five miles west of the zero point. The elevation of the receiving unit above the zero point was approximately 500 feet.

3.2 SURFACE SHOT

At 0600 in the morning prior to the surface shot, the operating personnel were transported to the receiver station. At 0645 the timing signal turned on the transmitters.

Great difficulty was experienced in receiving the transmitter carriers (radiation-free field frequency) due to the low sensitivity of the receivers. Nearby communication transmitters caused much interference

[redacted]

due to the broad band pass of the receivers. At times it was impossible to distinguish between the radiac transmitter signals and the interference.

At 0900 (zero time), the surface shot was detonated. The transmitters in positions one and two operated satisfactorily. The transmitter in position three failed shortly after detonation. Transmitters four and five, monitored by the P2V-2 project airplane circling nearby, were not picked up positively for several reasons:

(1) The range of the transmitters at altitude appeared to be of the order of three miles. At the further ends of the elongated flight path, the signal intensity faded out.

(2) The signal faded during banks. It was this difficulty that led to the elongated flight path. A circular orbit of smaller radius simply meant that the airplane was in a constant bank.

(3) Interference was present at altitude despite the radio silence on the ground. The origin of this interference is not known and is difficult to ascertain inasmuch as the line-of-sight range at altitude extends over a large area.

Transmitters one and two continued to transmit radiation intensities but the indications fell off rapidly during the 15 minute initial period. Although much effort was put forth to keep other transmitters off the air for at least 15 minutes, much interference was encountered making it impossible to record any further information at the end of 10 minutes. Radiation intensities recorded from transmitters one and two are presented in Figures 3.1, 3.2, and brief data from transmitter three in Figure 3.3. No data on transmitters four and five are available.

Since no data was obtained from transmitters four and five, no direct comparison could be made with the data obtained from Bureau of Standards dosimeters located nearby. (See project 2.1a report.) Transmitters one, two, and three were located much closer to the zero point than any of the Bureau of Standards dosimeters and, again, no direct comparison is practicable. This matter is discussed again in Section 4.4, Comparison of Data.

3.3 UNDERGROUND SHOT

On 27 and 28 November 1951, preparations were made to measure the gamma radiation from the underground shot. At 1145 on 29 November 1951 all the radiac transmitters came on and the receivers were adjusted to the carrier signals. At 1200 the detonation occurred. All but one radiac transmitter functioned satisfactorily. No interference from other transmitters was experienced until +15 minutes. Good data were

recorded for about 25 minutes after zero time. Radiation intensities recorded from units one, two, and three are presented in Figures 3.4, 3.5, and 3.6.

Aerial reception of unit four was good but no shift due to gamma radiation was apparent, i.e., it radiated only the radiation-free field frequency. Unit five was received only between +26 minutes and +40 minutes due to interference. It remained at a constant level of 16 r/hr during this period. No figures have been presented to illustrate the performance of these units.

The limited data obtained from transmitter five at 3,000 feet permits some comparison with the dose rate data obtained in project 2.1a of the National Bureau of Standards. This comparison is briefly made in Section 4.4, Comparison of Data.

3.4 AN/USQ-1 DROPPED FROM P2V-2

One of the two objectives of the present project was to drop a number of telemetering units into the crater areas and monitor them from the project P2V-2 airplane. Four units were dropped altogether without success, the basic difficulty being failure to secure proper erection of the antennae. Two subsequent series of test drops involving 10 units at the test site confirm this belief.

Only two units were dropped near the crater of the surface shot. Interference prevented any hope of receiving their radiation and no further units were dropped.

An additional two units dropped into the area around the crater of the underground shot failed to perform. Further drops were abandoned pending a solution to the antennae erection problem. It was evident, however, the antennae erection problem was not likely to be solved with the present equipment and efforts have since been devoted to securing a new and better design.

All units dropped were launched from an altitude of about 800 feet, the airplane's speed at the time of drop being about 150 knots. As a rule, after one practice drop to gauge the effects of wind, the units can be placed in a square approximately fifty feet on a side. The practice drops were made with dummy units similar in weight and size to a normal AN/USQ-1 unit.

3.5 RESULTS

The results obtained from the fixed telemetering units are tabulated in Tables 3.1 and 3.2, the curves obtained being identified by an appropriate figure number.

[redacted]

PROJECT 2.1b

No results are presented for the dropped telemetering units due to their unsatisfactory performance. The results obtained are essentially a better appreciation of the present design deficiencies and the remedial measures which must be incorporated in the improved design now under development.

[redacted] [redacted]

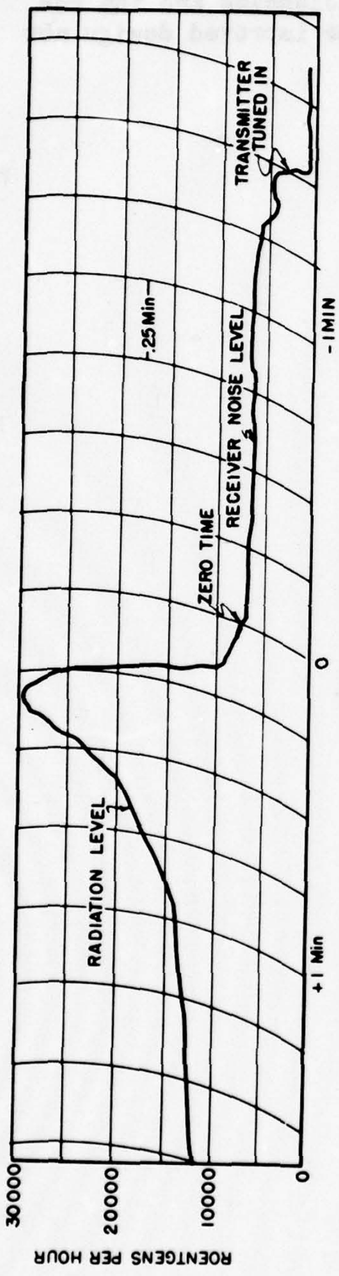

Figure 3.1 Roentgen/Hour Versus Time - 1000 Feet - Surface Shot

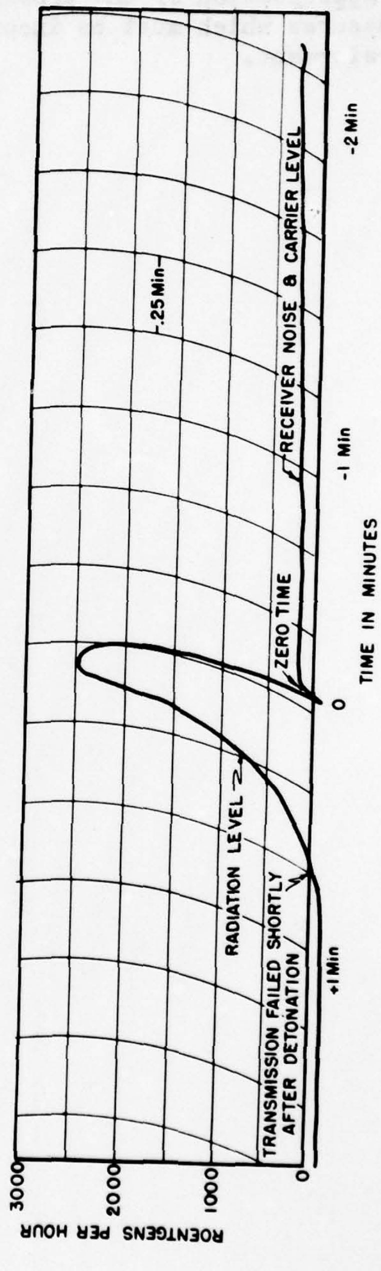

Figure 3.2 Roentgen/Hour Versus Time - 1250 Feet - Surface Shot

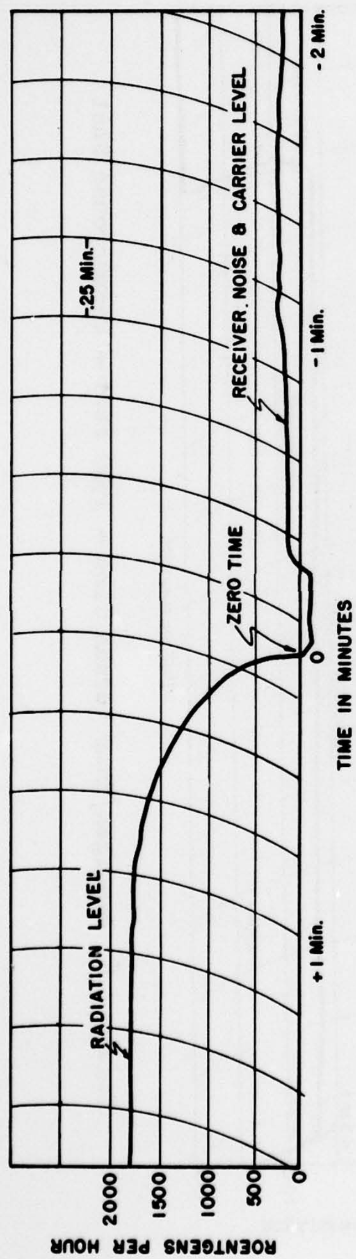

Fig. 3.3 Roentgen/Hour Versus Time - 1500 Feet - Surface Shot

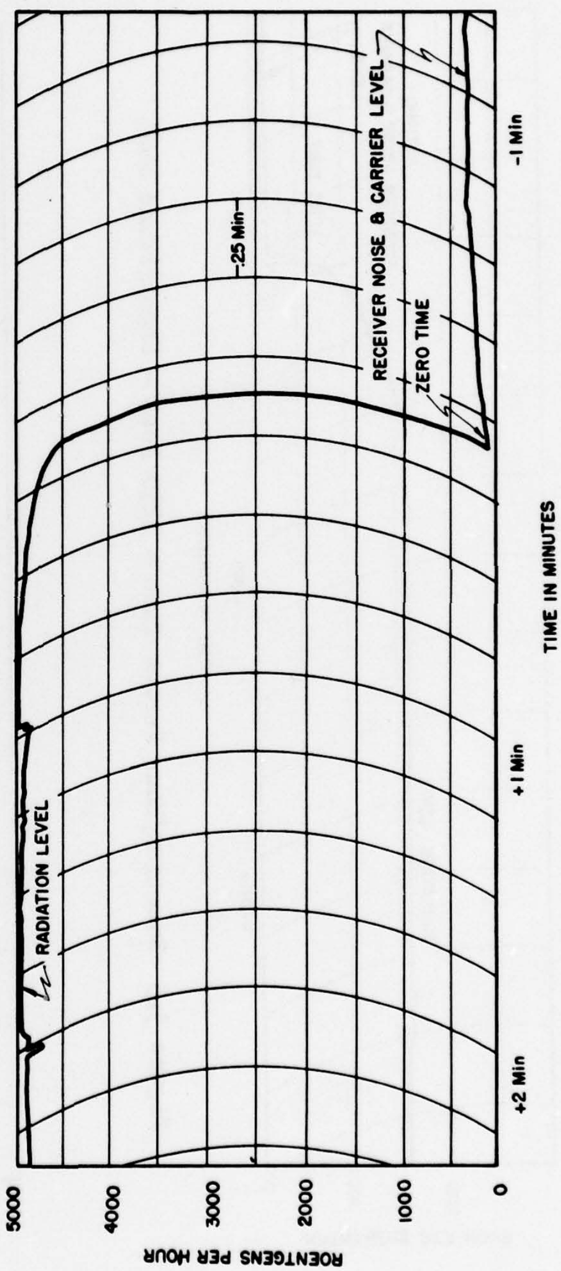

Figure 3.4 Roentgen/Hour Versus Time - 1000 Feet - Underground Shot

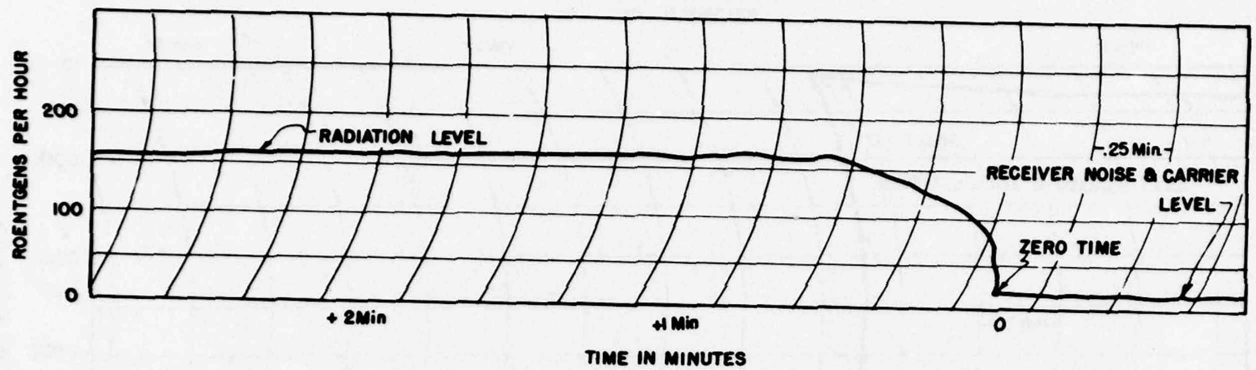

Figure 3.5 Roentgen/Hour Versus Time - 1250 Feet - Underground Shot

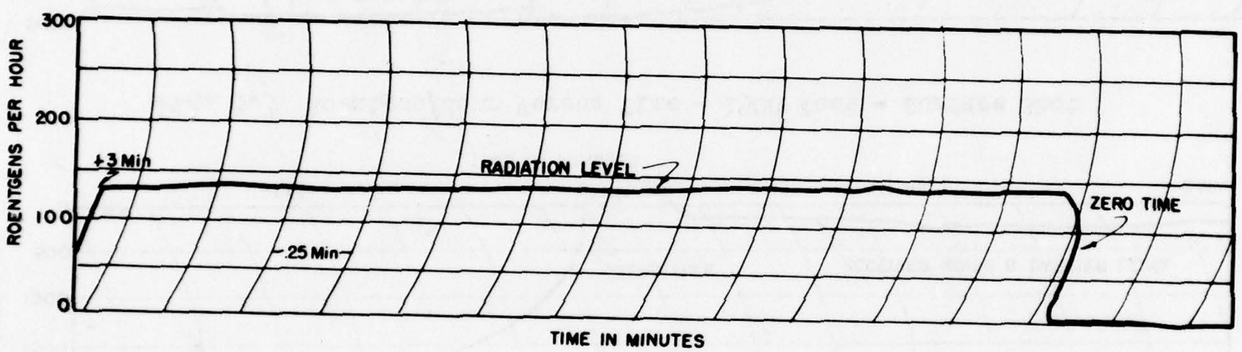

Figure 3.6 Roentgen/Hour Versus Time - 1500 Feet - Underground Shot

TABLE 3.1

Tabulation of Results - Surface Shot

Distance From Zero Point (Ft)	Frequency (Mc/Sec)	Intensity Range (R/Hr)	Performance	Monitored By	Peak* Intensity (R/Hr)	Figure On Which Data Is Shown
1000	167.04	50,000	Received	Mobile unit	29,750 at +20 secs. (fell rapidly)	3.1
1250	169.64	5,000	Failed after detonation	Mobile unit	2,500 at +8 secs.	3.2
1500	171.24	5,000	Received	Mobile unit	1,800 at +53 secs.	3.3
2000	165.10	500	Not received (interference)	Project airplane	No data	Not shown
3000	163.0	500	Not received (interference)	Project airplane	No data	Not shown

*Estimated error +20 per cent

TABLE 3.2

Tabulation of Results - Underground Shot

Distance From Zero Point (Ft)	Frequency (Mc/Sec)	Intensity Range (R/Hr)	Performance	Monitored By	Peak* Intensity (R/Hr)	Figure On Which Data Is Shown
1000	169.5	5,000	Received	Mobile unit	5,000 + at +8 secs.	3.4
1250	171.12	500	Received	Mobile unit	165 at +8 secs.	3.5
1500	168.00	500	Received	Mobile unit	140 at +8 secs.	3.6
2000	165.30	15	Received unmodulated	Project airplane	No data indicated	Not shown
3000	163.00	15	Received +26 to -40 mins. only	Project airplane	Constant 15 r/hr	Not shown

*Estimated error +20 per cent

CHAPTER 4

DISCUSSION

4.1 GENERAL

The AN/ADR-4 surface-radiation survey equipment measures the gamma intensity at altitude over a contaminated area and, by correcting for attenuation due to distance and absorption or scattering by the intervening air, plots a theoretical estimate of the gamma intensity at ground level. The advantages and limitations of this equipment are outlined in the report on Project 2.1c-2 of Operation JANGLE. The AN/ADR-4 has three limitations which the AN/USQ-AN/ARR-29 telemetering system was intended to alleviate:

(1) The AN/ADR-4 does not provide absolute information; it requires an extrapolation of information obtained at altitude with a corresponding possibility of error. The AN/USQ-1 transmitter, on the other hand, measures gamma intensity at ground level and the uncertainties inherent in the AN/ADR-4 measurements are not present.

(2) The intensities computed with the AN/ADR-4 are average values over an area which is some three hundred feet on a side at an altitude of five hundred feet and which increases in size roughly with the square of the altitude. The AN/USQ-1, on the other hand, measures the intensity at a point; it would indicate "hot spots" which the AN/ADR-4 would "smear" into an average value over an area.

(3) The intensity contours determined by the AN/ADR-4 are valid for the time of the survey but subsequent contours must either be determined directly or estimated from experimental decay curves. The AN/USQ-1, on the other hand, provides regular signals of intensity level extending over a period of approximately forty-eight hours, depending upon the duration of the transmissions, their frequency, and battery life. Moreover, these signals can be obtained remotely at a distance depending only on the transmitter radiation pattern, field strength, and receiver characteristics.

It is for the reasons detailed that the AN/ADR-4 and the telemetering system are regarded as complementary. In particular, it should be noted that the telemetering system was not primarily designed to measure high intensity levels or rapid changes of gamma radiation; it was intended to determine the comparatively low intensities present in a contaminated area. Nevertheless, the AN/USQ-1 time constant, estimated at about 0.1 second, makes it useful in estimating a gamma intensity curve during those periods when it is not changing too rapidly.

4.2 DISCUSSION OF DATA

As previously noted, the three innermost or high range AN/USQ-1 units were calibrated with x-ray equipment of the National Bureau of Standards, using 1 Mev radiation from that source. The over-all error in calibration is estimated at about plus or minus twenty percent. This estimate is considered to be approximately correct for the telemetering system as a whole for radiation of constant or slowly varying intensity.

The telemetering system was intended to measure the instantaneous dose rate due to gamma radiation from ground contaminated by an atomic detonation. In designing the AN/ARR-29 recorder, therefore, it was considered sufficient to require that it follow an input sine wave signal of three cycles per second with negligible error. The time constant of the AN/ARR-29 recorder is therefore well below one-third of a second. A consideration of its circuits indicates that the AN/USQ-1 transmitter should likewise have a time constant of about one-tenth of a second and the over-all time constant of the system should certainly not be more than one-half of a second.

This maximum predicted value has not, however, been actually confirmed by laboratory test, primarily due to limited time and personnel. Laboratory tests to determine the cumulative time constant are now underway. It is emphasized, however, that these tests will be of technical interest in interpreting the data of the present project and it is not intended to suggest that the value of the time constant, whatever it may prove to be, is a limitation of the military usefulness of the telemetering system.

At first glance, it might be suggested that varying paper speed of the AN/ARR-29 recorder could be a significant source of error. During the field tests, however, the recorders were started well in advance of zero time to avoid any lag in starting and their speed was checked with a stop watch.

The AN/USQ-1 transmitters were designed for intermittent, not continuous operation. The accumulation of heat over the fifteen minute period therefore led to a shift in the radiation-free field signal. But this source of error was eliminated by redetermining the radiation-free signal at check points occurring at three-minute intervals as indicated on Figures 3.1 through 3.6 inclusive. The displacement of the continuous curves at these points is to be taken as zero level in estimating radiation intensity.

To sum up, the curves shown in Figures 3.1 through 3.6, inclusive, may be in error by an indeterminate amount during the first half-second and by as much as twenty percent at succeeding instants but it is not evident that there is any major source of error in the system itself which would account for any wide departure from data secured by other projects at nearby points.

4.3 COMPARISON OF DATA

In Project 2.1a, Gamma Radiation as a Function of Time and Distance, the National Bureau of Standards obtained gamma dose rate data over an extended area surrounding both the surface and underground shots. In the surface shot, Project 2.1a stations 2 and 8 were on a line 10° NE at radii of 2000 and 3000 feet as compared with AN/USQ-1 at the same radii on a line 20° NE. At these locations, the 2000-foot stations were approximately 350 feet apart and the 3000-foot stations about 520 feet apart. Again, in the underground shot, Project 2.1a stations 103 and 109 were on a line 35° NE at radii of 2000 and 3000 feet with AN/USQ-1 on a 20° NE bearing at the same radii, with corresponding separations of approximately 870 and 1300 feet.

It was intended that the data from Projects 2.1a at these stations would provide a rough check on the data obtained in the present project. Unfortunately, the AN/USQ-1 at the 2000 and 3000 foot radii were not received by the monitoring project airplane, due to interference, except from plus 26 to plus 40 minutes in the case of the 3000-foot AN/USQ-1 during the underground shot. The AN/USQ-1 units which were received were at 1000, 1250, and 1500 feet and there were no Project 2.1a dosimeters in their vicinity. The AN/USQ-1 at 3000 feet, received during the underground shot, was some 1300 feet from the nearest Project 2.1a station. In a strict sense, therefore, no comparison of data can be made.

While no direct comparison is possible, it can be said that the AN/USQ-1 from 1500 feet inward indicated intensities much less than those recorded by Project 2.1a dosimeters at the 2000 and 3000-foot radii. The explanation of this apparent disagreement cannot be confidently given but, presumably, it lies in one of the following categories:

(1) There might conceivably be a large error in the AN/USQ-1 telemetering system which is not evident under laboratory conditions but which is induced by the detonation shock waves. While this is a possibility, it is not considered probable. The units have operated successfully after an air drop from 500 feet on concrete pavement.

(2) It is conceivable that the concrete mounts might have shielded the units sufficiently to reduce the radiation intensity at each unit but it is not a likely explanation. The units had a fairly wide "field of view" and at the high radiation energy levels encountered the concrete would hardly offer sufficient shielding to account for the comparatively low intensities measured.

(3) Finally, it is suggested that the actual fall out was such that the 20° NE bearing was a region of low intensity at least out to 1500 feet. The absence of Project 2.1a data within the 2000-foot radius and the relatively wide separation of that project's stations at

greater radii make it impossible either to affirm or deny the possibility. The Project 2.1a iso-dose contour lines do indicate that rapid intensity fluctuations could well have occurred within the 2000-foot radius.

4.4 DISCUSSION OF EQUIPMENT

4.4.1 AN/USQ-1 Transmitter

The air drops have demonstrated the same antenna erection deficiencies as were encountered in Operation GREENHOUSE. It has been mentioned that these deficiencies have previously been recognized but that the time between GREENHOUSE and JANGLE did not permit redesign or other corrective measures.

Air monitoring of the units indicates that the reception range is more limited than had been originally believed. This may be in large measure due to old batteries.

The units clearly need some method to facilitate adjustment of the basic frequency so that it can be shifted away from interfering frequencies.

4.4.2 AN/ARR-29 Receiver

The present receiver has two major deficiencies which led to difficulties in Operation JANGLE:

(1) The sensitivity is not sufficiently high.

(2) The present telemetering system requires a broad frequency spectrum since each transmitter deviates at a total of 500 Kcs. at maximum radiation intensities and there are five different transmitter frequencies normally in use. A receiver to accept all of these frequencies must necessarily have a broad frequency response. Moreover the adjacent channel rejection of these receivers was inadequate. In Operation JANGLE this design feature led to interference from transmitters operating as much as a megacycle or two away from the receiver tuned frequency.

CHAPTER 5

CONCLUSIONS

5.1 GENERAL

The following conclusions are believed to be reasonable:

(1) The present telemetering system is a necessary and desirable adjunct to the AN/ADR-4 surface-radiation equipment.

(2) The major problems existing at its inception have been solved for the most part. These included problems in launching technique, resistance to shock on landing, and design of a compact radiation-detecting transmitting circuit.

(3) The current problems are those involved in getting all air-dropped units to operate properly rather than approximately 25 per cent. Clearly, however, these are problems solvable by present techniques.

(4) The system can be used to measure the initial gamma radiation from an atomic detonation and subsequent fall-out. It should be recognized, however, that such measurements will require interpretation in the light of the characteristics of the system.

UNCLASSIFIED [redacted]

CHAPTER 6

RECOMMENDATIONS

6.1 GENERAL

It is recommended that the present telemetering system be improved in design to eliminate the limitations previously discussed. These improvements should include:

(1) A reliable method of antenna erection.

(2) Increased reception range.

(3) Ability to be launched at high speeds.

(4) Use of new, improved Geiger tubes instead of an ionization chamber. This recommendation is made in view of very recent developments in Geiger tube performance which are discussed briefly in the closing paragraphs below.

(5) Provide a rapid means for altering the transmitter frequencies within the 160-170 Mc band.

(6) Narrowing of the receiver band width.

(7) Increase receiver sensitivity.

(8) Use of a coded pulse transmission from transmitter to receiver to minimize interference from other signals and background noise.

(9) Insure that the overall design is such that the transmitters can be launched from a carrier-based airplane carrying a suitable receiver. Emphasis should be placed on a system that can be affixed to, or removed from, the airplane in a short time without modification of the airplane. A system possessing these features is now under development. The first components of the new design should be available in the spring of 1953.

6.2 DISCUSSION

The recommendation for the use of a Geiger tube is based on the following information:

(1) The new Geiger tubes have a good energy response curve, varying within ± 40 per cent over the range 50 kev to 3 kev.

[redacted] UNCLASSIFIED [redacted] UNC... ED

(2) The new tubes produce approximately 2.5 microamperes at 500 r/hr. These comparatively high outputs mean that the d-c amplifiers characteristic of ionization chanber circuits would not be necessary. The elimination of d-c amplifiers virtually eliminates the problem of drift.

(3) The high output permits the use of low impedance circuits, reducing the resistances values encountered from about 1000 to one megohm. The use of high impedance circuits has always been questionable inasmuch as the AN/USQ-1 are likely to be stored for several years when in service use and their high impedance electrical characteristics are likely to change during that time.

It is true that the use of Geiger tubes would limit the dose rate range to not more than 500 r/hr, but values over 500 r/hr are not likely to be of major interest in military operations. Geiger tubes require high voltage but the coded pulse technique recommended requires high voltage as well and the use of Geiger tubes places no added requirement.

It should be understood, however, that the foregoing recommendations are tentative and are likely to be modified as development work proceeds. For example, the coded pulse transmission technique presents certain difficulties due to reflecting objects which may cause delayed pulses to arrive and interfere with pulses received directly from the transmitter. If this problem proves to be operationally significant, pulse coded transmissions would have to be abandoned and the necessity of providing high voltage for the Geiger tube alone would seriously impair their value.

The entire problem of securing a completely satisfactory telemetering unit is currently under extended discussion between the Navy and its contractors. It is not intended to accept any final design until its various features have been discussed with experienced personnel in the many fields contributing to, or interested in, its ultimate use.

[redacted] UNCLASSIFIED

OPERATION JANGLE

PROJECT 2.1c-1

AERIAL SURVEY OF DISTANT CONTAMINATED TERRAIN

by

William E. Harlan
Major, USAF

June 1952

Headquarters, U. S. Air Force
Office for Atomic Energy, DCS/O
AFOAT-1

[redacted] UNCLASSIFIED

PREFACE

The fall-out of radioactive debris from atomic explosions has been of considerable interest to meteorologists and to health physicists alike. The trajectory and intensity of this fall-out is not entirely predictable because of the influence of various phenomena such as local meteorological conditions, terrain, and to the height to which the atomic cloud rises. Consequently, a more direct means may be used to determine the degree of contamination in the areas of interest. One method, which consumes a considerable amount of time, is to employ ground parties equipped with radiac sets to establish the fall-out plot. A more rapid method was employed during Operation JANGLE. Three aircraft, equipped with radioactivity detection instruments, were assigned sectors of a grid out to 200 miles from the Test Site. Observations were relayed in flight to the Control Point where current radex plots were kept and areas which showed need for a more detailed survey were assigned to ground parties.

PROJECT 2.1c-1

CONTENTS

ILLUSTRATIONS

[redacted]

PROJECT 2.1c-1

ABSTRACT

The fall-out of radioactive debris following each of the atomic weapons tests in Operation JANGLE was plotted by means of instrumented aircraft taking measurements at low altitudes downwind from the Test Site. Iso-intensity lines were plotted at the Control Point on the basis of data relayed from the aircraft by radio. These plots are not intended to be quantitative but do effectively delineate the fall-out area and indicate the effects of terrain on the trajectory of low clouds.

1.0 OBJECTIVE

The objective of Project 2.1c-1 was to determine by use of instrumented aircraft the fall-out of radioactive debris from the clouds resulting from the Surface and Underground explosions of Operation JANGLE and to test and compare various types of airborne instruments for the instantaneous detection of radioactivity. This project was performed also during Operation BUSTER at the request of the Atomic Energy Commission.

2.0 GENERAL PLAN

Three C-47 type aircraft, instrumented with radioactivity detection devices were directed over the area downwind from the Test Site about four hours after shot time. These aircraft covered a pre-set grid pattern at an average altitude of 600 feet. Intensity readings were relayed by radio to the Control Point where iso-intensity lines were plotted. In this manner an area of 6000 square miles was covered following each shot with an average flight time of four hours.

3.0 INSTRUMENTATION

Two general methods of detection were used: (1) instantaneous detection with continuously recorded results, and (2) the exposure of filter papers which required post-flight analysis before the presence of radioactive material could be determined. Both methods are essential for a representative fall-out pattern because the instantaneous detection instruments will not discriminate between airborne particulate material and that deposited on the ground.

Three types of instantaneous detection equipment were used: (1) Atmospheric-Conductivity Equipment, (2) a Scintillation Gamma Detector, and (3) a Geiger-Mueller instrument. A description of each follows.

3.1 Atmospheric-Conductivity Apparatus

This instrument measures the changing ionization in the air which may in turn be related to the presence of radioactive matter. The intensity of the radioactive field is recorded as a function of the rate of collection of ions passing through a cylindrical condenser. In the simplified schematic, the voltage drop across R_1 caused by ion collection on the center probe is converted to AC voltage by the vibrating condenser C_1. This voltage is amplified, phase-rectified, and

measured by a recording potentiometer. The slope of the recorded trace is proportional to the change of the ionization produced, for example, by the presence of nuclear debris in the air surrounding the aircraft.

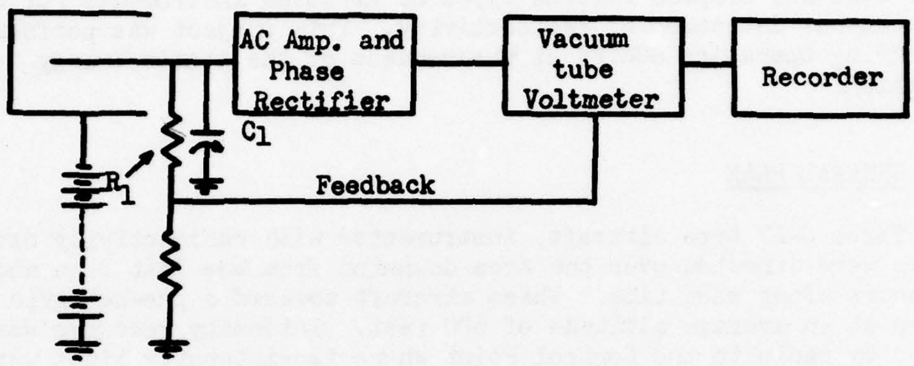

The time constant for the particular instrument used was about one second for 90 per cent response. For further details of this equipment, air-flow requirements, sensitivity, and altitude dependence, see ORNL 341, "An Aerial Survey of Radioactivity Associated with Atomic Energy Plants."

3.2 Scintillation Gamma Detector

Only one of the aircraft participating in these tests was equipped with scintillation equipment. Because of the general knowledge of the principle of scintillation counter operation, no discussion will be presented. The particular instrument used employed a NaI(Th) crystal, two inches in diameter and two inches thick, viewed by a 5819 photomultiplier tube. The detector head was placed in the rear of the aircraft, between the floor and the outer skin. The signal was passed to a pulse-height selector with an energy bandpass of from .23 to 1.6 mev.

3.3 Geiger-Mueller Type Instrument

This equipment was for a special purpose and is discussed in Section 5.0.

4.0 FILTER EXPOSURE

Each aircraft carried a filter box for exposing two one-square-

foot filters with about 600 cfm through each filter. Filters were exposed throughout the whole mission, the left filter being changed each hour, the right each ten minutes. The one-hour exposures were made to meet the requirements of another program. In order to establish the detailed structure of the low clouds of debris encountered in the flight and differentiate between terrain contamination and airborne debris which record indiscriminately on the detection equipment, exposures of a minute or less would be desirable but impractical. A compromise was effected with the ten-minute exposures.

5.0 IN-FLIGHT EVALUATION OF INSTRUMENT READINGS

It is evident that unless an instrument reading can be attributed in whole or in part to ground contamination or to airborne radioactive particles, an unrepresentative fall-out plot will result. An aid in differentiating these two sources of signals is the short duration filter. If high activity is found on a short duration filter and the detection instruments show an abnormal reading for the same period, it is evident that suspended particulate material is responsible for the greater part or all of this abnormal reading. But this information is available only after the flight has been completed.

A method of in-flight filter counting was used for the first time during Operation BUSTER which gave instantaneous indication of the collection of activity on the filter. This consisted of placing a Geiger-Mueller tube behind the filter and reading the counting-rate from a recorder which ran at the same speed as the recorders assigned to the detection instruments. By the use of this monitor as a cross-check on the other instruments, an instantaneous decision could be made as to the cause of an indication of abnormal activity.

The effectiveness of the continuous filter-monitor is demonstrated by portions of the records from flights following two of the BUSTER shots. Correspondence of the two traces is indicated by the letters adjacent to them on a precise time basis. The curves, of course, are not identical. The upper trace records the concentration of activity in the air; the lower trace the amount collected on the filter. Figure 1 shows traces taken on the flight following BUSTER Baker, which indicate that about 90 per cent of the activity was due to airborne material. The indication of a high concentration at <u>A</u> on the conductivity trace is accompanied by an indication of a rapid collection of debris on the filter at <u>A</u>'. Similarly, a slower accumulation of filter debris is to be noted at <u>B</u>' and <u>C</u>' corresponding to conductivity above normal at <u>B</u> and <u>C</u>.

Under different meteorological conditions, BUSTER Dog left considerable surface contamination from fall-out. This is shown in Figure 2 by the absence of buildup on the filter monitor with a corresponding high reading on the Atmospheric-Conductivity record.

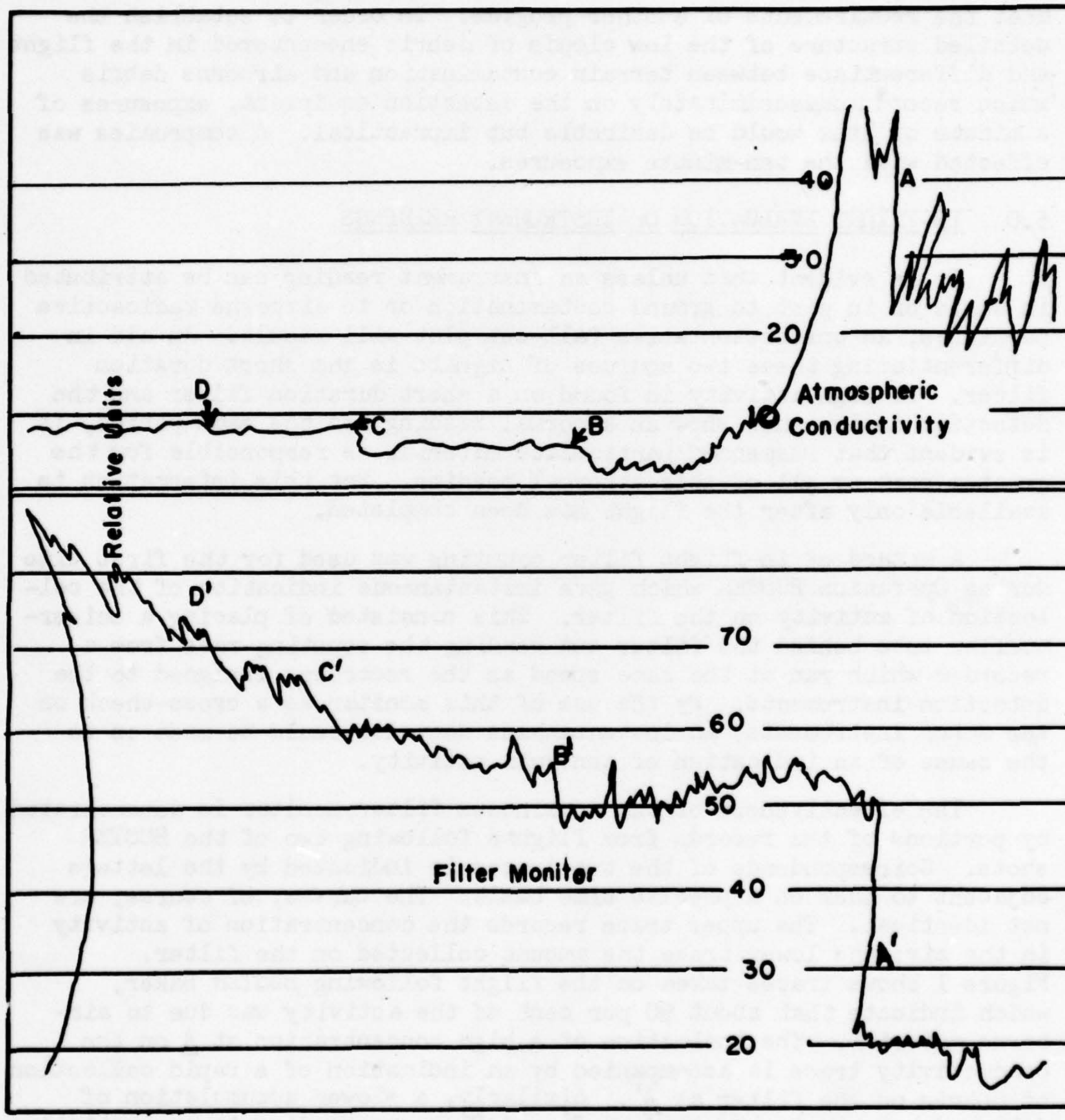

Figure 1 Specimen of Atmospheric-Conductivity and Filter Monitor Trace for BUSTER Test Baker

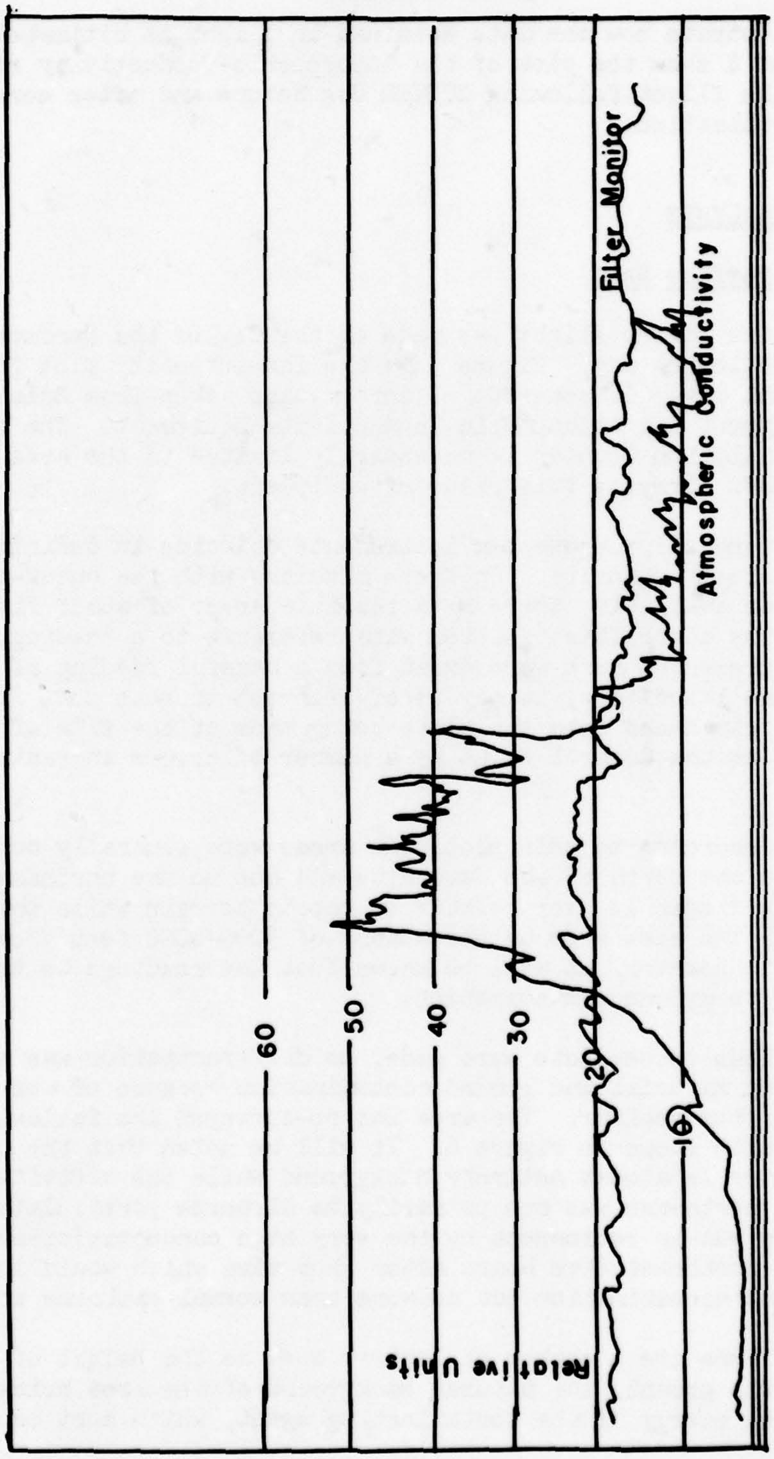

Figure 2 Specimen of Atmospheric-Conductivity and Filter Monitor Trace for BUSTER Test Dog

To illustrate how the data obtained in flight is ultimately used, Figures 3 and 4 show the plot of the Atmospheric-Conductivity records taken from the flight following BUSTER Dog before and after correction for filter collection.

6.0 DATA ANALYSIS

6.1 Surface Shot

One survey flight was made on the day of the Surface shot and on the following day. Figure 5 is the iso-intensity plot for the flight on shot day. It consists of information taken from Scintillation Counter Equipment and Atmospheric-Conductivity Equipment. The coverage of the Scintillation Counter is necessarily limited to the area covered by the aircraft carrying this piece of equipment.

Generally, these two instruments coincide in defining the areas of greatest intensity. On these missions with the check-points and navigation available, there is a possible error of about five miles in locating the aircraft's position with reference to a reading. While these plots presented here were drawn from a careful reading of the records in the laboratory, it may be of interest to note that further errors were introduced into the plots being made at the time of the measurements at the Control Point by a number of errors in radio transmission.

According to this plot, two areas were generally contaminated: One to the north of the Test Site and one to the northeast. The more easterly finger is over relatively smooth terrain while the other is blocked on the east side by elevations of 5000-6000 feet above the valley floor. However, it will be shown that the readings to the east were not due to ground contamination.

When these plots were made, no differentiation was made between airborne material and ground contamination because of the failure of the filter box monitor. The area was re-surveyed the following day with the results shown in Figure 6. It will be noted that the northeasterly sector is almost entirely background while the activity encountered to the northeast was due primarily to airborne particulate debris. This is borne out in retrospect by the very high conductivities encountered to the northeast five hours after shot time which would indicate extreme ground contamination but no more than normal airborne activity.

There are a number of factors such as the height of the aircraft above the ground, the natural background of the area being surveyed, and the energy of the contaminating agent, which must be considered

PROJECT 2.1c-1

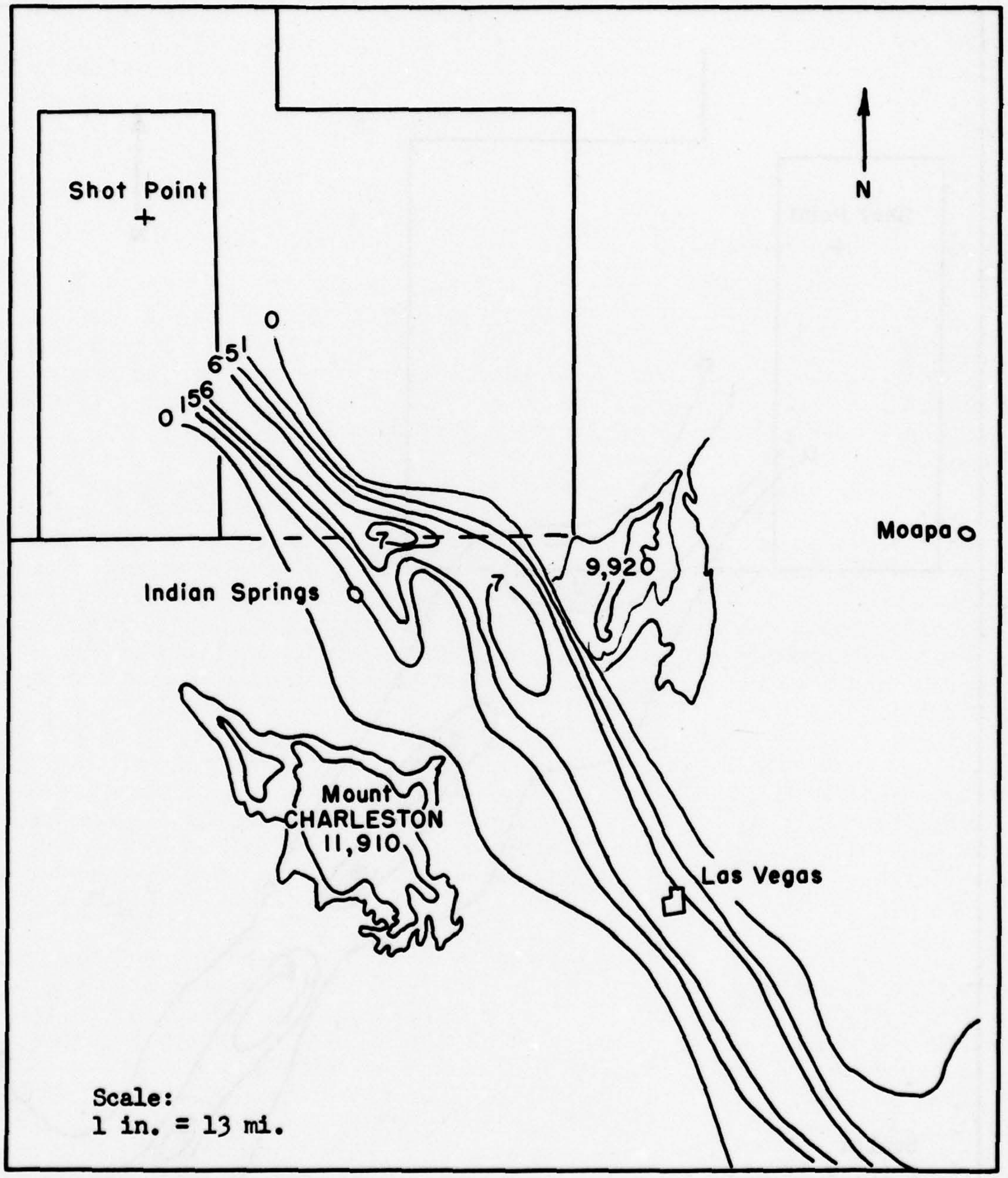

Figure 3 Fall-out Pattern from Analysis of Atmospheric-Conductivity Readings Uncorrected for Effect of Airborne Debris

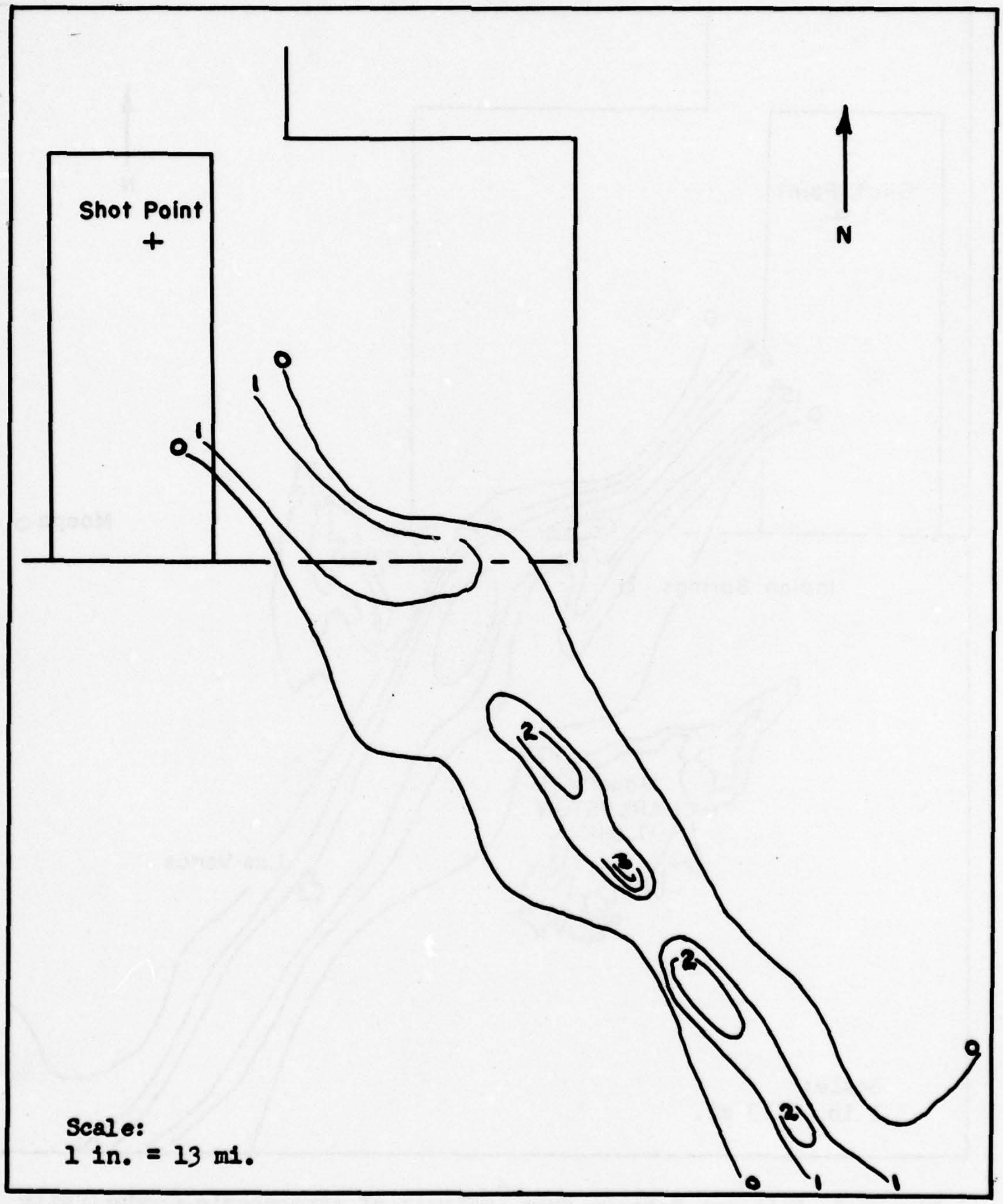

Figure 4 Final Fall-out Pattern from Atmospheric-Conductivity Measurements after Correction for Airborne Debris

PROJECT 2.1c-1

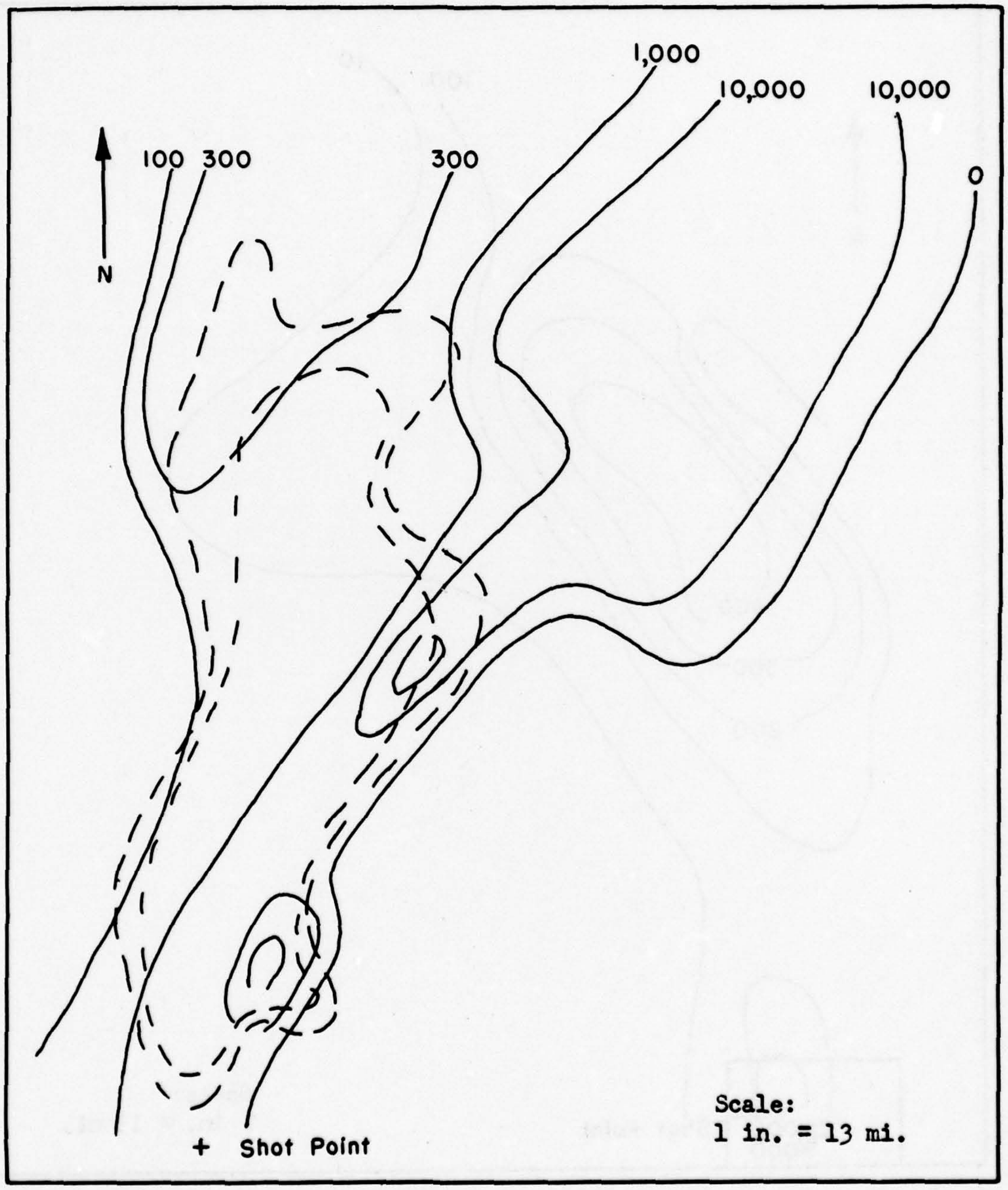

Figure 5 Fall-out Pattern for JANGLE Surface (H + 5 hours) as Determined by (1) Atmospheric-Conductivity (solid lines) and (2) Scintillation Counter (broken lines). Numbers at end of Isolines are in relative units only.

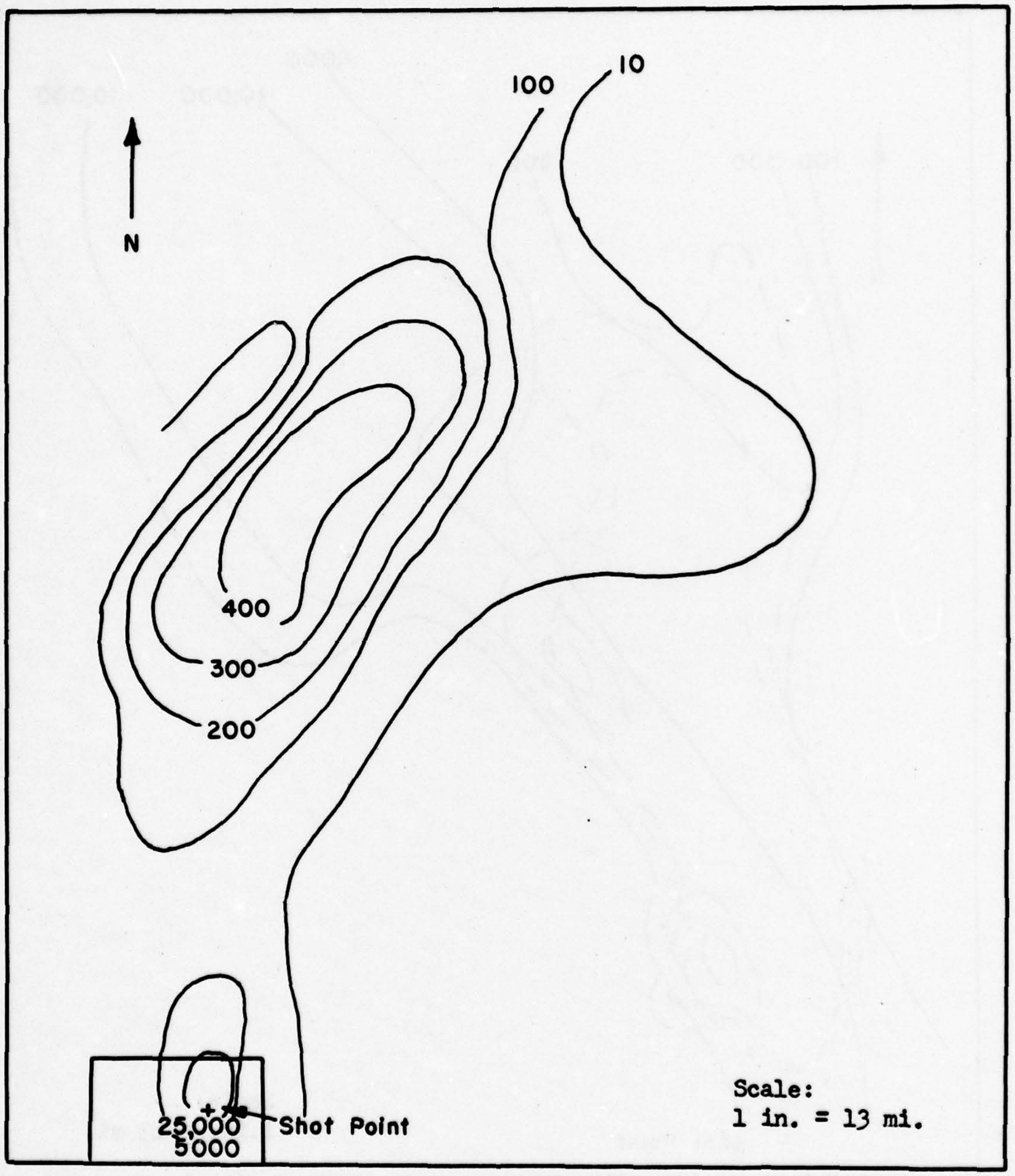

Figure 6 JANGLE Surface Fall-out Pattern (H + 30 hours) as Determined from Atmospheric-Conductivity Measurements Uncorrected for Airborne Debris Assumed to have Dispersed in 30 Hours.

in converting Atmospheric-Conductivity and Scintillation Counter measurements in an aircraft to dosage rates on the ground. In some cases, it is estimated that this conversion can be made accurate to within a factor of two, but more conversion data is required before any reliance can be placed on such calculations. The mission was designed to establish relative values to delineate the contaminated areas to indicate any necessity for survey by ground parties.

6.2 Underground Shot

Survey flights were postponed until the day after the Underground shot because such high contamination had been encountered on the shot-day flight of the Surface shot. Iso-intensity lines plotted from data taken from this flight are shown in Figure 7. The plot is a combination of Atmospheric-Conductivity and Scintillation Counter measurements and represents the intensity at the 600-foot level. It will be noted that the area of contamination resembles closely that found on the second-day flight following the Surface shot. It appears that terrain features of the area tend to localize the fall-out from clouds resulting from surface and underground atomic explosions by contrast to the very low fall-out in the general area resulting from air drops, which might be expected from the maximum altitude of the clouds resulting from the JANGLE Surface and Underground explosions. This observation applies to the general area out to fifty miles and should not be construed as applying to the immediate vicinity of an explosion out to one or two miles.

7.0 RECOMMENDATIONS AND CONCLUSIONS

It follows that effective terrain survey by aircraft requires the knowledge of the exact position of the aircraft at all times. There must also be available equipment to differentiate between measurements attributable to ground contamination and to suspended particulate matter. The problem presented by these two radiation components may be resolved by two methods: (1) the use of a filter monitor to determine the presence of airborne material while in flight, or (2) delay the survey for a period of twenty-four hours during which time most of the airborne material will settle out, as demonstrated by the JANGLE Surface shot.

These tests have been held during periods of good weather, a condition which allows the Atmospheric-Conductivity equipment to be used to its best advantage. It should be kept in mind, however, that should the occasion arise for monitoring the contamination from an enemy bomb, the presence of smoke from the fires would render the equipment useless.

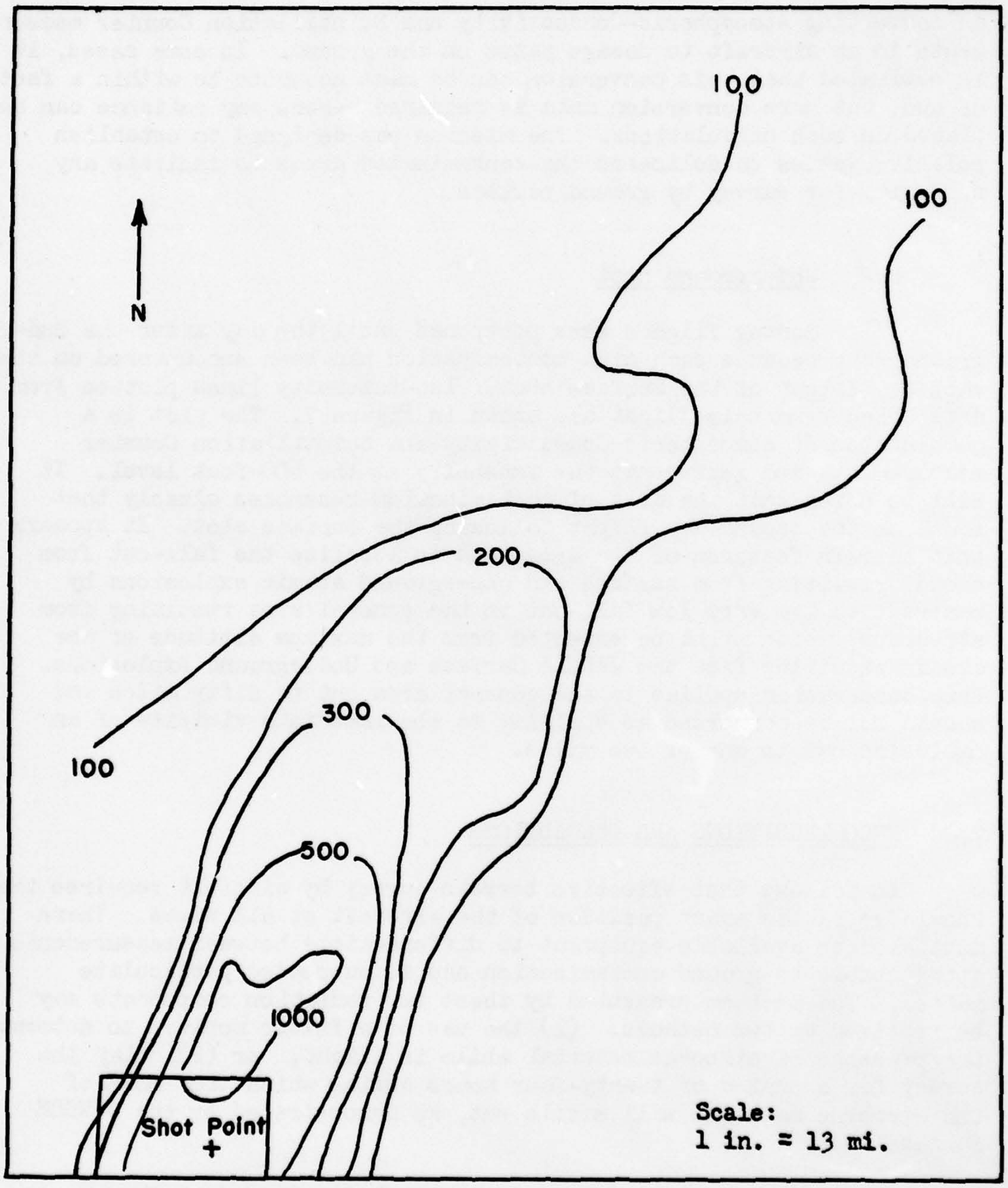

Figure 7 JANGLE Underground Fall-out Pattern as Determined by Atmospheric-Conductivity Uncorrected for Airborne Debris

From a tactical standpoint, it is recommended that this equipment be entirely replaced by Scintillation Counters and similar instrumentation not subject to atmospheric conditions.

It is concluded that areas of contamination are readily and rapidly detectable by the combination of techniques employed in this program. It appears to be quite feasible to determine iso-dose lines very rapidly but at present there exists only meager data to effect the conversion from readings of the highly sensitive apparatus required to detect ground activity even at the minimum safe altitudes.

It is recommended that measurements of the type reported here be made as the occasion of future bomb tests arises. Emphasis should be placed on obtaining conversion factors by correlating actual ground measurements over extended areas with aircraft observations, relating such factors as aircraft altitude, equipment calibrations, and areal extent of contamination with such measurements. Flights over the target areas in BUSTER tests indicate that aircraft measurements can also indicate the general level of contamination at the shot point once the conversion factors are well established.

[redacted] UNCLASSIFIED

OPERATION JANGLE

PROJECT 2.1c-2

AERIAL SURVEY OF LOCAL CONTAMINATED TERRAIN

by

JOHN H. TERRY
CDR., USN

and

GENE D. ROBERTSON
LT (jg)., USN

of

BUREAU OF AERONAUTICS

DEPARTMENT OF THE NAVY

DEPARTMENT OF THE NAVY
Bureau of Aeronautics
Washington 25, D. C.

DEPARTMENT OF THE AIR FORCE
Air Research and Development Command
Wright Air Development Center
Wright-Patterson Air Force Base

[redacted] UNCLASSIFIED

[redacted] UNCLASSIFIED

PROJECT 2.1c-2

CONTENTS

[redacted] UNCLASSIFIED

[redacted]

PROJECT 2.1c-2

CONTENTS (Cont.)

[redacted]

PROJECT 2.1c-2

ILLUSTRATIONS

PROJECT 2.1c-2

ILLUSTRATIONS (Cont.)

CHAPTER 4 RESULTS

TABLES

CHAPTER 2 INSTRUMENTATION

PROJECT 2.1c-2

ABSTRACT

The Navy and the Air Force have developed airborne radiac equipment to detect the presence of gamma-emitting radioactive contamination on the ground beneath an airplane. The equipment measures the gamma dose rate at altitude, introduces a correction for altitude, and indicates average ground intensity in defined areas on the ground. This information, when correlated with knowledge of the airplane's course, ground speed and initial position, permits construction of an isodose contour map of the radioactive ground-contamination. Surveys made with these equipments in the two shots of Operation JANGLE show that they are satisfactory in principle but that the Navy instrument indicated excessively high (except over the craters) while the Air Force instrument indicated somewhat low. The origin of these errors is suggested and corrective measures recommended.

CHAPTER 1

HISTORICAL BACKGROUND

1.1 GENERAL

Operations SANDSTONE and CROSSROADS underlined the hazard due to radioactive contamination of the surface incident to an atomic explosion. The possibility of outlining a contaminated area by aerial survey was recognized at least as early as 1946 and development contracts for various types of automatic ground survey recording equipment, designed for aircraft installation, were let in 1948 or soon thereafter. Among these equipments were the Navy AN/ADR-4 and the Air Force Type F-1.

These equipments were available in sufficient quantity by late 1950 to propose them for tests in Operation GREENHOUSE. A Navy P2V-2 and an Air Force B-17 were equipped with all of the airborne radiac equipment then available and were flown to Eniwetok to participate in Operation GREENHOUSE in the spring of 1951.

The two aircraft participated in three of the shots of Operation GREENHOUSE. The ground survey equipments performed as intended but the small aize of the atoll islands hardly permitted a full evaluation, except possibly in the case of the shot on Runit Island where the contaminated area was sufficient to permit the plotting of contour lines of isodose gamma intensity. It was therefore considered particularly desirable to secure confirmatory evidence of the adequacy of the equipments in the surface and underground shots of Operation JANGLE where extensive high-intensity, contaminated areas were anticipated. Accordingly both the P2V and the B-17 radiac aircraft were proposed and accepted for participation in Operation JANGLE.

[redacted]

CHAPTER 2

INSTRUMENTATION

2.1 AN/ADR-4 GROUND SURVEY EQUIPMENT

2.1.1 Purpose

The purpose of this equipment is to obtain, in flight, sufficient information to make a surface radioactivity contour map of the gamma-radiation intensity that would be encountered by a man walking on the ground beneath the airplane. The intensity contour maps so obtained are intended to provide ground troops with an estimate of the dosage they might expect in a given time interval after entry to the contaminated area.

2.1.2 Principle of Operation

This equipment is a three-channel, directional, gamma-intensity meter. Each channel is sensitive to a different cone of radiation representing three adjacent areas on the ground in a line perpendicular to the flight path of the airplane making the survey. The radiation in each cone is measured at the aircraft and presented graphically as the logarithm of the average intensity in the cone.

The detection elements are high pressure, gamma-sensitive, ionization chambers. Each channel has two ionization chanbers associated with it, one receiving gamma radiation nondirectionally, the other shielded from radiation coming from the particular cone concerned. The outputs of the two chambers are subtracted and the resultant is proportional to the radiation in the shielded cone. The logarithm of this resultant is recorded graphically as a function of time, one curve being obtained for each of the three channels. Figure 2.1 shows the radiation intensity versus mean photon energy for constant current output of the ionization chambers used.

A fourth pair of ionization chambers introduces a correction for attenuation due to air between the airplane and ground. One of the pair is unshielded, receiving radiation nondirectionally, the other is surrounded by a plastic material having the same average atomic number as air. The thickness of the plastic material was selected to be in equal in absorption to 500 feet of air. The ratio of the output of the shielded chamber to that of the unchielded chamber is therefore proportional to the decrease in intensity of the received radiation in traversing 500 feet of air. Since the plastic is similar in its characteristics to air, the ratio correctly takes into account the changes in absorption due to changes in the energy distribution or spectrum of the received radiation.

[redacted]

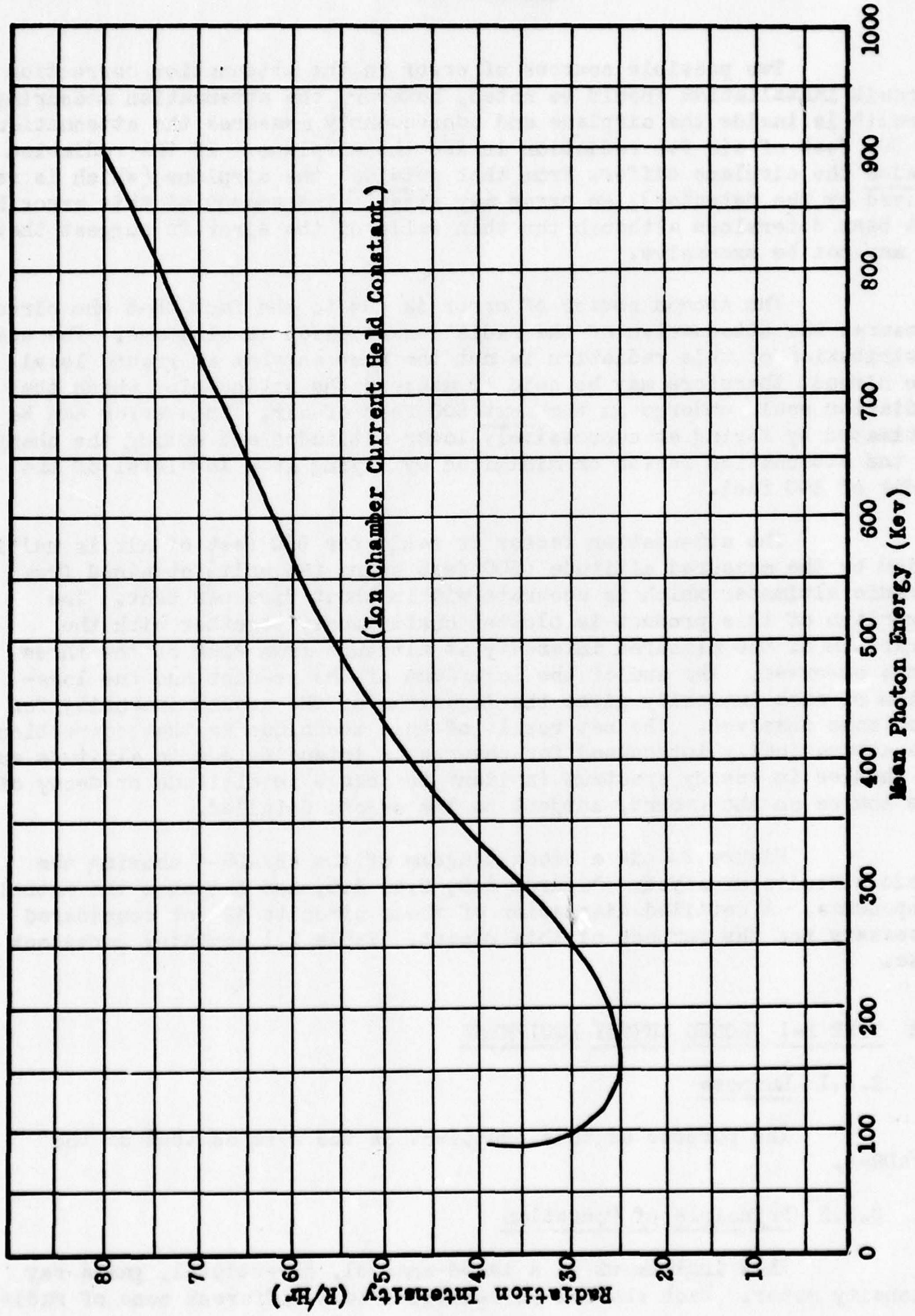

Figure 2.1 Radiation Intensity versus Mean Photon Energy - AN/USQ-1 Ionization Chamber

Two possible sources of error in the attenuation correction circuit installation should be noted, however, the attenuation measuring circuit is inside the airplane and consequently measures the attenuation of 500 feet of air for radiation inside the airplane. If the radiation inside the airplane differs from that outside the airplane (which is received by the detector), an error may exist. The amount of this error has not been determined although the thin walls of the aircraft suggest that it may not be excessive.

The second source of error is due to the fact that the circuit measures the attenuation of the radiation received at altitude. The energy distribution of this radiation is not the same as that at ground level. The circuit therefore may be said to measure the attenuation which the radiation would undergo in the next 500 feet of air. This error can be estimated by flying at successively lower altitudes and noting the change in the attenuation factor or minimized by flying at a low level of the order of 500 feet.

The attenuation factor or ratio for 500 feet of air is multiplied by the measured altitude (500 feet being the unit) obtained from a radio altimeter which is accurate within about five per cent. The logarithm of this product is plotted continuously together with the logarithm of the measured intensity at altitude from each of the three cones observed. The sum of the logarithm of the product and the logarithm of each intensity gives the logarithm of the ground intensity for each cone observed. The net result of this technique is that corrections are automatically introduced for changes in intensity due to altitude and to changes in energy spectrum incident to change in altitude or decay of the source on the ground, subject to the errors detailed.

Figure 2.2 is a block diagram of the AN/ADR-4 showing the basic circuits employed. Figures 2.3, 2.4, 2.5, and 2.6 show the actual components. A detailed discussion of their circuits is not considered necessary for the purpose of this report. Table 2.1 contains pertinent data.

2.2 TYPE F-1 GROUND SURVEY EQUIPMENT

2.2.1 Purpose

The purpose of this equipment is the same as that of the AN/ADR-4.

2.2.2 Principle of Operation

This instrument is a three-channel, directional, gamma-ray intensity meter. Each channel is sensitive to a different cone of radi-

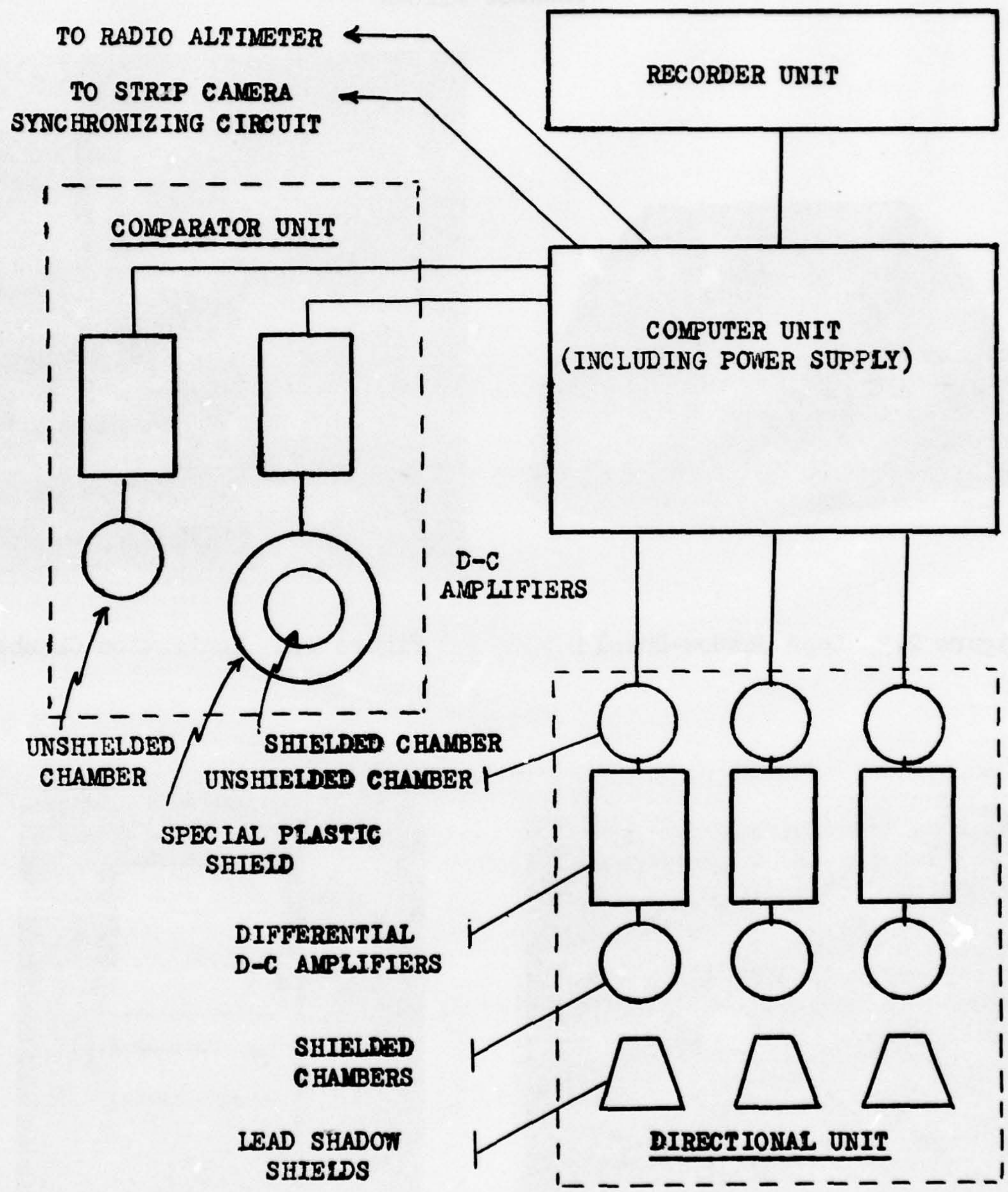

Figure 2.2 Block Diagram of AN /ADR-4 Surface-ra diation Survey Equipment

ation representing three adjacent areas on the ground in a line perpendicular to the line of flight of the aircraft. The radiation in each cone is measured at the aircraft and, by electronic computation, this information is extrapolated to average ground intensities in defined areas on the ground.

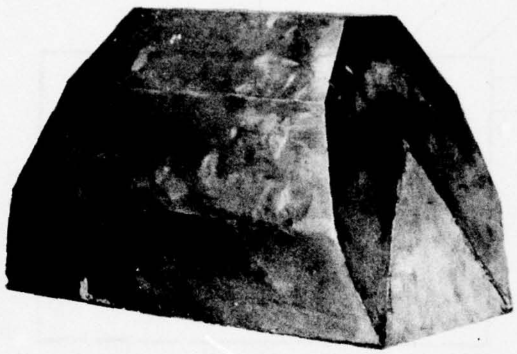

Figure 2.3 Lead Shadow-Shield

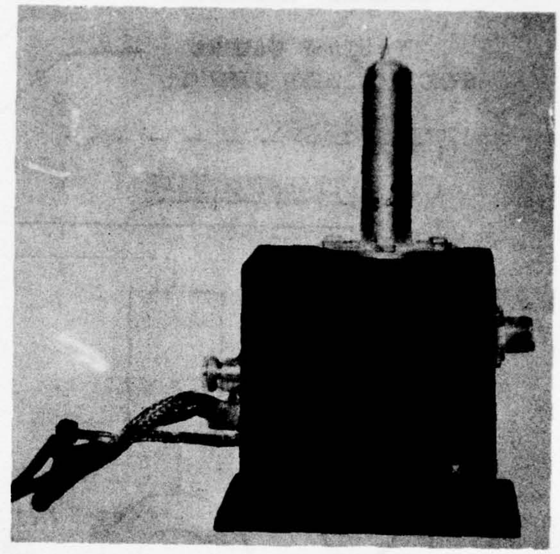

Figure 2.4 Ionization Chamber

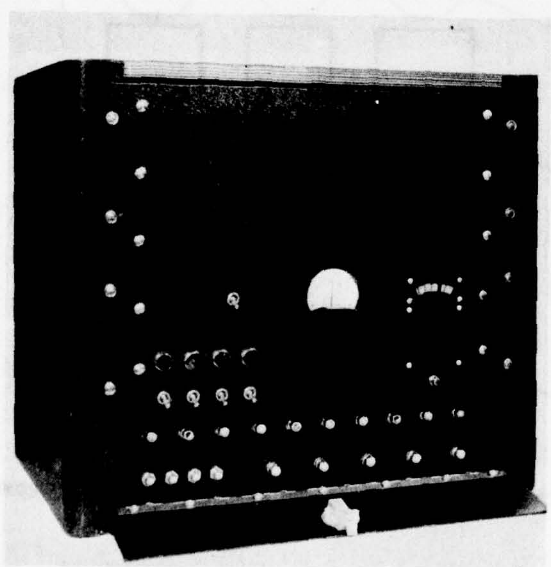

Figure 2.5 Computer Unit

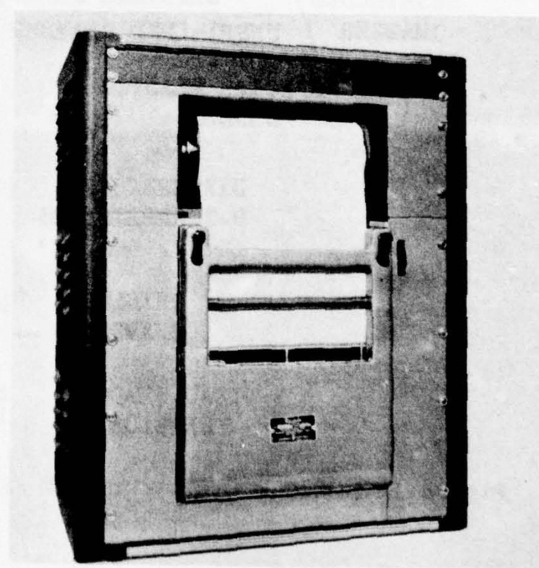

Figure 2.6 Recorder Unit

AN/ADR-4 Surface-radiation Survey Equipment

PROJECT 2.1c-2

TABLE 2.1

Data for AN/ADR-4 Surface-radiation Survey Equipment

Physical Data

Unit	Weight (lb)	Height (in.)	Width (in.)	Depth (in.)
Directional head	40	20	20	40
Computer	70	20	21	12
Recorder	40	30	20	12
Lead shadow shield	170	12	8	6
Comparator	50	20	20	12

Power Requirements

DC	AC
None	115 v, 500 va 400 cps

Miscellaneous Data

Gamma Intensity range (intensity at ground level) . . .	0.5-500 r/hr
Scanning Aperture	Three 30°-channels arranged to give a total angle of 90°

Phosphor-photomultiplier combinations are employed as detection elements. Two photomultiplier tubes are used in coincidence in each channel to suppress noise. Directionality is obtained by lead shielding excluding radiation from all directions except in the desired solid angle.

The signals from the directional detectors are amplified, appearing as a d-c input to the computer unit. This d-c voltage is applied to an exponentially tapered potentiometer. The slide of the potentiometer is positioned by a servomechanism motor so that the angular position is a linear function of the altitude of the aircraft. This is accomplished by establishing equality between the output voltage of an AN/APN-1 radio altimeter and a standard voltage obtained from an electronic standard cell. This design would appear to introduce a correction for altitude and attenuation which is strictly valid only for one value of radiation energy or for an average value thereof.

After amplification and modulation of an oscillator, a resultant 25-cycle signal, whose amplitude is proportional to gamma ground intensity, is fed to the recorder. The recorder uses the signals to drive pens through electromagnetic voice coils. The pens are heating elements which present the information on heat-sensitive recording paper whose speed is synchronized with the film speed of an S-11 camera. The relation of intensity to ground position is obtained by superposition or comparison of a strip film exposed in flight and the intensity record.

Figure 2.7 is a block diagram of the F-1 equipment showing the basic circuits employed. Figures 2.8, 2.9, 2.10, 2.11, 2.12, and 2.13 show the actual components. Table 2.2 contains pertinent data.

2.3 AN/ADR-1 RECORDING DOSIMETER

2.3.1 Purpose

This instrument is an automatic, continuous-recording gamma dosimeter, giving a graphic plot of instantaneous dose rate, and counter type dials giving integrated dosage. The information so presented is intended for use by air crews entering a contaminated air mass. Amber and red warning lights are provided to indicate when predetermined levels of intensity are reached.

2.3.2 Principle of Operation

The detecting elements of the AN/ADR-1 are high pressure ionization chambers. One chamber covers the range 0-20 mr/hr, the other the range 20-2,000 mr/hr. The outputs of the chambers are amplified and ultimately recorded on a moving logarithmic scale by inking pens whose deflection gives a continuous curve, the amplitude of the curve at any point being proportional to the instantaneous dose rate.

Amber and red warning lights are provided to indicate when predetermined levels of intensity are reached. Means are provided for

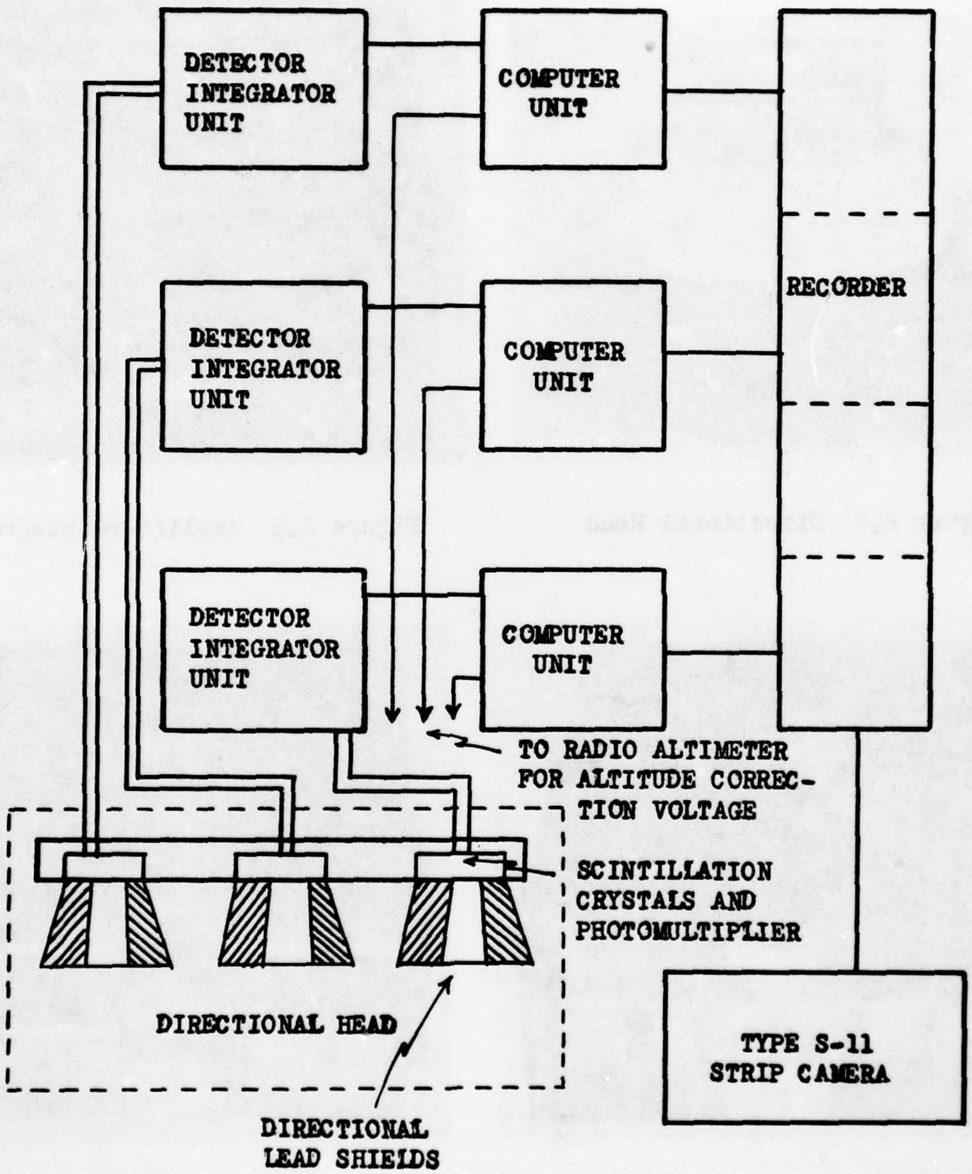

Figure 2.7 Block Diagram of Type F-1 Surface-radiation Survey Equipment

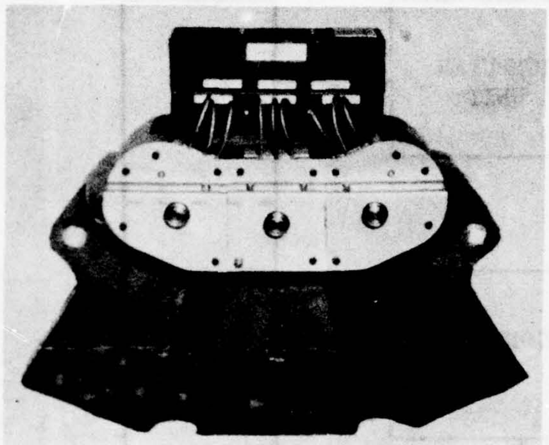

Figure 2.8 Directional Head

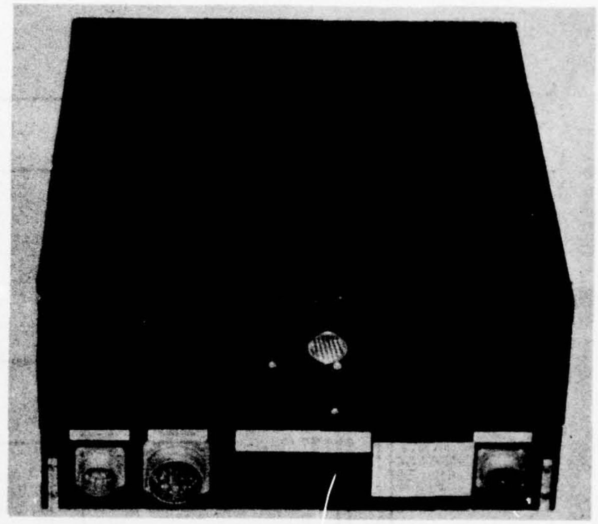

Figure 2.9 Amplifier-integrator

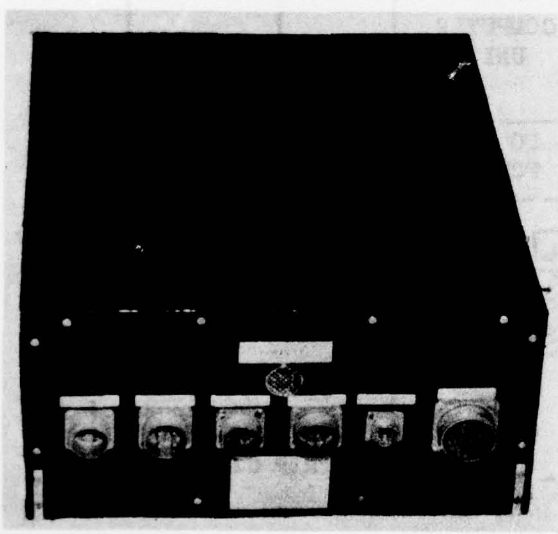

Figure 2.10 Computer Unit

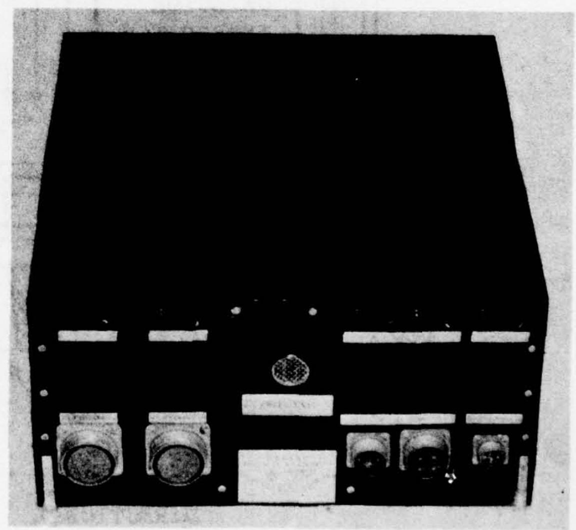

Figure 2.11 Power-supply Unit

Type F-I Surface Radiation Survey Equipment

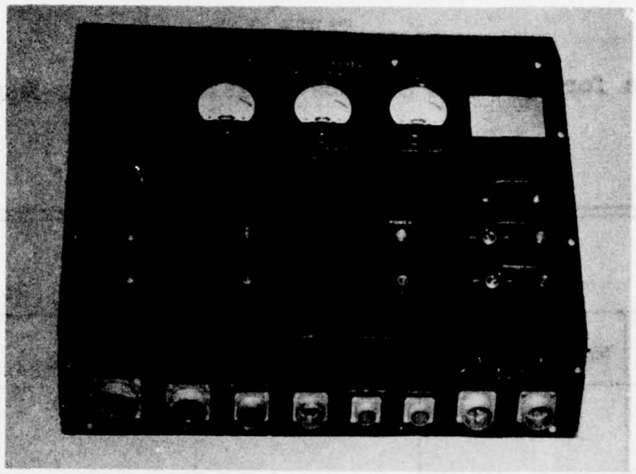

Figure 2.12 Recorder of Type F-1 Surface-radiation Survey Equipment

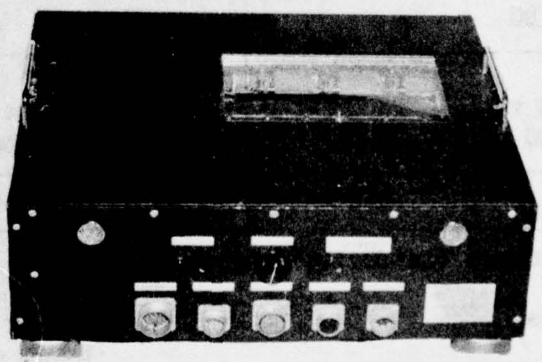

Figure 2.13 Control Unit of Type F-1 Surface-radiation Survey Equipment

TABLE 2.2

Data for Type F-1 Surface-radiation Survey Equipment

Physical Data				
Unit	Weight (lb)	Height (in.)	Width (in.)	Depth (in.)
Directional head	500	16	25	13
Amplifier-integrator	30	10	20	19
Computer	30	12	20	19
Power-supply	60	10	20	19
Control	20	11	20	14
Recorder	60	8	23	22
Power Requirements				
DC		AC		
28 v 100 w		115 v, 700 va 400 cps		
Miscellaneous Data				
Gamma intensity range (intensity at ground level) . . .			0.5-500 r/hr	
Scanning aperture			70° by 12° divided into three equal sections	

transmitting signals to accessory equipment at predetermined levels should such be necessary, e.g., to close an intake valve on a pressurized airplane.

Figure 2.14 is a block diagram of the ADR-1 showing the basic components and their interconnections. Figures 2.15, 2.16, 2.17, 2.18 and 2.19 show the actual components. Table 2.3 contains pertinent data.

2.4 <u>INSTALLATION OF SURVEY EQUIPMENTS AND DOSIMETER</u>

The detector units for the AN/ADR-1 gamma dosimeters were installed in the nose sections of the P2V-2 and the B-17. The ionization chambers of the AN/ADR-4 and the phosphor-photomultiplier detectors of the Type F-1 equipment were installed in the waist sections, well aft of the wing and as remote as practicable from large scattering masses such as the airplane's engines.

2.5 <u>HEADING AND ALTITUDE MEASUREMENT</u>

2.5.1 <u>Heading</u>

The heading of the aircraft in flight is determined by reference to a gyro fluxgate compass indicator. These indications are estimated to be correct to within one degree. The indicated heading, however, is the same as the direction of the ground track only in a no-wind condition or when the airplane has a velocity component with respect to the air which is equal and opposite to the wind at the altitude of flight. In practice, either the airplane is directed toward a salient object in the field of view or a correction is introduced subsequently when the wind is known. The error in ground track plotting due to wind is usually not significant, however, since the winds are usually small compared to the air speed of the airplane and the time of transit across the contaminated area is of the order of a minute or less. Moreover, with constant winds, the error is a simple linear function of time and a correction can readily be introduced in final estimates. Further comments on position and heading determinations are contained in Chapter 3, Operations.

2.5.2 <u>Altitude</u>

Radio altimeter measurements are accurate to within about five per cent. An error of fifty feet in a survey conducted at one thousand feet is not considered likely to introduce an appreciable error in estimates of attenuation; at least it will be small compared to other possible sources of error.

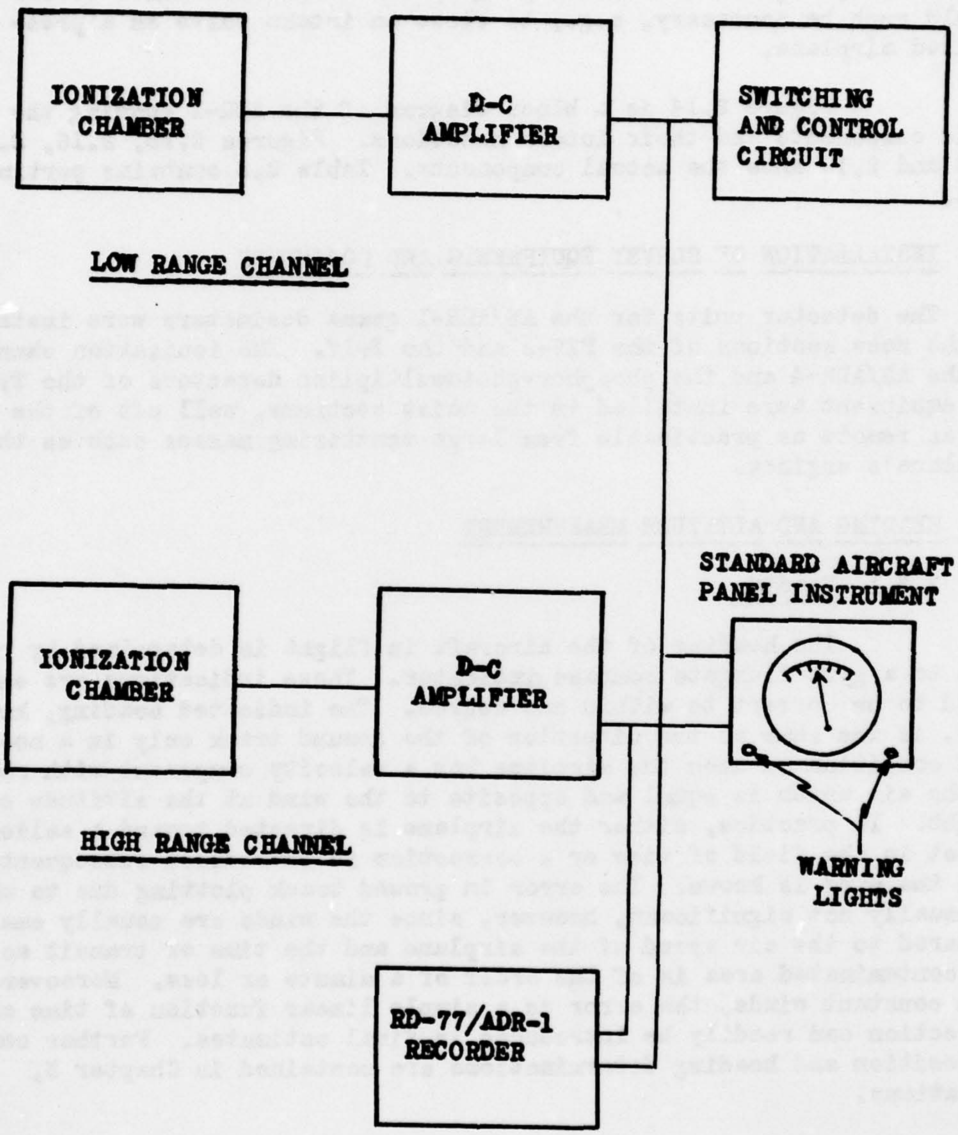

Figure 2.14 Block Diagram of AN /ADR-1 Gamma Dosimeter

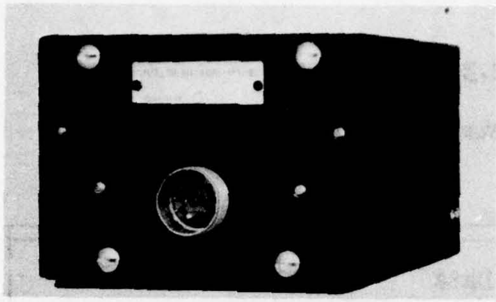

Figure 2.15 Detector Unit

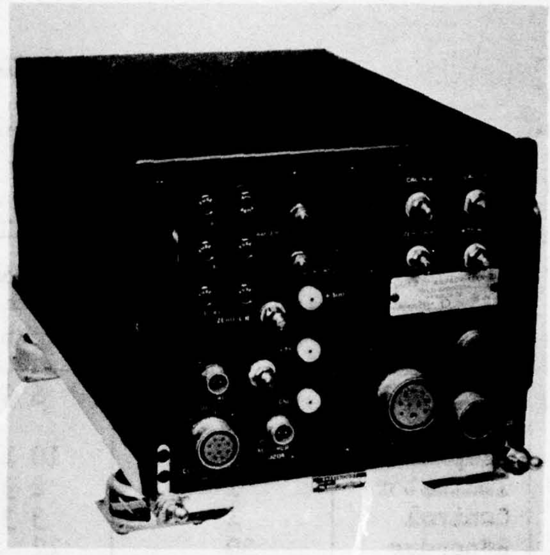

Figure 2.16 Power-supply and Amplifier Unit

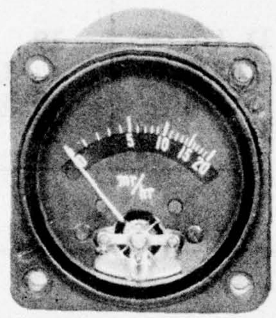

Figure 2.17 Indicator Unit

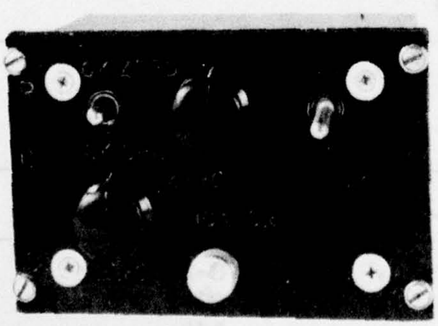

Figure 2.18 Control Unit

Figure 2.19 Recorder Unit

AN/ADR-1 Gamma Dosimeter

TABLE 2.3

Data for AN/ADR-1 Gamma Dosimeter

Physical Data				
Unit	Weight (lb)	Height (in.)	Width (in.)	Depth (in.)
Detector	10	6 3/4	8 1/4	12 1/4
Power-Amplifier	28	10 1/8	11 1/4	19
Indicator	1	2 3/8	2 3/8	4 3/4
Control	1	3 3/4	5 3/4	5 3/8
Recorder	30	12	11	19

Power Requirements	
DC	AC
28 v 50 w	115 v, 200 va 320-1760 cps

Indicator Scales	
No. 1	0-20 mr/hr
No. 2	20-2,000 mr/hr

Recorder Scales	
No. 1	0-20 mr/hr
No. 2	20-2,000 mr/hr
Dosimeter.	100 r

PROJECT 2.1c-2

CHAPTER 3

OPERATIONS

The two project aircraft were based at Kirtland Air Force Base, Albuquerque, New Mexico, throughout the duration of the tests, proceeding to the Nevada site on each shot day. On arrival at the site, each aircraft occupied its specified orbit approximately five miles from the zero point. The P2V-2 usually orbited at about 8,000 feet above the terrain, the B-17 at about 10,000 feet.

From zero time to about +1 hour both aircraft were engaged in monitoring gamma intensity telemetering units AN/USQ-1 mounted on concrete blocks on the ground near the crater. (See report on Project 2.1b, Gamma Radiation as a Function of Time with Droppable Telemeters.)

At about +1 hour, after the dust cloud had dissipated sufficiently to minimize the inhalation hazard, the two aircraft began ground survey operations.

Subsequent to the first shot, three overlapping parallel runs were made over the crater and in its vicinity at altitudes of 2,000, 1,500, and 500 feet. (See Fig. 3.1.) This method of survey was abandoned for the second shot for the following reasons:

(1) With no prior knowledge of the extent of the ground contamination, it is difficult to determine how many parallel runs need be made to adequately cover the area. For example, if the fallout lies in one narrow sector or lobe, the parallel run method is time-consuming at best unless, by accident, the passes happen to be oriented along the lobe.

(2) Lacking convenient reference points, the parallel run method does not permit an accurate determination of the airplane's position with respect to the crater except by subsequent correlation with ground photography during the runs. The only immediately available criterion in flight is the pilot's judgment of his lateral displacement with respect to the crater.

(3) The utilisation of ground photography for parallel run positioning is of doubtful value because the terrain around the crater is essentially featureless when viewed from an altitude of a thousand feet or more. Consequently an exhausting comparison must be made between a long film strip and the comparatively small scale maps of the area available which are hardly suitable for the purpose.

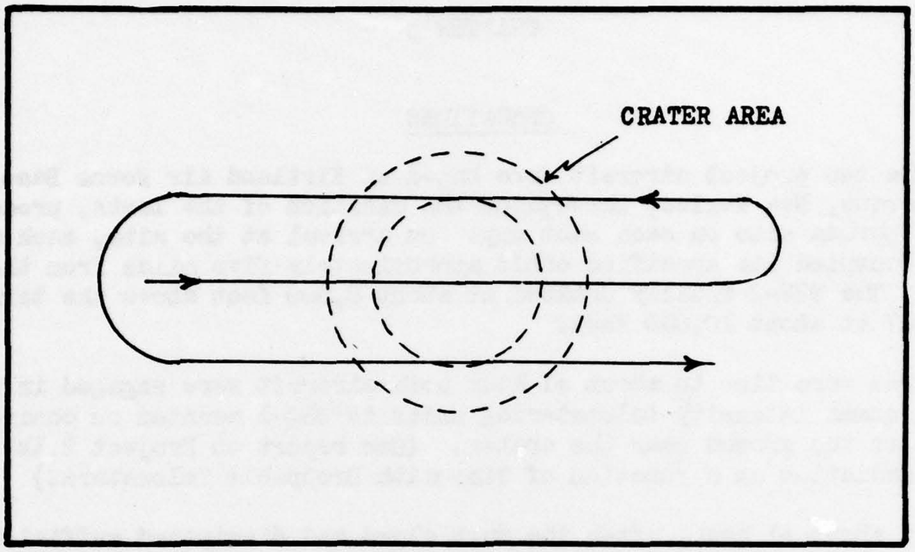

Figure 3.1 Surface Survey Flight Pattern for Surface Shot

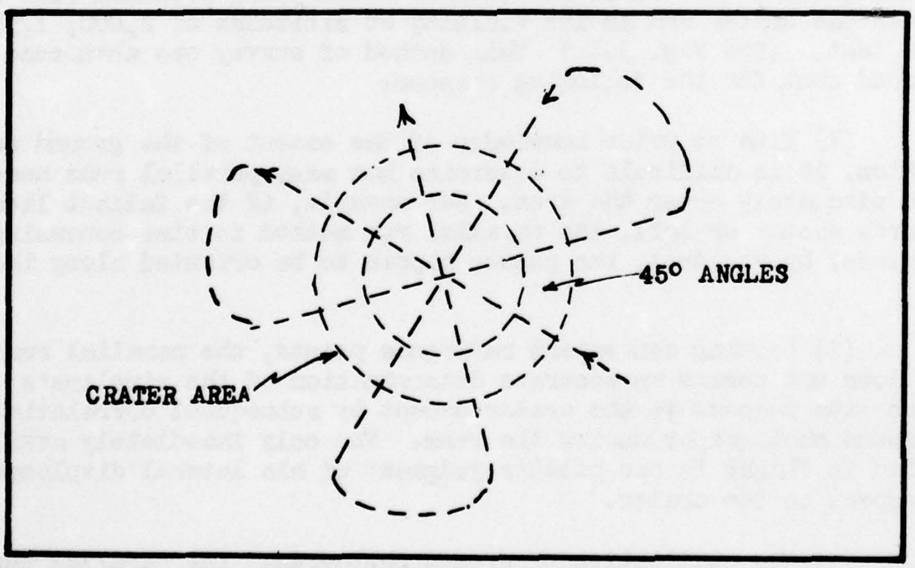

Figure 3.2 Surface Survey Flight Pattern for Underground Shot

It is to be noted that the parallel run method was initially utilized because of its value in similar operations in Operation GREENHOUSE. In that operation, however, the shots were detonated on small islands with well-defined shorelines and the entry and exit of the flight path could readily be ascertained by examination of a comparatively short film strip transecting a well-defined and indented shore line.

Consequently, a clover-leaf survey pattern was adopted for the underground shot, the aircraft making a series of runs at 45° angles to each other, all passing over the crater. (See Fig. 3.2.) Patterns were flown at altitudes of 4,000, 2,000, and 1,500 feet.

The clover-leaf pattern has the following advantages:

(1) Only the heading of the airplane, its ground speed, and its time of transit over the crater are required to obtain a reasonably accurate estimate of the airplane's position during the runs.

(2) The crater, being visible from the cockpit, permits the pilot to correct for drift due to wind.

(3) Ground strip photography is more easily used since the crater shows up as a distinctive feature in the otherwise uniform landscape and distances to other points on the path are readily estimated.

(4) The radial courses permit lobes and outlying areas to be more readily discerned as a matter of routine.

The limitations of the clover-leaf pattern are:

(1) It involves repeated passages over the crater and, if accomplished at low altitudes, might lead to somewhat higher dosages for crew members than in the parallel method. There is therefore an incentive to carry out the pass as fast as possible, especially if made at a low altitude.

(2) Radial passes over the crater may not be feasible if the crater lies near an abrupt rise in ground, e. g., a mountain. This constraint becomes particularly significant in the case of a low-altitude. high-speed pass as noted immediately above.

(3) Radial passes over the crater are not feasible if certain sectors are covered by dust clouds which entail a possible inhalation and contamination hazard when traversed by the surveying aircraft. It may therefore be necessary to wait for the cloud to drift completely off the area before starting to survey.

PROJECT 2.1c-2

An odograph was installed in the P2V-2 in anticipation of difficulties in flying a desirable pattern. This instrument gives a continuous plot of air position and of ground position if wind corrections are introduced. Its operation was not satisfactory, however, and little effort was expended to correct it inasmuch as the present scale of one-half mile to the inch is of little value in contour plotting. Efforts to secure an improved version are underway.

AD-A078 575 NATIONAL BUREAU OF STANDARDS WASHINGTON, D.C. 18/3, 18/8
OPERATION JANGLE. NEVADA PROVING GROUNDS, OCTOBER-NOVEMBER 1951, GAMMA RADIATION MEASUREMENTS, COSTRELL, LOUIS
UNCLASSIFIED WT-370 01 APR 52 AEC

3 OF 4
AD A 078575

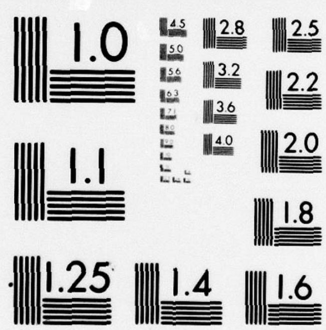

MICROCOPY RESOLUTION TEST CHART

CHAPTER 4

RESULTS

4.1 AN/ADR-4 SURFACE-RADIATION SURVEY EQUIPMENT

4.1.1 Surface Shot

Three parallel, overlapping paths were flown over the crater by the project aircraft at altitudes of 2,000, 1,500, and 500 feet. A peak value of 28,000 r/hr was obtained at H +1 hour. This value represents the average value of gamma ground intensity over an area 660 feet square, i.e., the average intensity in the middle cone measured at the aircraft and corrected for altitude and attenuation. Data was obtained on all runs but only the curve obtained on the crater pass at 1,500 feet is presented here in Figure 4.1.

Data on other passes, laterally and at other altitudes, is not included here inasmuch as it possesses no particular significance (1) because of uncertainty in aircraft position as detailed in Chapter 3, Operations, permitting no reliable correlation with actual ground measurements, (2) because of instrument design limitations detailed in Chapter 5, Discussion.

Figure 4.2 is a decay curve obtained from peak intensity readings at the same altitude over the crater on shot day and on the third and twelfth day following. The accepted $T^{-1.2}$ curve is drawn on the same graph for comparison.

4.1.2 Underground Shot

Figure 4.3 is a representative contour map based upon data taken at 1,500 feet approximately at H +2 hours and corrected by the $T^{-1.2}$ curve to H +1 hour. A clover-leaf pattern was used. The contour lines are markedly in error compared with actual ground readings except possibly directly over the crater. The nature of these errors is discussed in Chapter 5. Figure 4.4 is a plot of gamma intensity measured at ground level and corrected back to H +1 hour taken from a preliminary report of Project 2.1d.

4.1.3 Buster Shots

Figures 4.5 and 4.6 are intensity curves obtained during shots Dog and Easy of Operation BUSTER incidental and subsequent to the test of the AN/ADR-3 and Type D-1 radioactive-cloud trackers in Project 6.4,

Airborne Radiac Evaluation. The curves are representative only, being taken from passes over the zero point and omitting lateral pass data.

4.2 TYPE F-1 SURFACE-RADIATION SURVEY EQUIPMENT

Satisfactory operation of the Type F-1 equipment was obtained in the B-17 alone due to several factors, including the necessity of devoting the full attention of the limited personnel in the P2V-2 to the AN/ADR-4 surface-radiation survey equipment.

Curves comparable to those obtained for the AN/ADR-4 were obtained by the Type F-1 equipment but lower in magnitude by a factor of one hundred or more.

The curves which were obtained for the surface shot were plotted from data recorded during parallel passes and are therefore considered to be in error due to uncertainity in aircraft position, much as in the case of the runs by the P2V-2. The change of radiation intensity as the aircraft flew directly over the crater at an altitude of 2000 feet at approximately H - 1 hour subsequent to the surface shot is shown in Figure 4.13. Traces are shown for the center and right channels of the F-1 equipment. The left channel was inoperative at the time this data was gathered. The data may be compared with similar data obtained with the AN/ADR-4 at the same time and shown in Figure 4.1.

4.3 AN/ADR-1 GAMMA DOSIMETER

4.3.1 General

The AN/ADR-1 automatic recording dosimeter is a nondirectional detecting device giving a continuous plot of gamma intensity in the aircraft. The data so secured has no simple relation to ground contamination and therefore, in a sense, its accumulation may not appear relevant to this project. Nevertheless, the curves are believed to be of value for the following reasons:

(1) Curves taken at different altitudes over the craters or air burst zero points permit an estimate of attenuation due to the intervening air.

(2) A tentative set of rules might be formulated for estimating ground contamination, provided information is available on the nature of the burst (ground, surface, or air) and the peak intensity observed at zero point.

4.3.2 Surface Shot

Data were recorded, but discontinuously, due in part to power supply failures and in part due to the fact that the instruments went off scale (at 20 r/hr) when near or over the crater. The failure of the power supply was remedied in a short time but the instrument requires a comparatively long warm-up period to secure stable operation and most of the passes were completed before optimum operation had been reached. These fragmentary data are not presented in this report.

4.3.3 Underground Shot

Figures 4.7, 4.8, and 4.9 are curves obtained from passes over the crater at 1,000, 2,000, and 3,000 feet.

4.3.4 Buster Shots

Figure 4.10 shows data recorded on recording dosimeter AN/ADR-2 for shot #3 of BUSTER. The AN/ADR-2 is similar in principle to the AN-ADR-1, differing in construction, notably in the recording device. Figures 4.11 and 4.12 are curves taken during shots Dog and Easy of BUSTER on the AN/ADR-1.

CHAPTER 5

DISCUSSION

5.1 PRELIMINARY

The problem of determining gamma intensity at ground level from measurements made at altitude is not an easy one. It is comparable to the determination of the characteristics of a light source of diminishing intensity, whose physical extent, luminosity, and spectral distribution are unknown and which is shielded from observation by an absorbing and scattering medium whose attenuation coefficient is a function of radiation energy. In radioactive terms, the extent of the contaminated area, the ground intensity, the energy-frequency distribution, and the attenuation due to air are unknown. Moreover, operational limitations require that the data to be used be obtained in a reasonably limited number of passes over the area, and in a reasonably short time.

The present designs of the AN/ADR-4 and Type F-1 surface-radiation survey equipments are therefore based upon assumptions and approximations. Assumptions had to be made regarding the expected surface distribution (i.e. somewhere between a point source and an infinite plane), the attenuation of gamma radiation as a function of energy and distance, and the relative amounts of scattered and direct radiation to be expected at various distances and directions from the extended source. No satisfactory mathematical theory exists, except perhaps for very approximate calculations, and the only practicable approach has been to secure actual data at altitude by participating in a wide range of atomic detonations.

In brief, the purpose of the present project was not so much to provide actual information on ground intensity but rather to discover what design assumptions were incorrect as a guide in future development work.

5.2 JUSTIFICATION FOR SURFACE-RADIATION SURVEY EQUIPMENT

The difficulties encountered in obtaining satisfactory equipment are many, but the advantages accruing from its possession are marked. Aerial survey can be:

(1) Accomplished rapidly, not only in the area but by getting to the area in a minimum of time. For example, information can be obtained and made available to an approaching task force while it is a hundred miles from a beachhead on which troops are to be landed.

(2) Carried out over comparatively large areas. For example, a beachhead heavily bombed in breadth and depth could be quickly surveyed.

(3) Carried out in territory held by the enemy or under enemy fire with comparative safety.

(4) Carried out over high intensity areas otherwise inaccessible.

(5) Carried out without change of technique over land, sea, or beachhead.

It is these advantages which suggest that such equipment would be a valuable accessory in planning for a landing from the sea on a bombed beachhead or in an advance by ground forces into a contaminated area. The information obtained would enable a staff to estimate the length of time required to cross a contaminated area, or to remain in it, or to decide whether to avoid it, and to what extent it would be accessible to enemy troops.

5.3 CRITICISM OF SURFACE-RADIATION SURVEY EQUIPMENT

Some of the possible criticisms of the survey equipments may be enumerated as follows:

(1) Compared to most radiac measuring equipment, the survey equipment is heavy and bulky and requires a large airplane to employ it.

This criticism is becoming less significant in future designs. The Navy equipment, for example, is being packaged compactly so that it can readily be attached to or removed from an attack airplane available on almost all aircraft carriers. It can be held in reserve and brought forth for use when necessary, imposing no restrictions on aircraft operation in the interim.

(2) Being a rather complex item, any survey equipment will require maintenance facilities and personnel.

(3) If the atomic burst is an air burst, the residual contamination on the ground should rapidly decay to a low level and ground monitors should be able to outline the area as, and if, necessary. If the burst is on the surface or underground, the crater should be readily visible and a distance of closest approach can be specified.

This criticism, however, appears to assume that the altitude and yield of the air burst are known. This may be true of our own weapons but certainly not of those dropped by the enemy. It would appear to take little account of extensive fallout patterns in a high yield underground shot or even for a low air burst. Moreover, it does not encompass the possible use of radiological warfare agents over an extended area or its indirect equivalent, pattern bombing with atomic bombs over a large area.

(4) The survey equipments only measure the average intensity over a square 330 feet on a side at an altitude of 1,000 feet; therefore they do

not indicate "hot spots" in the area which may be of major importance to ground troops. Again, since its indications are averages, their significance for rough terrain is not clear. Is the contamination on the ridge tops alone, or in the valley as well?

The problem of "hot spots" is acknowledged. But it should be borne in mind that the survey equipment is intended to provide rapid information to a field commander, not to eliminate the use of portable survey equipment. As for rough terrain, it may be argued that use of an atomic bomb is not likely to be justified against such a target. Admittedly, however, such a rough area might be contaminated by fallout or drifting clouds or deliberate radiological warfare agents which the current survey equipments would perhaps not properly assess.

(5) Finally, it may be inquired whether the elaborate automatic survey equipments cannot be replaced by using a simple intensity meter in flight, noting the point of peak intensity and estimating the residual contamination field below the aircraft on the basis of patterns established on previous detonations of a like character.

This approach certainly cannot be summarily dismissed and its limitations as a makeshift method are being investigated. However, it appears to be about as reliable as a weather forecast. Any data so acquired would necessarily be sketchy and any variations from previous patterns would bring the entire estimate under suspicion.

In brief, the advantages of aerial ground survey appear to outweigh the disadvantages.

5.4 DISCUSSION OF TEST RESULTS

5.4.1 AN/ADR-4 Surface-radiation Survey Equipment

An examination of Figs. 4.1, 4.2, and 4.3 indicates that the AN/ADR-4 was in error in each of the JANGLE shots by an amount depending upon the distance from the zero point. For comparison, see Fig. 4.4, indicating actual ground level values. In Fig. 4.3, for example, at 500 yards the air survey indicates about 2,000 r/hr while the actual value appears to have been about 1,000 r/hr. At 1,000 yards due south, the AN/ADR-4 indicated 100 r/hr while the actual value appears to be about 1 r/hr or less.

The explanation of this marked difference is believed to be as follows: Both the surface and underground shots gave rise to an intensely hot crater area. The contamination around the craters was appreciable but relatively small, except in the down wind area north of the crater. As a result, even at large distances, the principal contribution to the radiation received by the AN/ADR-4 was due to scattered radiation from the crater and only a minor amount to radiation from the ground beneath. The crater radiation, being highly scattered, nevertheless appeared to come from the ground

beneath insofar as the AN/ADR-4 was concerned. The farther the distance from the crater, the greater became the percentage due to the crater, until even where there was no ground contamination an appreciable amount was being received from the crater and attributed to ground contamination. In brief, the AN/ADR-4 which had been designed to survey a uniformly varying contaminated area, failed to cope with a very hot source of limited dimensions.

Directly over the crater, all of the radiation was coming from the crater and from the ground immediately below the airplane. It is therefore believed that the peak values on the curves do not contain errors attributable to scattered versus direction radiation. Instead the errors here (the instrument reading high by a factor of four) is attributed to the fact that the ionization chambers were intended for use with radiation in the 300 Kev to 3 Mev range whereas the actual radiation is understood to have been largely in the 80-130 Kev range at ground level. Scattering would further shift the ground level energy distribution to lower energies at altitude. The present chambers have a peak response in the 100-250 Kev range (See Figure 2.1) and the unanticipated presence of radiation in quantity at low energies is believed to have led to excessively high readings. This additional source of error would, of course, also partially explain the high readings at distances well out from the center of the crater.

To the north of the craters, where the fallout was much higher, the AN/ADR-4 did begin to receive an appreciable fraction of radiation from the ground. Consequently, the general orientation of the contour pattern is not too far off. It is evident, however, that the crater radiation is still dominant and the actual northeasterly trend is obscured by the contribution from the almost due north elongation of the contour lines around the crater.

Figures 4.5 and 4.6 show ground intensity indicated during runs across the zero point areas of shots Dog and Easy of Operation BUSTER. Limited data on actual ground values are drawn as dotted lines on the same figures. Here again the equipment indicates high immediately over the zero point due to peaked response of the ionization chambers in the 100-250 kev region while the increasing error factor at distances further out is partially ascribable to scattered radiation from the zero point competing with ground contamination radiation beneath the airplane, as noted in previous paragraphs.

The differences among the curves are traceable to two sources:

(1) At higher altitudes, the field of view of the instrument covers a larger area at ground level and therefore the <u>average</u> intensity falls off. It will be observed that the peak intensity falls off with altitude as might have been predicted.

(2) The ground tracks of the airplane varied in direction from one another within a 30° angle and it is assumed that the curves might

reasonably differ if only due to assymmetry in the ground contamination pattern and the difficulty of passing exactly over the center of the explosion area on successive runs.

5.4.2 Type F-1 Surface-radiation Survey Equipment

The chief difficulty with the F-1 equipment is the instability of the amplifiers and the Brown converter oscillator with changes in operating temperature. The oscillator frequency must be adjusted immediately prior to use to compensate for temperature drift during warm-up. The amplifiers in the computer are very frequency selective and a slight change in input frequency causes a large variation in the output amplitude. Also at altitudes where the amplifier gain is near its maximum the amplifiers are in an unstable condition and are likely to begin self-oscillation at any transient disturbance.

The recorder does not have a great enough range. The useful range is 5 to 1 and should be at least 10 to 1. The pens are too fragile and the method of controlling the pen temperature requires the operator to constantly control the heat to prevent either burning the recording paper or loss of recording as the vibrations of the pens change amplitude with changes in ground intensity.

The equipment is not easily serviced and calibrated because many controls and test points are almost inaccessible when the equipment is normally installed in the plane.

There was a great disagreement between the indicated ground intensities of the Type F-1 and AN/ADR-4 Radiac Sets. The latter employs "shadow" shielding as described in Section 2.1.2 and the former employs shielding in all directions except toward the ground. In the AN/ADR-4 the difference between two fairly high levels of radiation is measured while in the F-1 the radiation in the ground-directed solid angle is measured directly. The F-1 equipment gave readings which were usually about one-hundredth as high as those obtained with the ADR-4.

Ground radiation intensity measurements given in Figure 4.12 were used as a standard in comparing results obtained with the two radiac sets. The nature of the data is such that wide variations in indication of ground radiation intensity are obtained depending upon assumptions made concerning the actual distribution within the contour lines provided. Three estimates were made of the ground dosage rate. The most probable dosage rate was obtained by assuming exponental interpolation between contour lines provided. The other two estimates were made as limiting permitted by the data used as a standard. Only rough estimates were possible inasmuch as the only data available from instruments used as standards was not sufficiently detailed to give an exact indication of the distribution of ground radiation intensity. A comparison of the data obtained by the

F-1 and ADR-4 Radiac Sets with the best ground radiation intensity estimate indicates that the F-1 reads low by a factor of approximately 3 while the ADR-4 reads high by a factor of approximately 40. Using the maximum possible estimate, the F-1 reads low by a factor of 25 while the ADR-4 reads high by a factor of 6. Using the lowest possible estimate, the F-1 reads correctly within 10% while the ADR-4 reads high by a factor of over 100.

5.4.3 <u>AN/ADR-1 Gamma Dosimeter</u>

Figures 4.7, 4.8, and 4.9 are curves obtained at altitude over the crater of the underground shot. Roughly, the intensity appears to fall off by a factor lying between three and four each additional 500 feet of altitude. This fact serves to vindicate the assumption made in designing the F-1 equipment that the radiation intensity decreases by a factor of 10 for each 1200 feet increase in air path. The curves represent the dose rate which an individual might have encountered at that particular time and place in that particular part of the project airplane, namely, the nose section. They do not represent the dose rate necessarily at any other part of the airplane. Specifically, it was observed that these instruments invariably read higher by a factor of ten than the values obtained by the radsafe monitor stationed amidships. In other words, the fuselage in certain sections of the airplane may constitute a rather effective shield.

Figures 4.11 and 4.12 are curves obtained in passes over the zero points of BUSTER shots Dog and Easy. They are evidently similar to the JANGLE curves but much lower in intensity level.

It is believed that the AN/ADR-1 curves will be of use in two ways:

(1) In conjunction with the known energy characteristics of gamma radiation at ground level, they should permit an estimate of the attenuation due to air. Such calculations will be complicated, however, by the fact that the sources at low altitudes are extended while at higher altitudes they approximate a point.

(2) As a basis for approximate rules which might enable an aerial observer equipped with nondirectional equipment to make some estimate of the probable ground intensity level and the extent of the contaminated area. Unsatisfactory though such rules might be, they could be of use in the interim period until equipment of the AN/ADR-4 or F-1 type is available in service.

5.4.4 Airborne Particulate Debris

Preliminary information obtained from Project 2.1c-1, Aerial Survey of Distant Contaminated Terrain, indicates that airborne particulate debris may be a source of radiation encountered in flight which would be incorrectly attributed to ground contamination. The significance of such debris with respect to the aerial survey detailed in the present report is not easy to assess since the copy of the report made available to the authors contained no quantitative data. However, it is believed that such cloud radiation would be at a very low intensity and introduce a significant error only over areas where the actual ground intensity was small and hence of little importance in a military way. Clouds of particulate matter would presumably introduce an error on the side of safety in any event. The smooth and continuous curves obtained with the AN/ADR-1 recording dosimeter in the project aircraft indicate that such clouds were not flown through during the course of the present survey. Moreover, after surveying the crater areas, the P2V-2 project airplane made several flights over low lying cloud resulting from the detonation at altitudes above the cloud of the order of two hundred feet. In all such flights, the increase in radiation level was barely perceptible. As a result, while the problem of aerial debris is not to be summarily dismissed and will certainly be considered in future tests, it does not appear on the basis of available information, to be a major limitation on the practicability of aerial survey of ground contamination.

UNCLASSIFIED

[redacted]

CHAPTER 6

CONCLUSIONS

6.1 AN/ADR-4 SURFACE-RADIATION SURVEY EQUIPMENT

The AR/ADR-4 surface-radiation survey equipment is not satisfactory in its present design status for aerial survey of a contaminated area. It does not discriminate between the scattered gamma radiation from the zero point or crater and the radiation from the ground beneath the surveying aircraft. It also is in error due to the energy dependent characteristics of its ionization chambers, possessing an undesirable peak response in the 100-250 kev region.

6.2 TYPE F-1 SURFACE-RADIATION SURVEY EQUIPMENT

1. The Type F-1 surface - radiation survey equipment is not a satisfactory instrument in its present form for aerial survey of a contaminated area. However, this equipment does have very good directional properties and indicates very definitely the relative radiation intensities in the three adjacent areas being surveyed simultaneously. The equipment appears to indicate ground gamma intensities below the actual values. The errors are considered to be due to the following facts:

(a) The equipment was not designed to operate in a radiation field where the energy level extends primarily from 80 to 130 KEV.

(b) A cobalt 60 source was used to calibrate the equipment.

(c) The calibration procedure is not precise enough to permit accurate calibration of the equipment.

6.3 AN/ADR-1 GAMMA DOSIMETER

The AN/ADR-1 gamma dosimeter is satisfactory in principle and operation provided its recording mechanism is kept under frequent observation to eliminate zero drift and to insure proper pen adjustment. The intensity values indicated by it will depend critically upon the location of the detecting elements in the surveying aircraft.

[redacted]

UNCLASSIFIED

CHAPTER 7

RECOMMENDATIONS

7.1 GENERAL

The present airborne radiac equipment intended for aerial survey of a contaminated area is complex, heavy, and expensive. The results obtained are subject to several appreciable errors and to others which may or may not be negligible. If the final equipment is to be of value, not only must these errors be reduced, they must be reduced to values considerably smaller than those which could be expected from an aerial survey conducted with a simplified version of the AN/ADR-1 recording dosimeter or even a simple direct-reading portable instrument. Or, if appreciable errors are to be tolerated, they must be justified by particularly valuable features of the equipment, such as automatic and continuous recording, simplicity of presentation, or ease of computation and correlation with the aircraft's ground track.

The recommendations listed below for particular equipments are those which are necessary to minimize known errors and to effect reductions in complexity and weight. It is not considered, however, that these recommendations should be put into effect until a preliminary investigation, based upon the results of the present report, has shown that a solution does exist which can be obtained in the present state of the arts and which can be obtained without excessive cost. If this investigation indicates that the problem of accurate aerial survey will always involve inherent and inescapable errors, further development of such special radiac equipment should be abandoned. Such an investigation is now being conducted by the Navy and its contractors.

Concurrently with such an investigation, a study should be made of the feasibility of aerial survey with a simplified AN/ADR-1 recording dosimeter or its equivalent. This study should assume measurements made at altitude and estimate the errors made in predicting ground level intensities utilizing extrapolation methods empirically obtained in past and future atomic tests intended to evaluate the methods and estimates selected.

When sufficient information is obtained from the investigation of present equipment and from the proposed study, the entire airborne radiac aerial survey program should be carefully reviewed in the light of the particular operational or tactical situation in which it is expected to be of use.

Irrespective of the particular technique of aerial survey which is adopted, it is recommended that particular attention be given to encouraging the development or utilization of navigational methods or equipment which will permit a more satisfactory determination of an aircraft's position

in its maneuvers over a limited area in order that better correlation between aircraft position and measured ground gamma intensity can be established. Such a program would require little direct support from radiac equipment funds since a similar requirement for accurate knowledge of aircraft position exists for more extensive programs, such as anti-submarine warfare.

7.2 AN/ADR-4 SURFACE-RADIATION SURVEY EQUIPMENT

It is recommended that this equipment be redesigned as follows:

(1) Introduce design changes to insure that only radiation from the ground beneath the aircraft determines the estimated values of gamma intensity at ground level.

(2) Modify the detecting ionization chambers to eliminate the peak response from the 100 kev region.

(3) Reduce the size and weight of the equipment and redesign it so that it can be installed on, or removed from, a carrier based aircraft as a packaged unit.

7.3 TYPE F-1 SURFACE-RADIATION SURVEY EQUIPMENT

It is recommended that this equipment be further developed as follows:

(1) Introduce design changes to insure circuit stability

(2) Improve the recording method

(3) Reduce the size and weight

(4) Investigate the effect of the shielding method on indicated intensities

7.4 AN/ADR-1 GAMMA DOSIMETER

It is recommended that this equipment be redesigned as follows:

(1) Reduce its size and weight

(2) Improve the reliability of its recording mechanism

(3) Adapt its improved design to permit incorporation in the packaged unit desired for the AN/ADR-4

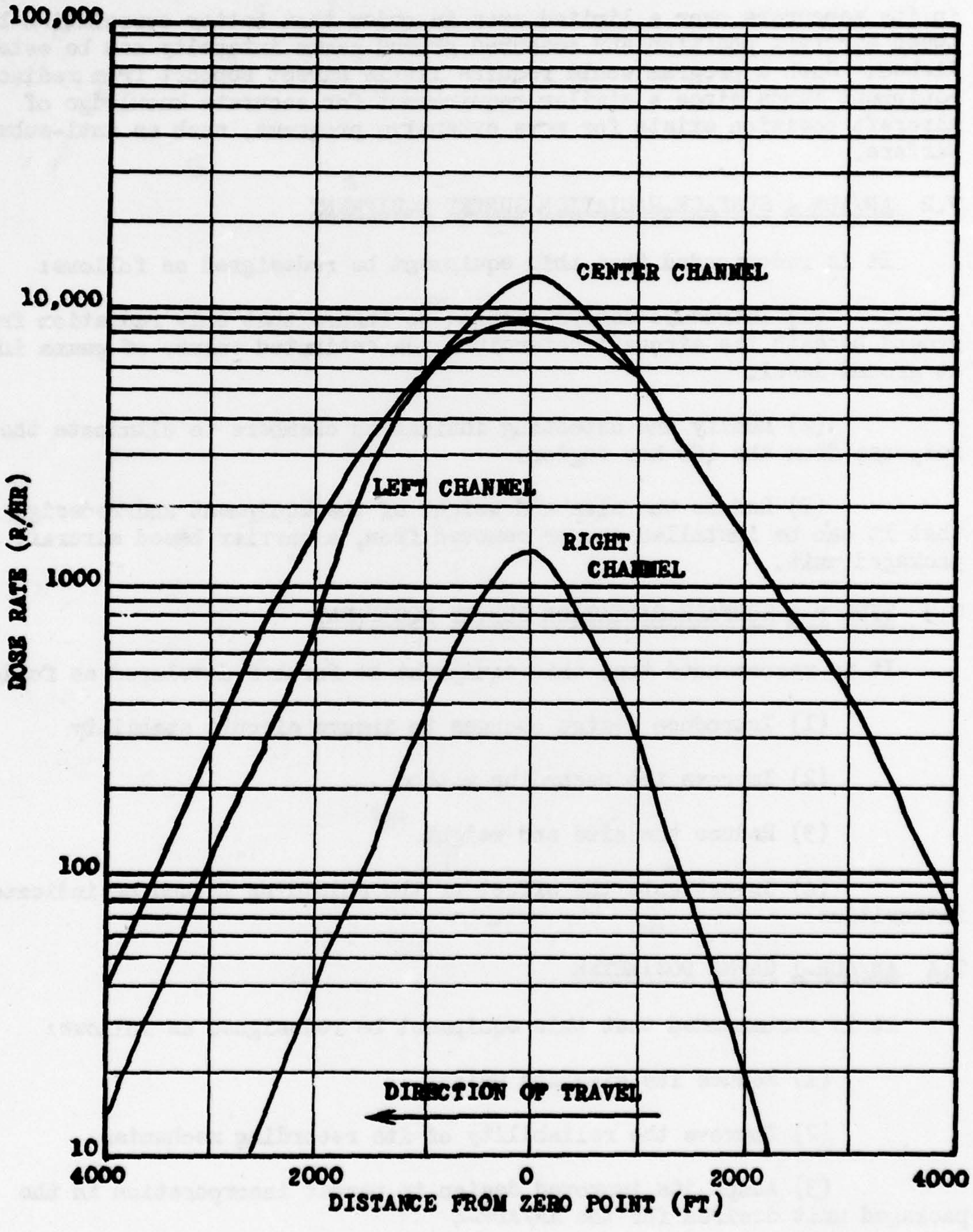

Figure 4.1 Gamma Intensity Near Ground Zero at H + 1 Hour Measured by AN/ADR-4 - Surface Shot

PROJECT 2.1c-2

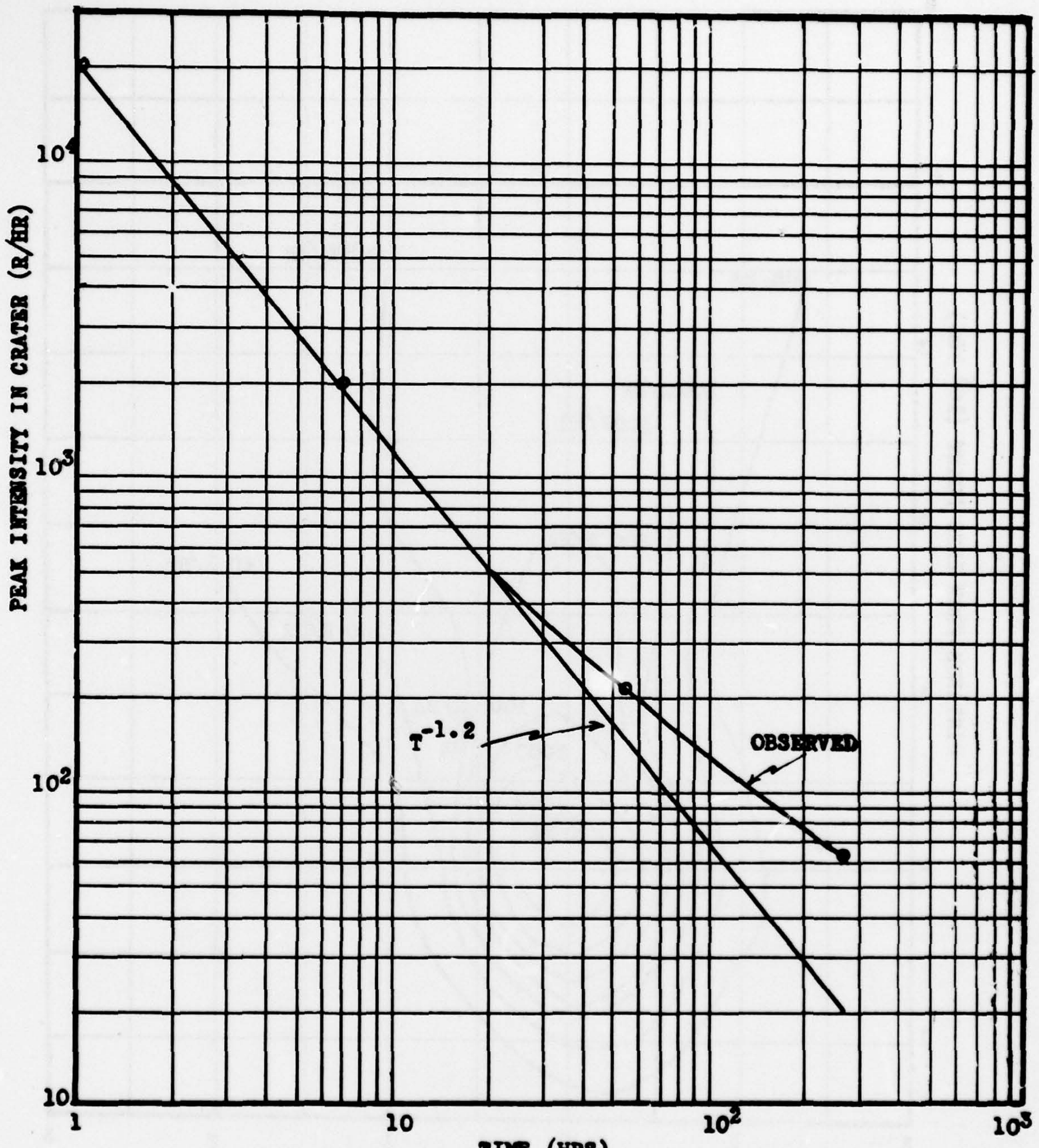

Figure 4.2 Gamma Intensity Near Ground Zero Measured by AN/ADR-4 - Surface Shot

[redacted]

PROJECT 2.1c-2

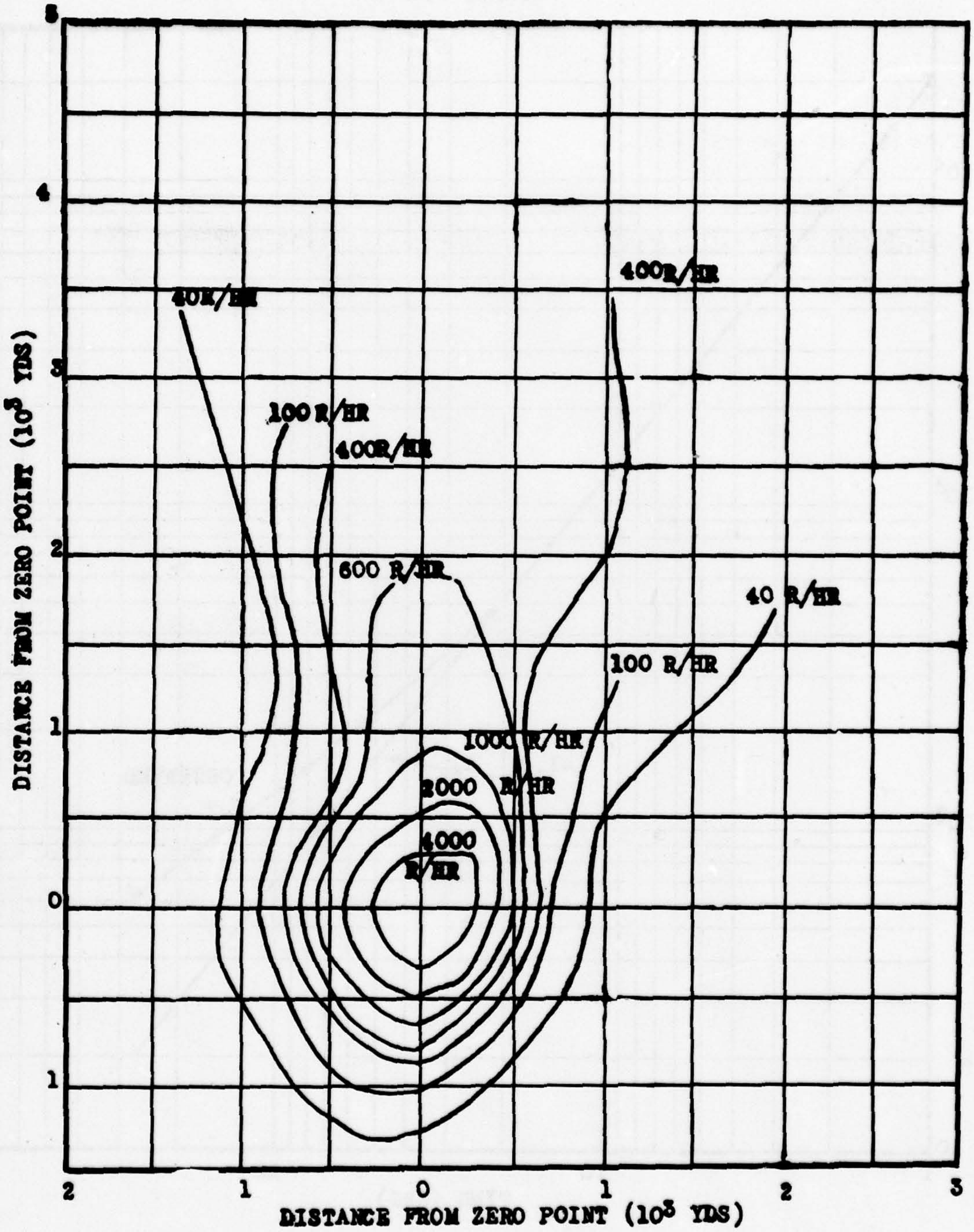

Fig. 4.3 Gamma Intensity Contour Map at H + 1 Hour Measured by AN/ADR-4 Surface Shot

[redacted]

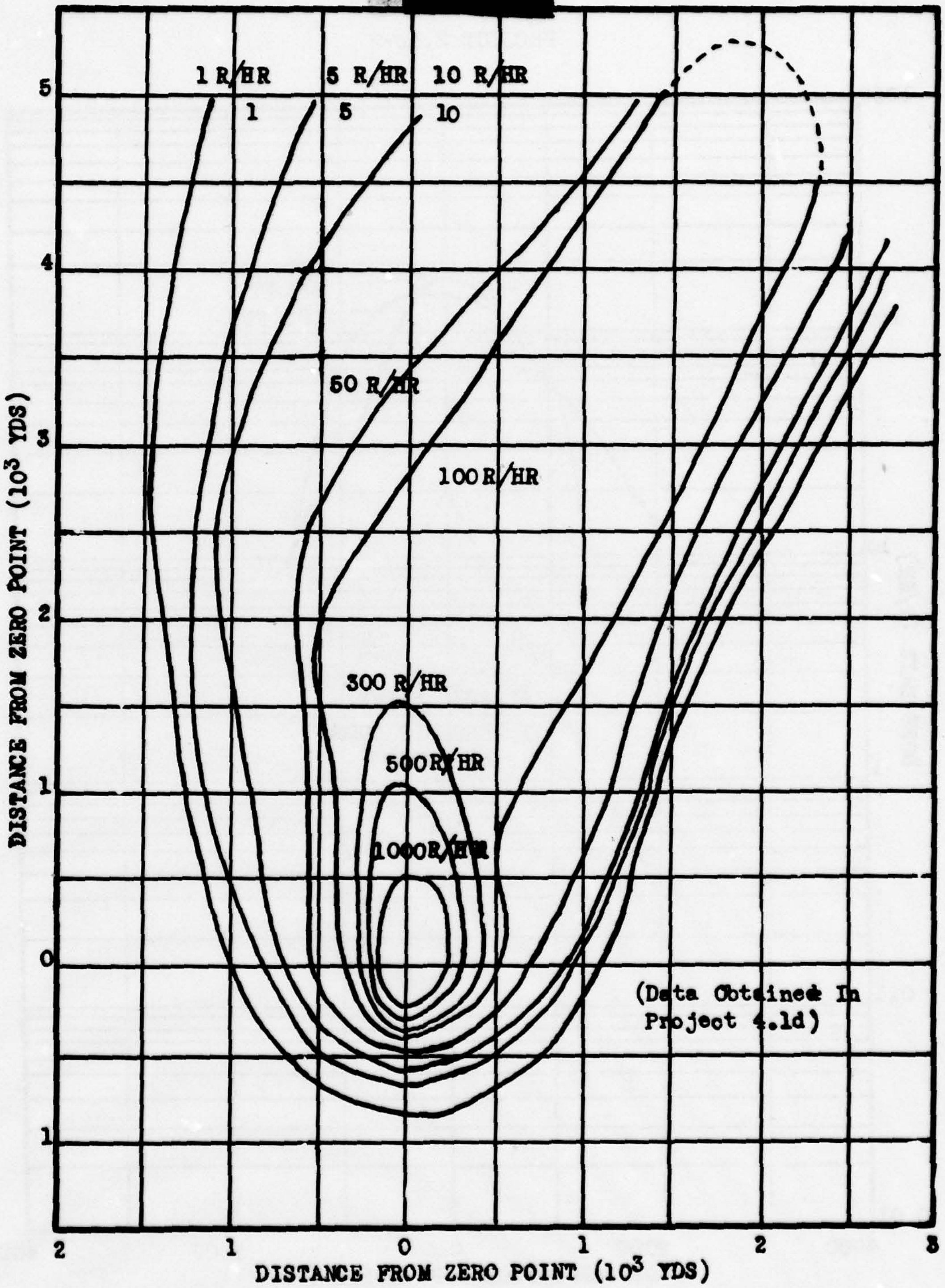

Fig. 4.4 Gamma Intensity Measured at Ground Level at H+1 Hour - Underground Shot

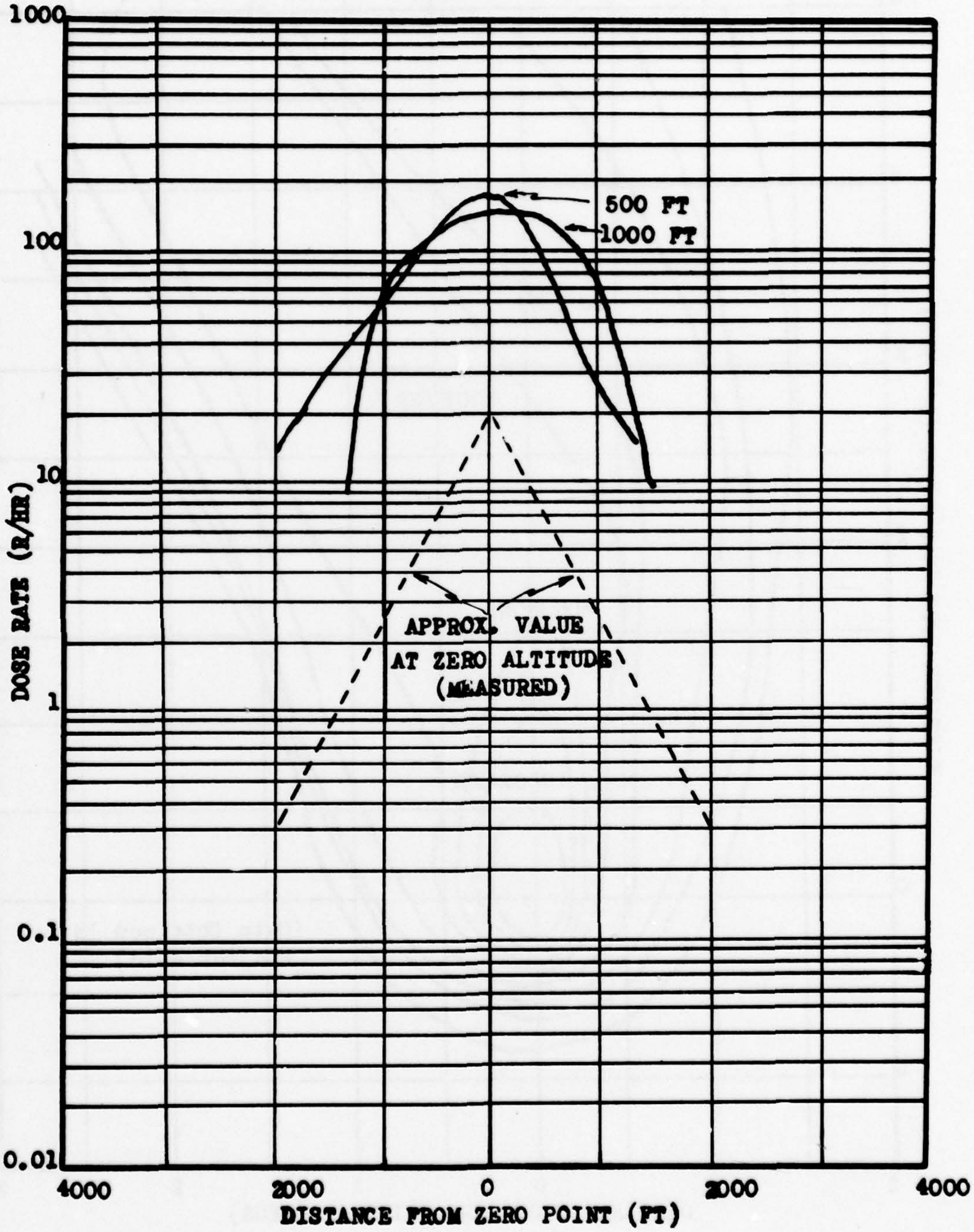

Fig. 4.5 Gamma Intensity Near Ground Zero at H+1 Hour Measured by AN/ADR-4 - Shot Dog of Operation BUSTER

PROJECT 2.1c-2

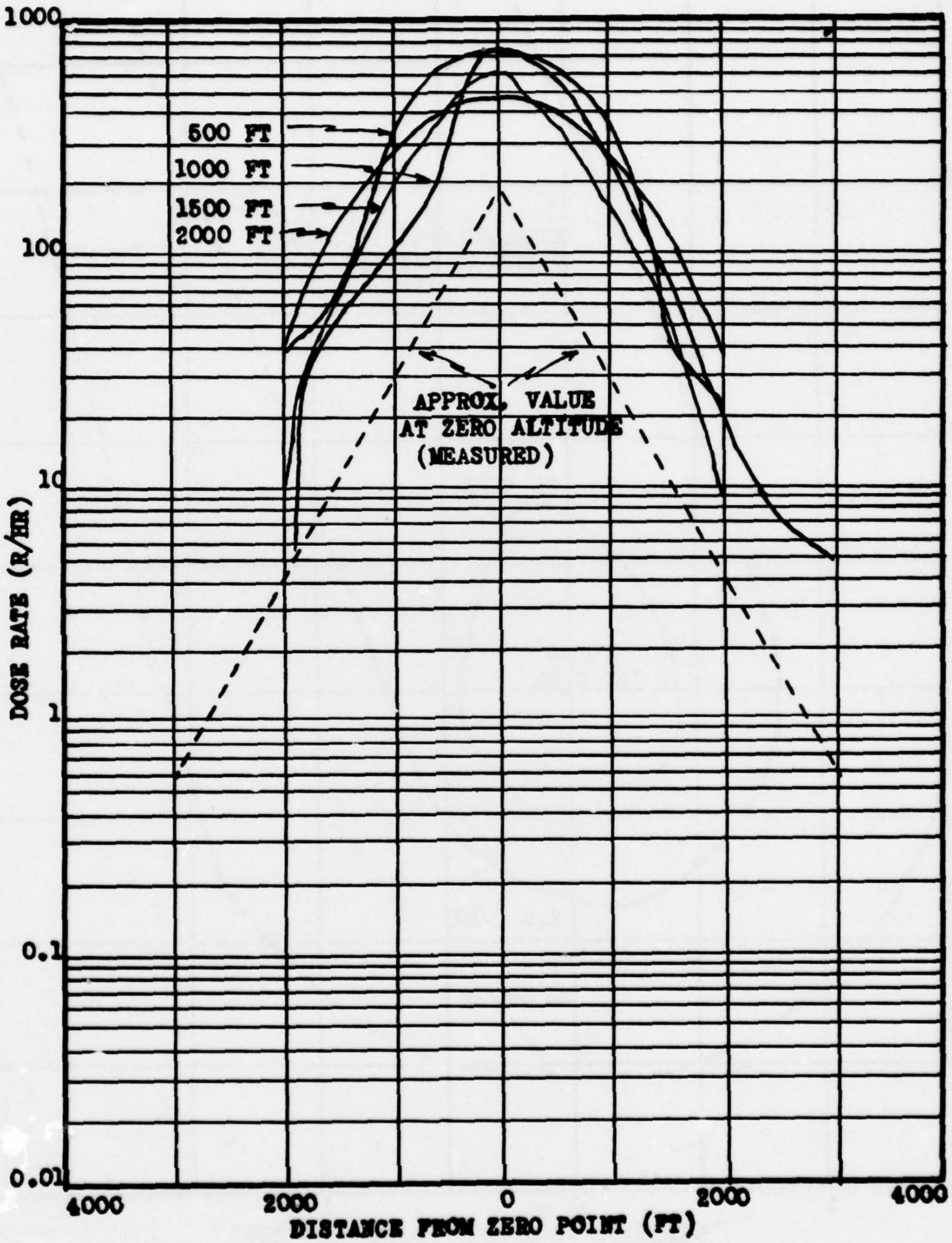

Fig. 4.6 Gamma Intensity Near Ground Zero at H+1 Hour Measured by AN/ADR-4 - Shot Easy of Operation BUSTER

[redacted]

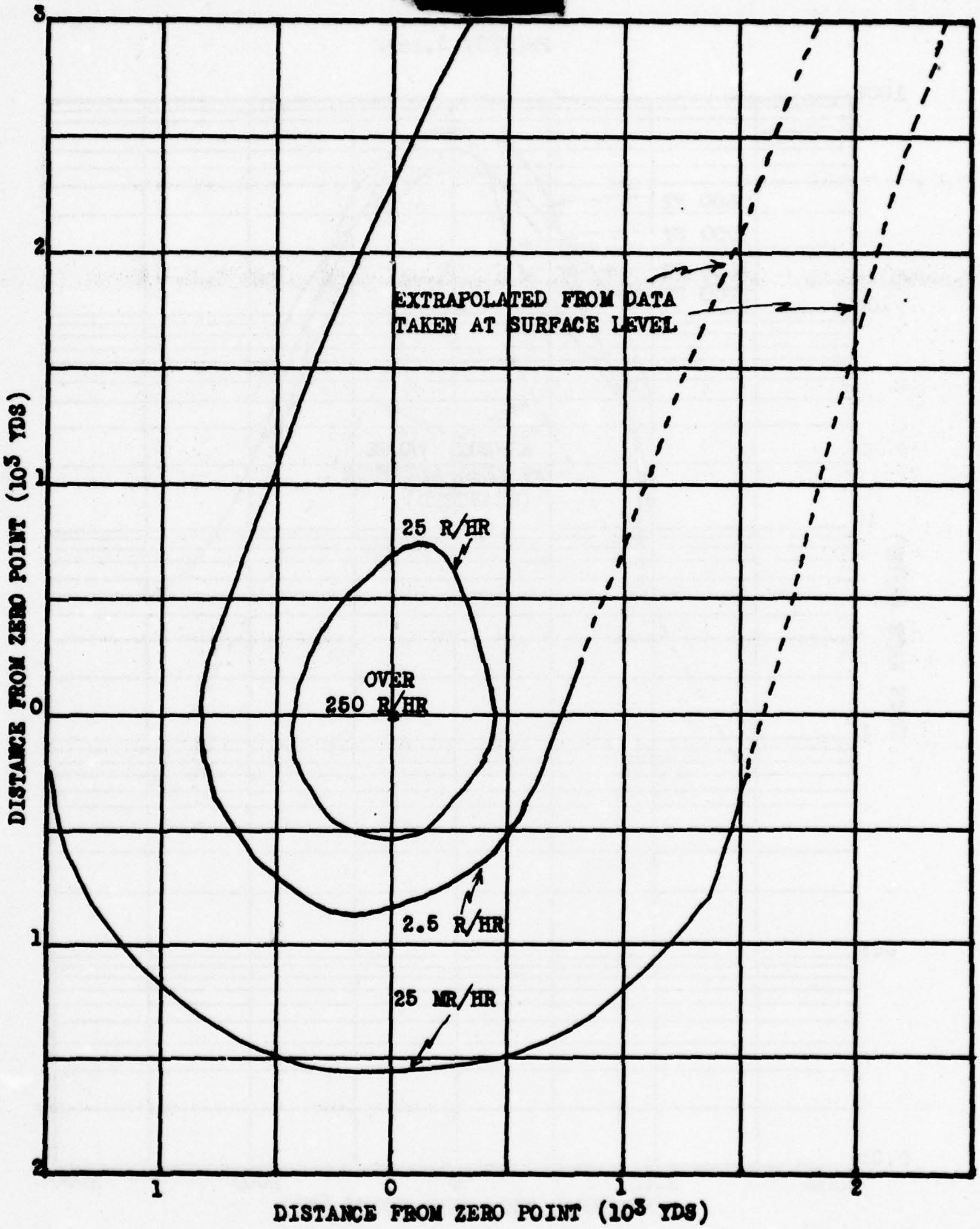

Fig. 4.7 Gamma Intensity Over Zero Point at H+1 Hour Measured by AN/ADR-1 - Underground Shot (1,000 Feet)

[redacted]

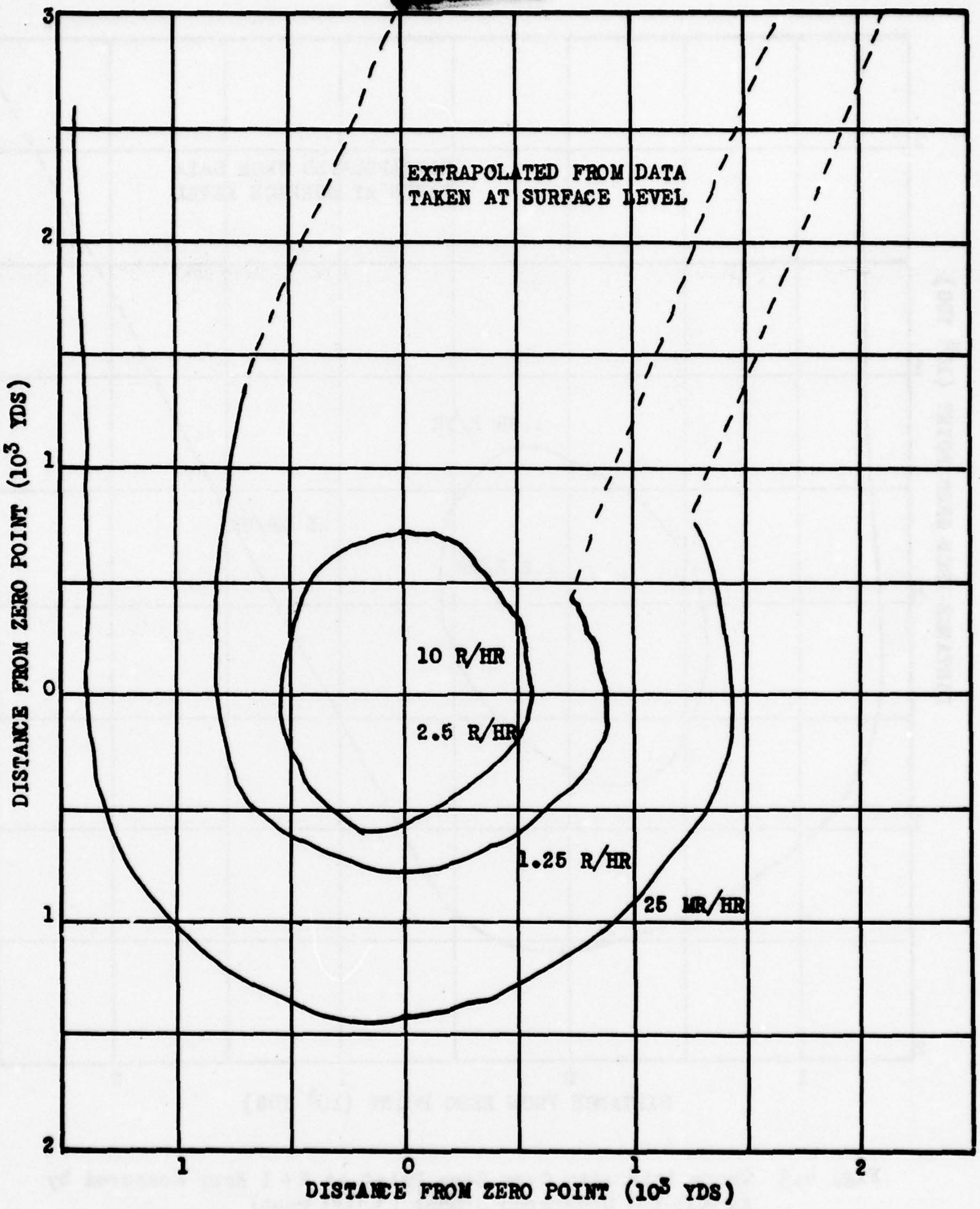

Fig. 4.8 Gamma Intensity Over Zero Point at H+1 Hour Measured by AN/ADR-1 - Underground Shot (2,000 Feet)

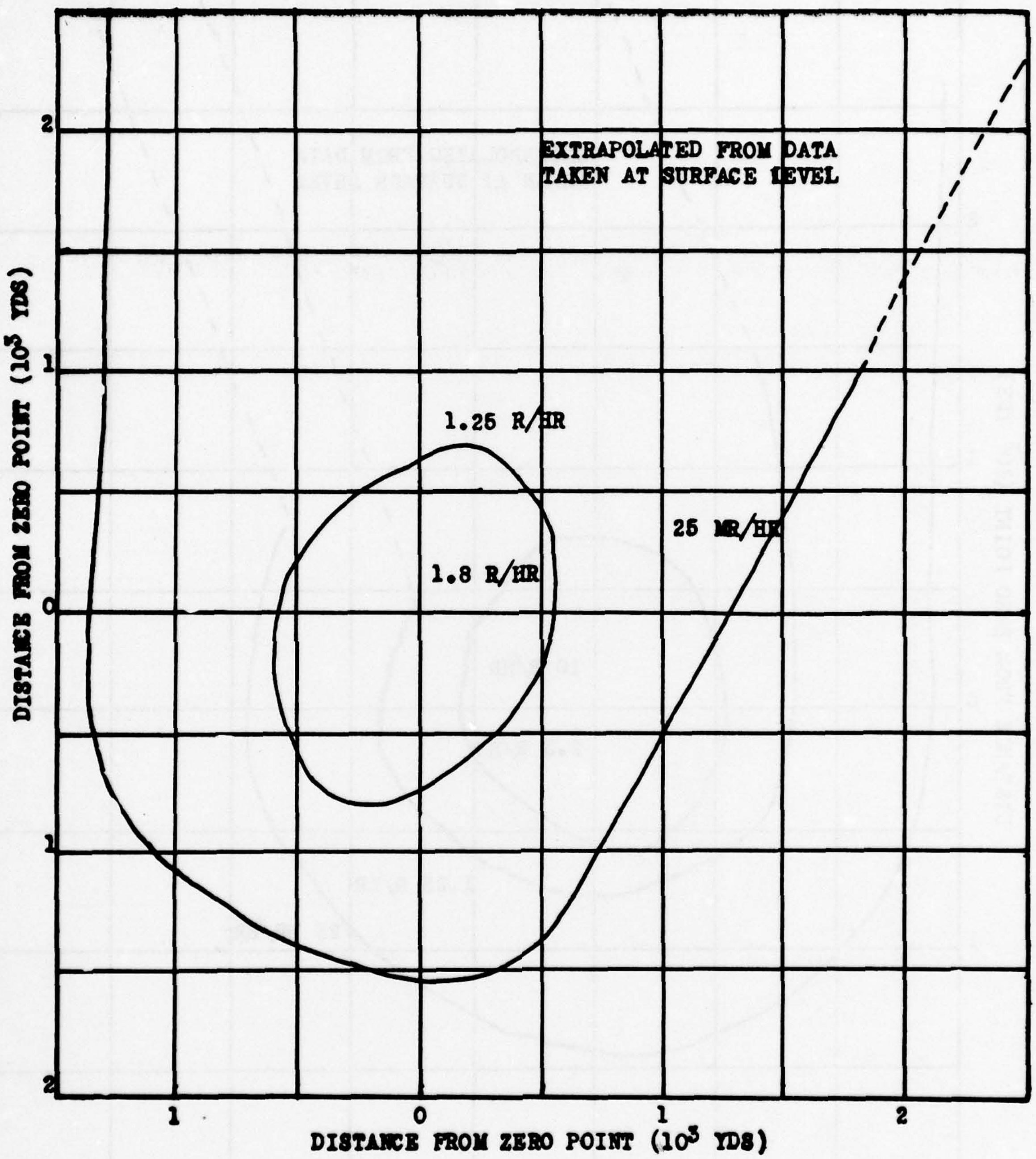

Fig. 4.9 Gamma Intensity Over Zero Point at H+1 Hour Measured by AN/ADR-1 - Underground Shot (3,000 Feet)

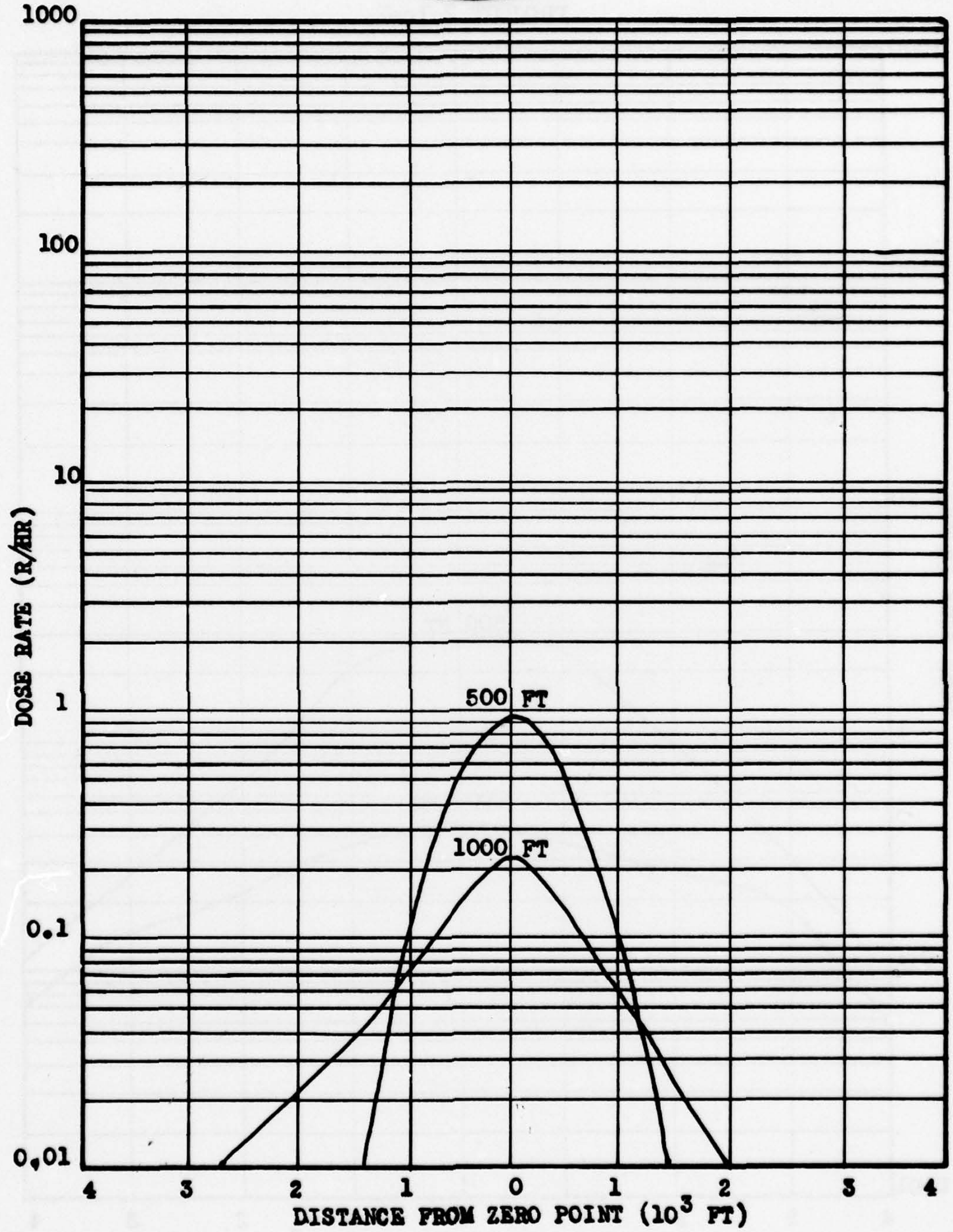

Fig. 4.10 Gamma Intensity Over Zero Point at H+1 Hour Measured by AN/ADR-2 - Shot Charlie of Operation BUSTER

UNCLASSIFIED [redacted]

PROJECT 2.1c-2

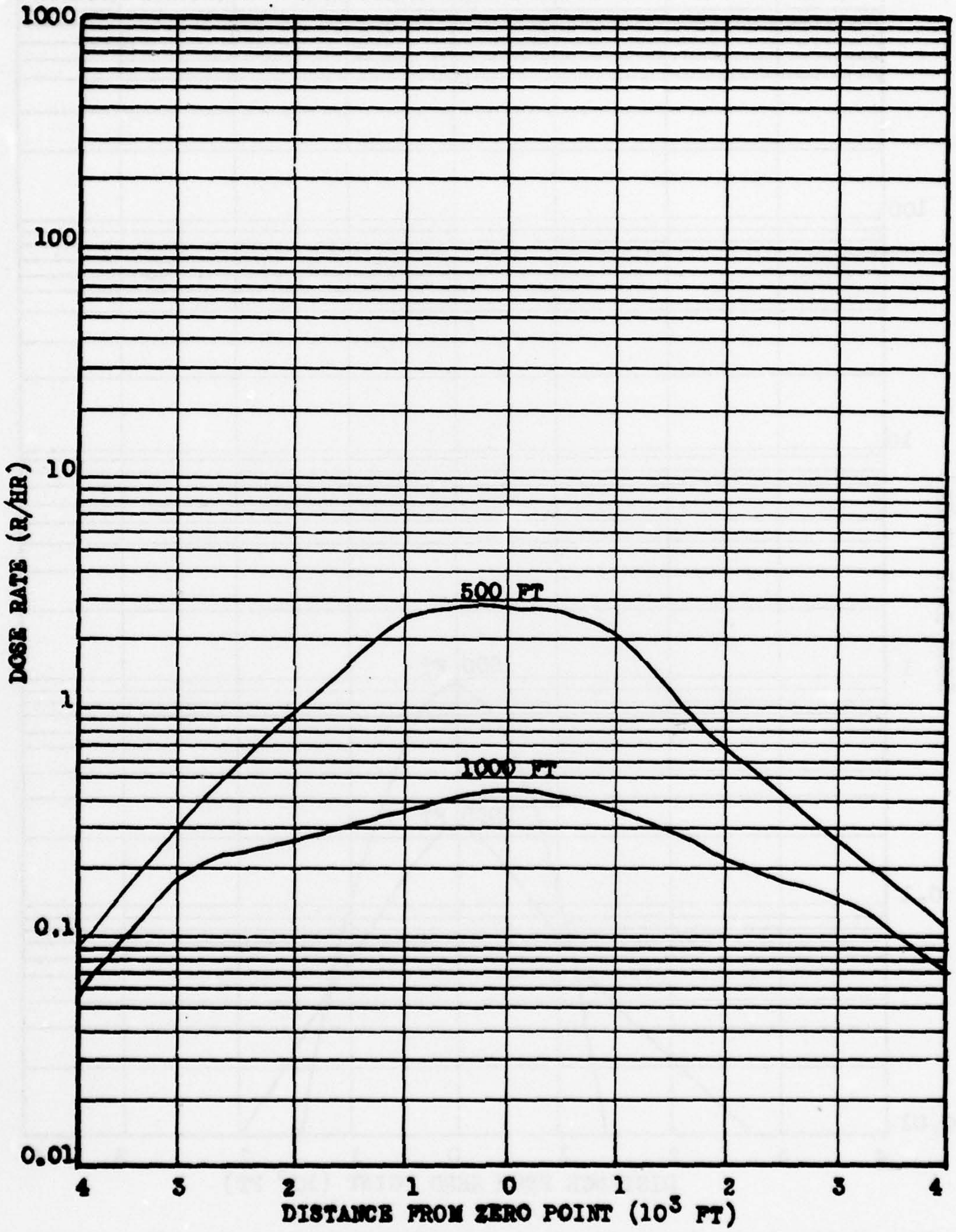

Fig. 4.11 Gamma Intensity Over Zero Point at H+1 Hour Measured by AN/ADR-1 - Shot Dog of Operation BUSTER

UNCLASSIFIED [redacted]

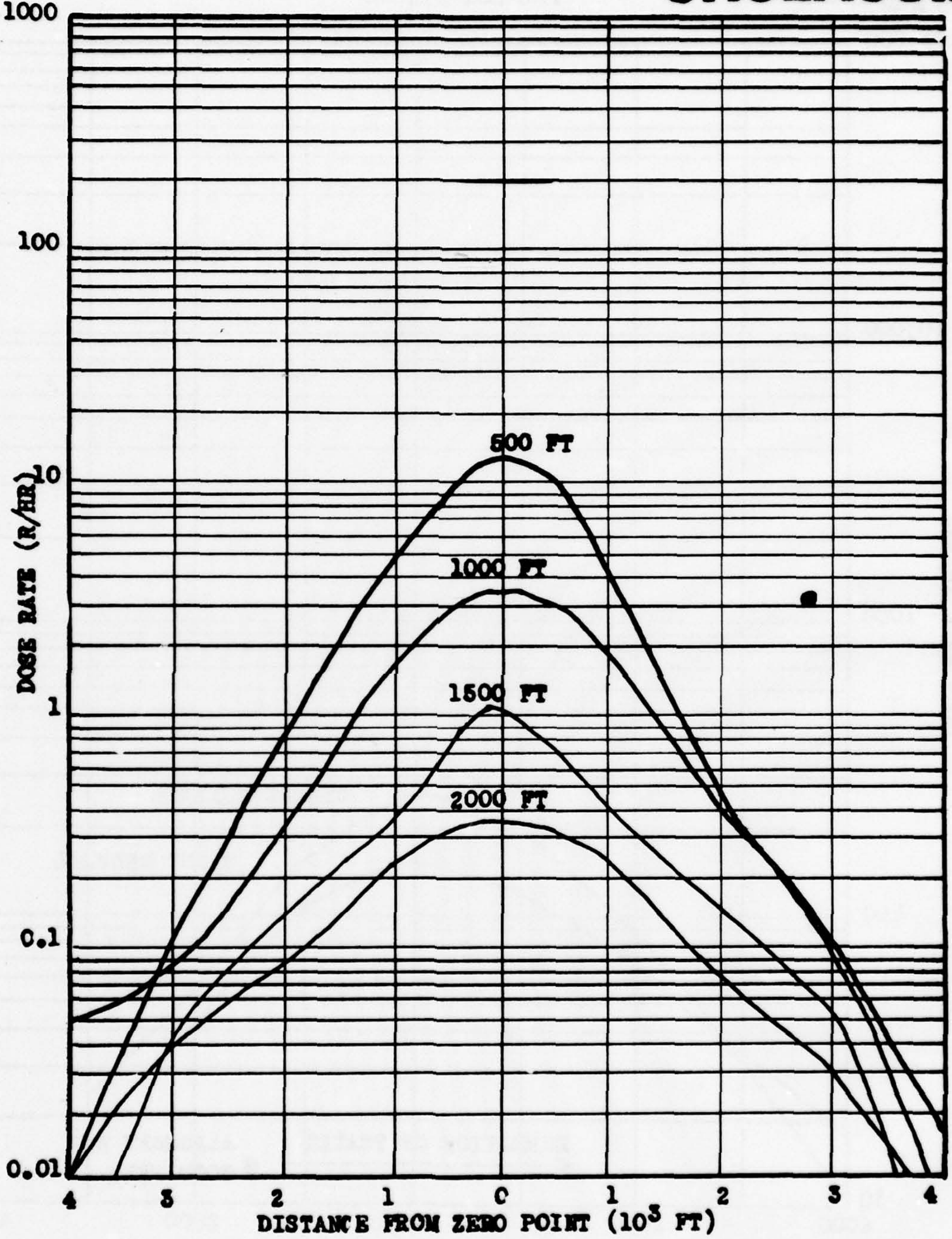

Fig. 4.12 Gamma Intensity Over Zero Point at H+1 Hour Measured by AN/ADR-1 - Shot Easy of Operation BUSTER

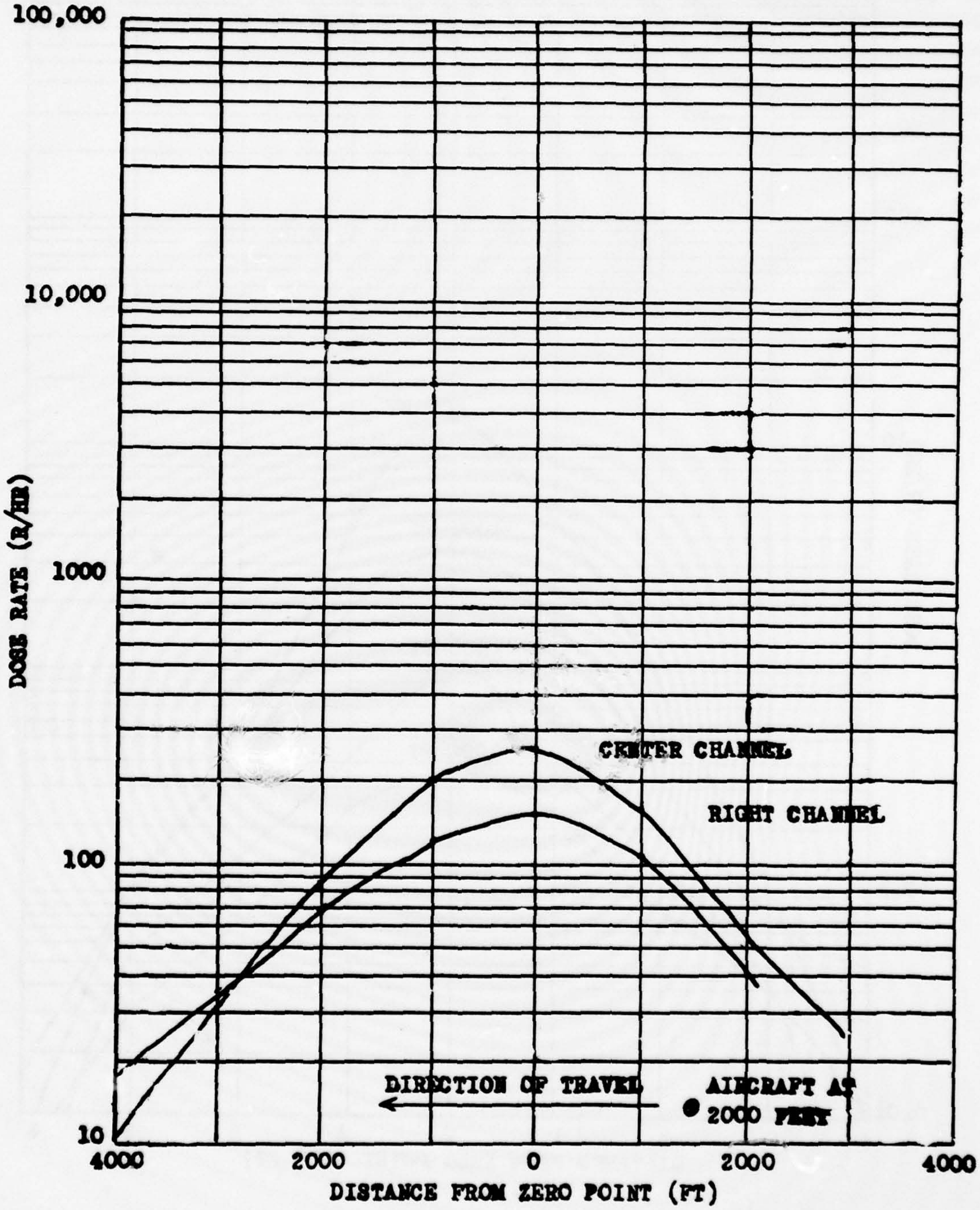

Figure 4.13 Gamma Intensity Near Ground Zero at H - 1 Hour
Measured by F-1 Equipment - Surface Shot

[redacted] UNCLASSIFIED

OPERATION JANGLE

Project 2.1d

MONITOR SURVEY OF GROUND CONTAMINATION (RADSAFE)

by

G. W. Johnson, CDR, USN

22 May 1952

Armed Forces Special Weapons Project

[redacted] UNCLASSIFIED

PREFACE

The purpose of this report is to collect the monitor survey information obtained for the surface and underground shots of JANGLE and to reduce it to usable form. The data used in the report were provided by the RadSafe group of Los Alamos, Program 2 surveys, and the Naval Radiological Defense Laboratory. The final contours were prepared in collaboration with Dr. W. E. Strope of the Naval Radiological Defense Laboratory.

PROJECT 2.1d

CONTENTS

ILLUSTRATIONS

TABLES

[redacted]

PROJECT 2.1d

ABSTRACT

The radiation field intensity was measured by monitor survey groups using AN/PDR-T1B instruments. The results were corrected to H+1 hour using the $t^{-1.2}$ decay law for the surface and underground shots. The final results are presented in the form of dose rate contours.

[redacted]

MONITOR SURVEY OF GROUND CONTAMINATION (RADSAFE)

1.1 INTRODUCTION

Among the important effects to be expected from a surface or underground explosion is that of residual contamination on the ground. Quantitative information on the radiation intensities and the associated areas for such explosions was lacking prior to the JANGLE operation. It was the purpose of Project 2.1d to provide for the determination of the extent and magnitude of the radiation fields as measured by monitor survey teams using the Radiac Training Set AN/PDR-T1B for making the measurements.

1.2 PROCEDURE

All instruments were calibrated with gamma rays from an equilibrium radium source prior to each survey. In making readings the instrument in general was held about 3 feet above the ground, although very little difference was noted in varying the height from 2 to 4 feet, and every attempt was made to get a representative reading. Non-uniformities in the field were practically absent until the wind became sufficiently strong to shift the contamination, at which time there was a localization of contamination in ditches and behind obstructions.

The plan to get the necessary measurements involved, in addition to the RadSafe surveys, the taking of readings at stations of other projects, mainly those of Projects 2.1a and 2.1d.

The station layouts and the detailed data are given in Appendices A, B, and C.

1.3 RESULTS

The results were reduced to gamma dosage-rate contours at one hour after each explosion. In all cases the monitor survey information was collected at times later than one hour and therefore it was necessary to correct it to one hour. The correction for decay was based on the $t^{-1.2}$ decay law which was shown to be the best approximation from monitor surveys and from gamma decay of samples from the field. The radiation fields for the surface shot are shown in Fig. 1 and those for the underground in Fig. 2. The detailed data on which the curves were based are given in Appendices A, B, and C.

The values for the fields in the lip areas given in Figs. 1 and 2 were obtained by extrapolation to the lip areas of the fields obtained by surveys in the surrounding areas as given in Figs. 1 and 2. Surveys of the lips of both craters on 25 January 1952 corrected back to H-1 hour gave an average value for the surface shot of 6000 r/hr with a peak value of 8500 r/hr, which agrees well with the extrapolated average value of 7500 r/hr. For the underground shot, the survey of 25 January gave an average value of 6000 r/hr with a peak

[redacted]

value of 7000 r/hr. The detailed values of the lip surveys of 25 January 1952 are given in Appendix C.

It must be emphasized that the particular distributions of contamination as found in Figs. 1 and 2 were a result of the particular wind conditions existing at the time of the detonation.

The wind pattern at the time of the surface shot (0900 PST, 19 November 1951) is given in Table 1.

TABLE 1

Wind Pattern at Time of Detonation - Surface Shot

Altitude above Surface Feet	Velocity Knots	Direction
0	2	190°
2000	13	170°
4000	26	180°
6000	32	200°
10,000	40	210°
12,000	44	210°
14,000	63	200°
16,000	54	200°

Following the surface detonation the wind pattern was unchanged for 12 hours. At that time the surface wind increased to 12 knots and continued to blow at 17 to 30 knots for about 24 hours. Accompanying the increase of wind at H-12 hours was a relatively heavy rainfall. The amount of precipitation was not measured by the weather observers at the site but it was sufficient to wet the desert surface to a depth of about 3/4 inch.

The effect of the rain was to stabilize the soil until about H-27 hours after which the soil had dried to such an extent that the wind was able to pick up dust again. For these reasons, the monitor survey data collected in the first 27 hours were considered to be more reliable than measurements made subsequently. Therefore, in drawing the contours the earlier measurements were given the greatest weight.

The wind pattern at the time of the underground shot (1200 PST, 29 November 1951) is given in Table 2.

PROJECT 2.1d

TABLE 2

Wind Pattern at Time of Detonation - Underground Shot

Altitude above Surface Feet	Velocity Knots	Direction -
0	calm	-
1000	3	100°
2000	8	190°
3000	12	210°
4000	17	210°
5000	22	220°
6000	21	220°
8000	25	240°

The surface winds remained less than 10 knots generally from the south for 48 hours following the shot, at which time the winds increased to about 20 knots. Since loose dust on the desert is moved about by winds of 15 to 20 knots, after 48 hours the distribution of radioactive material was modified by the winds. Therefore, in preparing the dose-rate contours, the measurements made prior to H-48 hours were given the greatest weight.

The assignment of the expected accuracy of the results is somewhat questionable but based on the overall performance of the survey instruments and the general consistency of the data, the radiation fields at a given point are probably accurate to ± 25 percent. Such accuracy is certainly adequate because except for the large downwind areas of relatively low intensity, the field gradients are so steep that errors of 25 percent in radiation field do not markedly affect the areas of contamination.

1.4 RECOMMENDATIONS

In future operations, in the event that another contaminating burst is fired, it is recommended that the station layouts for monitor survey follow the scheme that was used for the underground shot at JANGLE. The shape of the contaminated field following the surface shot was such that it lay between two arms of the radial arrangement of stations; and because of the narrowness and length of the contaminated areas, coverage of measurements was not as complete as desired. Because of this result, new stations for the underground shot in the downwind area were placed on arcs about the center of the explosion and therefore led to a more definite delineation of the field. Thus in future operations, if the need arises to determine the field contours, the stations should be so positioned that traverses are made at right angles to the expected direction of drift of the cloud at appropriate downwind positions. The upwind and crosswind contours are best determined by a radial arrangement of stations.

[redacted]

PROJECT 2.1d

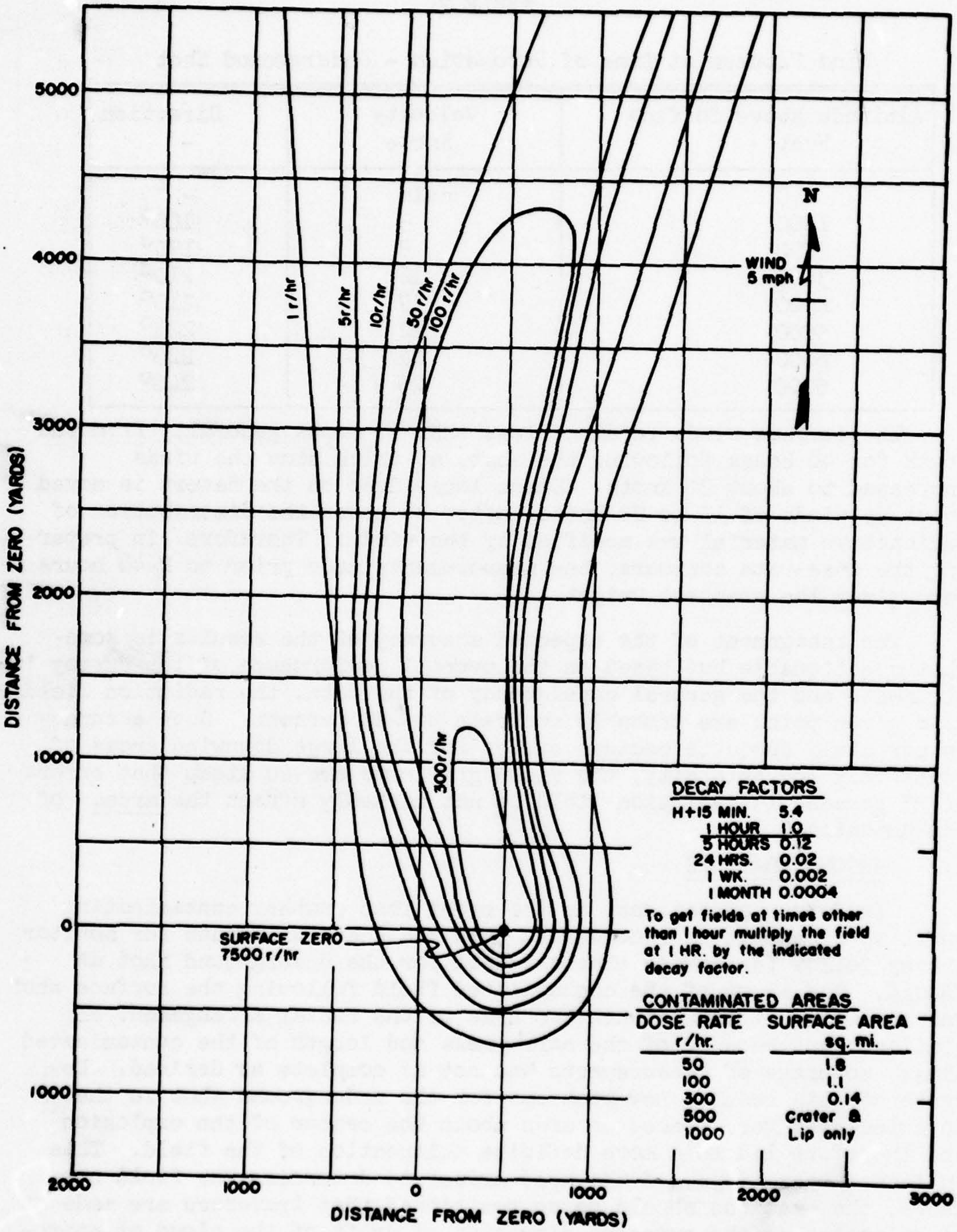

Fig. 1 Gamma Dose-Rate Contours at H+1 hour - Surface Burst

[redacted]

UNCLASSIFIED

[redacted]

PROJECT 2.1d

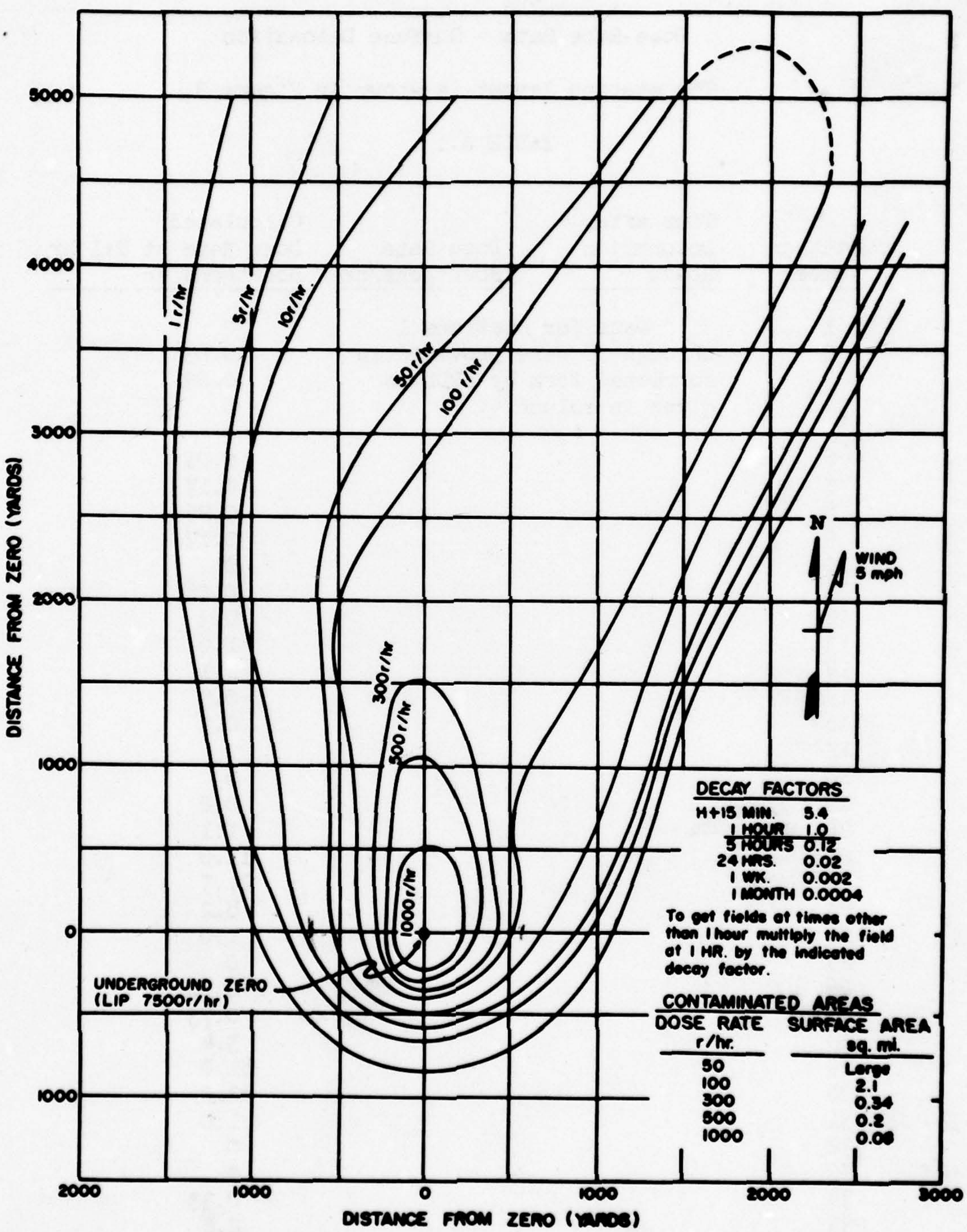

Fig. 2 Gamma Dose-Rate Contours at H+1 hour - Underground Burst

[redacted]

UNCLASSIFIED

UNCLASSIFIED

[redacted]

PROJECT 2.1d

APPENDIX A

Dose-Rate Data - Surface Detonation

The station layout is shown in Figure 3

TABLE A.1

Station Number	Time after Detonation Hours	Dose-Rate Roentgens/hr	Calculated Dose-Rate at H+1 hr Roentgens/hr
1	Data for stations 1		0
2	through 68 were provided in		0.03
3	corrected form by NRDL as		0.03
4	given in column 4.		0
5			0
6			0.05
7			0.17
8			0.25
9			0.17
10			0
11			0.06
12			0.3
13			1.0
14			1.1
15			0.5
16			0.3
17			0
18			0
19			0.2
20			1.1
21			11.0
22			27.5
23			8.2
24			1.0
25			0
26			0.06
27			0.33
28			3.4
29			81.0
30			42.0
31			1.0
32			0
33			0
34			0.33
35			2.6
36			208.0

[redacted]

UNCLASSIFIED

PROJECT 2.1d

TABLE A.1 (cont'd)

Station Number	Time after Detonation Hours	Dose-Rate Roentgens/hr	Calculated Dose-Rate at H+1 hr Roentgens/hr
37			540.0
38			11.0
39			0.5
40			0
41			0.12
42			0.33
43			16.5
44			480.0
45			208.0
46			3.4
47			0.10
48			0
49			0.12
50			0.58
51			71.0
52			350.0
53			170.0
54			1.4
55			0.06
56			0
57			0.12
58			1.4
59			93.0
60			350.0
61			91.5
62			0.94
63			0.01
64			0
65			69.0
66			115.0
67			115.0
68			115.0
69	5.5	0	0
	22	0	0
	50	0	0
70	6.	0.06	0.52
	22	0.018	0.74
	50	0.005	0.50
71	4.9	0.003	0.022

[redacted]

PROJECT 2.1d

TABLE A.1 (con't)

Station Number	Time after Detonation Hours	Dose-Rate Roentgens/hr	Calculated Dose-Rate at H+1 hr Roentgens/hr
72	4.9	0.22	1.48
	22.	0.032	1.31
	50.	0.008	0.88
73	5.4	0.080	0.60
	22	0.022	0.90
	50	0.008	0.83
74	5.4	0.010	0.76
	22	0.005	0.21
75	5.6	0.160	1.27
	22	0.034	1.39
	50	0.013	1.40
76	5.6	0.020	0.16
	22	0.005	0.21
77	5.5	2.40	18.5
	22	0.36	14.8
	50	0.165	18.1
	72	0.05	8.5
78	5.4	1.05	7.9
	22	0.080	3.3
	50	0.038	4.2
	72	0.012	2.0
79	50	0.31	34.
	72	0.20	34.
80	5.4	0.90	6.8
	22	0.033	1.4
	50	0.018	2.0
	72	0.008	1.4
81	50	0.017	1.0
	72	0.010	3.3
82	5.4	0.75	5.7
	22	0.012	1.0
	50	0.009	0.5

UNCLASSIFIED

[redacted]

PROJECT 2.1d

TABLE A.1 (cont'd)

Station Number	Time after Detonation Hours	Dose Rate Roentgens/hr	Calculated Dose-Rate at H+1 hr Roentgens/hr
83	50	0.0004	0.04
84	5.3	0.65	4.8
	50	0.007	.8
	72	0.002	.3
85	5.3	1.25	9.3
	22	0.12	4.9
	50	0.041	4.5
	72	0.026	4.4
86	96	0	0
87	96	0.03	7.2
88	22	1.0	41.
	72	0.20	34.
	96	0.10	24.
89	22	0.90	37.
	72	0.14	24.
	96	0.08	19.
90	5.2	0.81	5.8
	22	0.120	4.9
	50	0.055	6.0
	72	0.019	3.2
	96	0.010	2.4
91	72	0	0
92	72	0.036	6.1
	96	0.022	5.3
93	72	0.090	15.0
	96	0.050	12.0
94	72	0.180	31.0
	96	0.100	24.0
95	72	0.018	3.1
	96	0.010	2.4

[redacted]

UNCLASSIFIED

PROJECT 2.1d

TABLE A.1 (con't)

Station Number	Time after Detonation Hours	Dose-Rate Roentgens/hr	Calculated Dose-Rate at H+1 hr Roentgens/hr
96	72	0.120	20.0
	96	0.060	15.0
97	72	0.270	46.0
	96	0.110	26.0
98	72	0.008	1.4
99	72	0.090	15.0
	96	0.040	10.0
100	72	0.230	39.0
	96	0.100	24.0
101	72	0.038	6.5
	96	0.030	7.2
102	72	0.250	42.0
	96	0.120	29.0
103	6.0	2.10	18.0
	72	0.180	31.0
	96	0.090	23.0
104	72	0.026	4.4
	96	0.009	2.3

PROJECT 2.1d

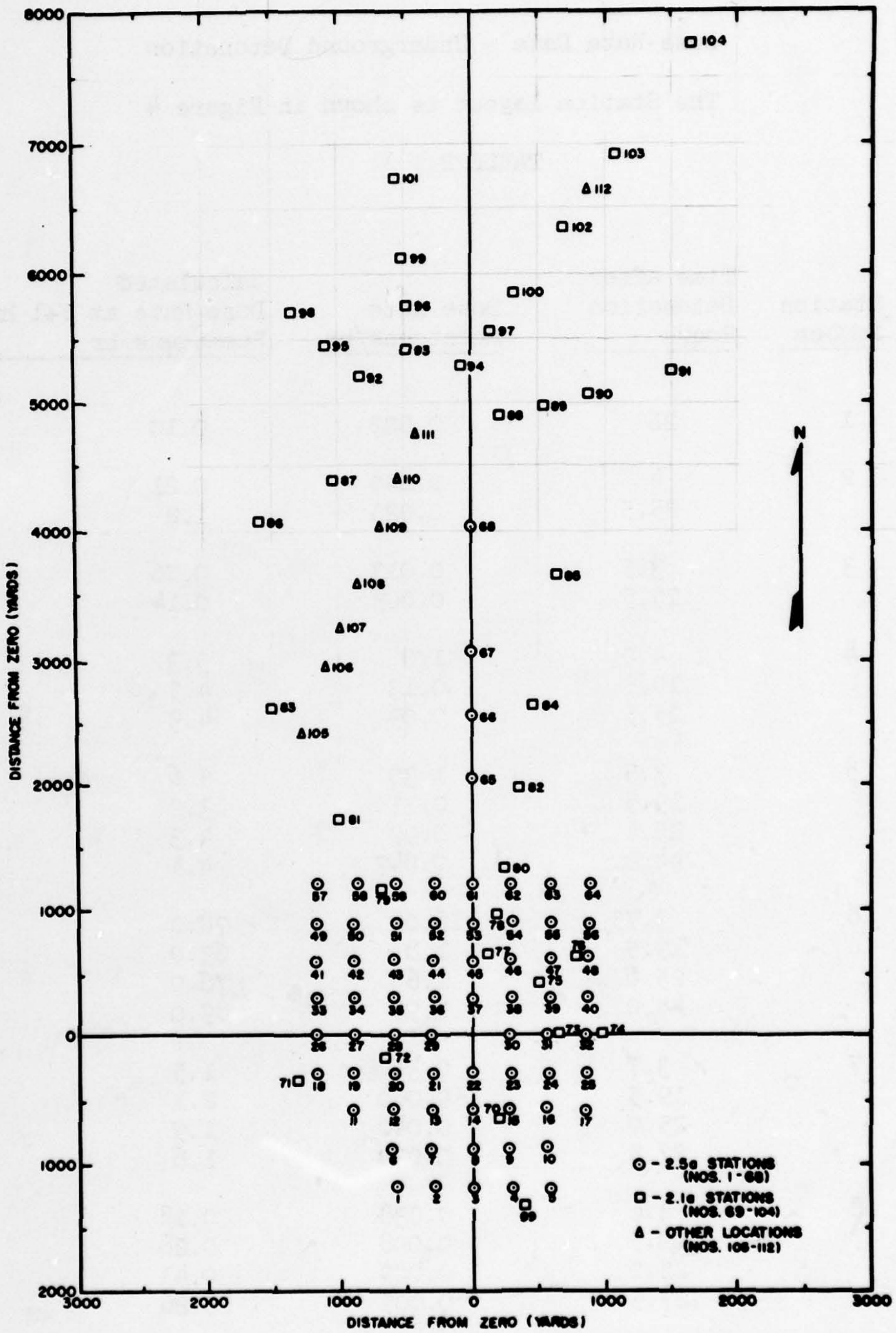

Fig. 3 Station Layout - Surface Shot

[redacted]

PROJECT 2.1d

APPENDIX B

Dose-Rate Data - Underground Detonation

The Station layout is shown in Figure 4

TABLE B.1

Station Number	Time after Detonation Hours	Dose-Rate Roentgens/hr	Calculated Dose-Rate at H+1 hr Roentgens/hr
1	26	0.002	0.10
2	4	0.040	0.21
	25.5	0.025	1.2
3	3.5	0.013	0.06
	25.5	0.003	0.14
4	4.0	1.0	5.3
	19.5	0.13	4.5
	25.5	0.09	4.3
5	3.5	1.30	5.6
	19.5	0.11	3.9
	25.5	0.09	4.3
	44.0	0.047	4.4
6	3.75	16.0	78.0
	19.5	1.8	63.0
	25.0	1.6	76.0
	44.0	0.95	89.0
7	3.7	0.30	1.5
	19.5	0.060	2.1
	25.0	0.040	1.9
	27.5	0.030	1.6
8	3.7	0.038	0.18
	19.5	0.008	0.28
	25.0	0.009	0.43
	27.5	0.005	0.26
9	25.0	0.002	0.09

[redacted]

[redacted]

PROJECT 2.1d

TABLE B.1 (con't)

Station Number	Time after Detonation Hours	Dose-Rate Roentgens/hr	Calculated Dose Rate at H+1 hr Roentgens/hr
10	19.5	2.50	87.0
	26.5	1.40	70.0
	44.0	0.95	89.0
11	24.5	10.0	460.0
12	24	6.0	270.0
13	19.5	0.38	13.3
	26.5	0.20	10.0
	44.0	0.15	14.0
14	24.5	9.0	415.0
15	24.0	0.7	31.5
16	19.5	0.26	9.1
	26.0	0.11	5.5
	44.0	0.10	9.3
17	24.5	7.0	320.0
	27.5	4.8	250.0
18	24.0	0.170	7.6
19	19.5	0.034	1.2
	26.0	0.012	0.6
20	24.5	3.6	166.0
	27.5	3.3	174.0
21	24.0	1.2	54.0
	27.5	1.0	53.0
22	26.0	0.009	0.5
23	24.5	1.7	78.0
	27.5	1.2	63.0
24	25.0	0.28	13.0
25	24.5	0.50	23.0
	27.5	0.40	21.0

[redacted]

[redacted]

PROJECT 2.1d

TABLE B.1 (con't)

Station Number	Time after Detonation Hours	Dose-Rate Roentgens/hr	Calculated Dose-Rate at H+1 hr Roentgens/hr
26	24.0	0.38	17.0
	27.5	0.30	16.0
27	24.5	0.16	7.4
	27.5	0.14	7.4
28	27.0	0.20	9.5
29	1.5	.01	.016
30	1.5	0.24	0.39
31	1.5	1.1	1.8
32	1.5	2.5	4.1
	19.5	0.10	3.5
	44.0	0.10	9.4
33	1.5	4.0	6.5
34	1.5	17.0	28.0
	19.5	0.50	18.0
	27.5	0.32	17.0
	44.0	0.22	21.0
35	19.5	4.0	140.0
	44.0	2.1	200.0
36	70.0	1.5	250.0
37	70.0	3.6	590.0
38	70.0	9.0	1480.0
39	2.0	0.008	0.018
	1.5	0.01	0.016
40	2.0	0.080	0.18
	1.5	0.050	0.08
41	2.0	0.170	0.39
	1.5	0.22	0.36

[redacted]

UNCLASSIFIED

[redacted]

PROJECT 2.1d

TABLE B.1 (con't)

Station Number	Time after Detonation Hours	Dose-Rate Roentgens/hr	Calculated Dose-Rate at H+1 hr Roentgens/hr
42	2.0	0.70	1.60
	1.5	0.48	0.78
43	2.0	3.8	8.7
44	2.0	20	46.0
	1.5	22	36.0
45	1.5	50	81.0
46	19	0.11	3.8
47	19	0.22	7.7
	27.5	0.10	5.3
	44	0.10	9.4
48	19	0.30	10.5
	27.5	0.14	7.4
	44	0.15	14.0
49	19	0.48	16.8
	27.5	0.30	15.9
	44	0.30	28.2
50	19	1.00	35.0
	27.5	0.50	27.0
	44	0.90	85.0
51	19	4.6	161
	27.5	3.6	191
	44	3.0	282
52	19	5.5	192
53	19	6.0	210
	27.5	3.5	186
54	19	4.2	147
	27.5	3.2	170
	44	2.8	263

[redacted]

UNCLASSIFIED

[redacted]

PROJECT 2.1d

TABLE B.1 (con't)

Station Number	Time after Detonation Hours	Dose-Rate Roentgens/hr	Calculated Dose-Rate at H+1 hr Roentgens/hr
55	19	5.5	192
	27.5	4.4	233
	44	3.1	292
56	19	5.2	182
	27.5	3.9	207
	44	3.5	329
57	19	4.2	147
	27.5	4.8	254
	44	2.8	263
58	19	2.6	91
	27.5	1.6	85
	44	1.5	141
59	19	2.0	70
	27.5	1.9	101
	44	1.4	132
60	19	1.8	63
	27.5	1.6	85
	44	1.4	132
61	19	1.3	46
	44	1.2	113
62	2.5	6.0	18
	19	0.5	18
	44	0.6	56
63	19	0.018	0.63
	44	0.015	1.4
64	2.5	0.060	0.18
	19	0.006	0.21
	44	0.009	0.85
65	19	0.004	0.14
66	19	Background	-
67	19	Background	-
68	27.5	3.3	175

[redacted]

TABLE B.1 (con't)

Station Number	Time after Detonation Hours	Dose-Rate Roentgens/hr	Calculated Dose-Rate at H+1 hr Roentgens/hr
69	27.5	1.4	72
70	27.5	1.2	62
71	27.5	0.44	23
72	27.5	0.28	15
73	27.5	0.20	11
74	27.5	0.30	16
75	27.5	0.16	8.5
76	24	0.60	27
	27.5	0.60	32
77	27.5	0.60	32
78	24	1.10	50
	27.5	0.80	42
79	27.5	2.8	148
80	24	3.2	144
	27.5	3.1	164
81	24	2.8	126
	27.5	2.8	148
82	27.5	1.6	85
83	27.5	0.26	14

PROJECT 2.1d

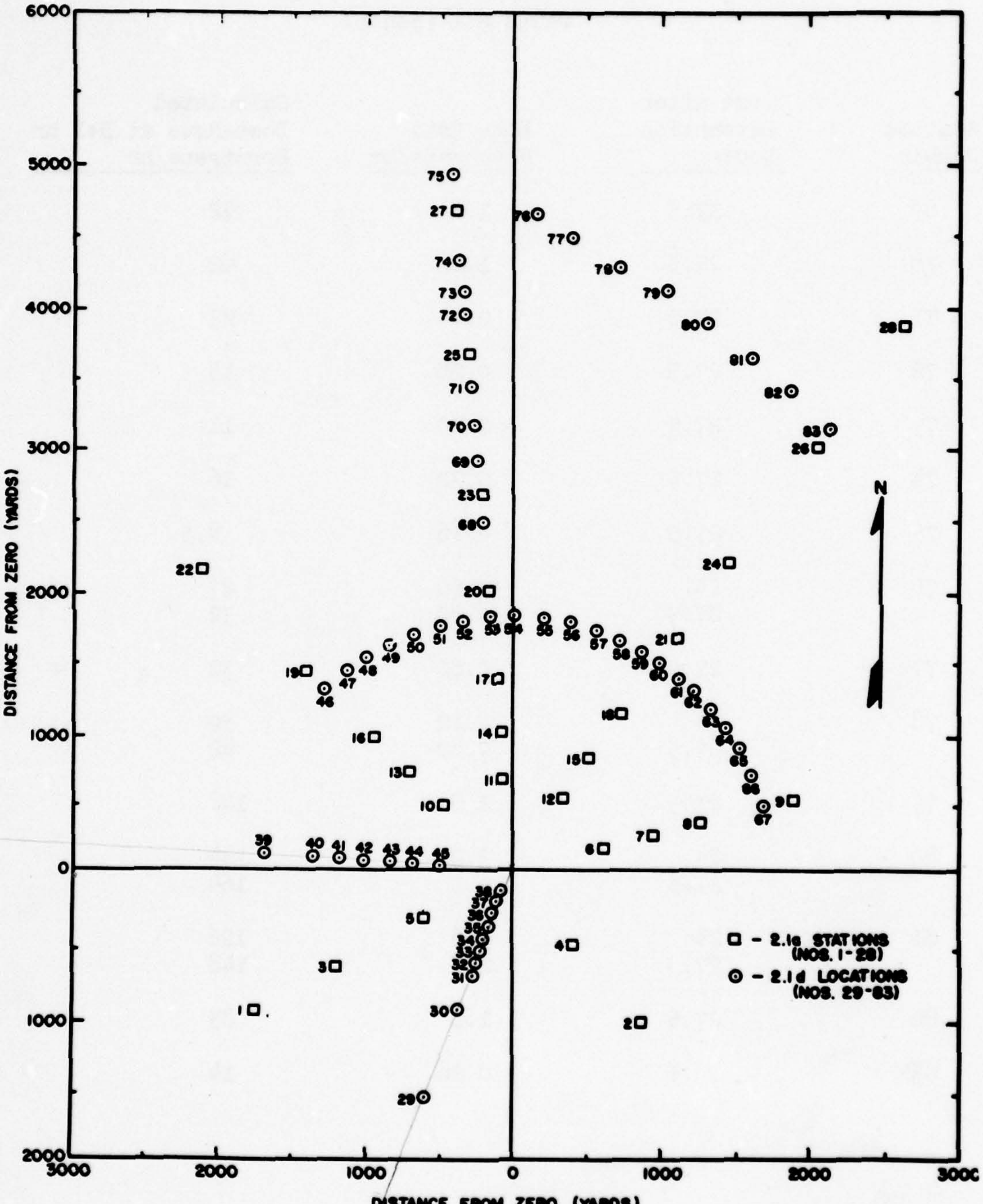

Fig. 4 Station Layout - Underground Shot

APPENDIX C

Surveys of Lips

On 25 January 1952 monitor surveys were made of the lip areas of the underground and surface shots. Readings were made at eight positions equally spaced on a circle surrounding the craters and are listed below.

TABLE C.1

Surface Shot

Station Number	Rate Roentgens/hr	Rate Corrected to H+1 hr Roentgens/hr
1	1.2	8600
2	1.1	7900
3	1.0	7200
4	0.90	6500
5	0.32	2300
6	0.50	3600
7	0.60	4300
8	1.0	7200
		Mean......6000 r/hr

Underground Shot

Station Number	Rate Roentgens/hr	Rate Corrected to H+1 hr Roentgens/hr
1	1.2	7000
2	1.0	5800
3	0.95	5500
4	0.90	5200
5	1.0	5800
6	1.0	5800
7	1.05	6100
8	1.10	6400
		Mean......6000 r/hr

[redacted]

UNCLASSIFIED

OPERATION JANGLE

Project 2.3-1

TOTAL DOSAGE

by

LT. COL. MERWIN B. FORBES
MR. ROSS G. LARRICK
CPL. EDWARD J. FULLER

March 15, 1952

SIGNAL CORPS ENGINEERING LABORATORIES

FORT MONMOUTH, NEW JERSEY

UNCLASSIFIED

[redacted]

[redacted]

PROJECT 2.3- UNCLASSIFIED

ACKNOWLEDGMENTS

The authors are greatly indebted to

Cpl. Lowell J. Smith

and

Sgt. Ernst S. Johnson

for their work in calibrating and processing the films.

The authors also wish to acknowledge the help and fine cooperative spirit of the various groups within Program 2 who so greatly aided them at the Nevada Test Site.

[redacted] UNCLASSIFIED

PROJECT 2.3-1

CONTENTS

UNCLASSIFIED

[redacted]

PROJECT 2.3-1

ILLUSTRATIONS

TABLES

[redacted]

UNCLASSIFIED

[redacted]

PROJECT 2.3-1

ABSTRACT

The total dosage of gamma rays in the radiation fields of atomic weapons exploded at and below the surface of the earth was measured as a function of distance and direction at fixed stations of Program 2 by using a number of photographic films of graduated sensitivity placed in National Bureau of Standards film badge holders. The dosage measurements obtained were in excellent agreement with those recorded by other projects during the operation. The methods used in this project give good results with a relatively high degree of accuracy with relatively small expenditure of manpower, equipment, and money. It is recommended that in future operations of this type, this method be used with a closer degree of coverage of the radiation field.

[redacted]

CHAPTER 1

HISTORICAL AND THEORETICAL

1.1 EARLY HISTORY

Photographic film has been used for radiation dosimetry purposes since early in the history of X-ray work. Basic work by L. A. Pardue, N. Goldstein and E. O. Wollan[1], in 1944, resulted in the development of film meters for monitoring radiations of different types and over wide potential ranges. L. J. Deal, J. H. Roberson, and F. H. Day[2], proposed a light metal container, housing a film packet. Approximately one-half of the film packet was exposed directly without any filter material, other than the containing wrapping. The other half is shielded on both sides by one millimeter of cadmium. The portion of the film exposed without filter is used primarily to pick up very soft radiations, including beta rays. The other half of the film filtered by the cadmium, detects gamma rays where the cadmium is interposed to minimize the wavelength dependence of the film emulsion.

1.2 LATER DEVELOPMENTS

M. Erlich and S. Fitch[3], have developed at the National Bureau of Standards, a film dosimeter which, using a series of film emulsions, covers the energy range from 115 kev up to 10 mev and a dosage range from 1 to 10,000 roentgens when properly calibrated. This type of film dosimeter was used by Project 2.3-1, to measure total dosage at the JANGLE operation.

1.3 THEORETICAL CONSIDERATIONS

Gamma rays affect a photographic film much like ordinary light, and consequently, gamma ray photography has much in common with ordinary optical photography. Photographic measurements of radiation dose must be calibrated in terms of the primary ionization measurements. Most gamma rays pass right through the film without interacting with the emulsion and only the small amount that is absorbed has any effect in exposing the film. The exposure is defined as a quantity proportional

[redacted]

to the intensity of the radiation times the time it strikes the film. The reciprocity law of Bunsen and Roscoe defines the exposure as equal to the product of intensity by time and implies that equal exposures should result in equal emulsion blackening. This law fails, if carried to extremes with ordinary light, but it has been shown by G. E. Bell[4], that the photographic effect of a given dose is independent of dosage rate over a range of X-ray intensities, varying by a factor of ten thousand. Also Bell could not detect any intermittency effect for X-rays, i.e., that resultant density was the same for a steady exposure as for intermittent exposures. Therefore, film can be used to record cumulative dosage from a source or series of sources or to measure total gamma dosage, including both initial and residual gamma radiation.

1.4 ENERGY DEPENDENCE OF FILMS

Unfortunately, there is no simple and direct relationship between film blackening and radiation dosage in roentgens, but in general, the photographic effect is dependent upon photon energy, the emulsion blackening per unit dose, decreasing with increasing photon energy[4,5,6]. To compensate for this energy dependence, metallic absorbers are placed between the source of radiation and the film. The absorbers counteract the high response of film emulsion to low energy radiations by attenuating the lower energies more strongly than the higher energies. In this way a film can be made to respond equally to equal dosages from different energy gamma rays. The response of both shielded and unshielded films was found to be independent of the energy of the radiation above 400 kev[2]. This response relationship continues up to energies at which pair production becomes prominent.

1.5 SCATTERING FROM IMMEDIATE OBJECTS

Secondary electrons, produced outside of the holder by gamma radiation would probably not reach the film emulsion due to absorption in the lead and tin. The Bakelite layer was designed to produce electronic equilibrium at the surface of the film; the point-to-point variation of the total energy absorbed in this layer parallels roughly the absorption of gamma rays. Electrons, whose energies are below about 10 mev, do not penetrate this layer of Bakelite; but electrons originating within this layer reach the film emulsion. Due to the orientation of the film holder with respect to Ground Zero, gamma rays scattered from any supporting material should not affect dosage readings appreciably.

CHAPTER 2

INSTRUMENTATION AND OPERATION

2.1 THE N. B. S. FILM BADGE HOLDER

The N. B. S. Film Badge Holder, Figure 2.1, consists of a bakelite container 8.25 mm wall thickness holding two dental size film packets and is covered with a layer of 1.07 mm of tin and a layer of 0.3 mm of lead. The lead filtration suppresses the lower energies more strongly than the higher one, except in the portion of the spectrum immediately below the K-absorption edge. This lead fluorescent radiation is stopped by the tin absorber. The bakelite serves as an "air equivalent" layer which produces electronic equilibrium at or near the surface of the film. A lead strip approximately 0.78 mm thick was wrapped around the periphery of the badge to protect the film from tangential radiation and at the same time cover the badge seam. The badge was sealed with paper masking tape.

TABLE 2.1

Types of Film Used

Emulsion Type	Packet Type	Sensitivity Range	Range Utilized
D-502 D-510	DuPont 552	0.5 R to 10 R 3 R to 50 R	0.5 R to 7.5 R 5 R to 25 R
D-510 D-605	DuPont 554	3 R to 50 R 20 R to 500 R	5 R to 40 R 25 R to 200 R
D-1290 "Adlux"	DuPont 556	20 R to 3,000 R	25 R to 1,000 R
E-548-0 (double coat)	Eastman 548	500 R to 10,000 R	1,000 R to 10,000 R

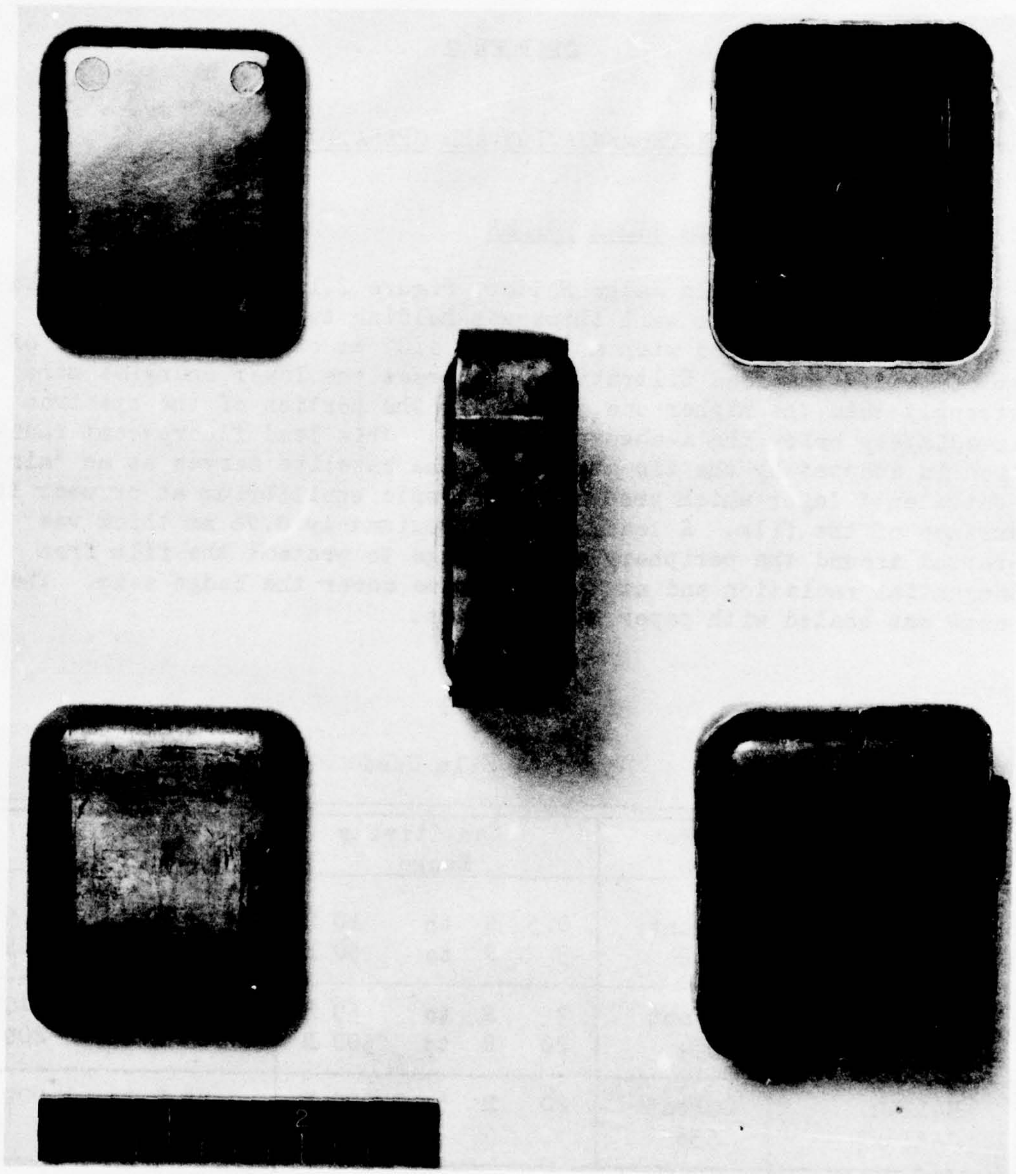

Figure 2.1 National Bureau of Standards Film Badge Holder Exploded View, Showing Component Parts

2.2 OPERATION

Film badges were placed at fixed stations of Program 2 (Figures 2.2 and 2.3) 3.5 feet above the earth normal to ground zero and in foxholes, tanks, and structures. The exposed films were recovered approximately 49 hours after the detonation of the atomic weapon. The films were then developed with agitation in Kodak Concentrated Dental X-ray developer (one part diluted with three parts of water) at 68 ± 0.5°F (20°C) for 5 minutes. Immediately thereafter the films were placed in a dilute acetic acid stop bath for fifteen seconds with agitation, removed and then immersed in Kodak Concentrated Dental X-ray Fixer (one part diluted with three parts of water) at 68 ± 0.5°F for 7 minutes and were agitated frequently. Afterwards the films were hung in a drying cabinet equipped with a blower system and remained there until dry. A set of control films and films calibrated with a Co^{60} source were processed along with each batch of film. The photographic transmission densities were read on an Ansco-Macbeth photoelectric densitometer (with range up to transmission densities of 6 on the Hurter and Driffield scale). The dosages were determined by comparing the densities with those of the Co^{60} calibrated films by means of density versus dosage curves (Figures 2.4, 2.5, 2.6, 2.7, and 2.8). The densitometer zero reading was corrected by means of the control film blanks so as to compensate for changes in film properties due to ageing or due to variation in the processing procedures between different batches of film. The film badges were stored in a cool, well ventilated room. Due to the short time interval between shots, and the prevailing temperature conditions, it was felt that refrigeration would not be required. Fresh sets of calibrated film were prepared just prior to each shot, each film being mounted so as to duplicate field conditions. The minimum distances from the Co^{60} source was twenty-five (25) centimeters so as to assure good geometry. In the calibration, both exposure times and distances were varied.

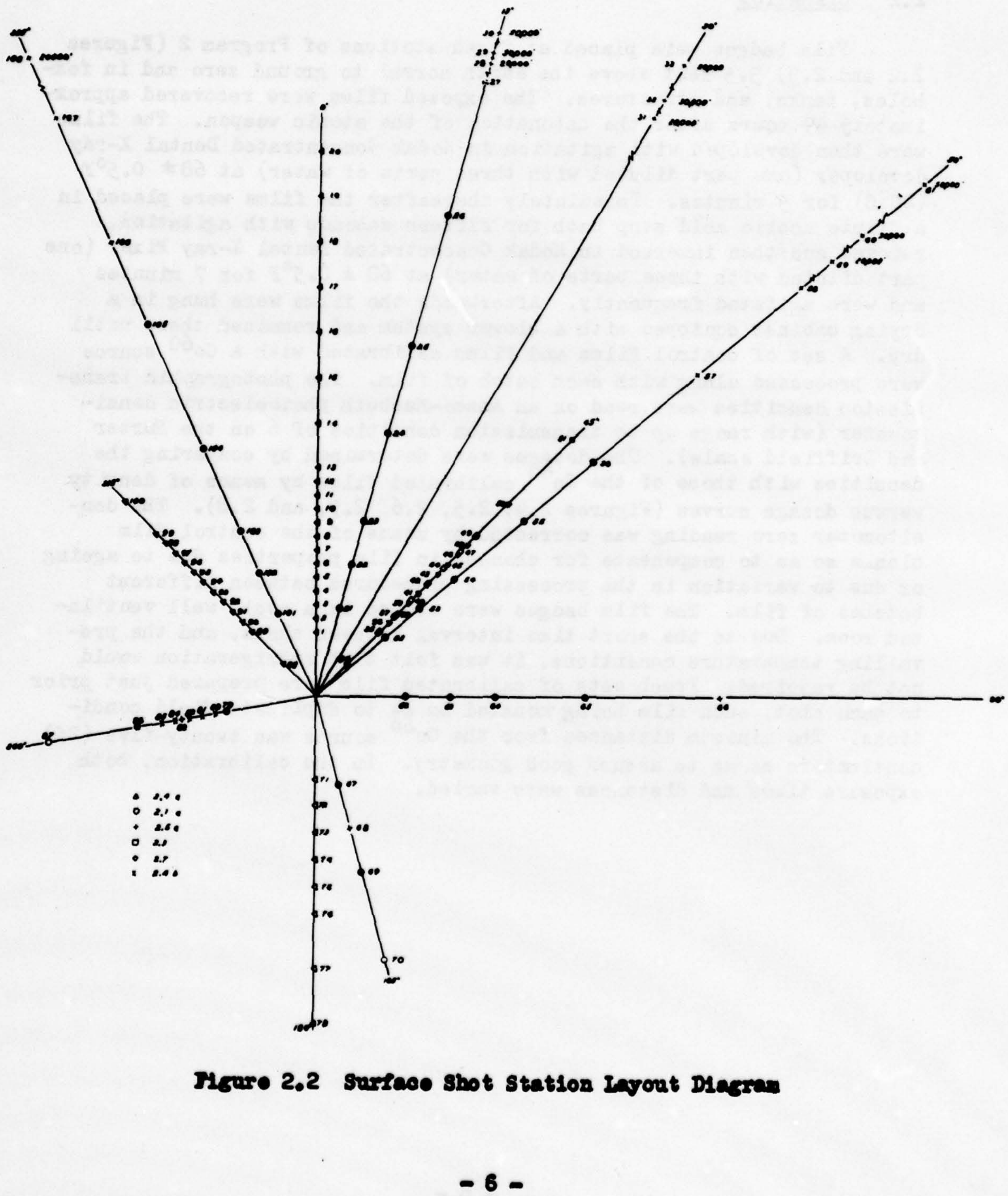

Figure 2.2 Surface Shot Station Layout Diagram

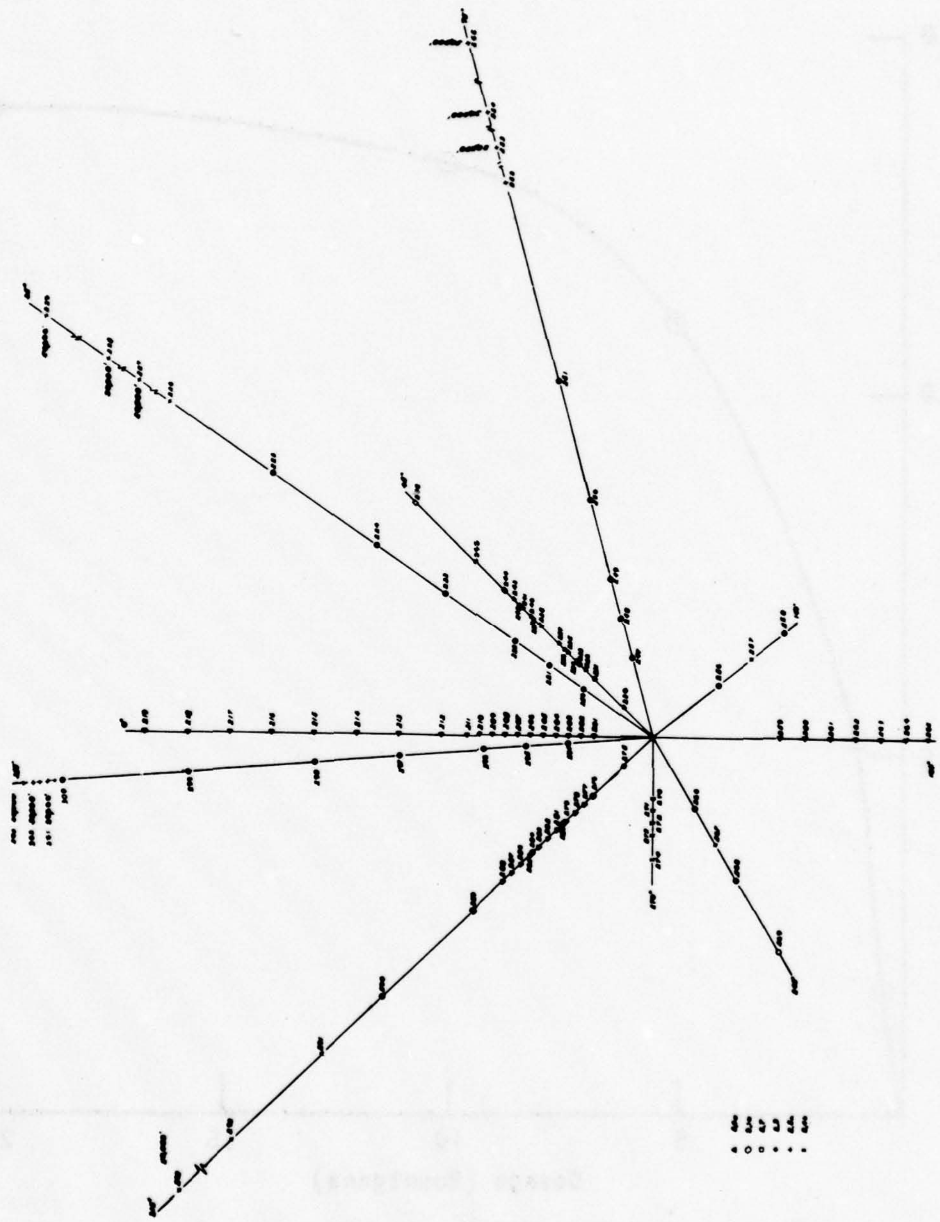

Figure 2.3 Underground Shot Station Layout Diagram

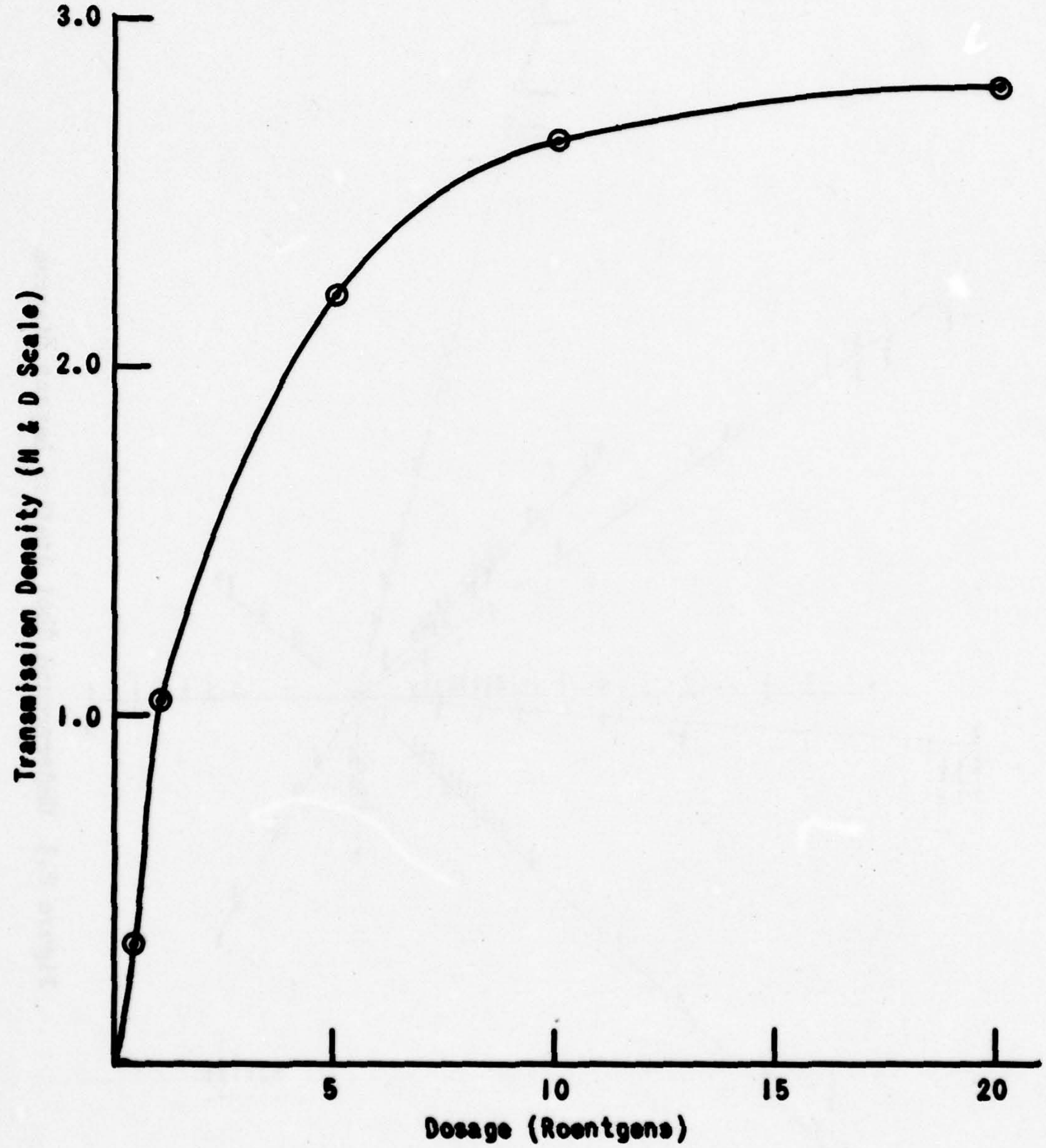

Figure 2.4 DuPont 502 Density vs Dosage Curve

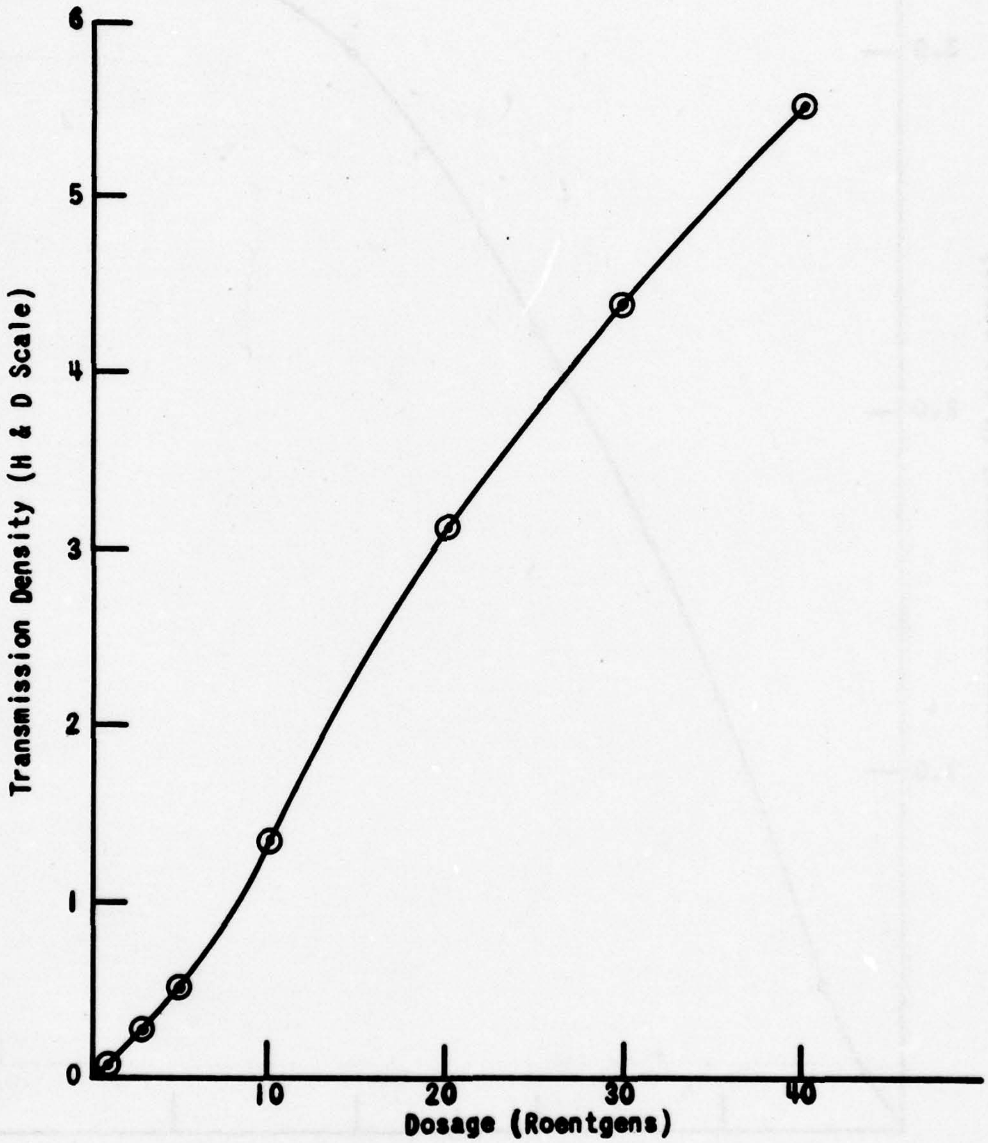

Fig. 2.5 Density vs Dosage Curve

UNCLASSIFIED

[redacted]

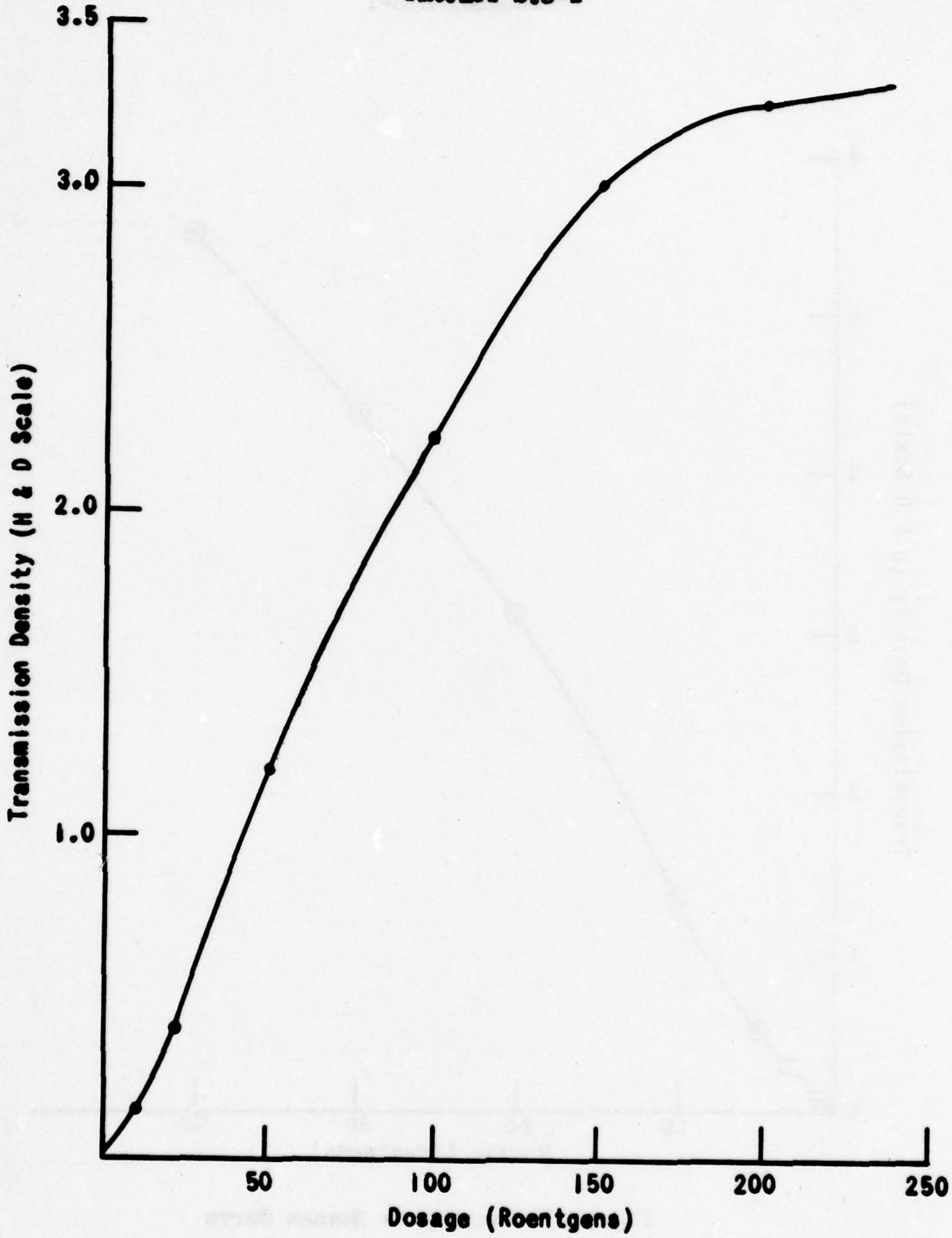

Figure 2.6 DuPont 605 Density vs Dosage Curve

[redacted]

UNCLASSIFIED

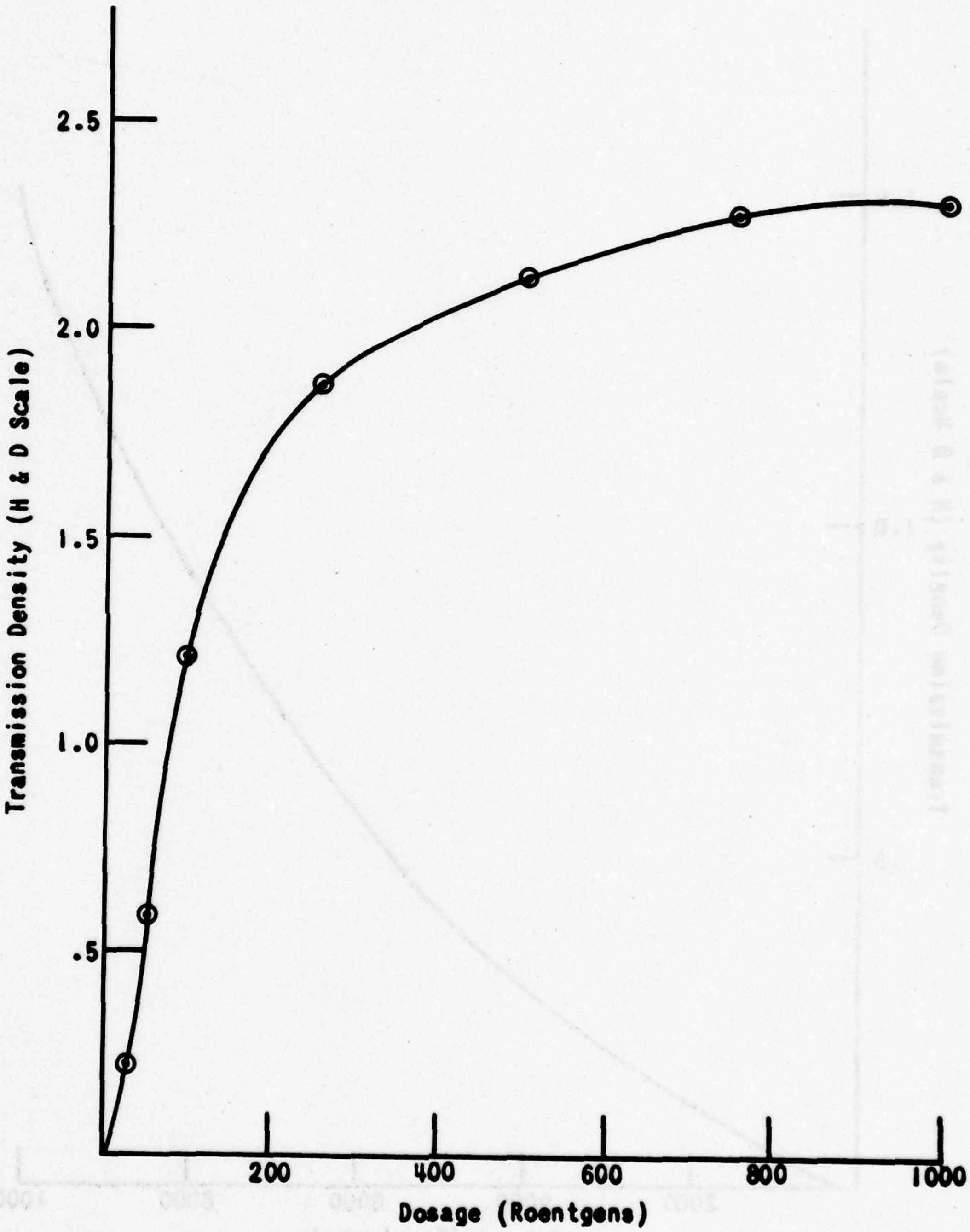

Figure 2.7 DuPont 1290 Density vs Dosage Curve

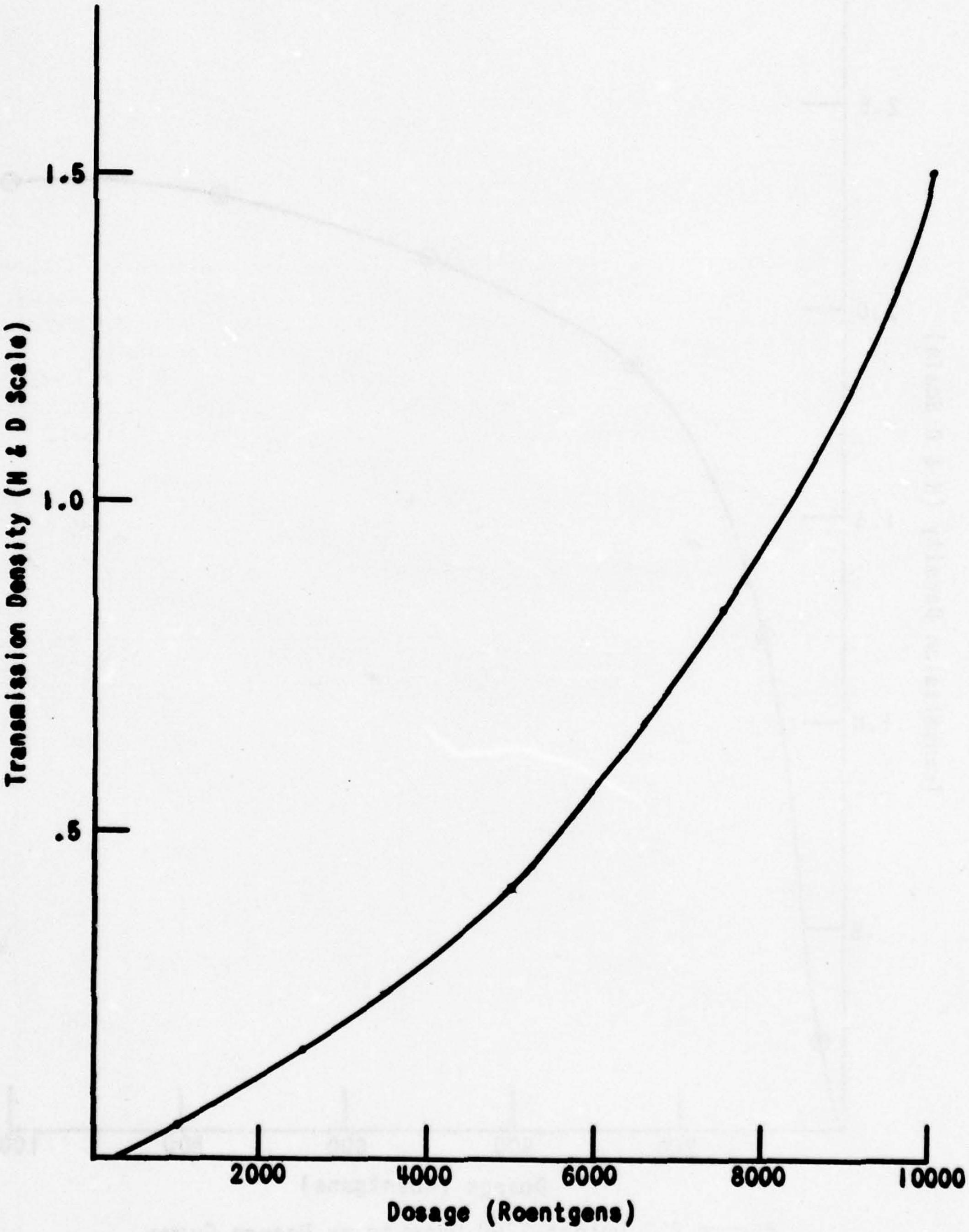

Figure 2.8 Eastman 548-0 (double coated) Density vs Dosage Curve

[redacted]

CHAPTER 3

RESULTS

3.1 GENERAL

Tabulations of the dosage measurements obtained appear in Tables 3.1 and 3.2. The dosages are based upon Co^{60} calibrations. An entry in the column headed "Film Badge Readings (R)" is the dosage in roentgens, for the station, provided the dosage was within the useful range of one or more of the film emulsions placed there. The column headed "Dose (R)" gives the best estimates of the dosages, in roentgens, at the various stations that can be derived from the data obtained.

TABLE 3.1

Total Dosage Measurements (Surface Shot)

Azimuth: 0 Degrees

Station Number	Distance ($d \times 10^3$ FT)	Project Number	Exposure (Hours)	Film Badge Readings (R)	Dose (R)
1	1.4	2.4a	27	4720	4720
2	1.7	2.4a	27	2320	2320
3	2.0	2.4a	27	1400	1400
4	2.3	2.4a	27	Above Range	1000
5	2.6	2.4a	27	1000,750	875
6	2.9	2.4a	27	505,500	500
7	3.2	2.4a	27	435	435
8	3.5	2.4a	27	245	245
9	3.8	2.4a	27	220	220
10	4.1	2.4a	27	138,142	140

[redacted]

[redacted]

TABLE 3.1 (Contd)

Total Dosage Measurements (Surface Shot)

Azimuth: 0 Degrees

Station Number	Distance ($d \times 10^3$ Ft)	Project Number	Exposure (hours)	Film Badge Readings (R)	Dose (R)
11	4.4	2.4a	27	126, 127	126
12	4.7	2.4a	27	127, 120	123
13	5	2.4a	27	128, 132	130
14	6	2.4a	27	178, 192	185
15	7	2.4a	27	Above Range	>300
16	8	2.4a	27	Above Range	>50
17	9	2.4a	27	Above Range	>50
18	10	2.4a	27	Above Range	>50
19	11	2.4a	27	Above Range	>50
20	12	2.4a	27	Above Range	>50

Azimuth: 15 Degrees

Station Number	Distance ($d \times 10^3$ Ft)	Project Number	Exposure (hours)	Film Badge Readings (R)	Dose (R)
21	2	2.1a, 2.5a	49,25	800(5) (700(4))	775
22	3	2.1a, 2.5a	49,25	110(4) 95(1)	106
23	4	2.1a, 2.5a	49,25	26(3) 20	25
24	6	2.1a, 2.5a	49,25	4	c5.0
25	8	2.1a, 2.5a	49,26	2.65 2.15	2.5
26	11	2.1a, 2.5a	29,27	13.8 10.6	13
27	14	2.1a, 2.5a	74,30	13.4, 10.1	12.6

[redacted]

TABLE 3.1 (Contd)

Total Dosage Measurements (Surface Shot)

Azimuth: 15 Degrees (Contd)

Station Number	Distance ($d \times 10^3$ Ft)	Project Number	Exposure (hours)	Film Badge Readings (R)	Dose (R)
28	20	2.5a	5	Above Range	> 50
29	30	2.5a	26	Above Range	> 50
30	50	2.5a	6	Above Range	> 50

Azimuth: 30 Degrees

Station Number	Distance ($d \times 10^3$ Ft)	Project Number	Exposure (hours)	Film Badge Readings (R)	Dose (R)
31	20	2.5a	6	Below Range	< 0.07
32	30	2.5a	7	Below Range	0.
33	50	2.5a	8	Below Range	< 0.05

Azimuth: 45 Degrees

Station Number	Distance ($d \times 10^3$ Ft)	Project Number	Exposure (hours)	Film Badge Readings (R)	Dose (R)
34	1	2.4a	27	8400	8400
35	2	2.4a, 2.3	6	840,750	800
36	2.3	2.4a	6	390,430	420
37	2.5	2.7	50	265,265	265
38	2.6	2.4a	6	220,240	230
39	2.9	2.4a	6	110,110	110
41	3.2	2.4a	6	63, 68	65
42	3.5	2.4a,2.3	6,49	40, 42	40
43	3.8	2.4a	6	25	25
44	4.	2.3	50	17.8,18.4,16	17.4
45	4.1	2.4a	6	14.5, 14.7	14.6
46	4.4	2.4a	6	10.6, 10.8	10.7

[redacted]

TABLE 3.1 (Contd)

Total Dosage Measurements (Surface Shot)

Azimuth: 45 Degrees (Contd)

Station Number	Distance ($d \times 10^3$ Ft)	Project Number	Exposure (hours)	Film Badge Readings (R)	Dose (R)
47	4.5	2.3	50	9.6, 9.8	9.7
48	4.7	2.4a	6	7.6, 7.4	7.5
49	5	2.3,2.4a	6, 50	4.4, 4.6, 4.8, 4.9	4.7
50	6	2.4a	6	Below Range	c.0.4
51	8	2.7	49	Below Range	c.0.2
Azimuth: 50 Degrees					
52	2	2.1a,2.5a	50, 6	715(4), 720(1)	715
53	3	2.1a,2.5a	50, 6	95, 85.	95
54	4	2.1a,2.5a	50, 6	19(2), 17, 10	18
55	6	2.1a,2.5a	50, 6	1(3), .5(1)	1
56	8	2.1a,2.5a	50, 6	Below Range	c 0.25
57	11	2.5a	6	Below Range	c.0.1
58	14	2.5a	8	Below Range	c.0.05
59	20	2.5a	7	Below Range	c.0.05
60	30	2.5a	6	Below Range	0.
61	50	2.5a	6	Below Range	c.0.05
Azimuth: 90 Degrees					
62	2	2.1a,2.5a	50, 7	715(3), 690(1)	715
63	3	2.1a,2.5a	50, 7	90, 90	90
64	4	2.1a,2.5a	50, 7	16.8, 16.5	16.8

[redacted]

TABLE 3.1 (Contd)

Total Dosage Measurements (Surface Shot)

Azimuth: 90 Degrees (Contd)

Station Number	Distance ($d \times 10^3$ Ft)	Project Number	Exposure (hours)	Film Badge Readings (R)	Dose (R)
65	6	2.4a,2.5a	50, 7	1.1(3)	1.1
66	9	2.5a	6	0.4(2)	0.4

Azimuth: 165 Degrees

Station Number	Distance ($d \times 10^3$ Ft)	Project Number	Exposure (hours)	Film Badge Readings (R)	Dose (R)
67	2	2.1a,2.5a	50, 6	690(2),635,600	656
68	3	2.5a	6	80, 75	78
69	4	2.1a,2.5a	50, 6	14.4,15.2,15.6,14.8	15.
70	6	2.1a	50, 6	0.73,0.8,0.86	0.8

Azimuth: 180 Degrees

Station Number	Distance ($d \times 10^3$ Ft)	Project Number	Exposure (hours)	Film Badge Readings (R)	Dose (R)
71	1.8	2.4a	3	960	960
72	2.4	2.4a	3	280, 280.	280
73	3.0	2.4a	3	78, 75	76
74	3.6	2.4a	3	30, 30	30
75	4.2	2.4a	3	11.6,11.6,10	11.
76	4.8	2.4a	3	5.2,5.2	5.2
77	6.	2.4a	3	0,0	0.
78	7.2	2.4a	3	0	0.

Azimuth: 260 Degrees

Station Number	Distance ($d \times 10^3$ Ft)	Project Number	Exposure (hours)	Film Badge Readings (R)	Dose (R)
79	2	2.1a,2.5a	50, 6	640(3) 620	635

TABLE 3.1 (Contd)

Total Dosage Measurements (Surface Shot)

Azimuth: 260 Degrees (Contd)

Station Number	Distance ($d \times 10^3$ Ft)	Project Number	Exposure (hours)	Film Badge Readings (R)	Dose (R)
80	2.25	2.4b	2	220, 415	300
81	2.55	2.4b	2	175, 187	181
82	2.85	2.4b	2	107, 106	106
83	3	2.5a	6	80	80
84	3.15	2.4b	2	65, 67	66
85	3.45	2.4b	2	35, 34	34
86	4	2.1a,2.5a	50,6	17.2,16,16,14.8	16
87	6	2.1a	50	1,0.8,0.9	0.9

Azimuth: 315 Degrees

Station Number	Distance ($d \times 10^3$ Ft)	Project Number	Exposure (hours)	Film Badge Readings (R)	Dose (R)
88	1	2.4a	28	Over Range	▸ 10,000
89	2	2.4a	28	960	960
90	2.3	2.4a	28	495, 595	542
91	2.6	2.4a	28	245, 265	255
92	2.9	2.4a	28	130, 130	130
93	3.2	2.4a	28	80, 86	83
94	3.5	2.4a	5	45, 49	47
95	3.8	2.4a	5	30, 31	31
96	4.1	2.4a	5	19.6, 17	18.3
97	4.4	2.4a	5	12.6, 13	12.8
98	4.7	2.4a	5	9.2, 9.6	9.3
99	5.	2.4a	5	5.9, 6.1	6.

TABLE 3.1 (Contd)

Total Dosage Measurements (Surface Shot

Azimuth: 315 Degrees (Contd)

Station Number	Distance ($d \times 10^3$ Ft)	Project Number	Exposure (hours)	Film Badge Readings (R)	Dose (R)
100	6.	2.4a	5	Below Range	c.1.5

Azimuth: 335 Degrees

Station Number	Distance ($d \times 10^3$ Ft)	Project Number	Exposure (hours)	Film Badge Readings (R)	Dose (R)
101	2	2.1a,2.5a	50	2560, 3240	2730
102	3	2.1a,2.5a	50,25	595, 595	595
103	4	2.1a,2.5a	50,25	130,143,162	145
104	6	2.1a,2.5a	50,25	8.4(3),8.5(2),9.6	8.7
105	9	2.1a,2.5a	50, 6	Below Range	c.0.5
106	11	2.5a	6	Below Range	c.0.1
107	14	2.5a	6	Below Range	c.0.05
108	20	2.5a	29	Below Range	c.0.02

NOTE: "c" means Approximately.

[redacted]

PROJECT 2.3-1

TABLE 3.2

Total Dosage Measurements (Underground Shot)

Azimuth: 0 Degrees

Station Number	Distance ($d \times 10^3$ Ft)	Project Number	Exposure (hours)	Film Badge Readings (R)	Dose (R)
201	1.4	2.4a	50	Over Range	$> 10^4$
202	1.7	2.4a	50	5500	5500
203	2	2.4a	50	3450	3450
204	2.3	2.4a	50	2425	2425
205	2.6	2.4a	50	2425	2425
206	2.9	2.4a	50	2625	2625
207	3.2	2.4a	50	2300	2300
208	3.5	2.4a	50	2075	2075
209	3.8	2.4a	50	1800	1800
210	4.1	2.4a	50	1800	1800
211	4.4	2.4a	50	2425	2425
212	5	2.4a	50	1800	1800
213	6	2.4a	50	Over Range	$> 10^3$
214	7	2.4a	50	850	850
215	8	2.4a	50	750	750
216	9	2.4a	50	295	295
217	10	2.4a	50	180	180
218	11	2.4a	50	135	135
219	12	2.4a	50	93	93

[redacted]

PROJECT 2.3-1

TABLE 3.2 (Contd)

Total Dosage Measurements (Underground Shot)

Azimuth: 35 Degrees

Station Number	Distance ($d \times 10^3$ Ft)	Project Number	Exposure (hours)	Film Badge Readings (R)	Dose (R)
220	2	2.1a,2.5a	50, 47	1925, 3450, 2740 2425, 2525, 3050	2700
221	3	2.1a,2.5a	50, 47	165,168,171,135	160
222	4	2.1a,2.5a	50, 47	20, 48, 80	50
223	6	2.1a,2.5a	50, 46	245, 195, 225	220
224	8	2.1a,2.5a	50, 46	60, 70	65
225	11	2.1a,2.5a	50, 46	74, 55	70
226	14	2.5a	16	30, 26	28
227	20	2.5a	27	4.1, 3.6	4
228	30	2.5a	26	1, 0.6	0.75
229	50	2.5a	140	Below Range	0

Azimuth: 45 Degrees

Station Number	Distance ($d \times 10^3$ Ft)	Project Number	Exposure (hours)	Film Badge Readings (R)	Dose (R)
231	2.0	2.4a,2.3	24	3850	3850
232	2.3	2.4a,2.3	24	1325	1325
233 234	2.55	2.3,2.7 2.4a	24	1000, 510	750
235 236	2.95	2.4a 2.3	24	180	180
237	3.2	2.4a	24	105	105
238	3.8	2.4a	24	42	42
239 240	4.05	2.3 2.4a	50	28	28
241	4.4	2.4a	24	Below Range	22
242	4.5	2.3	50	Below Range	22

[redacted]

PROJECT 2.3-1

TABLE 3.2 (Contd)

Total Dosage Measurements (Underground Shot)

Azimuth: 45 Degrees (Contd)

Station Number	Distance ($d \times 10^3$ Ft)	Project Number	Exposure (hours)	Film Badge Readings (R)	Dose (R)
243	4.7	2.4a	24	Below Range	15
244	5	2.4a,2.7	24	73	73
245	6	2.4a	24	40, 48	44
246	8	2.7	50	Below Range	4

Azimuth: 75 Degrees

Station Number	Distance ($d \times 10^3$ Ft)	Project Number	Exposure (hours)	Film Badge Readings (R)	Dose (R)
247	2	2.1a,2.5a	50	1325,1475,1800,1925	1650
248	3	2.1a,2.5a	50	100, 97	100
249	4	2.1a,2.5a	50	18, 18	18
250	6	2.1a,2.5a	50	Below Range	2
251	9	2.1a,2.5a	50	Below Range	0
252	14	2.5a	50	Below Range	0
253	20	2.5a	50	Below Range	0
254	30	2.5a	50	Below Range	0
255	50	2.5a	50	Below Range	0

Azimuth: 140 Degrees

Station Number	Distance ($d \times 10^3$ Ft)	Project Number	Exposure (hours)	Film Badge Readings (R)	Dose (R)
256	2	2.1a,2.5a	50	1325, 1475	1400
257	3	2.5a	50	95, 100	97
258	4	2.1a,2.5a	50	Below Range	20
S23	6 +	2.1a	50	Below Range	0

[redacted]

[redacted]

PROJECT 2.3-1

TABLE 3.2 (Contd)

Total Dosage Measurements (Underground Shot)

Azimuth: 180 Degrees

Station Number	Distance ($dx10^3$Ft)	Project Number	Exposure (hours)	Film Badge Readings (R)	Dose (R)
259	3	2.4a	3	119	119
260	3.6	2.4a	3	36, 35	35
261	4.2	2.4a	3	21, 18, 17	19
262	4.8	2.4a	3	10, 9.6	10
263	5.4	2.4a	118	19, 18	18
264	6.	2.4a	118	15, 14	14
265	6.6	2.4a	118	17, 16	16

Azimuth: 240 Degrees

Station Number	Distance ($dx10^3$Ft)	Project Number	Exposure (hours)	Film Badge Readings (R)	Dose (R)
266	2	2.1a,2.5a	50, 27	10^3, 1150, 1325	1150
267	3	2.5a	26	92	92
268	4	2.1a,2.5a	50, 26	Below Range	20
269	6	2.1a	50	Below Range	2

Azimuth: 270 Degrees

Station Number	Distance ($dx10^3$Ft)	Project Number	Exposure (hours)	Film Badge Readings (R)	Dose (R)
270	1.5	2.4b	4	3175	3175
271	1.8	2.4b	4	1325	1325
272	2.1	2.4b	4	800, 1000	900
273	2.4	2.4b	4	345	345
274	3.	2.4b	4	80, 97	89

[redacted]

[redacted]

PROJECT 2.3-1

TABLE 3.2 (Contd)

Total Dosage Measurements (Underground Shot)

Azimuth: 315 Degrees

Station Number	Distance ($d \times 10^3$ Ft)	Project Number	Exposure (hours)	Film Badge Readings (R)	Dose (R)
275	1	2.4a	50	Over Range	$>10^4$
276	2	2.1a,2.5a	50	1800,2000,2400	2000
277	2.3	2.4a	4.5	625	625
278	2.6	2.4a	4.5	340	340
279	2.9	2.4a	50	170	170
280	3.0	2.1a,2.5a	50, 23	180, 170, 132	165
281	3.2	2.4a	4.5	118	118
282	3.5	2.4a	4.6	83	83
283	3.8	2.4a	4.6	55	55
284	4.	2.1a,2.5a	50	47, 50	50
285	4.1	2.4a	50	40	40
286	4.4	2.4a	4.6	30	30
287	4.7	2.4a	4.6	Below Range	23
288	5	2.4a	4.6	21, 20, 18	20
289	6	2.1a,2.5a	22,50	Below Range	5.5
290	9	2.1a,2.5a	50	Below Range	2.
291	11	2.5a	50	Below Range	0
292	14	2.5a	50	Below Range	0
293	20	2.5a	50	Below Range	0

[redacted]

PROJECT 2.3-1

TABLE 3.2 (Contd)

Total Dosage Measurements (Underground Shot)

Azimuth: 355 Degrees

Station Number	Distance ($dx10^3$ Ft)	Project Number	Exposure (hours)	Film Badge Readings (R)	Dose (R)
294	2	2.1a,2.5a	50	3400,4200,4000,4400	4000
295	3	2.1a,2.5a	50	2600,3000	2800
296	4	2.1a,2.5a	50	2075,2175,1925	2060
297	6	2.1a,2.5a	50	705, 650	690
298	8	2.1a,2.5a	50	300, 270, 375	320
299	11	2.1a,2.5a	50	93, 96	95
300	14	2.1a,2.5a	50	27, 26	26
301	20	2.5a	28	5.5, 5.1, 5.6	5.5
302	30	2.5a	26	2.3, 1.9	2.0
303	50	2.5a	24	1.4, 1.35	1.4

3.2 ISODOSE CURVES

Total dosage isodose curves (Figures 3.1 and 3.2) are based upon the results compiled in Tables 3.1 and 3.2. The recovery times varied for some of the stations but the majority were exposed 50 hours.

Total dosage in first hour isodose curves (Figures 3.3 and 3.4) are based on the total dosage measurements and the National Bureau of Standards (Project 2.1a) dose rate data at H+1 hour. Correction to 1 hour was made by subtracting from the film badge reading, the integrated dose rate between 1 hour and the time of collection of the film badge. The only total dosage values used were those which were recorded at National Bureau of Standards (Project 2.1a) stations where dose rates were also recorded.

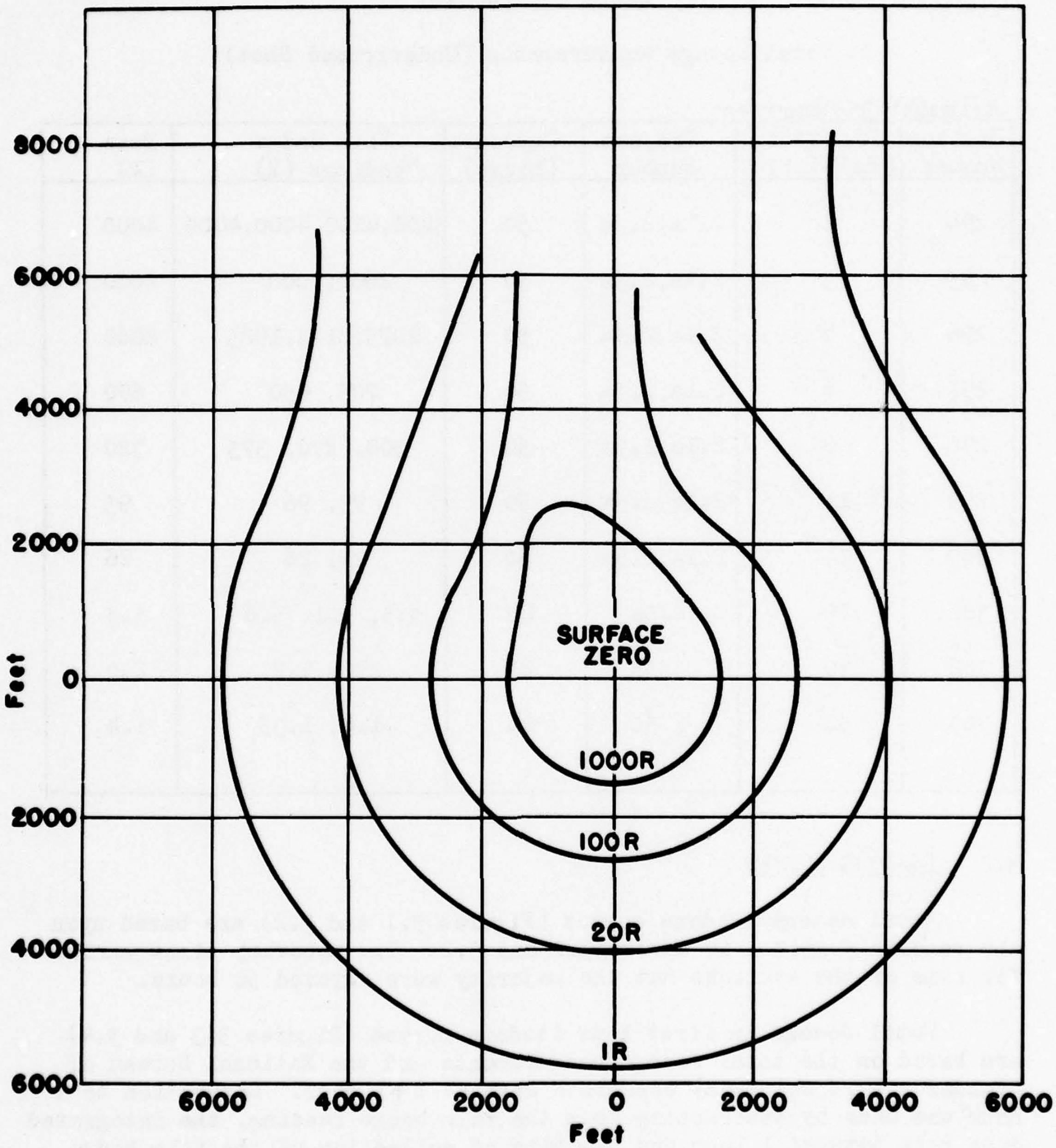

Figure 3.1 Total Gamma Dosage (50 Hours) Surface Shot

PROJECT 2.3-1

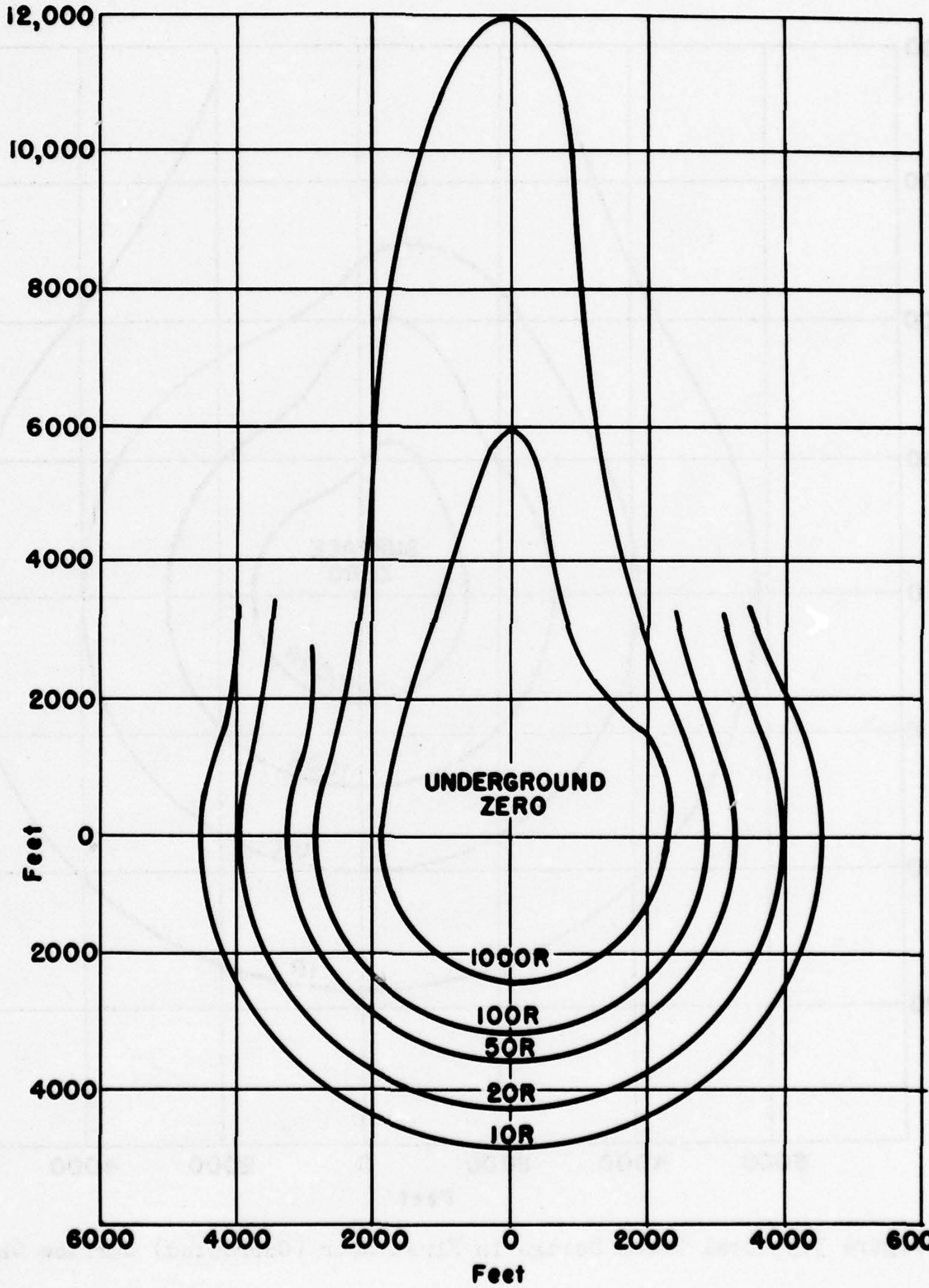

Figure 3.2 Total Gamma Dosage (50 Hours) Underground Shot

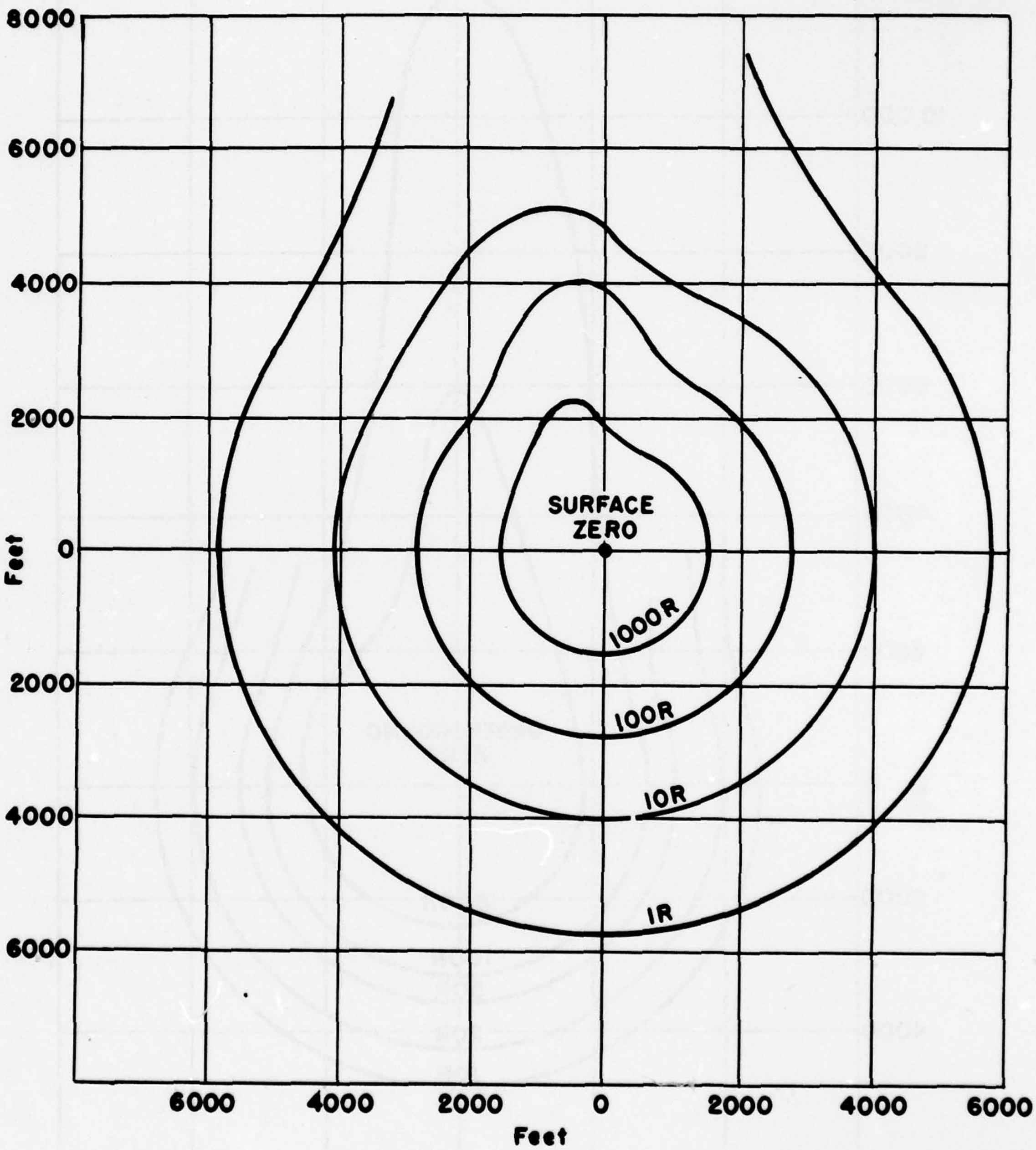

Figure 3.3 Total Gamma Dosage in First Hour (Corrected) Surface Shot

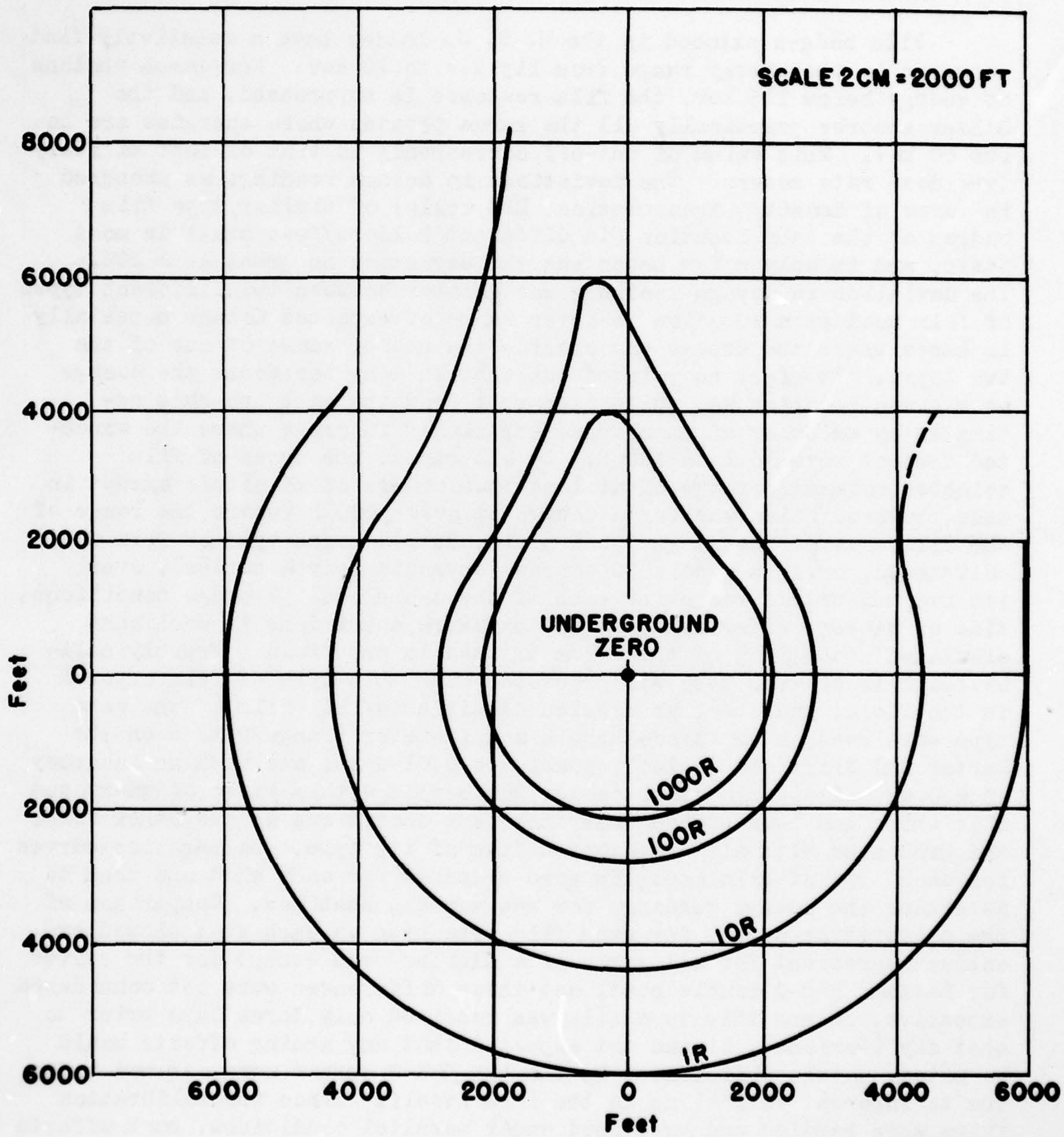

Figure 3.4 Total Gamma Dosage in First Hour (Corrected) Underground Shot

3.3 RELIABILITY AND ERRORS

Film badges exposed in the N. B. S. holder have a relatively flat response in the energy range from 115 kev to 10 mev. For gamma photons of energy below 115 kev, the film response is suppressed, and the holder absorbs practically all the gamma photons whose energies are below 80 kev. This value of cut-off corresponds to that of most military type dose rate meters. The deviations in dosage readings as measured in terms of density (transmission, H&D scale) of similar type film badges at the same location (in different holders) was small in most cases, and in only a few cases was the deviation as great as ± 20%. The deviation in dosage readings was greater between two different types of film used at a location to cover range of expected dosage especially in cases where the dosage was outside the useful range of one of the two types. It might be pointed out that in many instances the dosage at a given location was quite different from the best pre-shot estimates by an order of magnitude, especially in areas where the expected dosages were 10 R to 100 R. In all cases, the types of film selected covered a range of at least two orders of magnitude except in case the prediction was for a dosage of over 5000 R (where the range of the film covered the range 750 R to 10,000 R). Each type of film was calibrated, using a Cobalt 60 source (approximately 4 curies), over its maximum usable range for each of the two shots. Storage conditions, time of storage after exposure and exposure conditions in each case simulated conditions of the films exposed in the field. Freshly calibrated film of each type was processed with this type of film exposed in the field, and the transmission densities of all film of the same type were read on an Ansco-Macbeth densitometer (range 0 to 6 on the Hurter and Driffield Scale; readable to 0.01 unit, and with an accuracy of ± 0.02 unit). The densitometer was zeroed with a piece of unexposed film which had been stored under the same conditions as the other film, and processed with all the exposed film of its type. Calibration curves for each type of film emulsion were prepared for each shot and used to determine the dosage readings for the various stations. Comparison of the calibration curves for each film type used on each shot showed excellent agreement for all types of emulsions used except for the curves for Eastman 548-0 double coat, and these differences were not considered excessive. Since this type film was received only three days prior to shot day (Surface), it was not expected that any ageing effects would be noted, so the differences in the two 548-0 curves were assumed to be due to inherent variations in the film itself. Since the calibration films were handled and processed under parallel conditions, such effects as ageing of films, changes in the gamma of a film for any reason, and even errors in processing such as the discovery by the National Bureau of Standards after Operation JANGLE that the developing bath thermometer had a temperature error of -1.2°C, would not introduce any additional

errors to the dosage readings. It is believed that the dosage readings reported herein are not in error by more than ±10%, since they are averages of two or more film readings which themselves are averages of five readings on the individual piece of film. Each isodose curve shown represents an average of about a thousand film badge readings at over 100 stations, and as such any contour is more accurate than the dosage measurement at any one station.

APPENDIX A

Film Badge Readings Animal Cages (Project 2.7)

A. 1 CAGE LOCATION

The animal cages were located along arcs at 2500, 5000, and 8000 feet from ground zero; distance along the arcs between cages was measured from the northeast (azimuth 45 degrees) radial line, measured to right (R), or left (L) as an observer faced toward ground zero. Film Badge readings and estimated dosages are given in Tables A.1 and A.2 for the surface and underground shots respectively.

TABLE A.1

Total Dosage Measurements; Project 2.7 (Surface Shot)

2500 Foot Arc

Location (Ft)	Exposure (hours)	Film Badge Readings (R)	Dose (R)
350 L	49	260, 270	265
175 L	49	270, 280	275
0	49	267, 262	265
175 R	49	298, 300	295
350 R	49	298, 308	300
700 R	49	285, 295	290

5000 Foot Arc

600 L	49	Below Range	4.2
300 L	49	Below Range	4.6
300 R	49	Below Range	5.1

PROJECT 2.3-1

TABLE A.1 (Contd)

Total Dosage Measurements; Project 2.7 (Surface Shot)

5000 Foot Arc (Contd)

Location (Ft)	Exposure (hours)	Film Badge Readings (R)	Dose (R)
600 R	49	6.2, 6.0	6.2
900 R	49	6.4, 6.8	6.6
1200 R	49	7.1,7.4,8.0	7.5

8000 Foot Arc

800 L	49	Below Range	0.21
400 L	49	Below Range	0.24
0	49	Below Range	0.24
400 R	49	Below Range	0.24
800 R	49	Below Range	0.30
1200 R	49	Below Range	0.28
1600 R	49	Below Range	0.30

PROJECT 2.3-1

TABLE A.2

Total Dosage Measurements; Project 2.7 (Underground Shot)

Location (Ft)	Exposure (hours)	Film Badge Readings (R)	Dose (R)
2500 Foot Arc			
50 R	12, 50	1150, 1475	1310
225 R	12, 50	1325, 1325	1325
400 R	12, 50	1325, 1475	1400
575 R	12, 50	2685, 2850	2740
750 R	50	2525	2525
925 R	50	2425	2425
1100 R	12, 50	Lost, 2960	2960
1275 R	12	2425	2425
1450 R	---	Lost	
1625	12	2075	2075
1800	12	1800	1800
1975	12	1800	1800
2150	---	Lost	
5000 Foot Arc			
600 L	6	Below Range	7
300 L	6	Below Range	10
300 R	6, 50	68, 76	72
600 R	6, 50	195, 260	230
900 R	6, 50	250, 340	295

TABLE A.2 (Contd)

Total Dosage Measurements; Project 2.7 (Underground Shot)

5000 Foot Arc (Contd)

Location (Ft)	Exposure (hours)	Film Badge Readings (R)	Dose (R)
1500 R	50	350	350
2100 R	50	335	335
2400 R	50	285	285
Others		Lost	

8000 Foot Arc

Location (Ft)	Exposure (hours)	Film Badge Readings (R)	Dose (R)
20 R	6	Below Range	4
420 R	6	Below Range	9
820 R	6	Below Range	15
1220 R	6	30, 35	33
2020 R	6	292	292
Others		Lost	

BIBLIOGRAPHY

1. L. A. Pardue, N. Goldstein, E. O. Wollan
MDDC 1065, (Ch 1553; A-2223)

2. L. J. Deal, J. H. Roberson, F. H. Day
Amer. J. Roent. and Rad. Ther., 1948, 5 p 731

3. M. Erlich and S. Fitch
Nucleonics, 1951, 9, p 5

4. G. E. Bell
Br. J. of Radiol., 1936, 9, p 578

5. A. Bouwers
Acta Radio, 1925, 4, p 368

6. G. C. Henny
Am. J. Roent. and Rad. Ther., 1941, p 895

[redacted]

UNCLASSIFIED

OPERATION JANGLE

PROJECT 2.3-2

FOXHOLE SHIELDING OF GAMMA RADIATION

by

THOMAS G. WALSH

27 June 1952

UNCLASSIFIED

ENGINEER RESEARCH AND DEVELOPMENT LABORATORIES

[redacted] [redacted]

[redacted] UNCLASSIFIED

PROJECT 2.3-2

CONTENTS

UNCLASSIFIED

[redacted] [redacted]

PROJECT 2.3-2

ILLUSTRATIONS

TABLES

[redacted]

PROJECT 2.3-2

ABSTRACT

This project was designed by the Corps of Engineers to evaluate the protection afforded by foxholes against the gamma radiation emitted by atomic weapons detonated on the surface and beneath the ground. Film dosimeters were used to measure total gamma ray doses at different depths in one and two-man foxholes as well as in soil pipes sunk into the ground. The film dosimeters were contained in National Bureau of Standards' type holders and responded to gamma radiation of energy greater than 120 Kev. In the report, all doses are given in terms of roentgens and a reading of 650r (roentgens) is taken as the lethal dose; that is, the dose which will cause death to nearly 100 per cent of exposed personnel.

The major conclusions of this experiment, based on the data obtained in the above manner, follow:

1. Standard foxholes, as described in FM 5-15, provide excellent protection to personnel from the gamma radiation emitted during the detonation of an atomic weapon on the surface of the ground. The results show that the doses in the bottom of such foxholes located in the crosswind direction during Operation JANGIE were less than 10 per cent of the surface doses at identical locations. Since the foxholes were located outside of the major fall-out pattern, the complete dose measured was due to scattered prompt radiation. If the foxholes had been located downwind, however, the doses would have been higher, since fall-out into the foxhole and scattered radiation from the contamination on the surface would contribute more significantly to the total dose. There are indications that these contributions will not materially change the per cent of surface-received radiation reaching trained personnel in the bottom of the foxholes. An increase of surface contamination will increase the surface dose as well as the dose at the bottom of the foxhole, thereby maintaining the ratio between the two. The contaminated matter that falls into the foxhole can easily be removed by occupying personnel before it has time to increase the doses received to any great extent.

2. Except in those areas covered by extensive fall-out, foxholes also provided effective shielding in the case of the underground detonation of Operation JANGIE. The doses at the bottom of the foxholes varied from about 24 to 38 per cent of the surface doses at distances greater than 2500 feet from the burst. A great portion of this

[redacted] [redacted]

dose, about 90 per cent, was obviously due to radioactive matter that fell into the foxhole, because the doses measured in the holes during the surface shot were approximately 10 per cent of those measured during the underground shot of identical yield. It is expected that both bursts contributed equally to the doses as far as prompt radiation is concerned.

3. The doses obtained from the detonation of atomic weapons on the surface or underground receive contributions from prompt gamma radiation, radiation emanating from column and cloud, and from residual activity due to fall-out of radioactive matter. No base surge activity was evident.

4. The complete doses at the bottom of the foxholes after the surface burst of this operation were attributable to scattered prompt radiation in addition to a small contribution from the column and cloud; no material contribution from fall-out or residual activity was evident. This lack of effect undoubtedly resulted from the location of the foxholes in the crosswind direction. If the foxholes had been located downwind, there would have been a material contribution from fall-out and residual activity. It is not expected that this would falsify the conclusions drawn in this report on the effectiveness of foxholes as protection for personnel against gamma radiation. (See conclusion 1, above.)

5. The major portion of the total dose measured at the bottom of the foxholes after the underground burst apparently came from fall-out matter in the foxhole. Contamination on the surface of the ground surrounding the foxhole contributed only about 10 per cent to the doses at the bottom of these structures, and prompt radiation could not contribute more than evidenced in the surface burst since both weapons were the same size. Yet, in all cases the doses were considerably higher during the underground detonation, leading to the obvious conclusion that matter falling into the foxholes played the most important role. Also, the doses in the two and one-man foxholes were equal, although the two man foxhole had twice the opening area. If the column or cloud activity contributed greatly to these doses, it could be expected that the doses in the two-man foxhole would be about twice as great as those in the one-man structure.

CHAPTER 1

INTRODUCTION

1.1 OBJECTIVE

The main objective of this project was to determine the protection that foxholes provided from the gamma radiation emitted by surface or underground bursts of atomic weapons. Total gamma radiation intensities at different levels in foxholes were measured by means of film detectors, and the results were analyzed to determine the contributions to the total doses from prompt gamma radiation, from the residual activity due to fall-out, and from column and cloud activities.

1.2 HISTORICAL

Operation JANGLE was the first test in which atomic weapons were detonated on the surface of the ground and underground. No experimental data, therefore, existed prior to this operation concerning the intensity of gamma radiation that would result from such detonations, how this intensity would vary with distance, and the shielding from radiation afforded by foxholes. Since the results obtained by Cerar in an unnumbered project performed during Operation RANGER and the author during Operation BUSTER proved that foxholes provided excellent protection from the radiation emitted during an air burst atomic weapon, the Office of the Chief of Engineers suggested that measurements also be made during the surface and underground bursts of Operation JANGLE allowing a complete picture of the effectiveness of foxholes as shields against radiation to be determined. The project was assigned to the Special Projects Branch of the Engineer Research and Development Laboratories and was carried out as Project 2.3-2 of Operation JANGLE.

The gamma measurements were accomplished by means of National Bureau of Standards' type film dosimeters. The calibration, distribution, collection and development of the film dosimeters were performed by the personnel of Project 2.3-1, Operation JANGLE, and a complete description of the film detectors is found in that report.

AD-A078 575 NATIONAL BUREAU OF STANDARDS WASHINGTON, D.C. 18/3, 18/8
OPERATION JANGLE. NEVADA PROVING GROUNDS, OCTOBER-
NOVEMBER 1951, GAMMA RADIATION MEASUREMENTS, COSTRELL, LOUIS
UNCLASSIFIED WT-370 01 APR 52 AEC

4 OF 4
AD A
078575

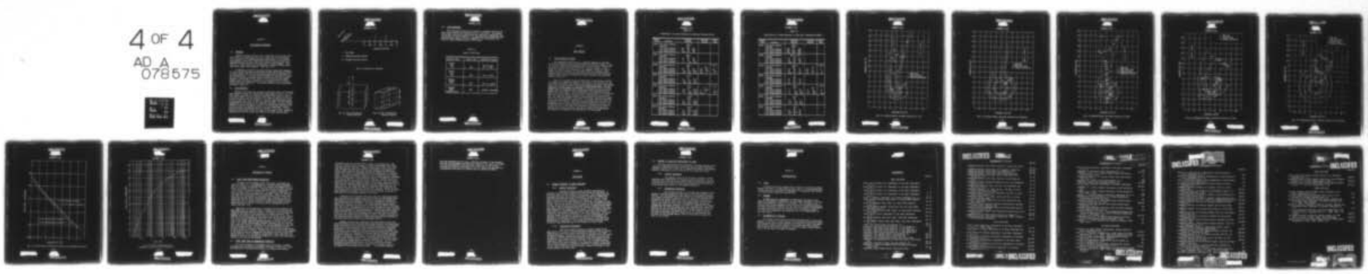

END
DATE
FILMED
6-80
DTIC

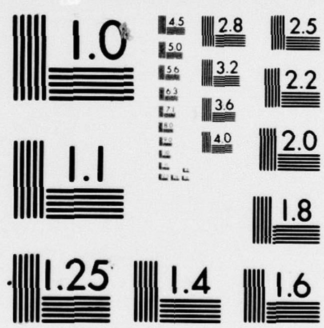

MICROCOPY RESOLUTION TEST CHART

[redacted]

CHAPTER 2

EXPERIMENTAL PROCEDURE

2.1 FOXHOLES

Standard two-man foxholes were constructed at the Nevada Test Site at 500 foot intervals from 2000 to 5000 feet from the points of detonation of the underground and surface shots. The foxholes were placed so that their longitudinal axes lay along a line which extended 45° East of North from the location of the weapon. (See Fig. 2.1.) Each foxhole was instrumented in eleven different positions with gamma film detectors. (See Fig. 2.2.)

In addition, there were one-man foxholes constructed adjacent to those two-man foxholes located 3000 and 4000 feet from the target in such a manner that their longitudinal axes were perpendicular to the northeast line. At these latter distances a soil pipe 48 inches long and 6 inches in diameter was also sunk flush with and perpendicular to the surface of the earth. The soil pipes were instrumented along the central vertical axes at depths of 16, 32, and 48 inches with gamma detectors. The one-man foxholes were instrumented as shown in Fig. 2.3.

2.2 FILM DETECTORS

Briefly, the films were arranged in National Bureau of Standards' type holders to cover the sensitivity ranges given in Table 2.1. The film holder consisted of a bakelite container which held two dental size film packets, and was covered with a layer of 1.07 mm of tin and a layer of lead 0.3 mm in thickness. The lead suppresses gamma rays of low energy, less than 0.1 Mev, and tends to make the film response independent of the energy of the incident radiation. The tin, placed between the lead and bakelite, filters the fluorescent radiation from the lead, while the bakelite serves as an "air equivalent" layer to produce electron equilibrium near the surface of the film. A lead strip was also placed around the edges of the badge to stop tangential radiation and the whole unit then sealed with paper masking tape.

[redacted] [redacted]

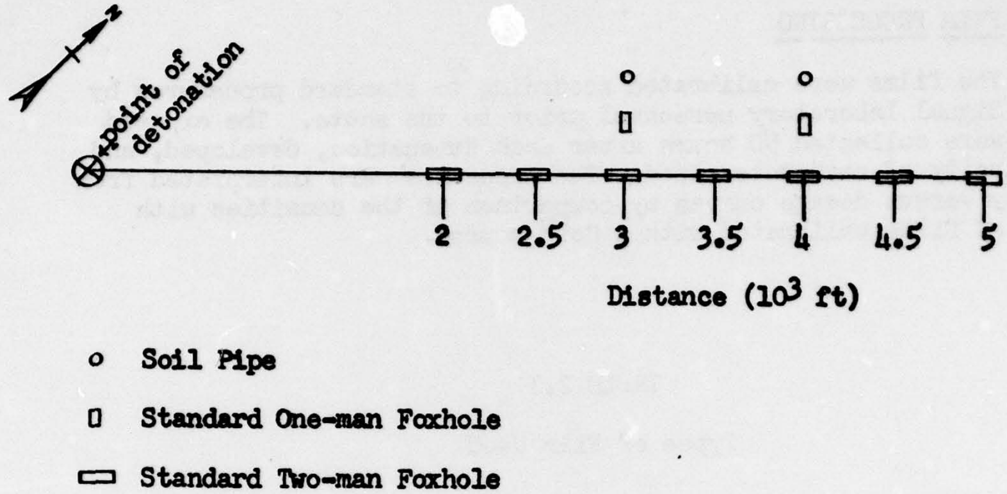

Fig. 2.1 Location of Foxholes

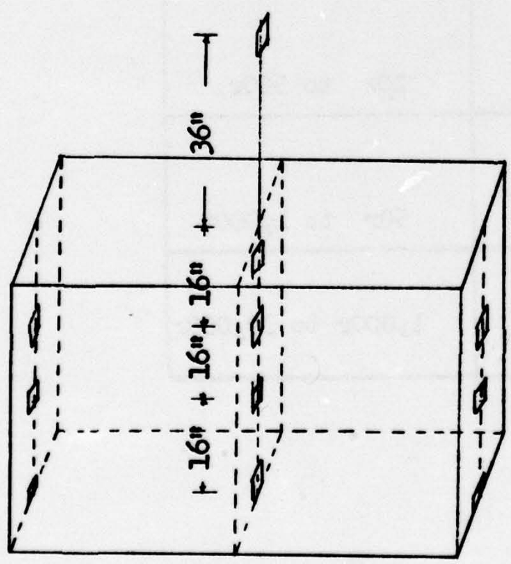

Fig. 2.2 Film Locations in Two-man Foxholes

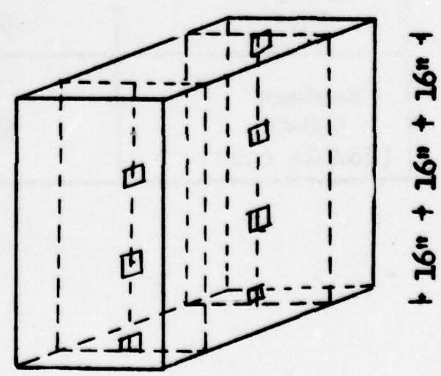

Fig. 2.3 Film Locations in One-man Foxholes

2.3 FILM PROCESSING

The films were calibrated according to standard procedures by Evans Signal Laboratory personnel prior to the shots. The exposed films were collected 50 hours after each detonation, developed, and the density of each determined. The exposures were interpreted from density versus dosage curves by comparison of the densities with those of films calibrated with a Co^{60} source.

TABLE 2.1

Types of Film Used

Emulsion Type	Packet Type	Sensitivity Range
Dupont 502 510	552	0.5r to 10r 3r to 50r
Dupont 510 605	554	20r to 500r
Dupont "Adlux" 556	556	50r to 1,000r
Eastman 548-0 (double coat)	548	1,000r to 10,000r

CHAPTER 3

TEST RESULTS

3.1 GAMMA RADIATION RESULTS

The integrated gamma doses in roentgens measured in foxholes at various distances from the detonations are shown in Tables 3.1 and 3.2 for the surface and underground bursts respectively. These doses are given for five different levels in a two-man foxhole, 3 feet above the surface of the ground, at the surface, and 16, 32, and 48 inches below the surface. At each level below the surface, three doses are given in the two-man foxholes and two doses in the one-man foxhole, representing the results of films located in the positions shown in Fig. 2.2.

Figs. 3.1 through 3.6 are reproductions of the results obtained in Project 2.1A, Operation JANGLE. They depict the dose rates at one hour after the bursts, the total dose received in the first ten minutes and in one hour for both the surface and underground shots. The presentation of these graphs is necessary in this report since the film badges were not collected until fifty hours after the bursts and the graphs give an estimate of the contribution that residual radiation made to the total doses. On these graphs the locations of the foxholes have been superimposed to facilitate the evaluation of the results. Fig. 3.7 shows the prompt radiation expected from detonations of weapons of the size employed in the tests. The curves show the logarithm of the dose received as a function of the distance from the point of detonation to the films. Fig. 3.8 shows the theoretical value of the integrated dose at any time after the burst assuming a dose rate of 1 r per hour at 1 hour after the detonation and a decay law of $t^{-1.2}$. Total doses for any other dose rate may be obtained by multiplying the values on the graph by the desired rate at H+1 hours.

[redacted]

PROJECT 2.3-2

TABLE 3.1

Distribution of Gamma Radiation in Foxholes (Surface Burst)

Range (ft)	Location	Two-man Foxhole			One-man Foxhole		Soil Pipe
2000	36" Above Surface		800 r				
	Surface		700				
	16" Below Surface	230	205	415			
	32" Below Surface	24	58	136			
	48" Below Surface	12.8	22	62			
2500	36" Above Surface		230 r				
	Surface		220				
	16" Below Surface	35	60	85			
	32" Below Surface	7	15	26			
	48" Below Surface	4	8.5	13.3			
3000	36" Above Surface		110 r				73 r
	Surface		90			55	
	16" Below Surface	23	36	55	6.8	6.6	10
	32" Below Surface	7.6	12.4	19.4	2.5	2.4	0.5
	48" Below Surface	2.5	4.8	6.7	1.6	1	0
3500	36" Above Surface		41 r				
	Surface		---				
	16" Below Surface	3	---	9.7			
	32" Below Surface	1.6	2.8	3.4			
	48" Below Surface	.54	.99	1.9			
4000	36" Above Surface		17 r				17 r
	Surface		9.6			—	
	16" Below Surface	1.6	3	5.6	—	0.35	—
	32" Below Surface	0.6	1.12	1.62	—	—	0.17
	48" Below Surface	—	0.54	0.57	0.39	—	—
4500	36" Above Surface		9.8 r				
	Surface		4.6				
	16" Below Surface	1	1.8	3.5			
	32" Below Surface	0.5	0.7	1.04			
	48" Below Surface	0.21	0.4	0.57			
5000	36" Above Surface		4.8 r				
	Surface		2.7				
	16" Below Surface	0.6	0.99	2.95			
	32" Below Surface	0.3	0.5	0.75			
	48" Below Surface	0.17	0.2	0.38			

[redacted]

UNCLASSIFIED

[redacted]

PROJECT 2.3-2

TABLE 3.2

Distribution of Gamma Radiation in Foxholes (Underground Burst)

Range (ft)	Location	Two-man Foxhole			One-man Foxhole		Soil Pipe
2000	36" Above Surface		3850 r				
	Surface		2300				
	16" Below Surface	1150	--	800			
	32" Below Surface	700	1000	555			
	48" Below Surface	200	200	200			
2500	36" Above Surface		1000 -- 550 r				
	Surface		78				
	16" Below Surface	78	98	115			
	32" Below Surface	43	56	50			
	48" Below Surface	73.4	94	96			
3000	36" Above Surface		175 r				155 r
	Surface		103			75	
	16" Below Surface	30	42	37	20	--	7
	32" Below Surface	22	23	20	15	11	3
	48" Below Surface	43.5	45	54	41	38	3
3500	36" Above Surface		--				
	Surface		48				
	16" Below Surface	12	17	15			
	32" Below Surface	9	10	9			
	48" Below Surface	15	15	22			
4000	36" Above Surface		32 r				28 r
	Surface		22			14	
	16" Below Surface	6	7	15	7	4	2
	32" Below Surface	5	3.4	7.2	3.7	2.8	0
	48" Below Surface	6	8.4	8.6	5	9.8	1.1
4500	36" Above Surface		22 r				
	Surface		10				
	16" Below Surface	4	5	5			
	32" Below Surface	5.8	2.8	2.8			
	48" Below Surface	--	7.7	8.9			
5000	36" Above Surface		73 r				
	Surface		23				
	16" Below Surface	15	15	67			
	32" Below Surface	21.5	22.6	15			
	48" Below Surface	--	21	19			

[redacted] [redacted]

UNCLASSIFIED

PROJECT 2.3-2

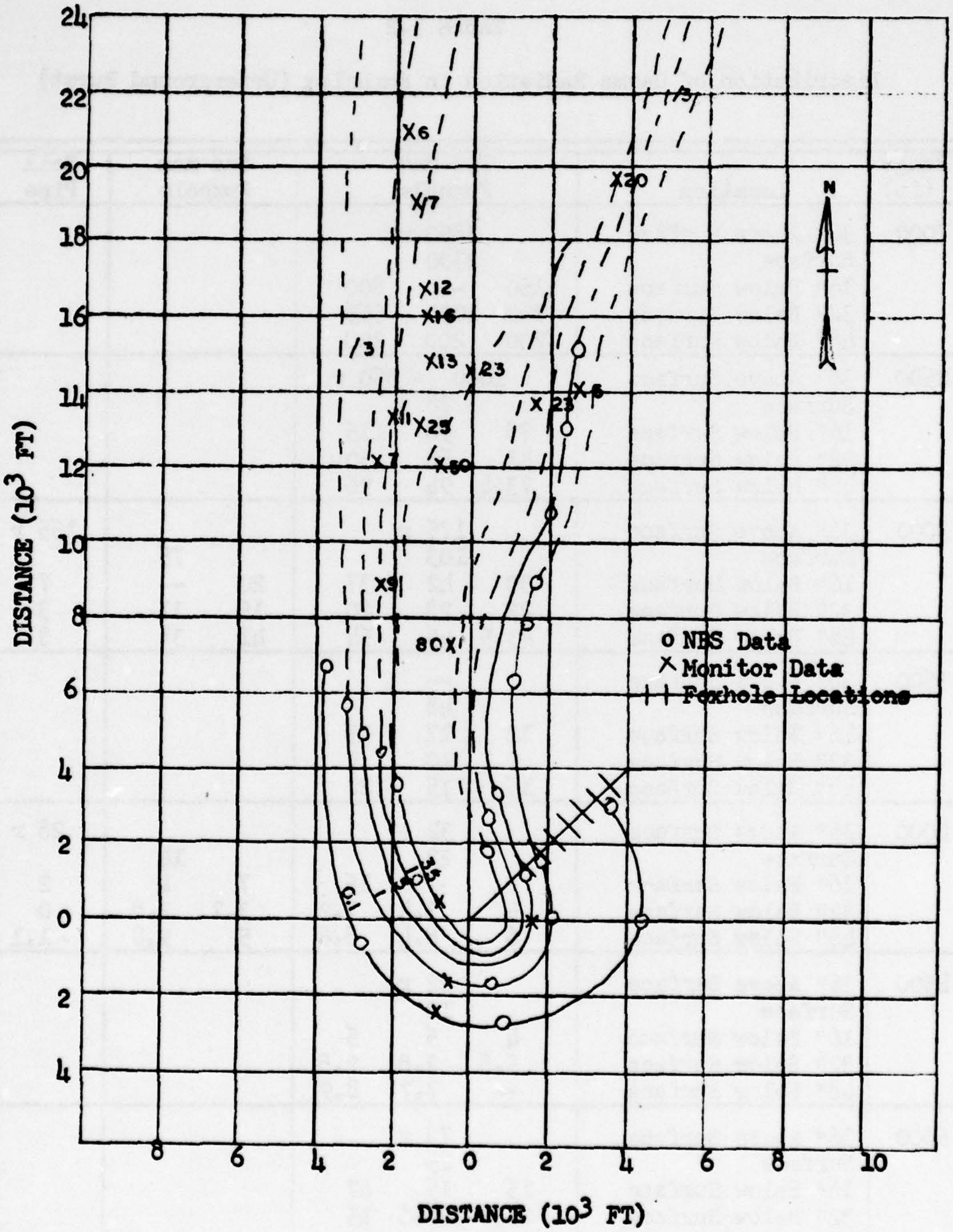

Fig. 3.1 Surface Burst, Iso-Rate Contours At 1 Hr.

PROJECT 2.3-2

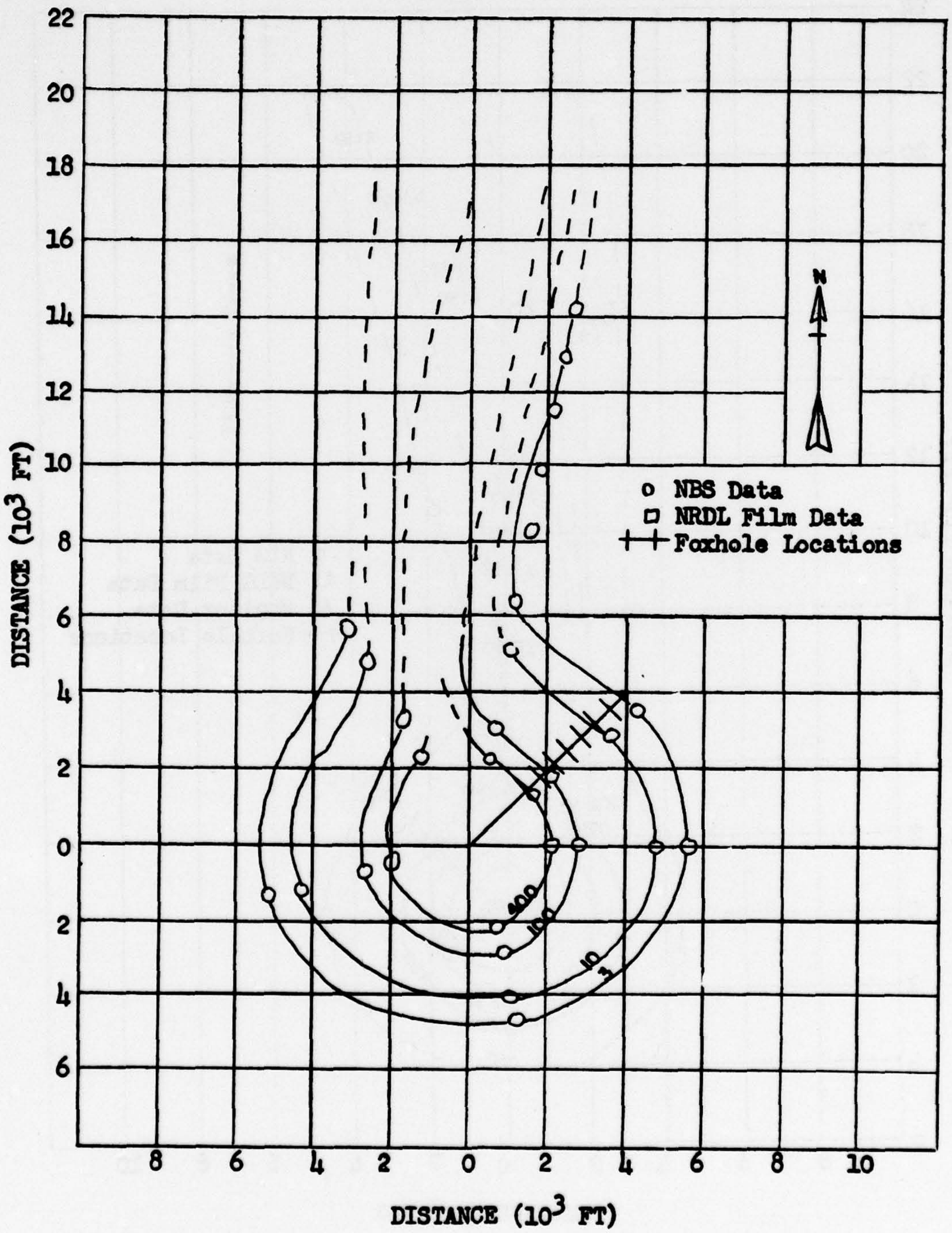

Fig. 3.2 Surface Burst, Iso-Dose Contours at 10 Minutes

PROJECT 2.3-2

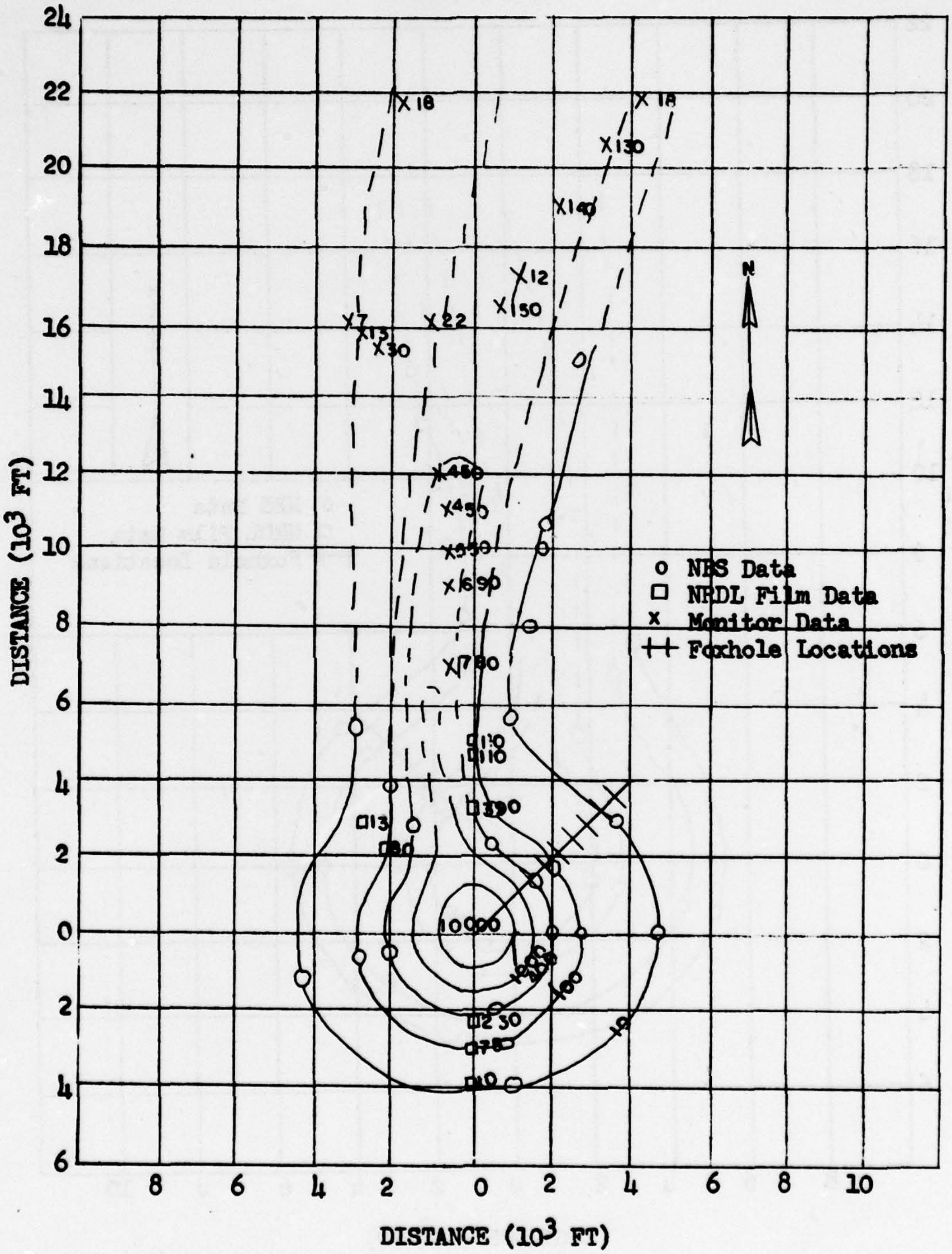

Fig. 3.3 Surface Burst, Iso-Dose Contours At 1 Hour

PROJECT 2.3-2

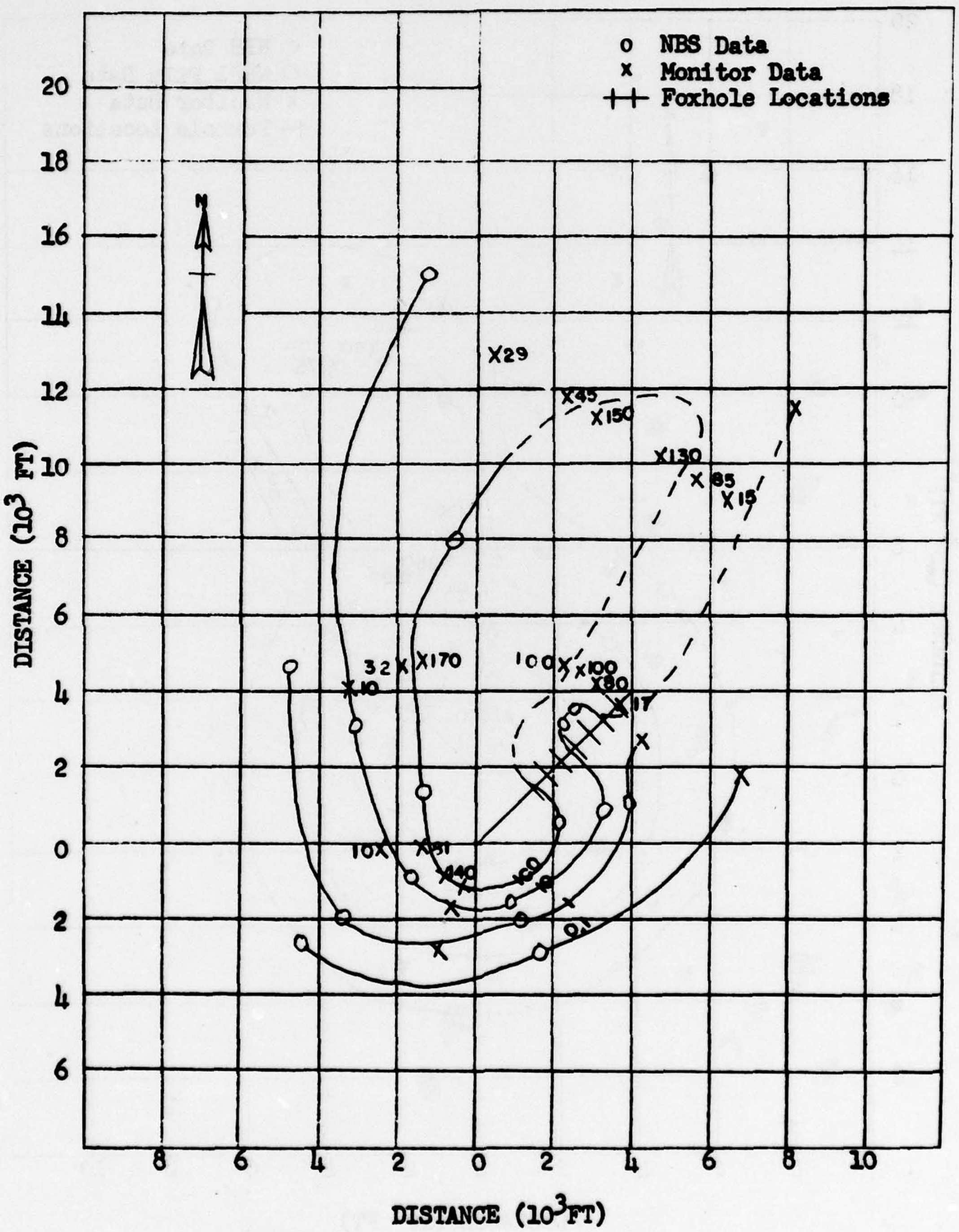

Fig. 3.4 Underground Burst, Iso-Rate Contours at 1 Hour

[redacted]

PROJECT 2.3-2

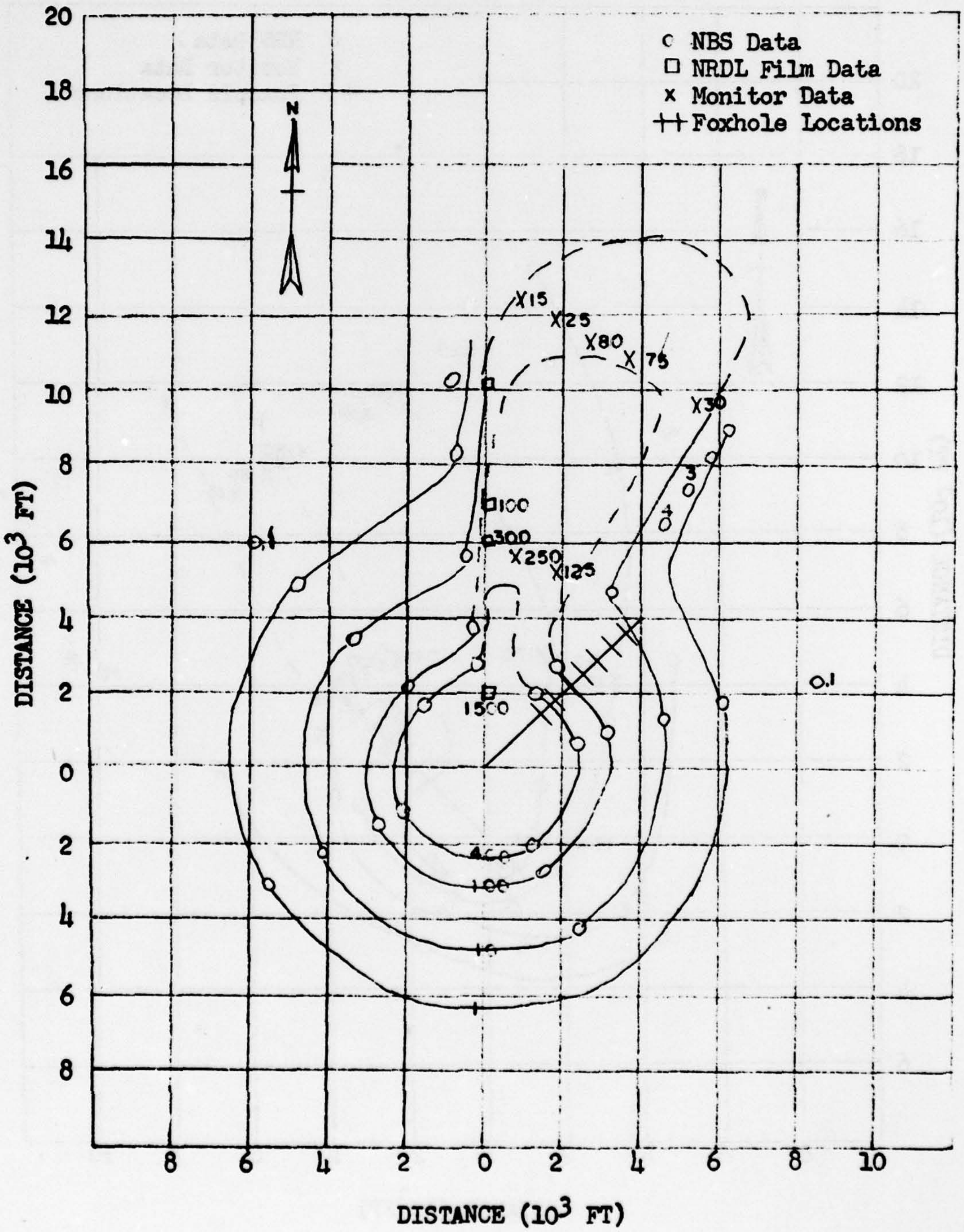

Fig. 3.5 Underground Burst, Iso-Dose Contours At 10 Minutes

[redacted]

PROJECT 2.3-2

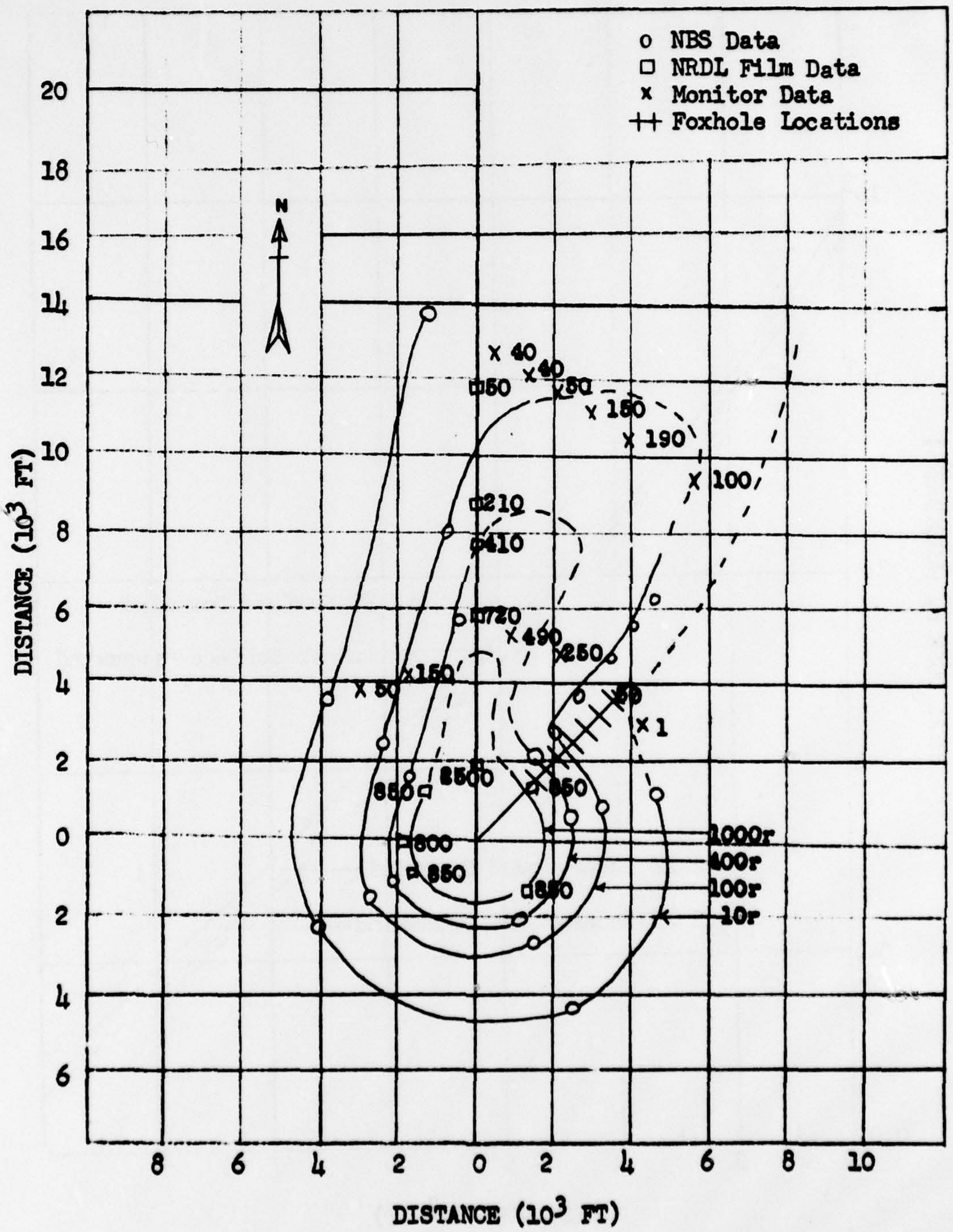

Fig. 3.6 Underground Burst, Iso-Dose Contours at 1 Hour

PROJECT 2.3-2

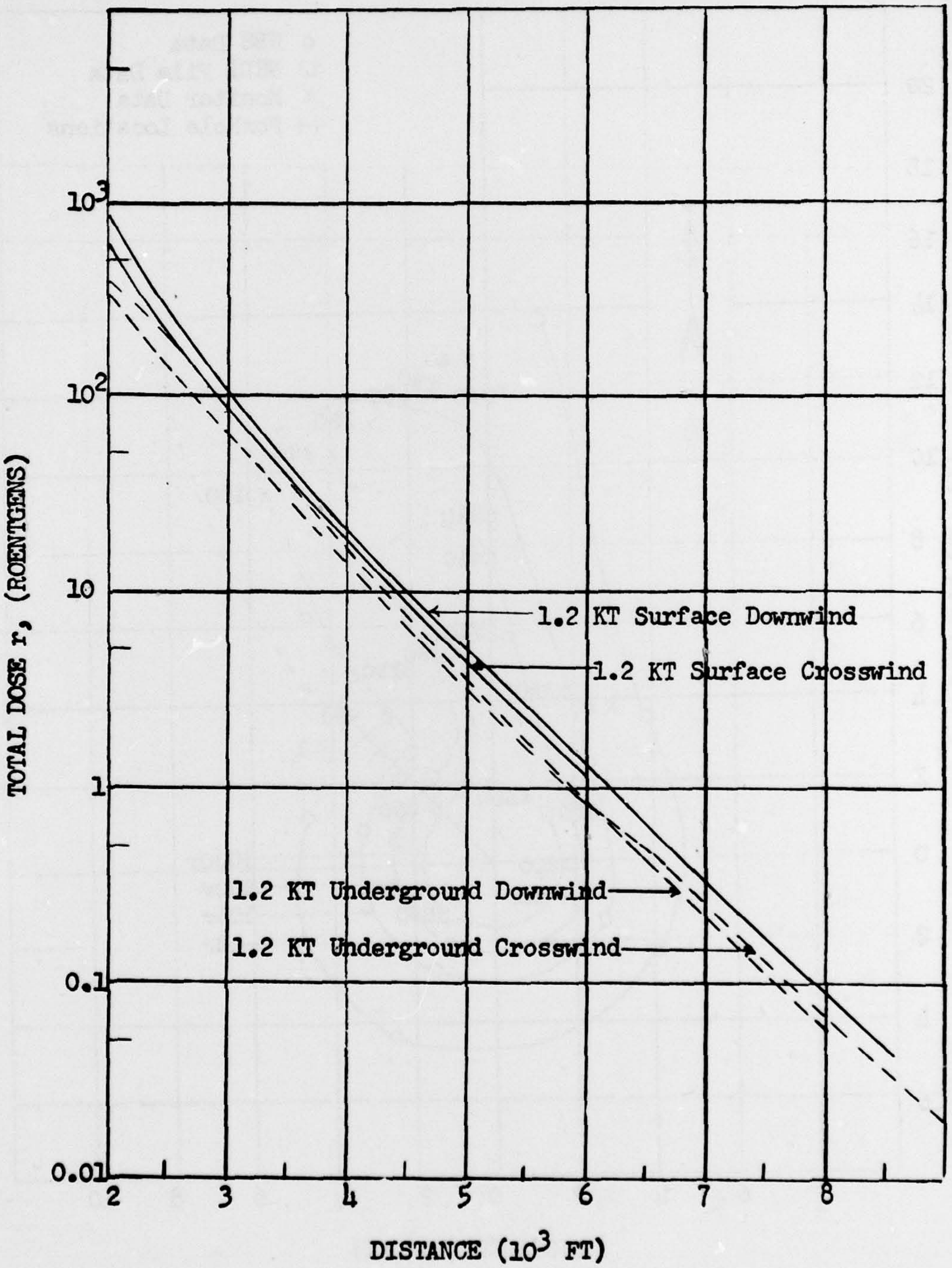

Fig. 3.7 Total Dose at 10 Seconds (Surface and Underground Bursts)

PROJECT 2.3-2

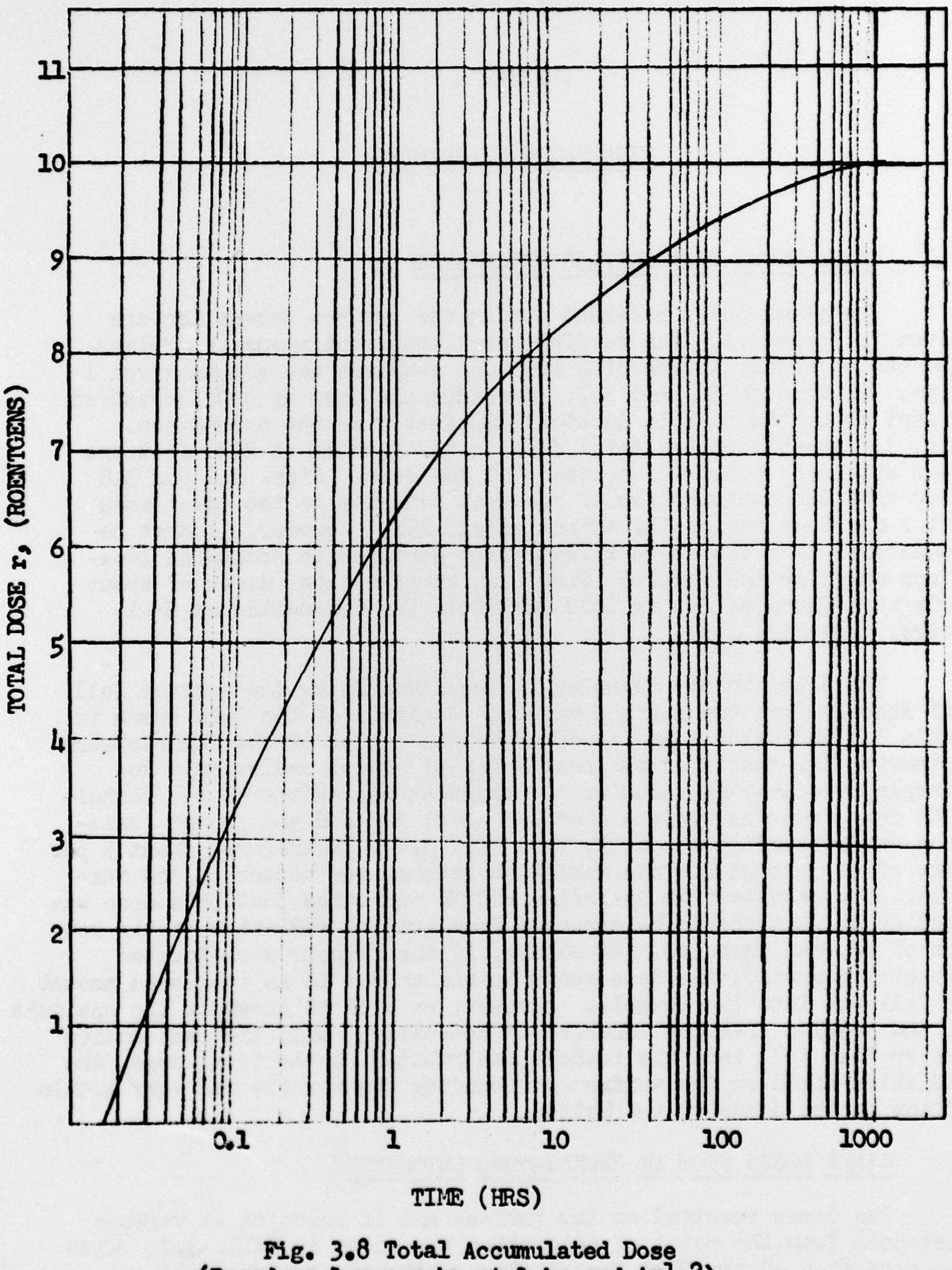

Fig. 3.8 Total Accumulated Dose
(Based on 1 r per hr at 1 hr and $t^{-1.2}$)

[redacted]

CHAPTER 4

DISCUSSION OF RESULTS

4.1 GAMMA DOSES FROM SURFACE DETONATION

The gamma doses recorded during the surface detonation are given in Table 3.1. The readings are consistent among themselves and can be easily interpreted from the contours and graphs given in Figs. 3.1 through 3.3 and 3.7. Consider the dose of 800r, measured 3 feet above the foxhole located 2000 feet from the detonation. Fig. 3.7 shows that the total dose to be expected at 2000 feet one hour after the burst was between 600 and 800r. Figs. 3.1 and 3.8 show that the contribution of residual activity to the total dose after one hour was small, approximately 15r. However, it must be remembered that the above illustration pertains to crosswind locations only; in the downwind direction surface total doses of about 800r were found as far as 7000 feet from the detonation at H+1 hours, (see Fig. 3.3).

The doses in the foxholes at locations below the surface fell off sharply from the surface values. Analysis of the data shown in Table 3.1 indicates that the doses at the bottom of the foxhole were primarily the result of the scattering of prompt radiation. For example, the average value of the films at the bottom of the foxhole 2000 feet from the surface shot was about 32r and the prompt radiation on the surface was 600r, (see Fig. 3.7). Therefore, about 5 per cent of the prompt surface radiation reached the bottom of the foxhole. The results from Operation BUSTER indicated that this dose was just about what should be expected from initial radiation at the bottom of two-man foxholes. Of course, if the foxhole were located directly downwind, the dose would be higher due to an increased amount of fall-out into the foxhole. However, as will be shown in the analysis of the results from the underground detonation, only the radioactive matter that fell into the foxhole contributed to the total dose, the radiation field on the surface surrounding the foxhole had very little effect on the doses at the bottom.

4.2 GAMMA DOSES FROM AN UNDERGROUND DETONATION

The doses received on the surface and in foxholes at various distances from the point of detonation are given in Table 3.2. With the exception of the 2000 foot station, all badges gave readings

[redacted]

consistent with the contours shown in Figs. 3.4 through 3.6. The 2000 foot station gave a reading of 3850r, considerably higher than expected from the contours. However, examination of Fig. 3.6 shows that although the total dose contours are accurate over large distances, small areas of very high activity existed in certain locations even though the surrounding areas gave relatively low radiation doses. This was undoubtedly caused by the concentration of a large amount of fall-out in these locations or by a higher specific contamination of the fall-out in that particular region. Consider the dose of 73r obtained 5000 feet from the burst. From Fig. 3.6 the total dose after one hour at the distance should be about 20r. Figs. 3.4 and 3.7 show that the residual radiation after one hour added about 27r, for a total of 57r. But, data from monitor readings as shown in Fig. 3.6 indicated that the total dose after one hour was 50r, instead of 20, in the area where the 5000 foot station was situated. If the 27r residual radiation were added to this, the result would be 77r which is very close to the reading obtained by the film.

Comparison of the results obtained during the underground burst with those during the surface burst showed that the total gamma doses were greater at all distances following the underground detonation. The increase was due primarily to the greater amounts of radioactive matter that fell from the floud. The doses dropped sharply beyond 2000 feet to reading of about 1000r at 2500 feet and 175r at 3000 feet, (see Table 3.2). Consideration of the doses recorded at these stations lead to an estimate of the effectiveness of foxholes as shields against gamma radiation from an underground burst. In the 2500 foot foxhole, a dose of less than 100r was measured at the bottom, while the dose 3 feet above the surface was approximately 1000r. Clearly, personnel on the surface would be exposed to lethal doses while those protected by foxholes would receive relatively unimportant doses.

Analysis of the doses obtained at the lower levels inside the foxholes indicated that only scattered prompt radiation and radioactive matter that fell into the foxholes contributed greatly to the measured doses and that the attendant surface radiation field was relatively unimportant. This conclusion arose from the fact that the films at the bottom of the two-man and one-man foxholes received about the same doses, see Table 3.2, although the one-man foxhole had only one-half the area of opening. Therefore, if the column and cloud contributed greatly to the doses at the bottom, a greater reading should be expected in the two-man foxhole. The same argument is true with respect to the surface contamination surrounding the foxholes. If this contamination contributed greatly to the doses inside the foxholes through radioactive decay, then it should have a greater effect on the badges in the two-man foxhole because of the greater opening.

This was seemingly not the case. Moreover, Reitmann of the Engineer Research and Development Laboratories, stated in his report on Project 6.2, Land Reclamation, that less than 10 per cent of the surface activity was found at the bottom of a 4 foot trench that was dug in a contaminated area after the surface burst of Operation JANGLE.

CHAPTER 5

CONCLUSIONS

5.1 FOXHOLE SHIELDING OF GAMMA RADIATION

5.1.1 Surface Detonation

Standard foxholes provide excellent protection to personnel from the gamma radiation emitted during the detonation of an atomic weapon on the surface of the ground. The results from the comparatively small sized weapon employed in Operation JANGLE show that 2000 feet from the burst, the location of the closest foxhole doses of about 60r were measured at the bottom of a foxhole, less than 10 per cent of the dose measured 3 feet above the surface of the ground. Due to the location of the foxhole in the crosswind direction, the dose at the bottom was caused primarily by scattered prompt radiation plus a small contribution from the residual activity of the fission products on the surface of the ground. In the downwind direction there would be a contribution from matter that falls out from the cloud into the foxhole in addition to the above mentioned. This fall-out will depend on the wind velocity for a given sized weapon, and although it is expected to increase the dose in the foxholes, especially in those located close to the detonation, it is relatively unimportant in comparison to the prompt and residual activity since it can be easily shoveled out of the foxhole in a short time.

5.1.2 Underground Detonation

With the possible exception of those located in the area close to the point of detonation where extensive fall-out occurs, foxholes also provide effective shielding in the case of an underground detonation. Even within this area of extensive fall-out, which at Operation JANGLE extended approximately 2000 feet, the high doses recorded in the foxholes could be greatly reduced by digging out the radioactive matter that fell into the hole. It is highly probable that one-half the doses recorded in the foxholes located within 2500 feet of the detonation at Operation JANGLE were directly attributable to this type of fall-out and most likely a higher percentage at distances greater than 2500 feet.

5.2 SOURCES OF RADIATION CONTRIBUTING TO DOSES

The doses obtained from the detonation of atomic weapons on the surface or underground receive contributions from prompt radiation, residual activity due to fall-out of radioactive matter, and possibly radiation emanating from the activity of the solumn and cloud.

5.2.1 Surface Detonation

The complete doses at the bottom of foxholes in this operation were attributable to scattered prompt radiation. No contribution from fall-out or cloud and column activity was evident but it is expected that fall-out would have increased the doses if the foxholes had been located in the downwind direction.

5.2.2 Underground Detonation

The greatest portion to the total dose measured at the bottom of foxholes apparently came from the fall-out matter in the foxhole. The contamination on the surface of the ground surrounding the foxhole contributes only about 10 per cent to the doses at the bottom and the prompt radiation could not contribute more than occurred in the surface burst since both weapons were the same size. Yet, in all cases the doses were considerably higher during the underground detonation leading to the obvious conclusion that matter falling into the foxholes played the most important role, also, the doses in the two and one-man foxholes were equal although the two-man foxhole had twice the opening area. If the column or cloud activity contributed greatly to these doses, it was expected that the doses in the two-man foxhole would be about twice as great as that in the one-man.

CHAPTER 6

RECOMMENDATIONS

6.1 TESTS

If future tests are planned which include the surface and underground detonation of larger weapons than 1.2KT, it is recommended that another project of this type be undertaken to investigate the validity of existing gamma radiation scaling laws.

6.2 STUDIES

A study should be undertaken to investigate the ratio of the doses at the bottom of foxholes to the dose rates existing on the surface surrounding the opening of the foxhole. It is possible that a constant ratio exists between the two that would facilitate predicting the doses expected in foxholes for all values of surface contamination. It seems that enough data are available for a preliminary study of this type and arrangements are being made for its accomplishment in the near future.

6.3 DISSEMINATION OF RESULTS

The results of this project should be disseminated to troop commanders in the field to form a basis for preliminary training and staff planning since these results together with those of Project 2.6, Operation BUSTER, present a good picture of the protection that foxholes afford against the nuclear radiation emitted by atomic weapons detonated in the air and on or under the ground.

[redacted]

DISTRIBUTION

	Copy No.
ARMY ACTIVITIES	
Asst. Chief of Staff, G-1, Department of the Army, Washington 25, D. C.	1
Asst. Chief of Staff, G-2, Department of the Army, Washington 25, D. C.	2
Asst. Chief of Staff, G-3, Department of the Army, Washington 25, D. C.	3- 6
Asst. Chief of Staff, G-4, Department of the Army, Washington 25, D. C.	7- 11
Chief of Ordnance, Department of the Army, Washington 25, D. C.	12- 14
Chief Chemical Officer, Temp. Bldg. T-7, Room G-522, Gravelly Point, Va.	15- 18
Chief of Engineers, Temp. Bldg. T-7, Room G-425, Gravelly Point, Va.	19- 21
The Quartermaster General, Second and T Sts. SW, Room 1139A, Washington 25, D. C.	22- 26
Chief of Transportation, Temp. Bldg, T-7, Room G-816, Gravelly Point, Va.	27- 28
Chief Signal Officer, Department of the Army, Washington 25, D. C.	29- 31
The Surgeon General, Main Navy Bldg., Room 1651, Washington 25, D. C.	32- 34
Provost Marshal General, Main Navy Bldg., Room 1065, Washington 25, D. C.	35- 37
Chief, Army Field Forces, Fort Monroe, Va.	38- 41
President, Army Field Forces Board No. 1, Fort Bragg, N. C.	42
President, Army Field Forces Board No. 2, Fort Knox, Ky.	43
President, Army Field Forces Board No. 3, Fort Benning, Ga.	44
President, Army Field Forces Board No. 4, Fort Bliss, Tex.	45
Commandant, The Infantry School, Fort Benning, Ga.	46- 47
Commandant, The Armored School, Fort Knox, Ky.	48- 49
President, The Artillery School Board, Fort Sill, Okla.	50- 51
Commandant, The AA&GM Branch, The Artillery School, Fort Bliss, Tex.	52- 53
Commandant, Army War College, Carlisle Barracks, Pa.	54- 55
Commandant, Command and General Staff College, Fort Leavenworth, Kans.	56- 57
Commandant, Army General School, Fort Riley, Kans.	58

[redacted] [redacted]

DISTRIBUTION (Continued)

	Copy No.
Commanding General, First Army, Governor's Island, New York 4, N. Y.	59- 60
Commanding General, Second Army, Fort George G. Meade, Md.	61- 62
Commanding General, Third Army, Fort McPherson, Ga.	63- 64
Commanding General, Fourth Army, Fort Sam Houston, Tex.	65- 66
Commanding General, Fifth Army, 1660 E. Hyde Park Blvd., Chicago 15, Ill.	67- 68
Commanding General, Sixth Army, Presidio of San Francisco, Calif.	69- 70
Commander-in-Chief, European Command, APO 403, c/o Postmaster, New York, N. Y.	71- 72
Commander-in-Chief, Far East, APO 500, c/o Postmaster, San Francisco, Calif.	73- 74
Commanding General, U. S. Army, Pacific, APO 958, c/o Postmaster, San Francisco, Calif.	75- 76
Commanding General, U. S. Army, Caribbean, APO 834, c/o Postmaster, New Orleans, La.	77- 78
Commanding General, U. S. Army, Alaska, APO 942, c/o Postmaster, Seattle, Wash.	79- 80
Director, Operations Research Office, 6410 Connecticut Ave., Chevy Chase, Md.	81- 83
Commanding Officer, Ballistic Research Laboratories, Aberdeen Proving Ground, Aberdeen, Md.	84- 85
Commanding Officer, Engineer Research and Development Laboratory, Fort Belvoir, Va.	86- 87
Commanding Officer, Signal Corps Engineering Laboratories, Fort Monmouth, N. J.	88- 89
Commanding Officer, Evans Signal Laboratory, Belmar, N. J.	90- 91
Commanding General, Army Chemical Center, Md. ATTN: Chemical and Radiological Laboratory	92- 93

NAVY ACTIVITIES

Chief of Naval Operations, Department of the Navy, Washington 25, D. C. ATTN: Op-36	94- 95
Chief, Bureau of Ships, Department of the Navy, Washington 25, D. C.	96- 99
Chief, Bureau of Ordnance, Department of the Navy, Washington 25, D. C.	100
Chief, Bureau of Medicine and Surgery, Department of the Navy, Washington 25, D. C.	101-102
Chief, Bureau of Aeronautics, Department of the Navy, Washington 25, D. C.	103-104
Chief, Bureau of Supplies and Accounts, Department of the Navy, Washington 25, D. C.	105-106
Chief, Bureau of Yards and Docks, Department of the Navy, Washington 25, D. C.	107-109

DISTRIBUTION (Continued)

	Copy No.
Chief of Naval Personnel, Department of the Navy, Washington 25, D. C.	110
Commandant of the Marine Corps, Washington 25, D. C.	111-113
Commander-in-Chief, U. S. Pacific Fleet, Fleet Post Office, San Francisco, Calif.	114
Commander-in-Chief, U. S. Atlantic Fleet, Fleet Post Office, New York, N. Y.	115
President, U. S. Naval War College, Newport, R. I.	116
Commandant, Marine Corps Schools, Quantico, Va.	117-118
Chief of Naval Research, Department of the Navy, Washington 25, D. C.	119-120
Commander, U. S. Naval Ordnance Laboratory, Silver Spring 19, Md.	121
Commander, U. S. Naval Ordnance Laboratory, Silver Spring 19, Md. ATTN: Aliex	122
Director, U. S. Naval Research Laboratory, Washington 25, D. C.	123
Commanding Officer and Director, U. S. Naval Electronics Laboratory, San Diego 52, Calif.	124
Commanding Officer, U. S. Naval Radiological Defense Laboratory, San Francisco 24, Calif.	125-128
Commanding Officer and Director, David Taylor Model Basin, Washington 7, D. C.	129
Commander, Naval Material Laboratory, New York Naval Shipyard, Naval Base, New York 1, N. Y.	130
Officer-in-Charge, U. S. Naval Civil Engineering Research and Evaluation Laboratory, U. S. Naval Construction Battalion Center, Port Hueneme, Calif.	131-132
Commanding Officer, U. S. Naval Medical Research Institute, National Naval Medical Center, Bethesda 14, Md.	133
Commander, U. S. Naval Ordnance Test Station, Inyokern, China Lake, Calif.	134

AIR FORCE ACTIVITIES

Assistant for Atomic Energy, Headquarters, United States Air Force, Washington 25, D. C.	135-136
Director of Operations, Headquarters, United States Air Force, Washington 25, D. C. ATTN: Operations Analysis Division	137-138
Director of Plans, Headquarters, United States Air Force, Washington 25, D. C. ATTN: AFOPD-P1	139
Director of Requirements, Headquarters, United States Air Force, Washington 25, D. C.	140
Director of Research and Development, Headquarters, United States Air Force, Washington 25, D. C.	141-142
Director of Intelligence, Headquarters, United States Air Force, Washington 25, D. C. ATTN: Phys. Vul. Branch, Air Targets Division	[illegible]

[redacted] CANCELED SECRET Security Information

UNCLASSIFIED

DISTRIBUTION (Continued)

	Copy No.
Director of Installations, Headquarters, United States Air Force, Washington 25, D. C.	145
Asst. for Development Planning, Headquarters, United States Air Force, Washington 25, D. C.	146
Asst. for Materiel Program Control, Headquarters, United States Air Force, Washington 25, D. C.	147
The Surgeon General, Headquarters, United States Air Force, Washington 25, D. C.	148
Commanding General, Strategic Air Command, Offutt Air Force Base, Nebr.	149-151
Commanding General, Air Research and Development Command, P.O. Box 1395, Baltimore 3, Md.	152-161
Commanding General, Air Materiel Command, Wright-Patterson Air Force Base, Dayton, Ohio	162-163
Commanding General, Air Materiel Command, Wright-Patterson Air Force Base, Dayton, Ohio. ATTN: Air Installations Division	164-165
Commanding General, Tactical Air Command, Langley Air Force Base, Va.	166-168
Commanding General, Air Defense Command, Ent Air Force Base, Colo.	169-171
Commanding General, Air Proving Ground, Eglin Air Force Base, Fla.	172-173
Commanding General, Air Training Command, Scott Air Force Base, Belleville, Ill.	174-176
Commanding General, Air University, Maxwell Air Force Base, Montgomery, Ala.	177-179
Commanding General, Special Weapons Center, Kirtland Air Force Base, N. Mex.	180-182
Commanding General, 1009th Special Weapons Squadron, 1712 G St. NW, Washington 25, D. C.	183
Commanding General, Wright Air Development Center, Wright-Patterson Air Force Base, Dayton, Ohio	184-187
Commanding General, Air Force Cambridge Research Center, 230 Albany St., Cambridge 39, Mass.	188-189
Commanding General, U. S. Air Forces in Europe, APO 633, c/o Postmaster, New York, N. Y.	190-191
Commanding General, Far East Air Forces, APO 925, c/o Postmaster, San Francisco, Calif.	192-193
Commanding General, Air Force Missile Center, Patrick Air Force Base, Cocoa, Fla.	194
Commandant, USAF School of Aviation Medicine, Randolph Air Force Base, Randolph Field, Tex.	195
Asst. to the Special Asst., Chief of Staff, United States Air Force, Washington 25, D. C. ATTN: David T. Griggs	196
The RAND Corporation, 1500 Fourth St., Santa Mo[illegible] Calif.	197-198

UNCLASSIFIED

[redacted] CANCELED SECRET CANCELED [redacted]

[redacted] Security Information [redacted]

UNCLASSIFIED

DISTRIBUTION (Continued)

	Copy No.
AFSWP ACTIVITIES	
Chief, Armed Forces Special Weapons Project, P.O. Box 2610, Washington 13, D. C.	199-207
Commanding General, Field Command, Armed Forces Special Weapons Project, P.O. Box 5100, Albuquerque, N. Mex.	208-210
Commanding Officer, Test Command, Armed Forces Special Weapons Project, P.O. Box 5600, Albuquerque, N. Mex.	211-213
OTHER ACTIVITIES	
Chairman, Research and Development Board, Department of Defense, Washington 25, D. C.	214
Director, Weapons System Evaluations Group, Office of the Secretary of Defense, Washington 25, D. C.	215
Executive Director, Committee on Atomic Energy, Research and Development Board, Department of Defense, Washington 25, D. C. ATTN: David Beckler	216
Executive Director, Committee on Medical Sciences, Research and Development Board, Department of Defense, Washington 25, D. C.	217
U. S. Atomic Energy Commission, Classified Document Room, 1901 Constitution Ave., Washington 25, D. C. ATTN: Mrs. J. M. O'Leary	218-220
Los Alamos Scientific Laboratory, Report Library, P.O. Box 1663, Los Alamos, N. Mex. ATTN: Helen Challenger	221-223
Sandia Corporation, Classified Document Division, Sandia Base, Albuquerque, N. Mex. ATTN: Wynne K. Cox	224-243

UNCLASSIFIED

[redacted]

AEC, Oak Ridge, Tenn., A31909